博士論文

Evaluation of thermal sensation in outdoor environment under mist spraying condition

（ミスト噴霧を有する屋外環境における温熱感覚評価に関する研究）

呉　元錫

Evaluation of thermal sensation in outdoor environment under mist spraying condition

by Wonseok Oh

A thesis submitted in partial fulfilment
of the requirements of the University of Tokyo
for the degree of Doctor of Philosophy

February 2020

Department of Architecture
Graduate School of Engineering
THE UNIVERSITY OF TOKYO

TABLE OF CONTENTS

TABLE OF CONTENTS ····· **1**

LIST OF FIGURES ····· **6**

LIST OF TABLES ····· **11**

NOMECLATURE ····· **13**

ABSTRACT ····· **17**

CHAPTER 1. INTRODUCTION ····· **21**

1.1. Fundamental of mist spraying system ····· 23

1.2. Literature review of mist spraying system ····· 24

1.3. Current issues ····· 25

1.4. Overall objectives of present thesis ····· 26

CHAPTER 2. BASIC THEORY ····· **29**

2.1. Environmental index for evaluating thermal environment ····· 31

2.1.1. Predicted mean vote (PMV) ····· *32*

2.1.2. Physiological equivalent temperature (PET) ····· *33*

2.1.3. Standard effective temperature (SET)* ····· *33*

2.1.4. Equivalent temperature ····· *34*

2.1.5. Wet-bulb globe temperature (WBGT) ····· *35*

2.1.6. UTCI (Universal thermal climate index) ····· *36*

2.2. Physiological human model ····· 36

2.2.1. Two-node model ····· *36*

2.2.2. Three-node model ····· *37*

2.2.3. 65-node model ····· *37*

CHAPTER 3. ASSESSMENT OF EXISTING ENVIRONMENTAL INDICES IN MIST SPRAYING ENVIRONMENT ····· 39

3.1. Background and objectives ····· 41

3.2. Experimental setup ····· 42

3.3. Survey research ····· 43

3.3.1. Subjects ····· *43*

3.3.2. Survey scale ····· *44*

3.4. Results and discussion ····· 45

3.4.1. Thermal sensation and thermal comfort ····· *45*

3.4.2. Outdoor weather condition ····· *48*

3.4.3. Acceptability in outdoor and mist spraying environments ····· *49*

3.4.4. Existing environmental indices and thermal sensation ····· *49*

3.4.5. Existing environmental indices and thermal comfort ····· *52*

3.5. Conclusion ····· 54

CHAPTER 4. ESTIMATION OF PHYSIOLOGICAL RESPONSES IN MIST SPRAYING ENVIRONMENT ····· 57

4.1. Background and objectives ····· 59

4.2. Literature review ····· 60

4.3. Mist spraying environment with sunshade ····· 61

4.3.1. Methodology ····· *61*

4.3.1.1 Overall experimental method ····· *61*

4.3.1.2 Environmental factors ····· *61*

4.3.1.3 Estimation of mean radiation temperature in outdoor ····· *64*

4.3.1.4 Review of mean radiation temperature estimation method ····· *65*

4.3.2. Subject experiment setup ····· *67*

4.3.2.1 Subject experiment protocol ····· *67*

4.3.2.2 Skin temperature measurement ····· *68*

4.3.3. Results and discussion ····· *70*

4.3.3.1 Environmental factors outdoor and mist spraying environment with sunshade ····· *70*

4.3.3.2 Infrared camera image of subject ····· *71*

4.4. Physiological human model in outdoor and mist spraying environments ····· 71

4.4.1. Experimental method for determining the clothing level ····· *71*

4.4.1.1 Thermal manikin experiment ····· *71*

4.4.1.2 Calculation method of clothing level ····· *72*

4.4.1.3 Results of thermal manikin experiment ····· *73*

4.4.2. Validation of two-node model ····· *74*

4.4.2.1 Calculation condition for validation of two-node model ····· *74*

4.5. Results and discussion ····· 75

4.5.1. Skin temperature variation ····· *75*

4.5.2. Calculation condition for standard condition ····· *77*

4.6. Conclusion ····· 80

CHAPTER 5. EVALUATION OF MIST SPRAYING ENVIRONMENT CONSIDERING MIST WETTEDNESS ····· 81

5.1. Background and objectives ····· 83

5.2. Experimental setup ····· 85

5.2.1. Operation conditions of mist spraying system ····· *85*

5.2.2. Measurements of environmental factors ····· *86*

5.2.3. Measuring mean radiant temperature (MRT) ····· *89*

5.2.4. Subject experiment setup ····· *90*

5.2.5. Statistical analysis ····· *91*

5.3. Concepts of mist wettedness ····· 92

5.3.1. Design of mist wettedness meter ····· *93*

5.3.2. Mist wettedness measurement ····· *95*

5.4. Results and discussion ····· 98

5.4.1. Environmental factors ····· *98*

5.4.2. Perspective on environmental index ····· *101*

5.4.3. Mist wettedness ····· *102*

5.4.4. Review of spraying condition ····· *102*

5.4.5. Subjective assessments ····· *104*

5.4.6. Overall skin temperature changes ····· *109*

5.4.7. Temperature differences in body segments ····· *110*

5.4.8. Skin temperature changes in maximum evaporative cooling condition ····· *112*

5.4.9. Overall skin temperature and thermal sensations ····· *114*

5.4.10. Correlation between thermal sensations and thermal comfort ····· *115*

5.4.11. Comparison with other outdoor researches ····· *117*

5.4.12. Perspective on adaptive thermal comfort ····· *118*

5.5. Conclusion ····· 121

CHAPTER 6. PHYSIOLOGICAL HUMAN MODEL CONSIDERING MIST WETTEDNESS ····· 125

6.1. Background and objectives ····· 127

6.1.1. Background and literature review ····· *127*

6.1.2. Objectives of developing human model considering mist wettedness ····· *128*

6.1. Methodology ····· 128

6.1.1. Environmental factors ····· *128*

6.2. Results and discussion ····· 136

6.2.1. Skin temperature variations ····· *136*

6.2.2. Heat loss causes in outdoor and mist spraying environment ····· *137*

6.2.3. Effectiveness area factor of evaporative heat loss by mist droplets ····· *138*

6.2.4. Heat loss causes considering effectiveness area factor ····· *140*

6.3. Conclusion ····· 142

CHAPTER 7. PROPOSAL OF NEW ASSESSMENTS FOR OUTDOOR AND MIST SPRAYING ENVIRONMENTS ····· 145

7.1. Proposal of O-PMV index ····· 147

7.2. Proposal of SET** index ····· 151

7.3. Proposal of mPMV index ····· 155

7.4. Comparison of proposed different environmental indices ····· 157

7.5. Conclusion ····· 157

CHAPTER 8. CONCLUSION AND FURTHER RESEARCH ····· 159

APPENDIX ····· 165

REFERENCE ····· 183

PUBLICATIONS ····· 193

ACKNOWLEDGMENTS ····· 197

LIST OF FIGURES

Fig. 1-1. Applications of mist spraying systems in different places. (a) Paris, France, (b) Kumagaya station, Japan, and (c) Roppongi, Tokyo, Japan. 23

Fig. 1-2. Overall research flow of proposal of new environmental indices in outdoor and mist spraying environments for thermal environment evaluation..... 28

Fig. 2-1. Schematic diagram and thermal resistance network model of two-node model. 37

Fig. 2-2. The schematic diagram and thermal network model of three-node model. 37

Fig. 2-3. The schematic diagram of 65-node model. 38

Fig. 3-1. Scene of (a) preliminary experiment (b) and concept diagram. 42

Fig. 3-2. Subjects' characteristics of age, height, and clothing insulation level. 44

Fig. 3-3. Tablets for survey research..... 44

Fig. 3-4. Probability density of the standard normal distribution $N(\mu, \sigma^2)$ of survey results before and after entering the mist spraying environment. Left is mTSV and right is CSV. ... 46

Fig. 3-5. Response rate results of mTSV (left) and CSV (right) before and before and after entering the mist spraying environment. 47

Fig. 3-6. The survey results (mean ± SD) of different age groups and the probability value (*p*-value) by paired sample t-test analysis between young (10–20) and old (70+) age groups.... 48

Fig. 3-7. Outdoor air temperature and relative humidity during experiment. 48

Fig. 3-8. The results of acceptability before and after entering the mist spraying environment (n = 1,110) 49

Fig. 3-9. Cumulative distribution functions (CDFs) analysis of modified thermal sensation vote (mTSV) for each environmental index in mist spraying environment. 51

Fig. 3-10. Cumulative distribution functions (CDFs) analysis comfort sensation vote (CSV) for each environmental index in mist spraying environment. 53

Fig. 4-1. Overall research flow for comparison of outdoor and mist spraying environments and validation of physiological human model. 59

Fig. 4-2. Measurement setup for measuring environmental factors in outdoor and mist spray environments. (a) Inside the mist spraying environment, inside*: Ultrasonic anemometer, WBGT meter, infrared H_2O analyzer, and cyclone type thermometer. (b) internal** indicates shortwave and longwave radiation, WBGT meter, (c) outside** indicates shortwave and longwave radiation and direct solar radiation installed outside the mist spray environment, and (d) outside*: ultrasonic anemometer, WBGT meter, and infrared H_2O analyzer..... 62

LIST OF FIGURES

Fig. 4-3. Mist spraying system installed in Fujisawa city, Kanagawa, Japan (August 3–4 and September 5, 2017), (a) The top view of mist spraying system and the position of measuring instruments. (b) Overall view of mist spraying system. 63

Fig. 4-4. Cyclone-type thermometer installed in mist spraying environment with a height of 0.2 m, 1.1 m, and 1.7 m. (a) is cylindrical cyclone separator and (b) is air compressors. 64

Fig. 4-5. Calculation results comparison for estimation method in outdoor and mist spraying environment..... 66

Fig. 4-6. Schematic diagram of subject experimental protocol showing timetable. Environmental conditions for outdoor and mist spraying environments correspond to (outdoor*, outdoor**) and (indoor*, indoor**) in Fig. 4-3. 67

Fig. 4-7. Points of measurement for calculation of overall skin temperature (this figure is referenced by a study by Choi et al. [87]). 68

Fig. 4-8. Environmental factor differences between outdoor and mist spraying environments during experiment. Outdoor environment and mist spraying environment correspond to (outside*, outside**), and (inside*, inside**) in Fig. 4-3, respectively. 70

Fig. 4-9. Results of infrared camera image of subjects. Left and right figures correspond to before and after entering mist spraying environment, respectively. 71

Fig. 4-10. Thermal manikin in climate chamber (naked (a), and clothed (b)). 72

Fig. 4-11. Results of changes in mean skin and core temperature before and after entering mist spraying environment. The environmental conditions before and after the mist correspond to the results of (outside*, outside**) and (inside*, inside**) in Fig. 4-3, respectively. 76

Fig. 4-12. Mean skin and core temperature change results for each mTSV scale. 78

Fig. 4-13. Mean heat losses and physiological responses change results for each mTSV scale. 79

Fig. 5-1. Mist spraying system installed at the Institute of Industrial Science of the University of Tokyo, Japan (July 23–August 4, 2018): (a) overall appearance of the mist spraying system; (b) a top view of the mist spraying system and the location of instruments; (c) Mist spraying generators (i.e. pressure pumps, water tanks and control devices). 88

Fig. 5-2. Equipment for measuring environmental factors in outdoor and mist spraying environments. (a) inside** representing shortwave and longwave radiation, direct solar radiation, and ultrasonic anemometers; inside* representing infrared H_2O analyzers and air temperature and humidity sensor; (b) displays air temperature and humidity sensor, shortwave and longwave radiation meters, ultrasonic anemometers, infrared H_2O analyzers installed outside, and (c) showing air temperature and humidity sensors in inside*. 89

Fig. 5-3. Schematic diagram of subject experimental protocol showing timetable. Experimental conditions for outdoor and mist spraying environments correspond to (outside) and (inside*, inside**) in Table 5-1b**,** respectively. 91

Fig. 5-4. Schematic diagram of heat loss on body surface by skin wettedness and mist wettedness. 93

LIST OF FIGURES

Fig. 5-5. Design of heating globe thermometer for measuring mist wettedness. 94

Fig. 5-6. Mist wettedness meter and its controller. 95

Fig. 5-7. Schematic diagram of measuring mist wettedness using heating globe thermometer. Heating globe thermometer and globe thermometer are placed in wetted and non-wetted areas inside mist spraying environment, respectively. 96

Fig. 5-8. Results of environmental factors (mean ± SD) in outdoor and mist spraying environment for operation modes. 99

Fig. 5-9. Existing environmental indices in outdoor environment and mist spraying environments (gap is difference of result of outdoor and mist spraying environments). 102

Fig. 5-10. Additional experiment was conducted with 20 cm scaffoldings, and subjects were stood on there during experiment (n = 5). 103

Fig. 5-11. Thermal sensation and thermal comfort results in outdoor and mist spraying environments for different operation mode of mist spraying system. 104

Fig. 5-12. Thermal sensations (mTSV, and TSV) and thermal comfort results in outdoor and mist spraying environments. (outdoor: before entering the mist spraying system, $mist_3$: 3 min. after entering the mist spraying system, $mist_{10}$: 10 min. after entering mist spraying environment) 106

Fig. 5-13. Changes in Individual thermal sensations (mTSV and TSV) and thermal comfort (CSV) in outdoor and mist spray environments. 107

Fig. 5-14. The mean of overall skin temperature and 95% CI variations with different operating conditions for the mist spraying system. 110

Fig. 5-15. Skin temperature changes in each body segment after entering the mist spraying environment. 111

Fig. 5-16. Correlation between air temperature and TSV in outdoor and mist spraying environments. 113

Fig. 5-17. Correlation between overall skin temperature and thermal sensations (mTSV and TSV). Pearson's correlation coefficient (r) and probability value (p) are represented. 114

Fig. 5-18. Correlation analysis of survey results. Pearson's correlation coefficient (r) and probability value (p) are represented. 116

Fig. 5-19. Correlation between thermal sensations (mTSV and TSV). Pearson's correlation coefficient (r) and probability value (p) are represented. 117

Fig. 5-20. Results of UTCI and mean TSV in outdoor and mist spraying environments. 118

Fig. 5-21. Correlation between air temperature and TSV in outdoor and mist spraying environments. 119

Fig. 5-22. Comparison with other outdoor thermal comfort studies. 121

LIST OF FIGURES

Fig. 6-1. Result of environmental conditions in the experiment (mean and 95% CI [confidence interval], n = 58). (a) air conditioning room, (b) outdoor environment, and (c) mist spraying environment..... 129

Fig. 6-2. Schematic diagram and thermal resistance network diagram of physiological thermal model considering mist wettedness. (a) 2NM with mist wettedness (b) 3NM with mist wettedness. (Thermal resistance, which affects heat transfer and evaporative heat loss is not the same, but it was simplified as a total resistance for easy understanding.) 130

Fig. 6-3. Evaporative heat loss concepts by skin wettedness and mist wettedness..... 135

Fig. 6-4. Comparison of results of overall body skin temperature by experiment (n = 65) and prediction (n = 58), (b) is for outdoor environment, and (c) is for mist spraying environment. 137

Fig. 6-5. Comparison of the results of heat loss by radiation, convection, evaporation on the human body in outdoor and mist spraying environments considering mist wettedness. 138

Fig. 6-6. Skin temperature variations for the effectiveness area factor of evaporative heat loss by mist wettedness. 140

Fig. 6-7. Comparison of the results of heat loss by radiation, convection, evaporation on the human body in outdoor and mist spraying environments considering mist wettedness and effectiveness area factor (the parentheses value is each heat loss percentage (%) for the total heat loss). (a): Ratio of heat loss causes to total heat loss for effectiveness area factor (2NM), (b): Ratio of heat loss causes to total heat loss for effectiveness area factor (3NM), (c): Results of heat loss causes in outdoor and mist spraying environments (2NM), and (d): Results of heat loss causes in outdoor and mist spraying environments (3NM)..... 142

Fig. 7-1. Overall research flow for proposing new environmental index. 147

Fig. 7-2. Heat loss in outdoor and mist spray environments (10 minutes). The statistically significant differences between outside and inside the mist spraying environment was analyzed by paired t-test..... 149

Fig. 7-3. Correlation between heat storage rate and mTSV (n is 72 for outdoor environment and 60 for mist spraying environment, r is the Pearson's correlation coefficient, and p is probability value). 150

Fig. 7-4. Correlation between heat storage rate and mTSV (n is 294 for outdoor environment and 231 for mist spraying environment, r is the Pearson's correlation coefficient, and p is probability value). 151

Fig. 7-5. Concept of SET** index considering skin wettedness and mist wettedness..... 152

Fig. 7-6. Correlation between results of SET* and SET** in outdoor and mist spraying environment..... 153

Fig. 7-7. Correlation results of mTSV to SET* and SET**. 154

Fig. 7-8. Correlation results of TSV to SET* and SET**. 155

Fig. 7-9. Correlation between heat storage (PMV method) and thermal sensations (mTSV and TSV) in outdoor environment and mist spraying environments. 156

Fig. 8-1. Summary of research flow. 161

LIST OF TABLES

Table 1-1. Maximum possible temperature drop due to mist spraying system. 24

Table 2-1. Environmental indices related to thermal comfort (refer to [28]) 32

Table 2-2. PET and UTCI equivalent air temperature categories in terms of thermal stress [45–47]. 33

Table 2-3. Risk level of heat disorders by Japan Amateur Sprots Association (1994) 35

Table 3-1. Measurement in preliminary research. 43

Table 3-2. Subjects characteristics. 44

Table 3-3. Survey scale in questionnaire. 45

Table 3-4. Calculation of *P* of mTSV and CSV. 50

Table 3-5. Results of each *P* distribution relevant to thermal sensation votes. 52

Table 3-6. Results of each *P* distribution relevant to thermal comfort votes. 54

Table 4-1. Field experiment of mist spraying system for the verifiacation of two-node model. 61

Table 4-2. Measurement for outdoor and mist spraying environment. 63

Table 4-3. Angular factor (F_i) between a person and surrounding surfaces. 66

Table 4-4. Characteristics of subjects 67

Table 4-5. Overall skin temperature calculation equations proposed by various researches. 69

Table 4-6. Experiment condition for determining clothing insulation level. 72

Table 4-7. Result of thermal manikin experiment for comfirming clothing insulation level. 74

Table 4-8. Calculation conditions of 2NM for validation of skin temperature. 75

Table 4-9. Calculation conditions of 2NM for comparison with thermal sensation results. 77

Table 5-1. Operation modes of mist spraying system. 86

Table 5-2. Measurements for mist wettedness. 87

Table 5-3. Characteristics of subjects. 91

Table 5-4. Measurements for mist wettedness. 94

Table 5-5. Environmental factors in outdoor and mist spraying environments. 101

LIST OF TABLES

Table 5-6. The results of environmental factors in additional experiment. 104

Table 5-7. Environmental factor results in outdoor and mist spraying environments. (baseline: standard condition, without air blowing: mist only, less mist: less amount of mist spray, without mist: air blowing only). 108

Table 5-8. Statistical analysis of effects of operation modes on thermal sensations and thermal comfort. Statistical significance was confirmed by probability value (*p*-value) in paired t-test. (CASE-1: baseline, CASE-2: without air blowing, CASE-3: less mist, CASE-4: without mist) 109

Table 5-9. The mean and 95% CI of the changes in skin temperature of each body segment before and after entering the mist spraying environment. 112

Table 5-10. Calculation conditions of 2NM in maximum possible temperature drop condition by mist spraying system. 113

Table 5-11. Mean and 95% CI of the changes in skin temperature of each body segment before and after entering mist spraying environment. 115

Table 5-12. Comfort temperature and mean air temperature in outdoor and mist spraying environments 120

Table 6-1. Environmental factors for calculation of heat loss causes in outdoor and mist spraying environments using 2NM and 3NM. 138

Table 6-2. The evaporative heat losses in 2NM and 3NM. 139

Table 6-3. Environmental factors for calculation of heat losses causes in outdoor and mist spraying environments using 2NM and 3NM. 141

Table 7-1. Utilized number of data for O-PMV index. 150

Table 7-2. Comparison of three different environmental indices. 157

Table 7-3. Summary of proposed new indices for outdoor and mist spraying environments .. 158

NOMECLATURE

Variables

A: surface area of globe thermometer (m^2)

A_D: surface area of human body (m^2)

A_{sk}: wetted surface area by natural diffusion and sweating (m^2)

A_{mist}: additional wetted surface area by mist droplets (m^2)

C: convective heat loss from clothed surface of the body (W m^{-2})

$c_{p,air}$: specific heat of air (1.005 kJ kg^{-1} K^{-1}),

C_g: heat capacity of globe thermometer (J K^{-1})

$C_{p,body}$: specific heat of human body (3500 J kg^{-1} K^{-1})

$C_{p,bl}$: specific heat of blood (4190 J kg^{-1} K^{-1})

C_{re}: sensible heat loss by respiration (W m^{-2})

Clo: clothing level (1 Clo = 0.155 m^2 K W^{-1})

D: diameter of globe thermometer (m)

E_{diff}: evaporative heat loss by natural diffusion of vapor from skin (W m^{-2})

E_{max}: maximum evaporative heat loss when the surface is completely wet (W m^{-2})

E_{mist}: latent heat loss by mist droplets on surface of body (W m^{-2})

E_{rsw}: evaporation heat loss by regulatory sweating (W m^{-2})

E_{sk}: latent heat loss by regulatory sweating and natural diffusion of vapor from skin (W m^{-2})

F: angular factor between a person and the surrounding surfaces

f_{clo}: ratio of clothing area to the body surface area

f_{eff}: effective area factor by radiation, 0.87 (-)

f_p: body's projected area factor by direct solar radiation (-)

f_r: the effective radiation area factors for the whole body

G: Griffiths constant

H: heat input into the heating globe thermometer (W)

h_c: convective heat transfer coefficient on surface (W m^{-2} K^{-1})

h_e: evaporative heat transfer coefficient for the outer air layer of a bared or clothed body (W m^{-2} kPa^{-1})

h_o: total heat transfer coefficient in a standard environment (W m^{-2} K^{-1})

h_r: radiative heat transfer coefficient on surface (W m^{-2} K^{-1})

I_{dH}: diffuse solar radiation on a horizontal surface ($S\downarrow - I_{dN} \cdot sin\beta$, W m^{-2})

NOMECLATURE

I_{dN}: direct solar radiation on a normal surface (W m^{-2})

K: effective conductance between core and skin (5.28 W m^{-2} K^{-1})

L: longwave radiation flux (W m^{-2})

$L\downarrow$: downward longwave radiation (W m^{-2})

$L\uparrow$: upward longwave radiation (W m^{-2})

L_{water}: specific latent heat loss of water (2264 kJ kg^{-1})

LR: coefficient of Lewis relation (16.5 K kPa^{-1})

M: metabolic heat production (W m^{-2})

m: total mass of body (kg)

$\dot{m}_{\mathrm{bl}}$: peripheral blood flow rate (L s^{-1} m^{-2})

m_{water}: water mass of vaporization (kg).

n: population, number of samples

Nu: Nusselt number

Pr: Prandtl number (e.g. approximately 0.707 at 27 °C air)

p: probability value

p^*: saturated water vapor pressure (kPa)

p^*_{gh}: saturated water vapor pressure at surface temperature of heating globe thermometer (kPa)

p_{air}: partial water vapor pressure in air (kPa)

p_{mist}: partial water vapor pressure in mist spraying environment (kPa)

Q: amount of energy (kJ)

Q_{conv}: convective heat transfer from skin (W m^{-2})

$Q_{\mathrm{core-sk}}$: heat transfer from core to skin (W m^{-2})

Q_{rad}: radiative heat transfer from skin (W m^{-2})

Q_{res}: heat loss by respiration (W m^{-2})

r: Pearson's correlation coefficient

R_{a}: thermal resistance at outer boundary (skin or clothing) (kPa m^2 W^{-1})

$R_{\mathrm{e,clo}}$: evaporative heat transfer resistance of clothing (kPa m^2 W^{-1})

R_{total}: total insulation (kPa m^2 W^{-1})

Re: Reynolds number

RH: relative humidity (%)

S: shortwave radiation flux (W m^{-2})

$S\downarrow$: downward shortwave radiation (W m^{-2})

$S\uparrow$: upward shortwave radiation (W m^{-2})

S_{core}: heat storage rate in core node (W m^{-2})

S_{sk}: heat storage rate in skin node (W m^{-2})

NOMECLATURE

S_{body}: heat storage rate in human body (W m^{-2})

S_{str}: mean radiant flux density on a human body (W m^{-2})

T: temperature (°C)

T_a: air temperature (°C)

ΔT_{air}: air temperature changes by vaporization of water

T_c: comfort temperature (°C)

T_{clo}: clothing surface temperature (°C)

T_{core}: core temperature of human body (°C)

$T_{core,n}$: core temperature of human body at physiological thermal neutral condition (36.8 °C)

t_{eq}: equivalent temperature

T_g: inside temperature of globe thermometer (°C)

T_{gh}: inside temperature of heating globe thermometer (°C)

T_{mist}: air temperature inside mist spraying environment (°C)

T_{mrt}: mean radiant temperature (°C)

T_{sk}: skin surface temperature (°C)

$T_{sk,n}$: skin surface temperature at physiological thermal neutral condition (33.7 °C)

T_{wet}: wet-bulb temperature (°C)

V_{air}: unit volume of air (m^3)

v: airspeed (m s^{-1})

W: external work (W m^{-2})

Greek letters

α: albedo on surface of globe thermometer (0.06)

α_k: absorptivity of the clothed human body by the shortwave radiation (0.7)

α_{sk}: mass fraction of skin compartment of human body

β: solar altitude

ε: longwave radiation emissivity (0.77)

k: thermal conductivity of air (e.g. 26.3×10−3 W m^{-1} K^{-1} at 27 °C)

λ: area ratio of bared body segments to total surface area of the body

μ: mean

μ_{mass}: mass ratio of the bared segments for the total mass of the body

ν: kinematic viscosity of air at atmospheric pressure (e.g. 15.89×10^6 m^{-2} s^{-1} at 27 °C)

ρ_{air}: density of air (1.2 kg m^{-3}),

ρ_{bl}: density of blood (1.06 kg L^{-1})

σ: Stefan-Boltzmann constant (5.67 × 10^{-8} W m^{-2} K^{-4})

ω_{sk}: skin wettedness

ω_{mist}: mist wettedness

Subscripts

all: overall value

bare: bared node in 3NM

clo: clothed node in 3NM

n: physiological thermal neural condition

Abbreviations

2NM: two-node model

3NM: three-node model

ASHRAE: American Society of Heating, Refrigerating and Air-Conditioning Engineers

BMI: body mass index

CI: confidence interval

CSV: comfort sensation vote

MEMI: Munich Energy-balance model for individuals

mTSV: modified Thermal Sensation Vote

O-PMV: outdoor predicted mean vote

OUT-SET*: outdoor standard effective temperature

PET: physiological equivalent temperature

PMV: predicted mean vote

SD: standard deviation

SET*: standard effective temperature

TSV: thermal sensation vote

UCB model: UC-Berkeley thermal comfort model

UTCI: universal thermal climate Index

WBGT: wet-bulb globe temperature

ABSTRACT

This thesis focuses on how to evaluate human's thermal sensation in mist spraying outdoor environments. The aim of this thesis is to clarify the thermal effects of the mist spraying outdoor environment on a human body and evaluate thermal sensation by proposing a method to predict the thermal state of the human body in these environments.

In recent years, a mist spraying system has been widely used to mitigate the fatal heat disorder of an outdoor environment during the summer season. Many studies reported that cooling effects by mist spraying are effective to improve the human's thermal sensation and thermal comfort. However, these results were mainly obtained through a survey research method, and there is a lack of quantitative understanding of the thermal effects of sprayed mist. Moreover, experimental studies in this field are limited since most of them are focusing on the measurement of two basic environmental factors such as temperature and humidity. A comprehensive investigation into mist spraying environments by measuring overall environmental factors is insufficient.

A field experiment of the mist spraying system has difficulty since it must be proceeded in outdoors in sunny days during the summer season, and the influence of the outdoor environmental factors on the human body is non-uniform and complex. For these reasons, it is difficult to clearly identify how the sprayed mist particles affect the human's thermal sensation and thermal comfort. Therefore, in the present study, experiments were conducted gradually for every summer for three years to measure the variations of overall environmental factors (temperature, radiation, humidity, and airspeed) due to mist particles in an outdoor environment, and the impact of these variations of environmental factors on improving thermal sensation and thermal comfort was evaluated. Moreover, the thermal state of the human body was investigated by measuring skin temperatures. Based on the experimental results, the physiological human model was developed which could predict the thermal state of the human body in outdoor and mist spraying environments well, and the environmental index was proposed to evaluate the thermal sensation using the prediction model.

The first experiment was conducted as a preliminary study. The effects of the mist spraying system on the human's thermal sensation and thermal comfort and the suitability of the existing environmental indices were examined. Specifications including outline, results, and analysis of the preliminary experiment are described in Chapter 3, and the details are as follows.

Evaluation of thermal sensation based on survey results and suitability existing environmental indices (Chapter 3)

1) Survey on variations in thermal sensation and thermal comfort between outdoor and mist

spraying environment (n = 1,110)

2) Examine the feasibility of conventional environmental indices (SET*, PET, WBGT, and UTCI) by measuring four environmental factors (temperature, radiation, humidity, and airspeed) in mist spraying environment

In the preliminary experiment, survey results showed that the subject's thermal sensation and thermal comfort were improved after they experienced the mist spraying environment. However, based on these survey results, the improvement level of the human's thermal sensation under certain environmental conditions cannot be grasped, and conventional environmental indices cannot be utilized to reflect the human's thermal sensation in the mist spraying environment appropriately. In order to solve this problem, not only the environmental factors of the mist spraying environment but also the skin temperatures of the subjects were measured through the second experiment. Based on the results from the second experiment, the validity of the prediction model to predict the physiological response of the human body was investigated. In addition, a correlation between the reported thermal sensation in the survey and the predicted results from the physiological model was analyzed to propose an evaluation method of human's thermal sensation which can be appropriately utilized in the outdoor and mist spraying environment. Further details are described in Chapter 4 including the following details:

Evaluation of mist spraying environment considering human's physiological responses (Chapter 4)

1) Survey of human's thermal sensation and thermal comfort in outdoor mist spraying environment (n = 12)
2) Measurement of environmental factors (temperature, radiant temperature, humidity, wind speed) in outdoor and mist spray environments and verification of the evaporative cooling effect of mist spraying system
3) Investigation of the thermal state of human body in outdoor and mist spraying environment by measuring the skin temperature
4) Prediction of skin temperature using measured environmental factors and two-node model, and verification of its feasibility by comparing with experimental results (Chapter 4)
5) Proposal of the new index (outdoor predicted mean vote (O-PMV)) to estimate human's thermal sensation in outdoor and mist spraying environment based on the correlation analysis between the reported thermal sensation in the survey and the predicted results from the physiological model (Chapter 7)

As a result of the second experiment, it was found that the skin temperature of the human body in the outdoor and mist spraying environment can be predicted with high accuracy by using the conventional two-node model. However, because of the deficient number of subjects participated in

the experiment, it was difficult to generalize this given fact.

As in Experiment 2, the skin temperature was well predicted under the shaded mist spraying environment condition, but there is a difficulty in predicting the skin temperature under non-shaded mist spraying environments. Moreover, the subjects reported that the mist spraying environment felt cooler than the outdoor environment under the same condition of heat load. Therefore, it was necessary to examine the influence of another environmental factor other than the basic four environmental factors (temperature, radiant temperature, humidity, airspeed). Since it is not known how much the evaporative heat loss at the human body surface caused by mist particles (mist wettedness) contributes to the cooling effect of the mist spraying system, an additional experiment was conducted to clarify this. In Chapter 5, the detailed overview, methodology, results, and analysis from the additional field experiment to consider the mist wettedness are described as follows.

Evaluation of mist spraying environment considering mist wettedness (Chapter 5)

1) Survey of human's thermal sensation and thermal comfort in outdoor and mist spraying environments according to the different operating conditions of mist spraying system (n = 65)
2) Examination of subjects' skin temperature variations according to the different operating conditions of the mist spraying system (n = 65)
3) Verification of the cooling effect of the mist spraying system by measuring the environmental factors in outdoor and mist spraying environments.
4) Proposal for the mist wettedness measurement method and its measurement.
5) Development of prediction model to predict a human's physiological response considering mist wettedness and its prediction accuracy by comparing with experimental results.

By suggesting an appropriate measuring method, the prediction model to predict human's physiological response was possible to be improved considering a mist wettedness. As a result of the developed prediction model considering the factor of mist wettedness, the skin temperature of the human body surface in outdoor and mist spraying environment could be estimated more accurately compared to the conventional prediction model, with a small temperature error of 0.5 °C between the experimental data. In conclusion, in outdoor environments, heat loss due to sweating was shown as 90% of total heat loss and it was the largest contributor. In mist spraying environments, convective heat loss due to the temperature drop was the largest, and the heat loss due to the mist wettedness was the second contributor which was shown to be 30%. Given this fact, it was found that the mist wettedness was the major environmental factor in the mist spraying environment.

In conclusion, based on the results of the three-step field experiment and its analysis, this thesis proposes the following three methods to clearly evaluate the human's thermal sensation in outdoor and mist spraying environments (Chapter 7).

ABSTRACT

1) Evaluation method using the correlation analysis between the heat load of the human body and the thermal sensation reported by the subject (O-PMV)
2) Evaluation method using prediction of human physiological response considering mist wettedness (SET**)
3) Evaluation method using correlation analysis between heat load using PMV calculation and thermal sensation reported by the subject (modified predicted mean vote (mPMV))

Chapter 1. Introduction

Chapter 1. Introduction

1.1. Fundamental of mist spraying system

The mist spraying system can mitigate the heat stress in outdoor hot environment. It utilizes the evaporation heat loss to cool down the outdoor air temperature by spraying the mist droplets in the air. High cooling effects with less water evaporation can be expected by using mist spraying systems. The evaporation of 1 g of water has the capacity to drop the 1 m^3 of air by 1.53 °C (Equation (1-1)).

$$Q = \rho_{\text{air}} V_{\text{air}} c_{\text{p,air}} \Delta T_{\text{air}} = L_{\text{water}} m_{\text{water}} \quad (1\text{-}1)$$

where Q is an amount of energy, ρ_{air} is density of air (1.2 kg m^{-3}), V_{air} is unit volume of air, $c_{\text{p,air}}$ is the specific heat of air (1.005 kJ kg^{-1} K^{-1}), and ΔT_{air} is the air temperature changes by vaporization of water. The L_{water} is a specific latent heat loss of water (2264 kJ kg^{-1}) and m_{water} is the water mass of vaporization in kg. Therefore, the mist spraying system is widely utilized in numerous outdoor places to mitigate a fatal heat disorder during the hot summer season as shown in Fig. 1-1.

(a) (b) (c)

Fig. 1-1. Applications of mist spraying systems in different places. (a) Paris, France, (b) Kumagaya station, Japan, and (c) Roppongi, Tokyo, Japan.

However, evaporative heat loss of water is proportional to the vapor pressure differences between the surface of the water and in the air as expressed in Equation (1-2). Therefore, the evaporation phenomenon does not occur when the partial water vapor pressure in the air exceeds the saturated vapor pressure of the water surface. Thus, the amount of evaporation of water cannot be increased

infinitely. In addition, the high relative humidity can make the human feel warmer and discomfort in hot environment.

$$E = \mathrm{LR}\, h_c\, (p^*_{\mathrm{water}} - p_{\mathrm{air}}) \quad (1\text{-}2)$$

where LR is the coefficient of Lewis relation (16.5 kg/kPa), p^*_{water} is the saturated water vapor pressure at surface temperature of water, and p_{air} is the partial water vapor pressure in the air.

As an example, maximum possible temperature drop due to evaporative cooling of mist spraying system can be obtained as shown in Table 1-1. The outdoor environment conditions were considered the average value obtained from the experiment. Evaporation heat loss due to mist spraying can be gained until relative humidity reaches 100% (i.e. adiabatic saturation process [1]). Air temperature is gradually lowered by mist evaporation and when air temperature drops to the maximum, it corresponds to the wet-bulb temperature. The air temperature can be lowered to the maximum by 6.2 °C when the outdoor temperature is 32.9 °C and the relative humidity is 58.7%.

Table 1-1. Maximum possible temperature drop due to mist spraying system.

Environmental factor	Outdoor environment*	Maximum
Air temperature T_a (°C)	32.9	26.7
Relative humidity RH (%)	58.7	100
Absolute humidity (g/kg DA)	18.57	22.28
Mean radiant temperature T_{mrt} (°C)	36.8	-
Airspeed v (m/s)	0.41	-

*Note: mean outdoor environment condition obtained from field experiment.

1.2. Literature review of mist spraying system

The recent increase in abnormal weather has led to an increase in human health and mortality due to extremely cold and hot weather [2–5]. Therefore, a variety of attempts have been made to prevent heat stress and heat disorder in the summer hot environment, such as blocking direct sunlight using a sunshade, utilizing highly reflective paint in roads and buildings, and using hand fans. In particular, the method of utilizing a mist spraying system to cool down the air temperature of the outdoor wide environment has been widely used. Basic research on the mist spraying system has been conducted to understand the thermal effects on the thermal environment and on the human body. For example, Mugele and Evans (1951) studied the mist spray distribution for various mist sizes [6]. Barrow and Pope (2007) performed a simple theoretical assessment of the evaporation time and travel distance of

spraying water in spray systems [7]. Numerical simulations have been developed to predict the heat and mass transfer of mist spraying systems, and the results confirm that outdoor air temperatures can drop to 9 °C during the dry summer season [8]. Three-dimensional numerical analysis to predict the cooling effect of the mist spraying system confirmed that the mist droplet size and air velocity were very important factors in the evaporation phenomenon [9].

Dry-mist spraying system was developed as a way to control heat island in outdoor environment [10]. The mean daily outdoor temperature was decreased up to 2 °C by mist spraying system. Previous studies in mist spraying experiments have shown that outdoor environments can reduce air temperatures by up to 5–7 °C when the air temperature was 35 °C with 50% relative humidity [11,12]. There were other studies that noted changes in outdoor air temperature and humidity [13,14], but these studies did not investigate the overall environmental factors of the thermal environment. Therefore, the thermal effects of the mist spraying system on the human body could not be fully understood. Farnham et al. attempted to understand the thermal effects of the mist spraying system on the human body by measuring the heat loss at the surface of a heated device that mimics the human body in a mist spraying environment [15]. In addition, the cooling effect of the mist spraying system was confirmed by measuring a skin temperature change of the arm before and after entering the mist spraying environment. The result showed a skin temperature drop to 1–3 °C within 10 seconds. However, studies on overall skin temperature have not been conducted.

Thermal sensation and thermal comfort are closely related to the four basic environmental factors: temperature, radiation, humidity, and airspeed, but so far, no overall review of basic environmental factors has been conducted in mist spraying environments. In addition, it is important to understand a heat exchange phenomenon with a thermal environment due to a physiological reaction of a human body in a hot environment such as an outdoor environment and a mist spraying environment. However, there have not been studied on human physiological responses in mist spraying environments.

In order to easily understand the thermal environment, the evaluation method using environmental index is widely used, but evaluation in an environment in which complex and non-uniform environmental factors exist, such as an outdoor environment, requires many challenges. Recently, as the research on the comfort of the outdoor environment has increased, environmental indices such as SET*, PET, and UTCI have been widely used. However, few attempts have been made to evaluate the thermal sensation using these environmental indices in a mist spraying environment [16,17].

1.3. Current issues

First, as the previous researches were focused on temperature and relative humidity changes by mist spraying system, studies on the thermal influence of the mist spraying environment on the human body, particularly with the overall consideration of influenceable thermal environmental factors, are lacking.

Therefore, it is necessary to verify the influence of the mist spraying system on thermal sensations and environmental factors in the outdoor environment by comparing environmental factors internal and external of mist spraying environment, including air temperature, humidity, radiation, and airspeed.

Thus, though thermal sensations in outdoor and mist spraying environment had been investigated in several studies, overall environmental factors had not been measured simultaneously. Therefore, it's hard to understand the degree of improvement in thermal sensing and thermal comfort after entering the mist spray environment at a given environmental condition.

Second, even if the overall environmental factors were measured in the outdoor and mist spray environment, it was not examined whether the existing environmental indices properly reflected the thermal sensations in the mist spray environment.

Third, the human body surface may wet by mist droplets, evaporative heat loss occurs on surface of the body. However, this evaporative heat loss cannot be captured by measuring basic four environmental factors (air temperature, radiation, humidity, and airspeed). In addition, the evaporative heat loss on the body surface by mist droplet has not been investigated. Therefore, understanding heat exchanges between mist spraying environments and the human body are insufficient.

Fourth, surveys that correspond to subjective evaluation were conducted in several studies. In addition, skin temperature changes in body parts have been performed the other studies. However, the whole skin temperature changes which can understand the overall thermal influences of the body by mist spraying environment has not been investigated yet.

Overall skin temperature changes in outdoor and mist spraying environments give information on the thermal effects of mist spraying environment on the human body. In addition, the comparative analysis of over skin temperature with thermal sensations and environmental factors is expected to provide a clue to evaluate the thermal sensation in outdoor and mist spraying environments.

1.4. Overall objectives of present thesis

The overall research flow of the present study is shown in Fig. 1-2. The first field experiment of the mist spraying system conducted in the plaza near Shimbashi Station in the summer of 2016. In Chapter 3, the results of the mist spraying system's effects on thermal sensation and thermal comfort with an enough subject are explained. In addition, the applicability of existing environmental indices in the mist spraying environment had been analyzed. However, since the insufficient data of outdoor environmental factors, the cooling effects of the mist spraying system could not understand, and not possible to grasp the degree of improvement of thermal sensations for the weather conditions.

In 2017, an additional mist spraying system experiment conducted at Fujisawa, Japan (Chapter 4). Environmental factors both outdoor and mist spraying environments were measured to investigate the cooling effects of the mist spraying system. The mist spray system was designed with the concept of

a bus stop, and sunlight was blocked by a sunshade. In addition, not only thermal sensations and thermal comforts but skin temperatures were also additionally measured as objective evidence. Though the physiological human model showed accurate predictions in the well-controlled climate chamber laboratory, there were not enough studies on whether the physiological human model predicted well even under complex thermal environmental conditions such as outdoor and mist spraying environments. Moreover, based on the prediction model, we investigated the thermal state of a human body that can be predicted well in outdoor and mist spraying environments, and explain its comparison results with thermal sensations and environmental factors.

Since there were not enough subjects to participate in the 2017 experiment, the 2018 experiment ensured a sufficient number of subjects and collected the results of thermal sensations, environmental factors, and skin temperatures (Chapter 5). Besides, we devised a way to measure the heat loss of evaporation (mist wettedness) on the human surface that presents in mist spraying environments.

Next, we developed a human physiological response human model considering mist wettedness (Chapter 6). Existing physiological models could not be applied to the mist spray environment because only the basic four environmental factors (air temperature, radiation temperature, humidity, and airspeed) were considered. Therefore, we developed a physiological human model that can utilize the mist wettedness obtained from the experiment and compared the results with the measured skin temperature changes to confirm the validity of the predictive model.

As a final step, environmental indices to evaluate the thermal sensations in mist spraying environments were proposed in Chapter 7.

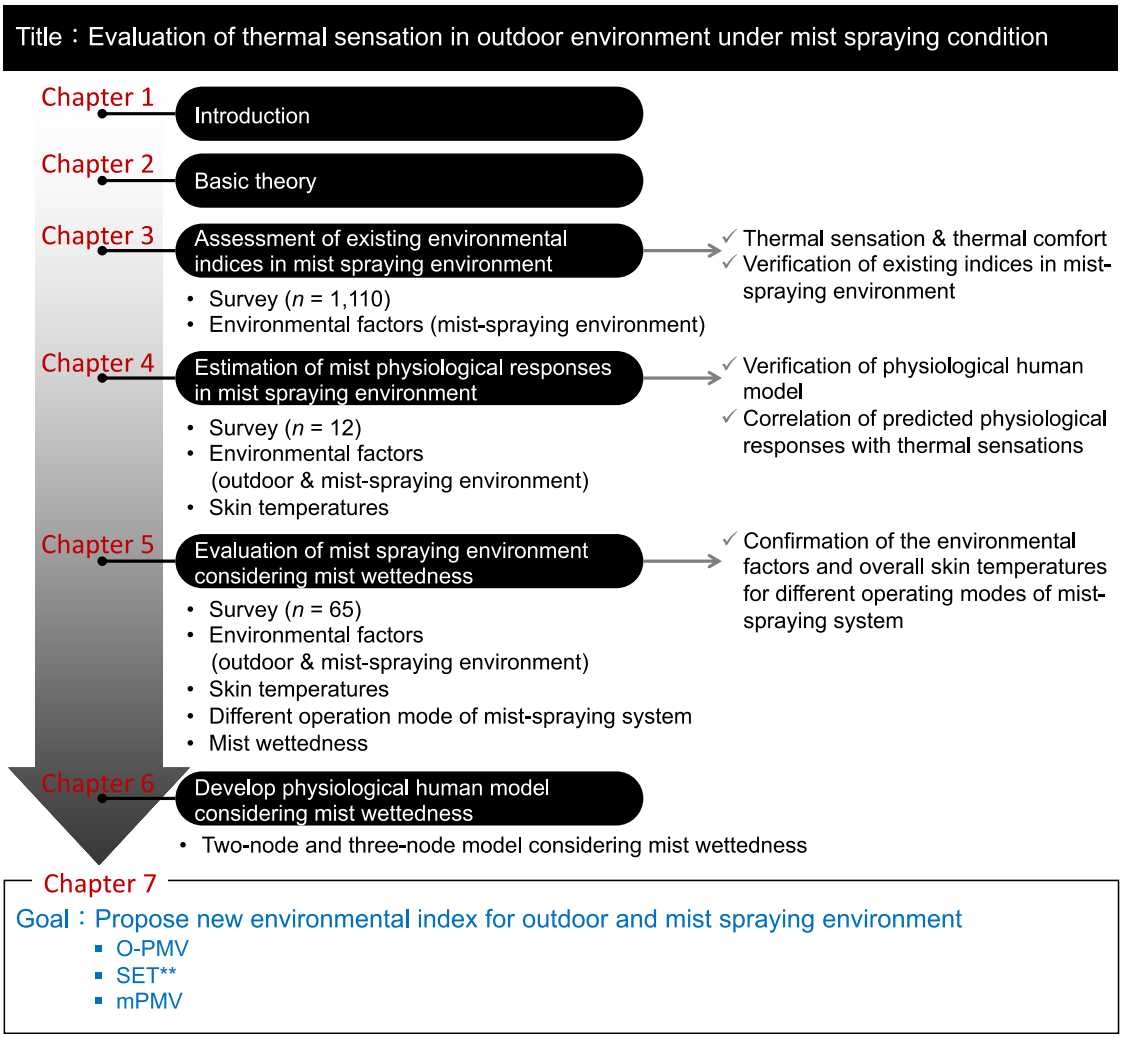

Fig. 1-2. Overall research flow of proposal of new environmental indices in outdoor and mist spraying environments for thermal environment evaluation.

Chapter 2. Basic theory

Chapter 2. Basic theory

2.1. Environmental index for evaluating thermal environment

In order to evaluate the thermal environment and estimate human's thermal sensation and thermal comfort, numerous kinds of thermal comfort indices have been proposed. Using these indices, the thermal interaction between a human body and the thermal environment is understandable (see Table 2-1). Fanger suggested the Predicted Mean Vote (PMV) and Predicted Percentage of Dissatisfied (PPD) to assess the thermal sensation and thermal comfort inside indoor environment. These indices were developed based on the correlation between survey results and the heat storage rate on a human body. Since Fanger's model does not consider the physiological responses, unpredictable results can be shown when it was applied to extreme environmental conditions, unlike in a near comfort thermal environment. By the way, the two-node model (2NM) considers the physiological responses such as sweating, blood flow regulation, and shivering in response to the thermal environment. Gagge et al. implemented this 2NM and compared the skin and core temperatures of the human body to verify its prediction accuracy and whether this model could properly evaluate the thermal state of the body. They suggested the Standard Effective Temperature (SET*) based on the 2NM.

By the way, since these proposed indices were mainly developed for indoor environment and validated in a climate chamber with the stable environmental condition, it is difficult to apply these indices to the outdoor environment. Recently, to extend the thermal comfort indices for the outdoor environment, Universal Thermal Climate Index (UTCI) [18] and Outdoor Standard Effective Temperature (OUT–SET*) [19] have been proposed to consider the effects of complex radiation environments on the human body. The wet-bulb globe temperature (WBGT) index was developed by Yaglou and Minard [20] and has been widely utilized for the analysis in thermal comfort assessment over 60 years [21]. Also, Höppe introduced the Physiological Equivalent temperature (PET) based on the Munich Energy-balance Model for Individuals (MEMI) considering thermo-physiological regulatory processes [22], and the calculation of PET index was revised by Walther and Goestchel, recently [23]. Some studies have applied the existing thermal comfort indices in outdoor environments to understand the effects of the outdoor environment on humans. Sharmin et al. confirmed the relationship between physiological equivalent temperature (PET) and sensation of pedestrians [24]. Sen and Nag studied the thermal susceptibility in a tropically hot and humid environment using existing environmental indices (e.g. PET, SET*, and PMV) [25]. Li et al. investigated the applicability of UTCI index to explore thermally comfortable conditions in an outdoor environment [26].

In mist spraying environment, it is difficult to measure environmental factors due to the presence of mist particles, and also, the thermal interactions between the human body and the mist spraying

environment have not been clearly clarified. For these reasons, the study on how to evaluate the mist spraying environment using environmental indices is insufficient. Oh et al. verified that 2NM could predict the human skin temperature accurately in outdoor and mist spraying environments. They proposed the new index of Outdoor Predicted Mean Vote (O-PMV) that can evaluate the thermal sensation in outdoor and mist spraying environments [27].

Table 2-1. Environmental indices related to thermal comfort (refer to [28])

Year	Index	Reference
1897	Theory of heat transfer	[29]
1905	Wet bulb temperature	[30]
1923	Effective temperature	
1929	Equivalent temperature (T_{eq})	[31]
1932	Corrected effective temperature (CET)	[32]
1937	Operative temperature (T_{op})	[33]
1955	Heat stress index (HSI)	
1957	Wet bulb globe temperature (WBGT)	[20]
1957	Discomfort index (DI)	[34]
1970	Predicted mean vote (PMV)	[35]
1971	New effective temperature (ET*)	[36]
1971	Wet globe temperature (WGT)	[37]
1972	Skin wettedness	[38]
1973	Standard effective temperature (SET*)	[39]
1986	Predicted mean vote (modified) (PMV*)	[40]
1999	Modified discomfort index (MDI)	[41]
1999	Physiological equivalent temperature (PET)	[22]
2000	Outdoor standard effective temperature (OUT-SET*)	[19]
2001	Environmental stress index (ESI)	[42]
2001	Universal thermal climate index (UTCI)	[43]

2.1.1. Predicted mean vote (PMV)

Fanger proposed the Predicted Mean Vote (PMV) index using the relation between thermal sensation scale and heat storage rate (S) can be expressed as Equation (2-1) [35,44]. Equation (2-2) describe the heat balance between thermal environment and human body. The heat storage rate is the difference between left and right side of the heat balance equation.

$$\mathrm{PMV} = [0.303\exp(-0.036\,M) + 0.028]\,S \tag{2-1}$$

$$M - W = 3.96 \cdot 10^{-8} f_{\mathrm{clo}} \left[(T_{\mathrm{clo}} + 273)^4 + (T_{\mathrm{mrt}} + 273)^4\right] + f_{\mathrm{clo}} h_{\mathrm{c}} (T_{\mathrm{clo}} - T_a) + 3.05 \left[5.73 - 0.007 (\mathrm{M} - \mathrm{W}) - p_{\mathrm{air}}\right] + 0.42 \left[(M - W) - 58.15\right] + 0.0173 M (5.87 - p_{\mathrm{air}}) + 0.0014 M (34 - T_{\mathrm{air}}) \quad (2\text{-}2)$$

2.1.2. Physiological equivalent temperature (PET)

The physiological equivalent temperature (PET) derived from the two-node model considering physiological responses of human body. This is based on the Munich Energy-Balance Model for Individuals (MEMI), which models the thermal conditions of the human body [22]. The range of thermal stress sensations corresponding to the PET index was reported as listed in Table 2-2. The PET calculation is basically based on the Pierce two-node model which consider the thermoregulation system, blood flow rate, sweating, and shivering [36]. Recently, the error of PET calculation was revised and the calculation code is available [23].

Table 2-2. PET and UTCI equivalent air temperature categories in terms of thermal stress [45–47].

Stress category	PET (°C)	UTCI (°C)
Extreme heat stress	> 41	> 46
Very strong heat stress		38 to 46
Strong heat stress	35 to 41	32 to 46
Moderate heat stress	29 to 35	26 to 32
Slight heat stress	23 to 29	
No thermal stress	18 to 23	9 to 26
Slightly cold stress	13 to 18	0 to 9
Moderate cold stress	8 to 13	−13 to 0
Strong cold stress	4 to 8	−27 to −13
Very strong cold stress	< 4	−40 to −27
Extreme cold stress		< −40

2.1.3. Standard effective temperature (SET)*

The new effective temperature (ET*) is defined as the temperature of a standard environment with no airspeed, uniform temperature (the conditions of air temperature and mean radiation temperature are the same), and 50% relative humidity [44]. The skin temperature and skin wettedness are calculated using a two-node thermoregulation model. This index is assuming the thermal influence of an environment on the human body is the same when the skin temperature and skin wettedness are the same in an actual environment the standard environment.

The standard effective temperature (SET*) index has been proposed to consider the various activity

and clothing insulation levels [39]. SET * is defined as the temperature of a standard environment with the same skin temperature and skin wettedness as the actual environment. The standard environment assumes that there is no air velocity, uniform temperature and 50% relative humidity, and a person takes clothes corresponding to activity level.

2.1.4. Equivalent temperature

The equivalent temperature is the most effective environmental index to evaluate the influence of air movement [48–50]. Using SET*, ET*, and PMV, the effect of airspeed is calculated along with the clothing, which involves the clothing insulation level and the clothing area factor. Moreover, it is difficult to identify the effect of airspeed on human body due to these indices are expressed by the mean value of the entire human body. However, the equivalent temperature (t_{eq}) can reflect the effect of airflow on each part of the body. In addition, this index is based on the heat exchange between a body and surrounding environment considering physical phenomena; it can evaluate the effect of airflow characteristics properly and directly. Moreover, this environmental index can evaluate each part of the human body and is thus able to confirm the local thermal effects of air movements. The equivalent temperature can also be used as an index to predict the thermal sensation in a nonuniform environment such as inside a vehicle with uneven airspeed, solar radiation, and temperature [48,49]. These days, equivalent temperature has been used as a method to evaluate the effect of personalized airflow systems [51,52] to improve the thermal sensation and thermal comfort. Equivalent temperature defined as the temperature of an imaginary ideal standard environment with the same radiant temperature and air temperature in a windless condition, where a person has the same heat loss by radiation and convection as that in an actual condition [53]. As described in Equation (2-3), when the heat loss of the human body is constant, the skin temperature is determined by radiation and convection.

$$Q_t = Q_r + Q_c = h_r(T_{sk} - T_{mrt}) + h_c(T_{sk} - T_a) = h_o(T_{sk} - t_{eq}) \quad (2\text{-}3)$$

This indicates that the skin temperature in the ideal environmental condition and the actual environment are equal and can be calculated by Equation (2-4).

$$t_{eq} = T_{sk} - \frac{Q_t}{h_o} \quad (2\text{-}4)$$

It is necessary to identify the skin surface temperature and the heat transfer coefficient of the human

body in a standard environment and an actual environment to determine the equivalent temperature. First, the heat transfer coefficients of each part of the human body under standard environmental conditions should be investigated. In general, the total heat transfer coefficient was calculated at 24 °C with an airspeed of 0.05 m/s which is considered a standard environment according to ISO 14505-2 [54]. The total heat transfer coefficient composed of radiative and convective heat transfer is not significantly changed by the difference between the environmental temperature and the human body temperature [55,56]. Second, by obtaining the skin temperature determined by the heat loss from the body and environmental factors of an actual thermal environment, the equivalent temperature can be determined. The equivalent temperature can be calculated by using the skin temperature under the same heat loss from the body and the same posture as a standard environment and the total heat transfer coefficient which is obtained from a standard environment.

2.1.5. Wet-bulb globe temperature (WBGT)

The Wet-Bulb Globe Temperature (WBGT) index was developed by Yaglou and Minard [20] to avoid the complex calculation of the Effective Temperature (ET) index and has been widely used to assess the thermal comfort in hot environment for over 60 years [21]. The WBGT index can be calculated using Equation (2-5). Since the WBGT calculation is very simple, it has an advantage which can be easily confirmed by even an inexperienced person. The above equation is used for outdoor environment with solar radiation, and the below equation is used for indoor environment. The WBGT index is commonly utilized to prevent heat disorders in Japan, and the risk level of heat disorders for the WBGT levels was recommended as listed in Table 2-3 [57].

$$\begin{aligned} \mathrm{WBGT_{out}} &= 0.7\,T_{\mathrm{wet}} + 0.2\,T_{\mathrm{g}} + 0.1\,T_{\mathrm{a}} \\ \mathrm{WBGT_{indoor}} &= 0.7\,T_{\mathrm{wet}} + 0.3\,T_{\mathrm{g}} \end{aligned} \tag{2-5}$$

Table 2-3. Risk level of heat disorders by Japan Amateur Sprots Association (1994)

Level	Recommendation	WBGT (°C)
Danger	Stop exercise in principle	> 31
Alert	Stop severe exercises	26 to 31
Advisory	Take rests frequently	25 to 26
Caution	Frequently hydration	21 to 25
Almost safe	Proper hydration	< 21

2.1.6. UTCI (Universal thermal climate index)

The Universal Thermal Climate Index (UTCI) is defined as the air temperature of the standard environment condition which has the same physiological responses as the actual environment condition. The UTCI can be expressed simply as Equation (2-7). The offset value is determined by radiation, wind speed, and humidity at the actual temperature values. The UTCI is calculated using the UTCI-Fiala model [58] and the UTCI-Clothing model [59]. The meteorological data is measured at a height of 10 m above ground, the wind speed v_x at a required height (x) can be converted by Equation (2-7). The range of thermal stress sensations corresponding to the UTCI values is listed in Table 2-2.

$$\mathrm{UTCI}(T_\mathrm{a}, T_\mathrm{mrt}, v, p_\mathrm{air}) = T_\mathrm{a} + \mathrm{offset}(T_\mathrm{a}, T_\mathrm{mrt}, v, p_\mathrm{air}) \tag{2-6}$$

$$v_x = v_{10\mathrm{m}} \cdot \frac{\log\frac{x}{0.01}}{\log\frac{10}{0.01}} \tag{2-7}$$

2.2. Physiological human model

2.2.1. Two-node model

The two-node model (2NM) was proposed to simply calculate the physiological thermoregulation human by Gagge from Stolwijk's 25-node model [36]. The two-node model considers physiological responses such as sweating, blow flow rate changes, and shivering. The schematic diagrams and thermal resistance network model of 2NM is described in Fig. 2-1. The human body is regarded as two nodes, the core, and the skin, and calculated considering the heat balance equation. In addition, a human body feels heat and cold based on the physiological neutral temperature. The 2NM was developed considering indoor environments and verified through laboratory experiments [39,60]. However, it was shown that the use of 2NM can be used to predict the thermal state of the human body in the outdoor environment [61]. In addition, SET * and PET indices which are based on 2NM, have been widely used to assess outdoor environments.

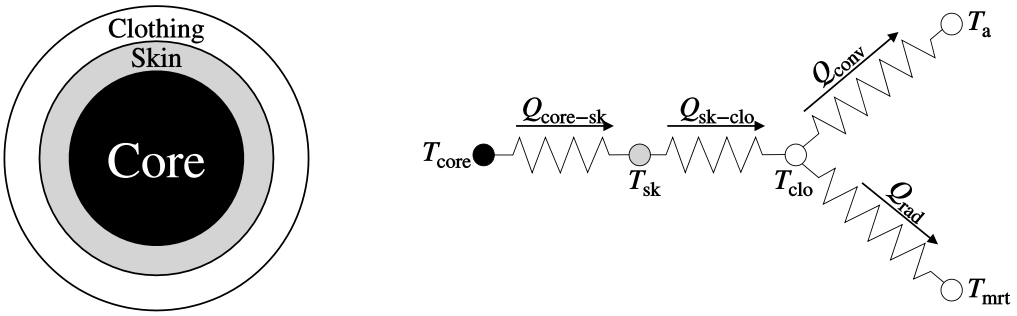

Fig. 2-1. Schematic diagram and thermal resistance network model of two-node model.

2.2.2. Three-node model

The 2NM is useful for analyzing overall thermal sensation and thermal comfort, but it has a limitation to understand local thermal discomfort and thermal sensation. Since the temperature differences exist between clothed skin and bared skin, Zolfahari and Maerefat had devised the three-node model (3NM) [62] which was considered core, bared skin, and clothed skin compartments as described in Fig. 2-2.

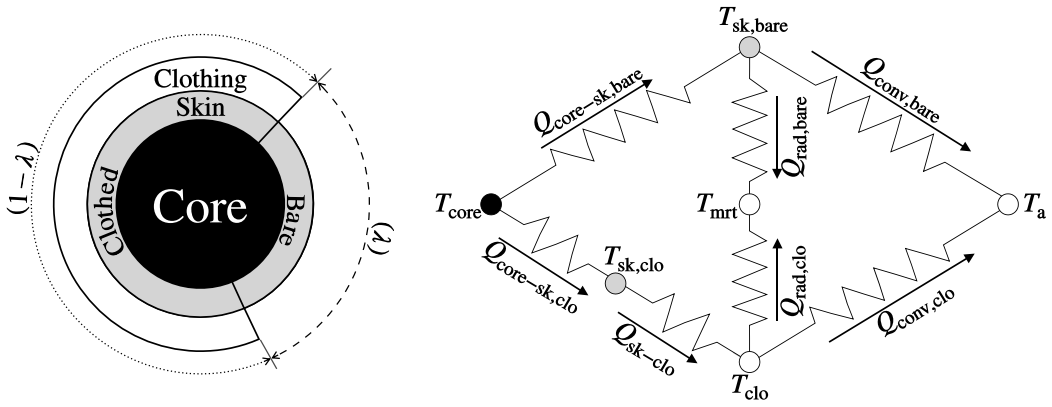

Fig. 2-2. The schematic diagram and thermal network model of three-node model.

2.2.3. 65-node model

The 65-node thermoregulation model was developed by Tanabe et al. [63] based on the Stolwijk model [64]. The 65-node model consists of 16 segments (head, chest, back, pelvis, left shoulder, right shoulder, left arm, right arm, left hand, right hand, left thigh, right thigh, left leg, right leg, left foot, and right foot segments) of human body, 4 layers (core, muscle, fat, and skin compartments) of each

segment, and central blood compartments as described in Fig. 2-3.

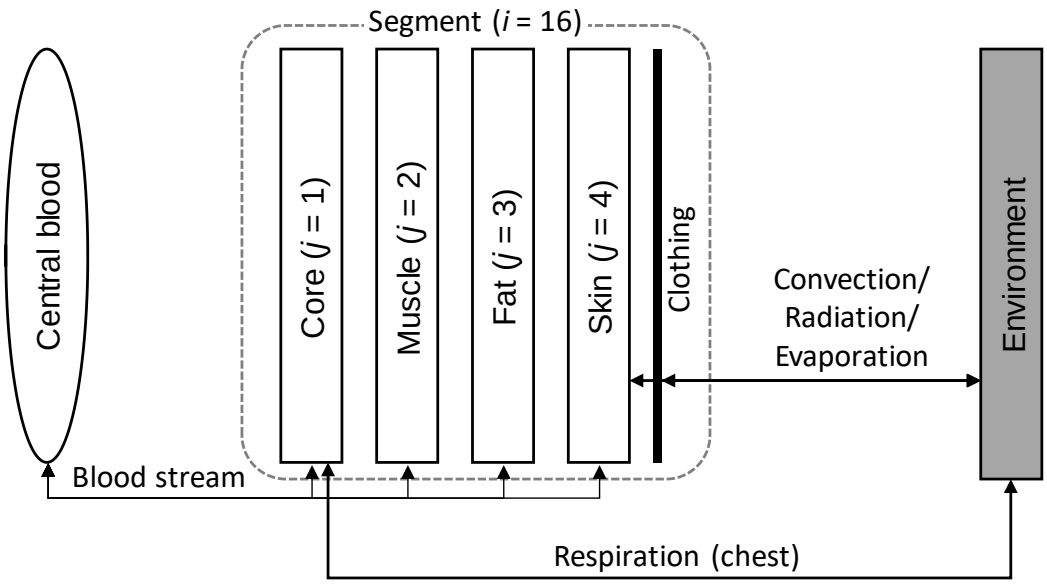

Fig. 2-3. The schematic diagram of 65-node model.

Chapter 3. Assessment of existing environmental indices in mist spraying environment

Chapter 3. Assessment of existing environmental indices in mist spraying environment

3.1. Background and objectives

Thermal environment influences a human's thermal sensations and thermal comfort. Essential environmental factors which can affect thermal sensations and thermal comfort are air temperature, humidity, airspeed, and radiant temperature. In addition, human's thermal sensation and thermal comfort depend on activity and clothing insulation levels. Since environmental index can be expressed only a single value, it helps to understand the complex interactions between the thermal environment and thermal sensations more easily. Various environmental indices have been proposed over the last century as listed in Table 2-1.

The most successful and widely used environmental index is the Predicted Mean Vote (PMV) index proposed by Fanger which can assess the human thermal sensation in an indoor environment based on the correlation between survey results and the heat storage rate. However, Fanger's model is only acceptable in environments with nearly comfortable conditions. Because PMV index does not consider physiological responses, applying this model in a certain environment with extreme conditions may result in an inconsistency with an actual sensation. Gagge et al. developed the simple two-node model (2NM) which considered the physiological responses such as sweating, blood flow regulation, and shivering in response to the thermal environment from Stolwijk's 25-node model. In addition, they suggested the Standard Effective Temperature (SET*) based on the 2NM.

However, these proposed indices were developed for an indoor environment and devised based on the results of a climate chamber with stable conditions, and therefore, they are difficult to an outdoor environment. In order to evaluate thermal comfort and thermal sensations in outdoor environments, the Universal Thermal Climate Index (UTCI) [18] and the Outdoor Standard Effective Temperature (OUT–SET*) [19] were proposed considering the effects of complex radiation environments on the human body. The wet-bulb globe temperature (WBGT) index was developed by Yaglou and Minard [20] to avoid the complex calculation, has been widely utilized to understand the outdoor thermal environment for over 60 years [21]. Additionally, Höppe introduced the Physiological Equivalent Temperature (PET) based on the Munich Energy-balance Model for Individuals (MEMI) taking thermo-physiological regulatory processes into consideration [22]; the calculation of the PET index was recently revised by Walther and Goestchel [23]. Some studies have applied the existing environmental indices to understand the outdoor thermal environments on human bodies. Sharmin et

al. investigated the correlation analysis between PET and thermal sensation of pedestrians [24]. Sen and Nag studied in tropically hot and humid environments using existing environmental indices (e.g. PET, SET*, and PMV) [25]. Li et al. investigated the applicability of UTCI index to evaluate the thermal comfort in an outdoor environment [26].

By the way, the mist spraying environment is more complex than the outdoor environment because mist particles exist in the air and evaporation occurs. However, there have not been studied on whether the existing environmental index can reflect the thermal sensations and thermal comfort in a mist spraying environment appropriately. Therefore, the present preliminary study confirmed the feasibility of existing environmental indices in the mist spraying environment and aimed to provide a foundation for the following studies. This chapter describes some part of my journal "Environmental index for evaluating thermal sensations in a mist spraying environment" [27].

3.2. Experimental setup

A field experiment was conducted to verify the effectiveness of the mist spraying system in Shimbashi station square in Tokyo. [65]. Shimbashi has been developed as a major railway hub of Tokyo and is a commercial district with many high-rise buildings. The installed experimental system has a sunshade which could block direct solar radiation, and the mist particles are sprayed in a 360° range to evaporate and cool down the air with a wide range of area. Also, air was blown by a fan to send the cooled air and mist droplets adjacent to the human body. A detailed overview of the experiment system is presented in Fig. 3-1. The experiments were conducted during the summer season except for the rainy days (August 4–12, 2016).

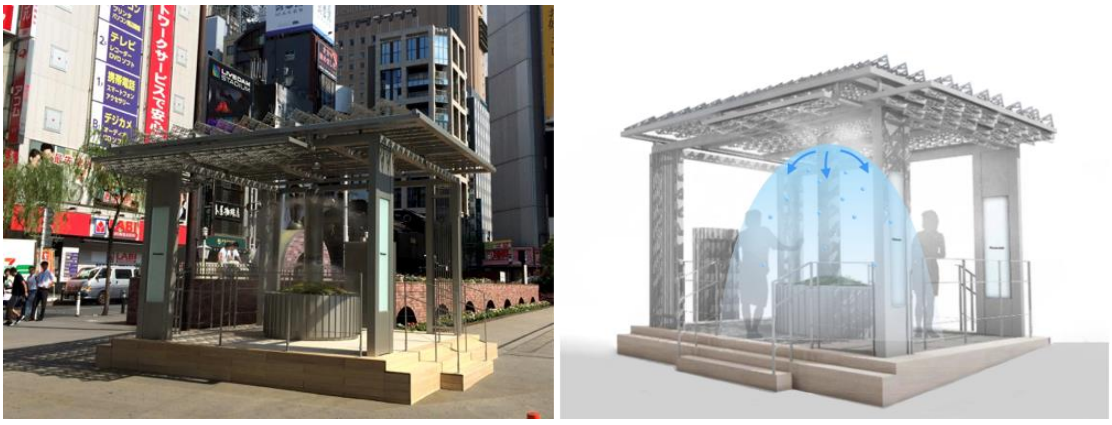

(a) (b)

Fig. 3-1. Scene of (a) preliminary experiment (b) and concept diagram.

The air temperature, radiation, humidity, and airspeed were measured inside the mist spraying environment. The details used instruments are listed in Table 3-1. In the experiment, environmental factors were measured only inside the mist spraying environment in Table 3-1. Then, conventional environmental indices were calculated using the measured environmental factors inside the mist spraying environment.

Table 3-1. Measurement in preliminary research.

Instrument	Environmental factors	Location†	Height (m)	Range	Accuracy
WBGT (401F)	air temperature (T_a)	mist spraying environment	1.1	0–60 °C	±0.5 °C
	globe temperature (T_g)			0–80 °C	±0.5 °C
	relative humidity (RH)			10–90%	±3.0%
Cyclone-type thermometer	air temperature (T_a)	mist spraying environment	1.1	−40–125 °C	±0.5 °C
SAT-600	airspeed (v)	mist spraying environment	1.1	0–60 m/s	±3.0%
LI-7200 RS	relative humidity (RH)	mist spraying environment	1.1	0–95%	

Note: Location† is the instrument position inside the mist spraying environment.

3.3. Survey research

3.3.1. Subjects

The survey research was conducted from August 4 to August 12, 2016. Any person can freely participate in the experiment and the subjects were 1,110 and included 342 women and 768 men between the ages of 10–70 range as described in Table 3-2 and Fig. 3-2. The surveys were conducted twice, and subjects reported the thermal sensations and thermal comfort before and after entering the mist spraying environments. The reporting time and answers of the questionnaire were recorded automatically on a tablet PC (Fig. 3-3) to identify the occupied duration that the subjects spent inside the mist spraying environment. The detailed survey questionnaires can be found in Appendix 1. If the residence time of subjects in the mist spraying environment is too short, i.e., a few seconds, the data was discarded as it was not suitable for understanding the proper effects of the mist spraying system. The average duration time in the mist spraying environment for all participants was about 1 minute. The reported sensations were used for correlation analysis with conventional environmental indices.

Table 3-2. Subjects characteristics.

Age (year)	Height (m)	Clothing level (clo)
n= 1,110 Mean ± SD (Standard deviation)		
47.8 ± 13.5	1.67 ± 0.07	0.42 ± 0.07

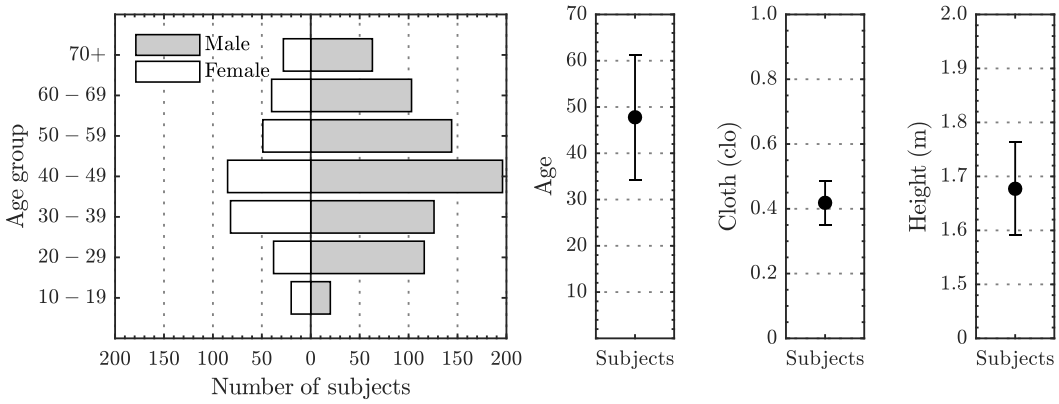

Fig. 3-2. Subjects' characteristics of age, height, and clothing insulation level.

Fig. 3-3. Tablets for survey research.

3.3.2. Survey scale

Questionnaires were collected before and after the subject entered the mist spraying environment to investigate the thermal effect of the mist spraying system on thermal sensation in hot weather. As a subjective assessment, modified thermal sensation vote (mTSV), thermal sensation vote (TSV) and comfort sensation vote (CSV) were used for the questionnaire as shown in Table 3-3. The TSV scale of the American Heating Association, Refrigerating and Air-Conditioning Engineers (ASHRAE), is

commonly used to assess a person's thermal sensation, but the word “warm” or “cold” means comfort in Japanese. Therefore, mTSV [66] is more suitable for indicating the thermal sensation of Japanese [67,68]. CSV was used on a seven-point scale.

Table 3-3. Survey scale in questionnaire.

Scale	mTSV	TSV	CSV
3	Very hot	Hot	Very comfortable
2	Hot	Warm	Comfortable
1	Slightly hot	Slightly warm	Slightly comfortable
0	Neutral	Neutral	Neutral
−1	Slightly cold	Slightly cool	Slightly uncomfortable
−2	Cold	Cool	Uncomfortable
−3	Very cold	Cold	Very uncomfortable

3.4. Results and discussion

3.4.1. Thermal sensation and thermal comfort

The survey results of modified thermal sensation vote (mTSV) and comfort sensation vote (CSV) before and entering the mist spraying environments are shown in Fig. 3-4. In the mTSV questionnaire, subjects reported 2.29 before and 0.23 after entering the mist spraying environment, which means that they reported thermal sensation between "very hot" and "hot" in outdoor and "neutral" in mist spraying environments. In the CSV questionnaire, subjects reported −1.28 before and 1.38 after entering the mist spraying environment, which implies that the “slightly uncomfortable” and "uncomfortable" feeling of subjects in the hot outdoor environment before entering the mist spraying environment changed to "comfortable" after entering the mist spraying environment.

Both thermal sensation and thermal comfort sensation were improved after entering the mist spraying environment, the result of the paired t-test analysis of mTSV and CSV before and after entering the mist spraying environment, a probability value (p-value) was revealed as less than 0.001.

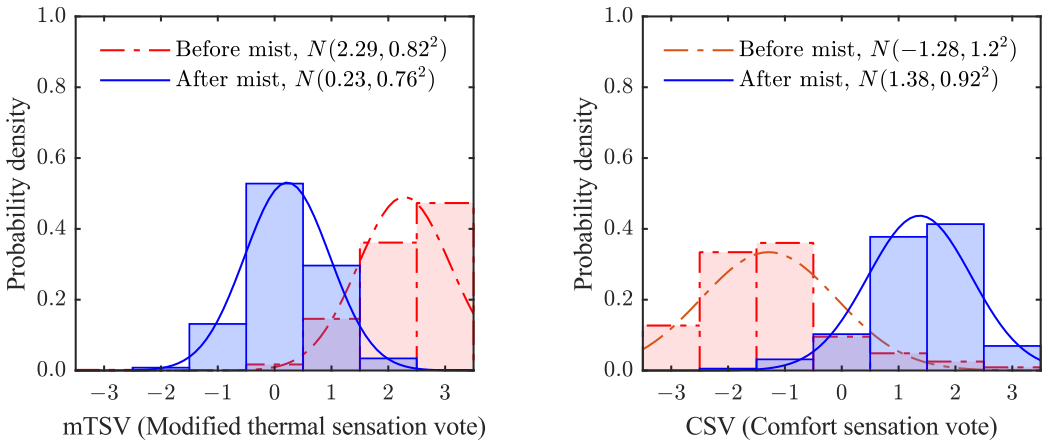

Fig. 3-4. Probability density of the standard normal distribution $N(\mu, \sigma^2)$ of survey results before and after entering the mist spraying environment. Left is mTSV and right is CSV.

The response rate results for each scale is illustrated in Fig. 3-5. Each thermal sensation and thermal comfort were described using the seven-point scale mentioned in Table 3-3 (i.e., mTSV(3) means very hot, and CSV(−3) means very uncomfortable). The summation ratio of mTSV (1), mTSV (2) and mTSV (3) accounted for 98% of the thermal sensation, which means that almost all participants report feeling hot in the summer outdoor environment before entering the mist spray system. However, it changed to 33% after entering the mist spraying environment. The summation ratio of CSV (−1), CSV (−2) and CSV (−3) was changed from 82% to 3.7% before and after entering the mist spraying system, which implicates that thermal comfort has been significantly improved. The summation ratio of the CSV (1), CSV (2) and CSV (3) was reported at 8.3% before entering the mist spraying environment and increased thermal comfort with 86% due to the evaporative cooling effect of the mist spraying system.

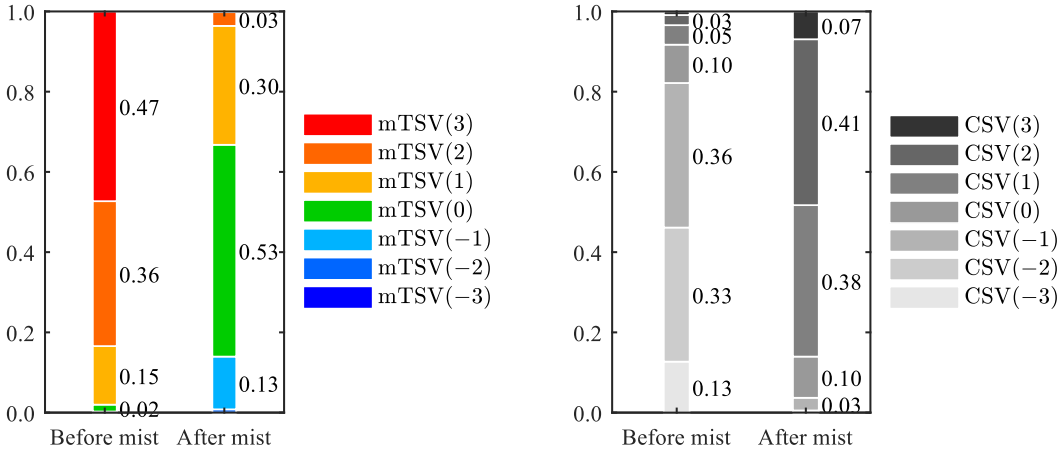

Fig. 3-5. Response rate results of mTSV (left) and CSV (right) before and before and after entering the mist spraying environment.

In the survey, the acceptability of the mist spraying environment was assessed to understand whether a person could accept the mist spraying thermal environment. As a result, the "Unacceptance" result dropped significantly from 45% to 7% after experiencing the mist spraying environment. Meanwhile, the "acceptable" result increased from 55% to 93%. In conclusion, most people felt that the mist spraying environment is acceptable in hot summer weather.

Tayler et al. reported that thermal comfort varies considerably between young and old during thermal change ($p < 0.05$) [69]. To investigate this tendency in the mist spraying environment, paired sample *t*-test analyses were performed as shown in Fig. 3-6. The result showed that the young group felt hotter than the old group in the outdoor environment (before entering the mist spray environment) with a significant difference ($p < 0.01$). However, CSV did not show a significant difference between the two groups ($p = 0.83$). On the other hand, the mTSV results showed no significant difference between the young and old groups ($p = 0.58$), in the mist spray environment (after entering the mist spray environment), but the CSV showed statistically different results between the young and the old group ($p < 0.001$). This result indicates that young people felt more comfortable inside the mist spraying environment than old people.

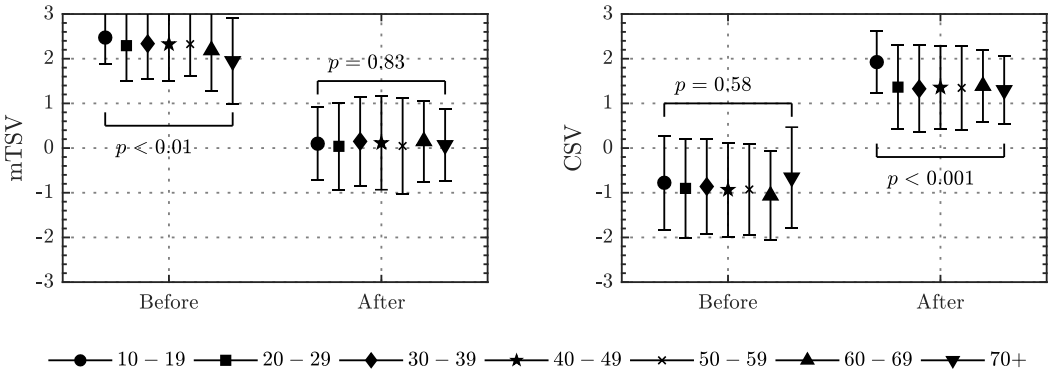

Fig. 3-6. The survey results (mean ± SD) of different age groups and the probability value (*p*-value) by paired sample t-test analysis between young (10–20) and old (70+) age groups.

3.4.2. Outdoor weather condition

The average and standard deviation of outdoor air temperature and relative humidity during the experiment resulted in 33.5 ± 2.2 °C and 50.7 ± 9.5%, respectively (Fig. 3-7).

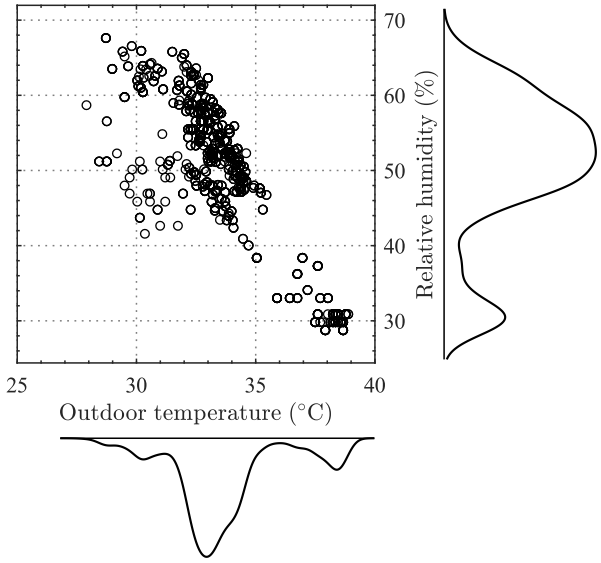

Fig. 3-7. Outdoor air temperature and relative humidity during experiment.

3.4.3. Acceptability in outdoor and mist spraying environments

The results of “Unacceptable” before and after entering the mist spraying environment changed from 45% to 7% as displayed in Fig. 3-6. Results of “Acceptable” answers changed from 55% to 93% after entering the mist spraying environment. These results represent that most people can accept the mist spraying environment in an outdoor environment during the hot summer season.

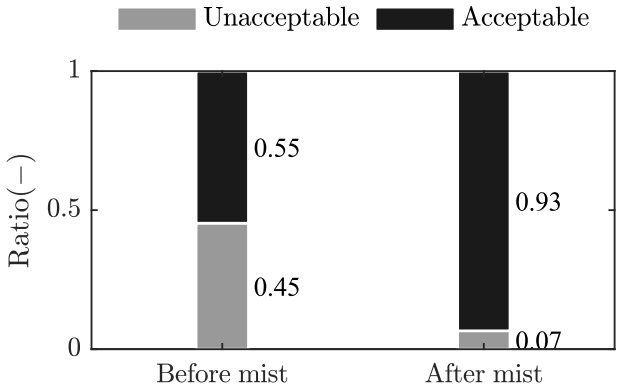

Fig. 3-8. The results of acceptability before and after entering the mist spraying environment (n = 1,110)

3.4.4. Existing environmental indices and thermal sensation

The existing environmental indices used to describe the thermal sensations of a person were investigated in a mist spray environment. If the environmental index has a statistically significant correlation with thermal sensation and thermal comfort, it can be considered as an appropriate evaluation index for estimating human thermal sensitivity. As the existing environmental indices, SET*, PET, WBGT, and UTCI indices were selected which were widely utilized in outdoor environments. Each environmental index was calculated using the measured environmental factors (air temperature, MRT, Relative humidity, and airspeed).

Fig. 3-9 shows the cumulative distribution function (CDF) of mTSV for each existing index, and Table 3-5 shows the mean and standard deviation (SD) of each normal distribution of P relevant to thermal sensation votes. The horizontal axis represents the value of each environmental index, and the vertical axis represents the cumulative ratio of P. The P is calculated using survey results, where P (1) is the cumulative probability densities of summation of mTSV (1), mTSV (2), and mTSV (3) as listed in Table 3-4. In other words, P (1) of mTSV represents the cumulative ratio of all participants who felt above the "slightly hot" level.

Table 3-4. Calculation of *P* of mTSV and CSV.

Sensations	Calculation of *P*
mTSV	$P(3) = \mathrm{mTSV}(3)$
	$P(2) = \mathrm{mTSV}(2) + \mathrm{mTSV}(3)$
	$P(1) = \mathrm{mTSV}(1) + \mathrm{mTSV}(2) + \mathrm{mTSV}(3)$
	$P(0) = \mathrm{mTSV}(0) + \mathrm{mTSV}(1) + \mathrm{mTSV}(2) + \mathrm{mTSV}(3)$
	$P(-1) = \mathrm{mTSV}(-1) + \mathrm{mTSV}(0) + \mathrm{mTSV}(1) + \mathrm{mTSV}(2) + \mathrm{mTSV}(3)$
	$P(-2) = \mathrm{mTSV}(-2) + \mathrm{mTSV}(-1) + \mathrm{mTSV}(0) + \mathrm{mTSV}(1) + \mathrm{mTSV}(2) + \mathrm{mTSV}(3)$
	$P(-3) = \mathrm{mTSV}(-3) + \mathrm{mTSV}(-2) + \mathrm{mTSV}(-1) + \mathrm{mTSV}(0) + \mathrm{mTSV}(1) + \mathrm{mTSV}(2) + \mathrm{mTSV}(3)$
CSV	$P(3) = \mathrm{CSV}(-3) + \mathrm{CSV}(-2) + \mathrm{CSV}(-1) + \mathrm{CSV}(0) + \mathrm{CSV}(1) + \mathrm{CSV}(2) + \mathrm{CSV}(3)$
	$P(2) = \mathrm{CSV}(-3) + \mathrm{CSV}(-2) + \mathrm{CSV}(-1) + \mathrm{CSV}(0) + \mathrm{CSV}(1) + \mathrm{CSV}(2)$
	$P(1) = \mathrm{CSV}(-3) + \mathrm{CSV}(-2) + \mathrm{CSV}(-1) + \mathrm{CSV}(0) + \mathrm{CSV}(1)$
	$P(0) = \mathrm{CSV}(-3) + \mathrm{CSV}(-2) + \mathrm{CSV}(-1) + \mathrm{CSV}(0)$
	$P(-1) = \mathrm{CSV}(-3) + \mathrm{CSV}(-2) + \mathrm{CSV}(-1)$
	$P(-2) = \mathrm{CSV}(-3) + \mathrm{CSV}(-2)$
	$P(-3) = \mathrm{CSV}(-3)$

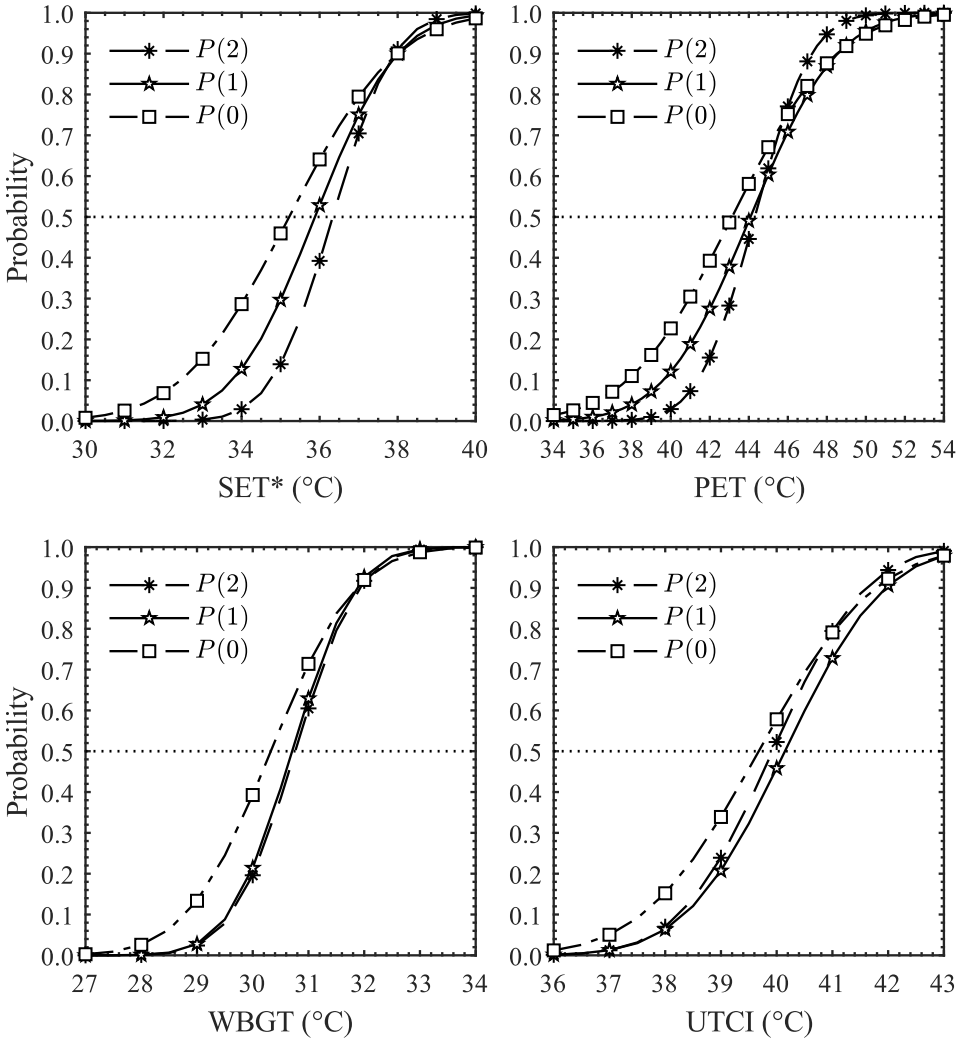

Fig. 3-9. Cumulative distribution functions (CDFs) analysis of modified thermal sensation vote (mTSV) for each environmental index in mist spraying environment.

Table 3-5. Results of each *P* distribution relevant to thermal sensation votes.

Environmental index	P	Mean (°C)	Standard deviation (SD, °C)
SET*	*P*(2)	36.3	1.23
	P(1)	35.9	1.65
	P(0)	35.1	2.07
PET	*P*(2)	44.6	2.28
	P(1)	44.1	3.49
	P(0)	43.1	4.20
WGBT	*P*(2)	30.8	0.89
	P(1)	30.7	0.89
	P(0)	30.3	1.19
UTCI	*P*(2)	39.9	1.31
	P(1)	40.1	1.41
	P(0)	39.6	1.56

3.4.5. Existing environmental indices and thermal comfort

In the CSV case, the value of *P* represents the sum of the reported CSV scale that was less when the *P* (0) was the cumulative probability density of the summation of CSV (0), CSV (−1), and CSV (−2)). In other words, the *P* (0) of the CSV refers to the cumulative ratio of all participants who felt more discomfort than "neutral" (see Fig. 3-10). Table 3-6 shows the mean and standard deviation (SD) of each normal distribution of *P* relevant to thermal comfort votes.

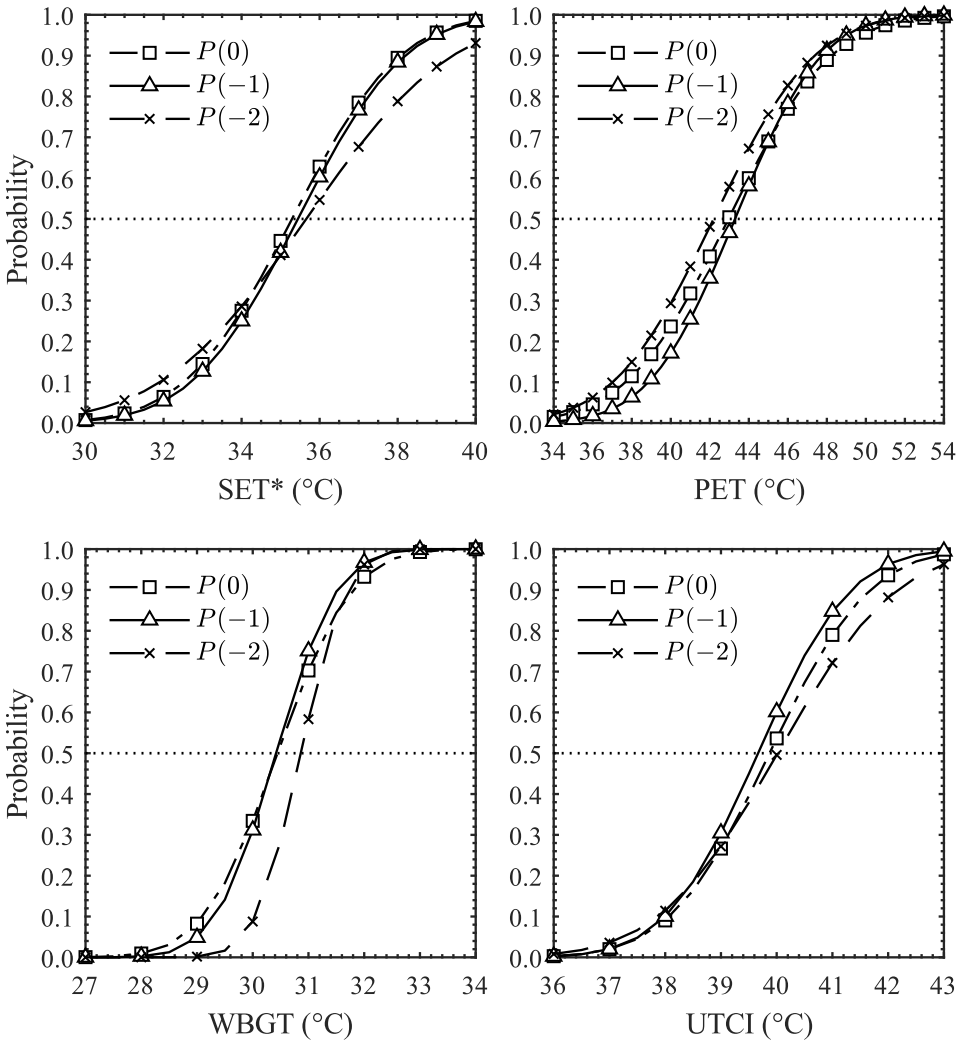

Fig. 3-10. Cumulative distribution functions (CDFs) analysis comfort sensation vote (CSV) for each environmental index in mist spraying environment.

Table 3-6. Results of each *P* distribution relevant to thermal comfort votes.

Environmental index	P	Mean (°C)	Standard deviation (SD, °C)
SET*	*P*(0)	35.3	2.16
	P(−1)	35.4	2.14
	P(−2)	35.7	2.93
PET	*P*(0)	43.0	4.12
	P(−1)	43.3	3.47
	P(−2)	42.2	4.04
WGBT	*P*(0)	30.4	1.04
	P(−1)	30.4	0.86
	P(−2)	30.8	0.64
UTCI	*P*(0)	39.9	1.40
	P(−1)	39.7	1.30
	P(−2)	40.0	1.68

The cumulative proportions of each *P* and each environmental index were positively correlated with mTSV and CSV results. Despite the same environmental conditions, the environmental index results had different ranges. PET results showed the widest range and WBGT showed the narrowest range. In mTSV results, each *P* distribution was best recognized for SET* but overlapped or reversed for PET, WBGT, and UTCI. In CSV results, each *P* distributions overlapped in all environmental indices. Each *P* distribution suggests that the sensation scale is properly reflected by the environmental index, thus overlapped or inverted *P* distribution suggests that the environmental index is hard to reveal each sensation.

3.5. Conclusion

From the preliminary experiment, it was found that the mist spraying system is effective to relieve heat stress in outdoor environment during the summer season. It was confirmed that among the examined existing environmental indices, only the SET* might be able to appropriately predict the mTSV in the outdoor mist spraying environment. However, even in the results of SET*, thermal sensations were not reflected in the range of low and high temperature properly. Therefore, from these results, it can be concluded that the existing environmental indices are inadequate for predicting thermal comfort in the outdoor environment where the mist droplets sprayed.

However, due to insufficient environmental condition data on the outdoor environment, it was not possible to examine how the weather affects the mist spraying system's cooling effect and thermal sensation changes. In addition, environmental indices were introduced to understand the complex thermal environments of a mist spraying environment. Though several studies reported the results of existing environmental indices in mist spraying environments, present study confirmed the existing

environmental indices could not adequately reflect the thermal sensation in mist spraying environments.

As the mist droplets exist in air of mist spraying environment, evaporation heat loss occurs when a human body wet in mist spraying environments. However, since existing environmental indices consider only four basic environmental factors, further research is necessary to extend the utilization of existing environmental indices on special environmental conditions such as mist spraying environments.

Chapter 4. Estimation of physiological responses in mist spraying environment

Chapter 4. Estimation of physiological responses in mist spraying environment

4.1. Background and objectives

As mentioned in Chapter 3, it has been found that SET* is likely to be utilized for the evaluation of mTSV in a mist spraying environment. However, in preliminary experiments, environmental factors were measured only in the mist spraying environment, so there was no useful data to understand the cooling effect of the mist spraying system in the outdoor environment. In addition, in order to understand the impact of the mist spraying system on the human body and to understand subjective assessments, such as surveys, it is necessary to investigate objective evidence, such as physiological reactions. Therefore, further experiments were conducted to confirm the applicability of Gagge's two-node model (2NM), which derives SET* in outdoor and mist spray environments.

This chapter discusses the details of the experiment, the comparison of environmental factors between outdoor and mist spray environments, and the changes in thermal sensations and thermal comfort after entering the mist spray environment. In addition, the environmental factors obtained in the field experiments were used to predict the physiological response through 2NM. The validity of the predictive model was confirmed by comparing the skin temperature with the experimental results (see Fig. 4-1).

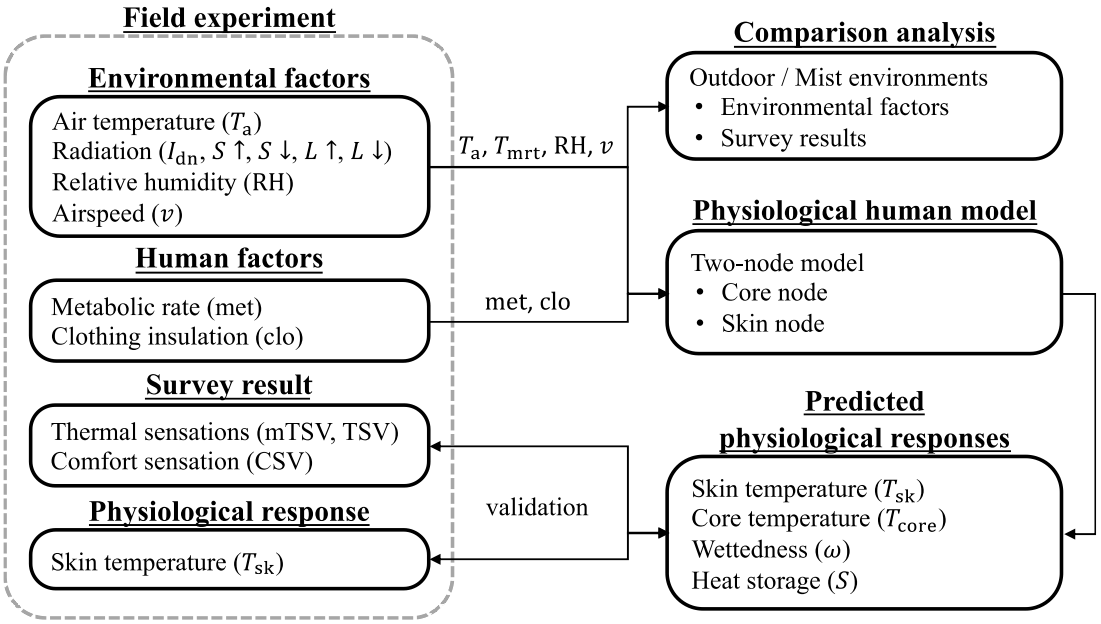

Fig. 4-1. Overall research flow for comparison of outdoor and mist spraying environments and validation of physiological human model.

4.2. Literature review

A survey is one of the best ways to investigate human's thermal sensations and thermal comfort in certain thermal environment. However, to conduct a survey is expensive and time-consuming, and the results from the survey are subjective. For these reasons, numerous kinds of environmental indices had been developed to assess the thermal environment and to estimate human's thermal sensations and thermal comfort in a more objective way [70]. The wet-bulb temperature (WBGT) index was developed by Yaglou and Minard [20] and has been widely utilized in thermal comfort evaluation over 60 years [21]. Particularly, the WBGT index is a commonly utilized to prevent heat disorders in Japan [57]. Gagge and Nishi proposed a standard effective temperature (SET*) that can consider human's physiological responses such as shivering, sweating and blood flow rate [36]. Höppe also introduced a physiological equivalent temperature (PET) based on the Munich Personal Energy Balance Model (MEMI), considering thermo-physiological regulatory processes [22]. In recent years, environmental indices such as Universal Effective Temperature (ETU) [71], Universal Thermal Climate Index (UCI) [18], and Outdoor Standard Effective Temperature (OUT-SET*) [19] have been suggested to consider the uneven radiation effects on the human body.

However, since the outdoor environment has non-uniform and complicated thermal conditions and the environmental factors vary greatly, it is not clear whether the conventional environmental indices can be utilized also in outdoor and mist spraying environments. In the previous publications, there was no comprehensive correlation analysis between the environmental index and human's thermal sensation and comfort in mist spraying environments. In addition, the suitability of the existing environmental index is not yet studied whether it can estimate the mist spraying environments properly where the humidity is high because of the mist particles. Therefore, this chapter presents the experiments to conduct subjective assessments and measurements of environmental factors in a mist spraying environment. In addition, each existing environmental index was calculated based on the measured environmental factors and compared with the results of subjective assessments.

Several studies have been published to understand the correlation between thermal sensations and environmental indices in mist spraying environments [15,17]. There have been attempts to predict skin temperature in outdoor environments [72], with various proposals for predicting the effects of radiation on the human body in outdoor environments [73,74]. However, a fundamental analysis comparing environmental index and human physiological response in outdoor and mist spraying environments is still insufficient. Therefore, additional studies are necessary to predict the thermal state of the human body in mist spraying environments. In this chapter, Gagge's two-node model [75] was used to estimate the thermal state of the body and was confirmed by comparison with the measured average skin temperature of the subject.

4.3. Mist spraying environment with sunshade

4.3.1. Methodology

4.3.1.1 Overall experimental method

During the summer season in 2017, a field experiment was carried out in Fujisawa, Japan (Table 4-1). The principle mechanism of the mist spraying system is the same as that of the initial preliminary experiment. However, in this experiment, the mist spraying system was assumed to be installed at the bus stop as shown in Fig. 4-3.

Table 4-1. Field experiment of mist spraying system for the verifiacation of two-node model.

Location	Number of subjects	Number of votes		Period
		Outdoor	Mist	
Fujisawa, Kanagawa	12 (9)[a]	72	60	August 3–4, and September 5, 2017 (10 am–12 pm, 1 pm–3 pm)

Note: [a]The number of subjects with measured skin temperatures.

4.3.1.2 Environmental factors

Four basic environmental factors (air temperature, radiation, humidity, and airspeed) were measured both inside and outside the mist spraying environment. Detail information about measuring equipment and measuring locations are listed in Table 4-2. Fig. 4-3 shows the installation of the mist spraying system, measuring equipment, and the scene of subject experiment. All measuring devices were installed at a height of 1.1 m, corresponding to the center of the standing human body. In previous studies, an accurate assessment of the thermal environment inside the mist spraying system is difficult was confirmed, because the measuring device is affected by mist droplets [15,76]. A conventional thermometer is difficult to use directly when wet with mist particles. Therefore, in the present study, the developed cyclone-type thermometer was used to measure the dry air temperature inside the mist spraying environment. The developed cyclone-type thermometer can separate the multi-phase mixture into liquid and gas (Fig. 4-4). Dry air and droplets can be separated by centrifugal and gravity-induced by an air compressor [77]. Two thermocouples were used to measure dry air temperature which was separated by the cyclone-type thermometers. Radiation was measured using short and longwave radiation meters and direct solar radiation meters. Relative humidity was induced by the mole fraction of water vapor in the air measured by an infrared H_2O analyzer. Regarding the measurement of airspeed, the hot-wire anemometer used ultrasonic anemometers because it could not accurately measure the wind speed when wet. In Fig. 4-3(a), inside* and inside** indicate where the device is wet or not due to mist droplets, respectively. Outdoor environmental factors (i.e. environmental factors

outside the mist system) were measured in areas without shading.

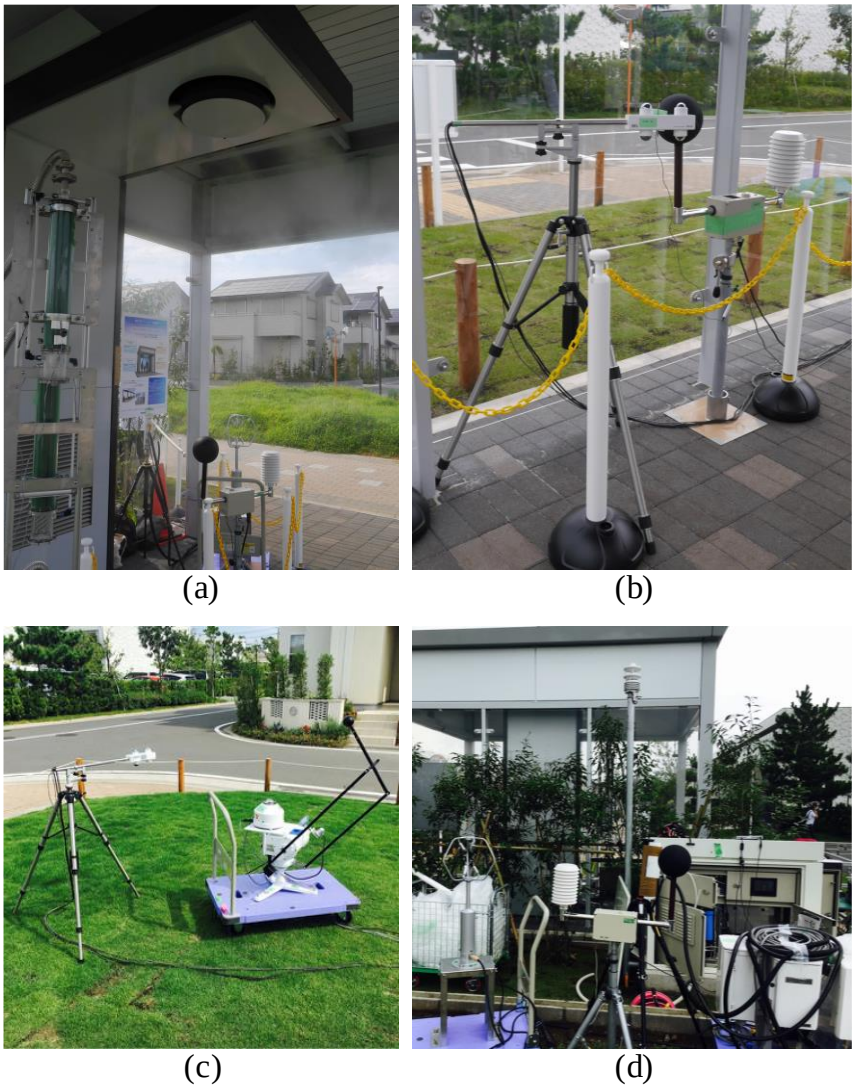

Fig. 4-2. Measurement setup for measuring environmental factors in outdoor and mist spray environments. (a) Inside the mist spraying environment, inside*: Ultrasonic anemometer, WBGT meter, infrared H_2O analyzer, and cyclone type thermometer. (b) internal** indicates shortwave and longwave radiation, WBGT meter, (c) outside** indicates shortwave and longwave radiation and direct solar radiation installed outside the mist spray environment, and (d) outside*: ultrasonic anemometer, WBGT meter, and infrared H_2O analyzer.

Table 4-2. Measurement for outdoor and mist spraying environment.

Instrument	Environmental factors	Location†	Height (m)	Range	Accuracy
WBGT (401F)	air temperature (T_a) globe temperature (T_g) relative humidity (RH)	inside** / outside*	1.1	0–60 °C 0–80 °C 10–90%	±0.5 °C ±0.5 °C ±3.0%
Cyclone-type thermometer	air temperature (T_a)	inside*	1.1	−40–125 °C	±0.5 °C
SAT-600	airspeed (v)	inside* / outside*	1.1	0–60 m/s	±3.0%
LI-7200 RS	relative humidity (RH)	inside* / outside*	1.1	0–95%	
MR-60	radiation ($S\uparrow$,$S\downarrow$,$L\uparrow$,$L\downarrow$)	inside** / outside**	1,1		
STR-22G	direct solar radiation (I_{dn})	outside**	-		

Note: Location† is the installation position of the instrument in and out of the mist spraying environment. Inside* is the wetted position by mist. Inside** is the area that does not get wet with mist droplets.

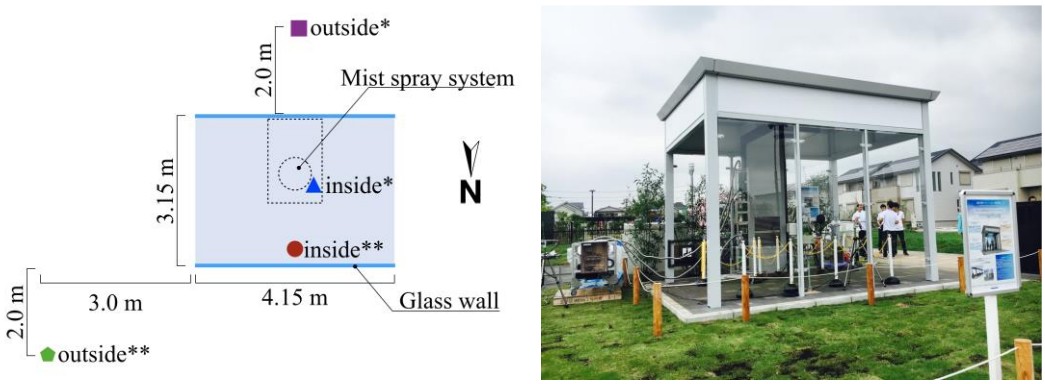

Fig. 4-3. Mist spraying system installed in Fujisawa city, Kanagawa, Japan (August 3–4 and September 5, 2017), (a) The top view of mist spraying system and the position of measuring instruments. (b) Overall view of mist spraying system.

(a) (b)

Fig. 4-4. Cyclone-type thermometer installed in mist spraying environment with a height of 0.2 m, 1.1 m, and 1.7 m. (a) is cylindrical cyclone separator and (b) is air compressors.

4.3.1.3 Estimation of mean radiation temperature in outdoor

Because the outdoor radiant environment is uneven and complex, the mean radiant temperature (MRT) was calculated to understand and simplify the effects of radiation on the human body. MRT can be derived in two ways. The first method described by Equation (4-1) uses the black globe thermometer and airspeed, while the second method uses upper and lower two-way longwave and shortwave radiation meter, and direct solar radiation by tracking the sun as shown (4-2).

$$T_{\mathrm{mrt}} = \sqrt[4]{\left(T_{\mathrm{g}} + 273.15\right)^4 + \frac{h_{\mathrm{cg}}}{\varepsilon D^{0.4}}\left(T_{\mathrm{g}} - T_{\mathrm{a}}\right)} - 273.15 \tag{4-1}$$

where, T_{mrt} is the mean radiant temperature, T_{g} is the globe temperature (0.15 m), h_{cg} is the mean convective coefficient ($1.1 \times 10^8 v^{0.6}$ for black globe, $1.335 \times 10^8 v^{0.71}$ for gray globe [78]), ε is the emissivity on the globe surface by longwave radiation assumed as 0.95, D is a diameter of the globe, T_{g} is the globe temperature, and T_{a} is the air temperature.

$$T_{\mathrm{mrt}} = \sqrt[4]{\frac{1}{\sigma}\left(f_{\mathrm{eff}}\left(\frac{\alpha_{\mathrm{k}}}{\varepsilon} \cdot \frac{I_{\mathrm{dH}} + S\uparrow}{2} + \frac{L\downarrow + L\uparrow}{2}\right) + \frac{\alpha \cdot f_{\mathrm{p}}}{\varepsilon} \cdot I_{\mathrm{dN}}\right)} - 273.15 \tag{4-2}$$

where, σ is the Stefan-Boltzmann constant (5.67×10^{-8}, W m^{-2} K^{-4}), f_{eff} is the effective body area

coefficient of the radiation assumed to be 0.87, I_{dH} is the diffused solar radiation on a horizontal surface calculated using the downward short radiation of $S\downarrow$, direct solar radiation on the normal surface of I_{dN}, and the solar altitude of β (i.e., $I_{dH} = S\downarrow - I_{dN} \cdot sin\beta$). $S\uparrow$ is the upward shortwave radiation, $L\downarrow$ is the downward longwave radiation, $L\uparrow$ is the upward longwave radiation, α_k is the absorption rate of the clothed human body by the shortwave radiation assumed to be 0.7, and f_p is the projection area coefficient of a standing human body by the direct solar radiation and was derived from Equation (4-3) proposed by Park and Tuller [79]. The solar altitude (β) was calculated with the recorded time and the location of Tokyo (latitude of 35° 33'N, longitude of 139° 46'E). Direct solar radiation was only measured on the outer side of the mist spraying environment because it did not reach the interior of the mist spraying environment.

$$f_p = 3.01 \times 10^{-7}\beta^3 - 6.46 \times 10^{-5}\beta^2 + 8.34 \times 10^{-4}\beta + 0.298 \quad (4\text{-}3)$$

All measuring instruments were installed where there is no influence of mist droplets. In previous publications, the results of MRT calculations using the two methods described above were not significantly different [74]. However, in our study, a clear difference was observed, because we used a 150 mm black globe thermometer that can be significantly affected by slow reaction light and the difference of shortwave radiation of black globe thermometer and the human body. Therefore, the second method (Equation (4-2)) was used to calculate the thermal radiation environment MRT around the body.

4.3.1.4 Review of mean radiation temperature estimation method

The radiant effect is the most important factor effecting thermal comfort in outdoor environment. Measuring six directional shortwave and longwave radiation fluxes and calculating the MRT using the Equation (4-4) and (4-5) is known as the most general method in outdoor environment.

$$S_{str} = \alpha_k \sum_{i=1}^{6} S_i F_i + \varepsilon \sum_{i=1}^{6} L_i F_i \quad (4\text{-}4)$$

where S_{str} is the mean radiant flux density on a human body, S is the shortwave radiation fluxes, L is the longwave radiation fluxes, F is the angular factor between a person and surrounding surfaces (see Table 4-3), and α_k and ε are the absorption coefficient for shortwave radiation (0.7) and the absorption coefficient for longwave radiation (0.5), respectively.

$$T_{\mathrm{mrt}} = \sqrt[4]{\frac{S_{\mathrm{str}}}{\varepsilon\,\sigma}} - 273.15 \tag{4-5}$$

Table 4-3. Angular factor (F_i) between a person and surrounding surfaces.

	East	South	West	North	Upward	Downward
Standing	0.220	0.220	0.220	0.220	0.060	0.060
Sitting	0.185	0.185	0.185	0.185	0.130	0.130
Globe	0.167	0.167	0.167	0.167	0.167	0.167

Meanwhile, six shortwave and longwave radiation meters were necessary for the comparison of outdoor and mist spraying environments. Therefore, the present study conducted the two-directional measuring method using Equation (4-2). In addition, globe thermometers (150 mm) were measured and calculated the MRT using Equation (4-1). The results are displayed in Fig. 4-5. The MRT calculated by measuring the globe thermometer and longwave and shortwave radiation meter showed similar results in the mist spraying environment. However, the globe thermometer showed higher MRT results than longwave and shortwave radiation meter. Because the direct solar radiation was blocked by a sunshade, MRT was dominated by longwave radiation. In addition, the absorptivity could not be modified after measuring the globe thermometer method, and the surface color of the globe thermometer should be changed gray color similar to the absorption coefficient for shortwave radiation on the human body.

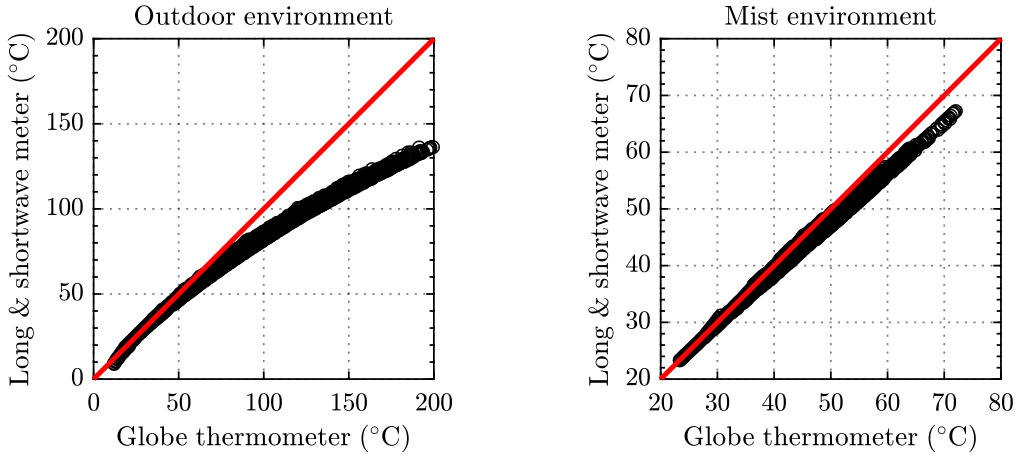

Fig. 4-5. Calculation results comparison for estimation method in outdoor and mist spraying environment.

4.3.2. Subject experiment setup

4.3.2.1 Subject experiment protocol

The experiment was conducted 4 participants daily for 3 days. The survey was carried out before and after entering the mist spraying environment as shown in Fig. 4-6. Detailed survey content can be found in Appendix 1. Twelve subjects participated in the experiment and six experiments were performed per subject. Detailed characteristics of the subjects are listed in Table 4-4. At the same time, only 9 of the subjects measured skin temperature due to equipment limitations. This time schedule of the experiment was designed considering bus stops in urban areas. In the experimental procedure, the subjects initially sat in a shady outdoor environment for 15-20 minutes and walked for 10 minutes outside the mist spray environment. After that, they entered the mist spraying environment for 10 minutes.

Table 4-4. Characteristics of subjects

	Age (year) Mean ± SD (standard deviation)	Weight (kg)	Height (m)	BMI
Men (n = 6)	37.6 ± 11.4	62.9 ± 7.8	1.69 ± 0.05	21.8 ± 2.2
Women (n = 6)	40.6 ± 11.1	52.6 ± 5.1	1.57 ± 0.03	21.4 ± 2.0
Total (n = 12)	39.1 ± 11.0	57.7 ± 8.3	1.63 ± 0.08	21.6 ± 2.0

n is number of subjects.

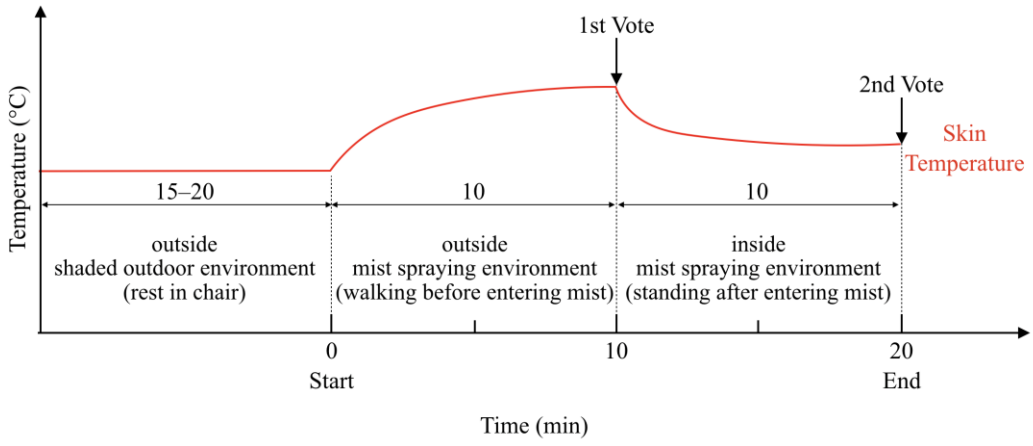

Fig. 4-6. Schematic diagram of subject experimental protocol showing timetable. Environmental conditions for outdoor and mist spraying environments correspond to (outdoor*, outdoor**) and (indoor*, indoor**) in Fig. 4-3.

4.3.2.2 Skin temperature measurement

In the experiment, the skin temperature was measured simultaneously to check the thermal state of the human body. The measured skin temperature was compared with the predicted results using a two-node model based on the measured environmental factors. Estimating overall skin temperature T_{sk} has been proposed in many studies [75,80–86]. In the present study, the overall skin temperature was calculated as the area-weighted average of the following seven points of the body parts: head, torso, forearm, hands, thighs, legs and feet, as shown in equation (4-6), as suggested by Hardy and Dubois [80,87] (T_i is the surface temperature of body segment i). The core temperature is difficult to measure, therefore oral temperature was measured and used it as a reference (see Fig. 4-7). During the experiment, the temperature was measured using an LT-ST08-12 sensor (accuracy is ± 0.01 °C) and recorded by LT-8 (Gram Corporation, Japan) at 10-second intervals.

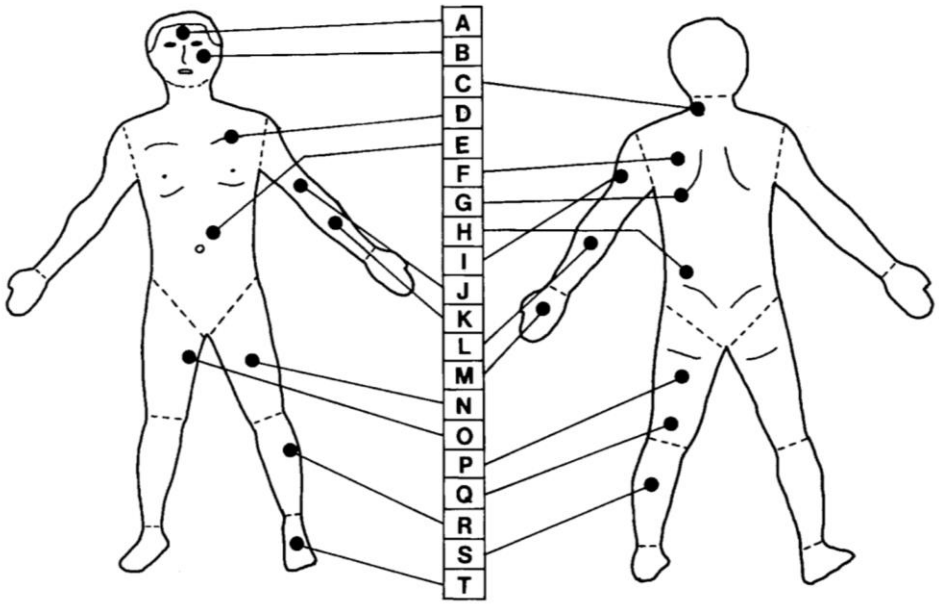

Fig. 4-7. Points of measurement for calculation of overall skin temperature (this figure is referenced by a study by Choi et al. [87]).

Table 4-5. Overall skin temperature calculation equations proposed by various researches.

Proposer	Points	Equation
Burton (1935) [86]	3	$T_{sk} = 0.5\ D + 0.14\ L + 0.36\ R$
Olsen (1984)	3	$T_{sk} = 0.5\ D + 0.14\ L + 0.36\ S$
Ramanathan (1964) [81]	4	$T_{sk} = 0.3\ D + 0.3\ I + 0.2\ N + 0.2\ R$
Houdas and Ring (1982)	4	$T_{sk} = 0.34\ D + 0.15\ L + 0.05\ M + 0.32\ N$
Houdas and Ring (1982)	5	$T_{sk} = 0.07\ B + 0.175\ E + 0.175\ H + 0.19\ J + 0.39\ Q$
Mitchell and Wyndham (1969) [82]	6	$T_{sk} = 0.14\ B + 0.19 + 0.19\ H + 0.11\ L + 0.05\ M + 0.32\ N$
Hardy and Dubois (1938) [80]	7	$T_{sk} = 0.07\ A + 0.35\ D + 0.14\ L + 0.05\ M + 0.19\ N + 0.13\ R + 0.07\ T$
Gagge and Nishi (1977) [75]	8	$T_{sk} = 0.07\ A + 0.175\ D + 0.175\ F + 0.07\ I + 0.07\ L + 0.05\ M + 0.19\ N + 0.2\ R$
Nadel et al. (1973) [83]	8	$T_{sk} = 0.21\ A + 0.1\ D + 0.17\ E + 0.11\ F + 0.12\ I + 0.06\ K + 0.15\ N + 0.08\ R$
Crawshaw et al. (1975) [84]	8	$T_{sk} = 0.19\ A + 0.08\ D + 0.12\ E + 0.09\ F + 0.13\ I + 0.12\ K + 0.12\ N + 0.15\ R$
Houdas and Ring (1982)	10	$T_{sk} = 0.2\ B + 0.05\ D + 0.125\ E + 0.2\ G + 0.05\ I + 0.05\ J + 0.05\ L + 0.125\ O + 0.075\ R + 0.075\ S$
Houdas and Ring (1982)	10	$T_{sk} = 0.06\ A + 0.12\ D + 0.12\ E + 0.12\ G + 0.08\ I + 0.06\ L + 0.05\ M + 0.19\ N + 0.13\ R + 0.07\ T$
Mitchell and Wyndham (1969) [82]	10	$T_{sk} = 0.1\ B + 0.125\ D + 0.125\ H + 0.07\ I + 0.07\ L + 0.06\ M + 0.125\ N + 0.125\ O + 0.15\ R + 0.05\ T$
Mitchell and Wyndham (1969) [82]	12	$T_{sk} = 0.07\ A + 0.0875\ D + 0.0875\ E + 0.0875\ F + 0.0875\ H + 0.14\ L + 0.05\ M + 0.095\ N + 0.095\ P + 0.065\ R + 0.065\ S + 0.07\ T$
Stolwijk and Hardy (1966) [85]	10	$T_{sk} = 1/10\ A + 1/10\ D + 1/10\ E + 1/10\ F + 1/10\ I + 1/10\ M + 1/10\ N + 1/10\ P + 1/10\ S + 1/10\ T$
Mitchell and Wyndham (1969) [82]	15	$T_{sk} = 1/15\ A + 1/15\ C + 1/15\ D + 1/15\ E + 1/15\ F + 1/15\ H + 1/15\ I + 1/15\ L + 1/15\ M + 1/15\ N + 1/15\ O + 1/15\ P + 1/15\ R + 1/15\ S + 1/15\ T$

In the present study, measuring skin temperature was conducted seven points method proposed by Hardy and Dubois (Equation (4-6))

$$T_{sk} = 0.07\ T_{head} + 0.35\ T_{trunk} + 0.14\ T_{forearm} + 0.05\ T_{hand} + 0.19\ T_{thigh} + 0.13\ T_{leg} + 0.07\ T_{foot} \quad (4\text{-}6)$$

4.3.3. Results and discussion

4.3.3.1 Environmental factors outdoor and mist spraying environment with sunshade

Mist droplets evaporated from the mist spraying system change the surrounding thermal environment. Fig. 4-8 shows the environmental factor differences between outdoor and mist spraying environments when subject experiments (n = 60) were performed. In the mist spraying system, the outdoor air temperature (mean ± SD (standard deviation)) was changed from 27.7 ± 0.9 °C to 26.3 ± 1.0 °C. MRT (mean ± SD) varied from 36.2 ± 6.1 °C to 23.6 ± 2.3 °C. The main reason for the difference in MRT between outdoor and mist spray system environments is that the surface temperature caused by mist droplets is lowered and the presence of a roof blocks direct sunlight. Because of the large amount of evaporated water, the relative humidity rose from 62.7 ± 7.9% to 70.3 ± 7.8%. Although air blowing was applied, the airspeed was not significantly different from the external mist spray system environment.

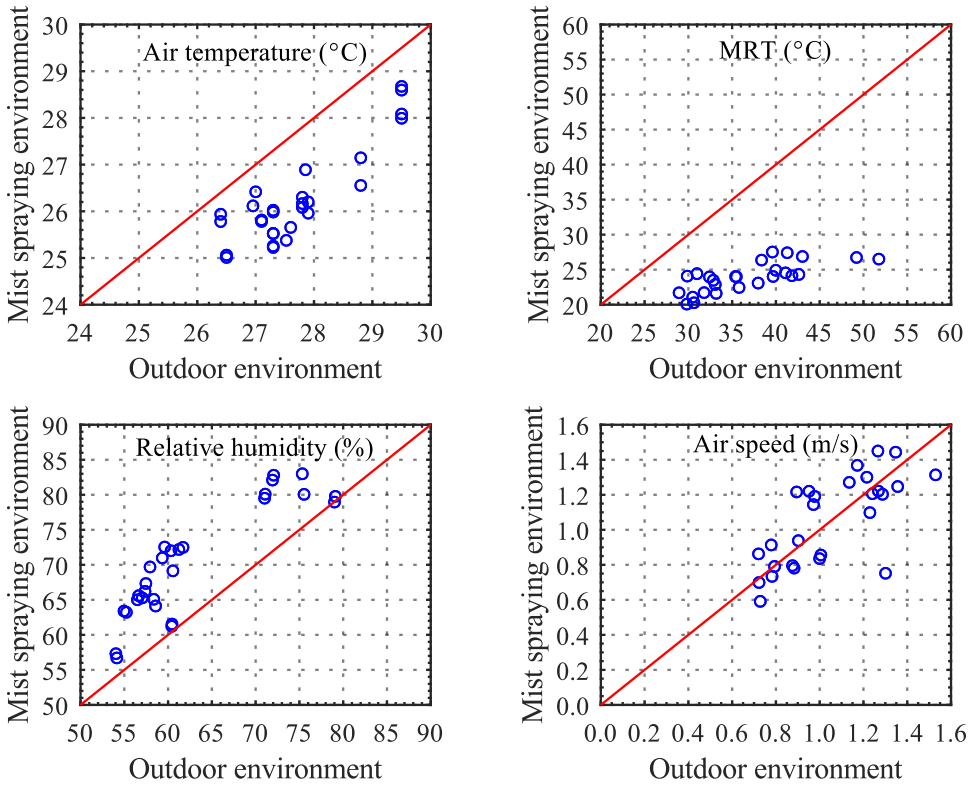

Fig. 4-8. Environmental factor differences between outdoor and mist spraying environments during experiment. Outdoor environment and mist spraying environment correspond to (outside*, outside**), and (inside*, inside**) in Fig. 4-3, respectively.

4.3.3.2 Infrared camera image of subject

Fig. 4-9 shows a few results captured by an infrared camera, before and after entering the mist spraying environment. The photographs were taken with the equipment, FLIR T660 with an accuracy of ± 1.0 °C. After entering the mist spraying environment, the upper body showed the greatest difference than before the mist, with about 1.0 °C difference. It was also found that the temperature difference between before and after entering the mist spraying environment appeared near the head part. Since infrared camera images are not perfectly precise, we only examined the tendency of the cooling effect by the mist.

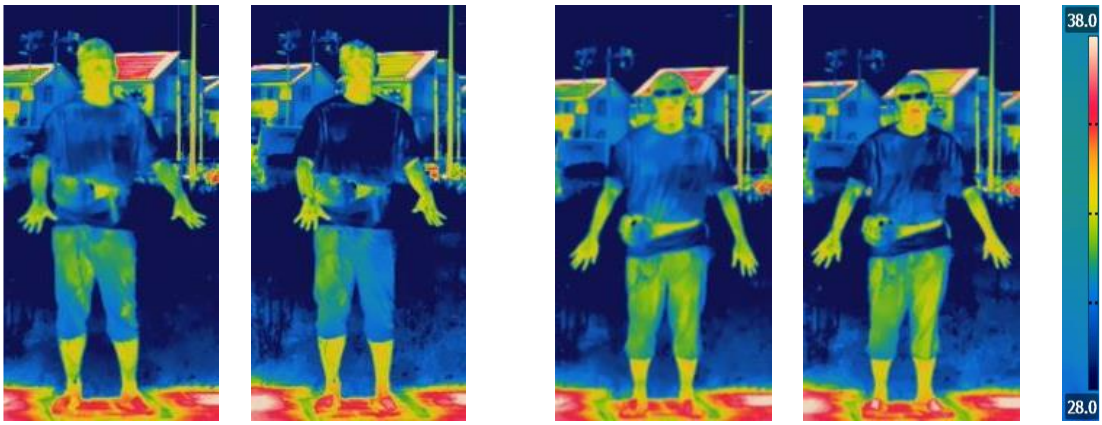

(a) Subject A (b) Subject B

Fig. 4-9. Results of infrared camera image of subjects. Left and right figures correspond to before and after entering mist spraying environment, respectively.

4.4. Physiological human model in outdoor and mist spraying environments

4.4.1. Experimental method for determining the clothing level

4.4.1.1 Thermal manikin experiment

The clothing level was measured in climate chamber in the University of Tokyo. The environmental conditions and thermal manakin were controlled as shown in Table 4-6. The climate chamber controlled at 28 °C. The controlling method of thermal manikin was used constant skin temperature. The skin temperature was set at 33 °C. The clothing insulation level was the same as in subject experiment.

Table 4-6. Experiment condition for determining clothing insulation level.

Climate chamber	
Air temperature (°C)	28
Thermal manikin	
Segments	16
Control type	Surface temperature constant (33 °C)
Clothing	Bra, Panty, Short pants, Short-sleeve shirts, Sandal
Posture	Standing posture

The experimental scenes are shown in Fig. 4-10. The naked manikin on the left figure is a condition for obtaining a total heat transfer coefficient in each segment, and the clothed figure on the right is for measuring the overall clothing insulation level.

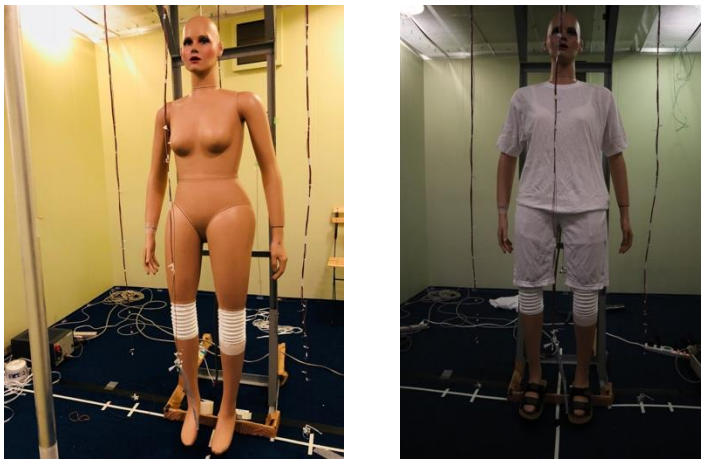

(a) (b)

Fig. 4-10. Thermal manikin in climate chamber (naked (a), and clothed (b)).

4.4.1.2 Calculation method of clothing level

The thermal resistance on the surface of the manikin and clothing insulation level of each segment can be calculated using Equation (4-7). Each thermal resistance at the outer boundary segment is calculated using Equation (4-8) with the results of a naked manikin experiment. The total insulation of each segment can be obtained using Equation (4-9) with the results of a clothed manikin experiment. However, since the clothing area factor is unknown, the overall clothing insulation level cannot directly be obtained from the above two experiments.

$$Q_{\mathrm{t}} = \frac{T_{\mathrm{sk}} - T_{\mathrm{o}}}{R_{\mathrm{clo},i} + \frac{1}{f_{\mathrm{clo},i} h_{\mathrm{t},i}}} \tag{4-7}$$

$$R_{a,i} = \frac{1}{h_{t,i}} = \frac{Q_t}{T_{sk} - T_o} \tag{4-8}$$

$$R_{\mathrm{total},i} = \frac{1}{R_{\mathrm{clo},i} + \frac{1}{f_{\mathrm{clo},i} h_{\mathrm{t},i}}} = \frac{Q_{\mathrm{t}}}{T_{\mathrm{sk}} - T_{\mathrm{o}}} \tag{4-9}$$

The clothing insulation is assumed to be the same in the clothed segment and no clothing insulation in the bare segment. Then, the overall clothing insulation level can be obtained using the overall clothing area factor estimation formula Equation (4-10) and iteration calculation with Equation (4-11)–(4-12).

$$f_{\mathrm{clo}} = 1 + 0.3\ \mathrm{Clo} = \frac{A_{\mathrm{clo}}}{A_{\mathrm{D}}} \qquad R = 0.155\ \mathrm{Clo} \tag{4-10}$$

$$f_{\mathrm{clo}} A_{\mathrm{D}} = A_{\mathrm{D}}(1 + 0.3\ \mathrm{Clo}) = \sum_{i=1}^{16} A_{\mathrm{clo},i} \tag{4-11}$$

$$\mathrm{Clo}_{\mathrm{all}} = \frac{\sum_{i=1}^{16} \mathrm{Clo}_i\, A_{\mathrm{clo},i}}{A_{\mathrm{clo}}} \tag{4-12}$$

4.4.1.3 Results of thermal manikin experiment

The result of the overall clothing insulation level obtained by thermal manikin experiment was 0.58 as summarized in Table 4-7. The clothing insulation is greatly influenced by the material of the clothes and the tightness of clothes on the body. In addition, the result was the female type of manikin and the types of underwear for men and women are different Therefore, since the results of this experiment could not represent the clothing level of all subjects, a value of 0.5 corresponding to the standard level of summer clothing was used for the calculation.

Table 4-7. Result of thermal manikin experiment for comfirming clothing insulation level.

i	Area (m^2)	Heat loss ($W\ m^{-2}$)		Cloth	$h_{t,i}$	$h_{t,i}$	$R_{cl,i}$	Clo_i
		Naked	Clothed					
Head	0.130	41.2	44.3	X	8.4	1.00	0.0138	−0.07
Back	0.130	37.7	22.2	O	7.7	1.26	0.1215	0.73
Chest	0.140	47.0	20.9	O	9.6	1.26	0.1349	0.95
Shoulder (Left)	0.073	42.1	27.1	O	8.6	1.26	0.0827	0.55
Shoulder (Right)	0.078	38.3	26.6	O	7.8	1.26	0.0856	0.51
Arm (Left)	0.050	42.4	48.9	X	8.7	1.00	0.0035	−0.11
Arm (Right)	0.050	39.5	45.7	X	8.1	1.00	0.0103	−0.12
Hand (Left)	0.037	56.2	54.7	X	11.5	1.00	−0.0069	0.00
Hand (Right)	0.038	46.8	50.6	X	9.6	1.00	0.0003	−0.06
Pelvis	0.165	43.3	14.7	O	8.8	1.26	0.2315	1.52
Thigh (Left)	0.160	46.6	23.2	O	9.5	1.26	0.1125	0.80
Thigh (Right)	0.166	42.9	20.8	O	8.7	1.26	0.1358	0.90
Leg (Left)	0.090	49.1	47.0	X	10.0	1.00	0.0074	0.01
Leg (Right)	0.090	47.2	46.5	X	9.6	1.00	0.0085	0.00
Foot (Left)	0.043	48.0	29.6	O	9.8	1.26	0.0678	0.52
Foot (Right)	0.043	49.7	30.5	O	10.1	1.26	0.0626	0.51
Total	1.483	44.1	30.3	-	9.0	-	0.09	0.58

4.4.2. Validation of two-node model

4.4.2.1 Calculation condition for validation of two-node model

The conditions of 2NM model for validation of skin temperature were listed in Table 4-8. Since the subjects' initial were not in a physiologically thermoneutral state on the experiment, initial skin temperatures were set the measured data. As the core temperature did not change significantly in a short time, initial core temperature was set at 36.8 °C which is the physiologically thermoneutral state [88]. Metabolic rate and clothing insulations were set to 1.2 and 0.5, respectively. Environmental factors measured at each condition were used to predict subjects' skin temperature changes in the outdoor and mist spraying environments. The measured environmental factors averaged at 1-minute intervals and applied it as input variables in 2NM.

Table 4-8. Calculation conditions of 2NM for validation of skin temperature.

Factor	Variables	Value
Human	Metabolic rate (met)	1.2
	Clothing insulation (clo)	0.5
	Initial mean skin temperature (°C)	Measured mean skin temperature (T_{sk})
	Initial core temperature (°C)	36.8
	Initial core temperature (°C)	$T_{body} = 0.1\,T_{sk} + 0.9\,T_{core}$
	Neutral mean skin temperature (°C)	$T_{sk}^{n} = 33.7$
	Neutral core temperature (°C)	$T_{core}^{n} = 36.8$
	Neutral body temperature (°C)	$T_{body}^{n} = 36.49$, $(0.1\,T_{sk} + 0.9\,T_{core})$
Environment	Air temperature	averaged at 1-minute intervals (before entering the mist spraying environment at 0–10 minutes and after entered the mist spraying environment at 10–20 minutes)
	MRT	
	Relative humidity	
	Airspeed	

4.5. Results and discussion

4.5.1. Skin temperature variation

Fig. 4-11 shows the results of the mean skin and core temperatures for nine subjects. In all cases, the initial skin temperature (mean ± SD) was 34.5 ± 0.63 °C, which is higher than the physiologically thermoneutral temperature. Skin temperature did not show a representative trend before entering the mist spraying environment but decreased in all subjects in mist spraying environment. The skin temperature (mean ± SD) changes before entering the mist system was 0 ± 0.18 °C for 10 minutes, which was 0.28 ± 0.40 °C higher than the predicted results. After entering the mist environment, the skin temperature changes (mean ± SD) in the measurement and prediction results decreased by 0.69 ± 0.27 °C and 0.60 ± 0.31 °C for 10 minutes, respectively. The difference in skin temperature changes between the experimental and calculated results was analyzed by paired *t*-test. In the results, the probability value (*p*-value) were 0.07 before entering the mist spraying environment and 0.23 after entering the mist spraying environment, respectively. This indicates that measured and predicted skin temperature changes are not statistically significant.

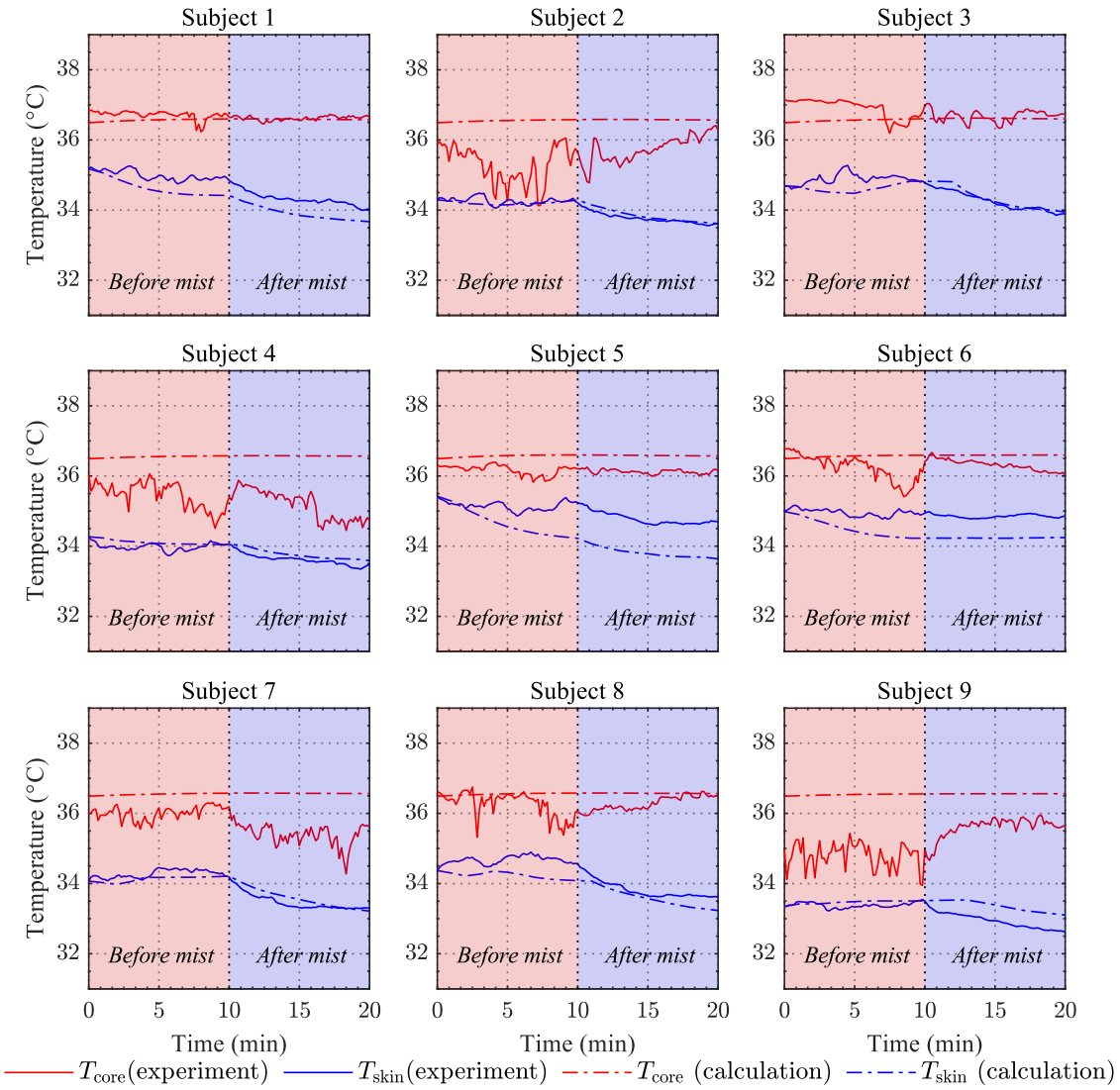

Fig. 4-11. Results of changes in mean skin and core temperature before and after entering mist spraying environment. The environmental conditions before and after the mist correspond to the results of (outside*, outside**) and (inside*, inside**) in Fig. 4-3, respectively.

The individual differences of subjects in measurement and prediction results can be understood to be caused by the uneven and complex environmental conditions of the mist spraying environment. The predicted results showed better accuracy within the mist spraying environment than outside, because direct solar radiation has a high impact on the human body in the outdoor environment but is blocked in the mist spraying environment by the sunshade. Meanwhile, the oral temperature, which is the baseline data for the core temperature, showed frequent fluctuations because the sensor position was unstable in the oral cavity and breathed during the experiment.

4.5.2. Calculation condition for standard condition

A correlation analysis between the predicted physiological response and mTSV was performed to confirm that the predictive model could identify thermal sensations even in a mist spraying environment. As a calculation condition, it is assumed that the human body in the physiological thermal neutral state is exposed to the measurement environment. Thus, the initial average skin temperature and core temperature were set to physiological thermal neutral conditions at 33.7 °C and 36.8 °C, respectively. Using the average value of the measured environmental factors, it is assumed that the environmental conditions are uniform. Detailed calculation conditions are described in Table 4-9.

Table 4-9. Calculation conditions of 2NM for comparison with thermal sensation results.

Factor	Variables	Value
Human	Metabolic rate (met)	1.2
	Clothing insulation (clo)	0.5
	Initial mean skin temperature (°C)	33.7
	Initial core temperature (°C)	36.8
	Initial core temperature (°C)	$T_{\mathrm{body}} = 0.1\,T_{\mathrm{sk}} + 0.9\,T_{\mathrm{core}}$
	Neutral mean skin temperature (°C)	$T_{\mathrm{sk}}^{n} = 33.7$
	Neutral core temperature (°C)	$T_{\mathrm{core}}^{n} = 36.8$
	Neutral body temperature (°C)	$T_{\mathrm{body}}^{n} = 36.49$, $(0.1\,T_{\mathrm{sk}} + 0.9\,T_{\mathrm{core}})$
Environment	Air temperature (°C)	Average value for measured data for 10 minutes and considered the stable environment condition during calculation
	MRT (°C)	
	Relative humidity (%)	
	Airspeed (m/s)	

The thermal state of the body was calculated for the outside (n = 72) and inside (n = 60) of the mist spraying environment where the survey was conducted. Results were sorted and averaged according to the results of mTSV scale. Fig. 4-12 Figure 4 12 shows the results of the average skin and core temperatures for each mTSV scale. When the results of the mTSV scale were high, the average skin temperature increased even more. Skin temperature increased outside the mist spraying environment but decreased inside the mist spraying environment. The core temperature increased more externally than inside the mist spraying environment, but there was no significant difference depending on the mTSV scale outside or inside the mist spraying system.

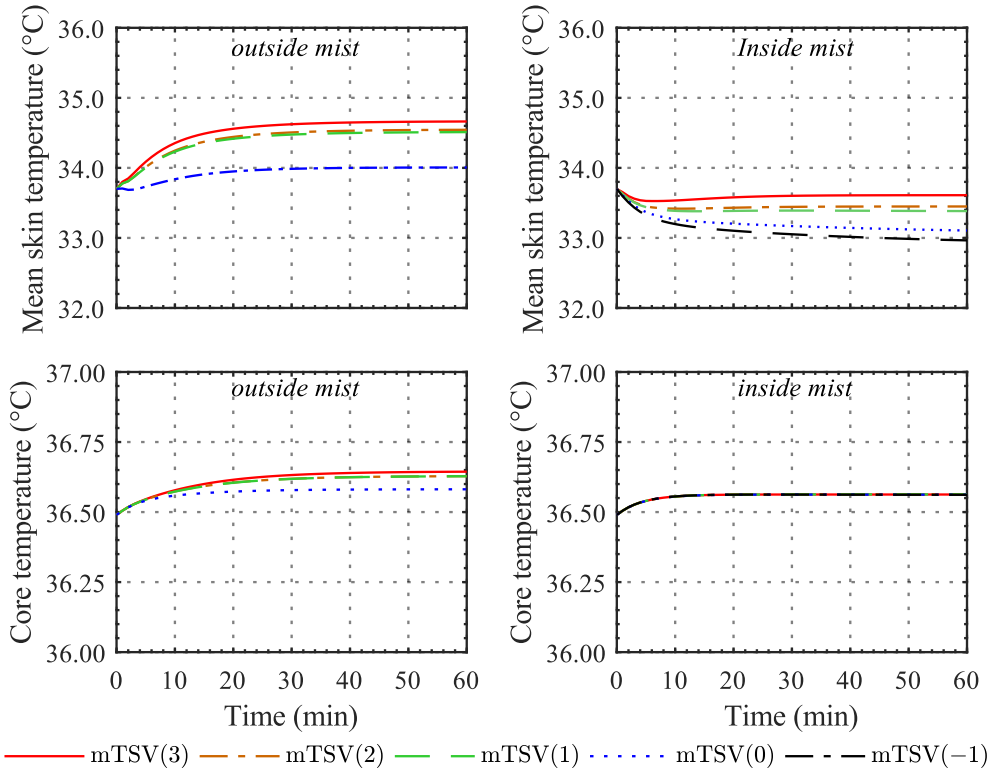

Fig. 4-12. Mean skin and core temperature change results for each mTSV scale.

Fig. 4-13 shows the results of the heat storage rate, sensible heat loss, latent heat loss, and skin wettedness. The heat storage rate was calculated using equation (4-13) introduced by Fanger [35]. The heat storage rate converged close to zero due to the temperature control response of the human body.

$$S_{\mathrm{body}} = (M - W) - E_{\mathrm{sk}} - Q_{\mathrm{res}} - Q_{\mathrm{rad}} - Q_{\mathrm{conv}} \tag{4-13}$$

where, S is the heat storage rate in the body, M is the production of metabolic heat, W is the mechanical work achieved, and E_{sk} is the sum of heat loss by the diffusion of water vapor through the skin and heat loss by evaporation of sweat on the skin surface. Q_{res} is latent heat loss and sensible heat loss due to breathing, Q_{rad} is radiant heat loss that occurs on the covering surface of the body and Q_{conv} is convective heat loss at the covering surface of the body.

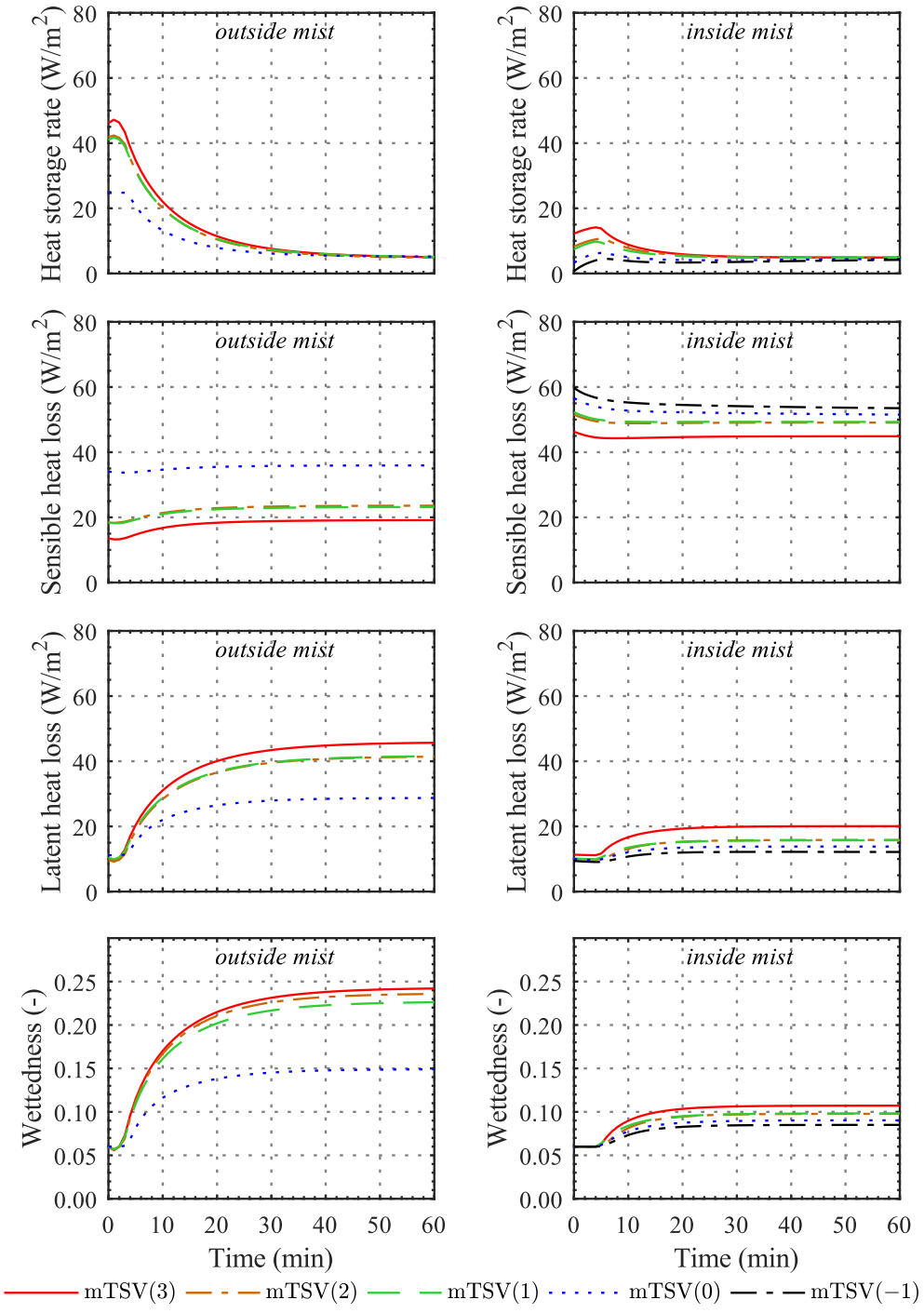

Fig. 4-13. Mean heat losses and physiological responses change results for each mTSV scale.

The mean skin temperature tended to increase with higher mTSV before and after entering the mist spraying environment. The core temperature did not change significantly under both conditions. Sensible heat loss decreased with increasing mTSV value, while latent heat loss and skin wettedness

increased. Due to the low ambient temperature, the existing heat losses in the mist spraying environment were higher than in the outdoor environment, but the skin wettedness was lower, resulting in lower latent heat losses. Therefore, the results can be summarized as follows: Under hot outdoor air temperature or hot weather conditions with high MRT, the sensible heat loss can be reduced, but latent heat loss may increase due to sweating caused by thermoregulation control.

4.6. Conclusion

This chapter describes the estimation of the physiological response of the human body in a mist spraying environment. Subjective assessments were conducted, and also, environmental factors and overall skin temperature were measured in outdoor and mist spraying environments. The thermal state of the human body was estimated using Gagge's two-node model along with the measured environmental factors. The two-node model was verified by comparing it with the subjects (n = 9) skin temperature data. The mean skin temperature changes (mean ± SD) before entering the mist system were 0 ± 0.18 °C in the experiment and 0.28 ± 0.40 °C in prediction. After entering the mist system, the skin temperature changes (mean ± SD) in the experiment and prediction results decreased by 0.69 ± 0.27 °C and 0.60 ± 0.31 °C for 10 minutes, respectively. As a result, the two-node model was observed to have high prediction accuracy for both outdoor and mist spraying environments. In addition, the thermal state of the body was calculated for the outside (n = 72) and the inside (n = 60) of the mist spraying environment in which the investigation was performed. Predicted physiological response results were sorted and averaged according to each mTSV scale. The results showed significant differences according to the mTSV scale. Predicting the physiological response of the human body using 2NM was well reflected in the thermal sensation in outdoor and mist spraying environments.

However, in the mist spraying environment, a human body gets wet by mist droplets. The smaller the diameter of the mist droplet, the faster it evaporates in the air and the body feels wet lesser. Although the field experiment in this chapter could not identify the evaporative heat loss due to mist droplets on the human body surface, it is necessary to clarify the mist environment and human body heat exchange to understand the thermal sensation, thermal comfort, and thermal state of the human body in mist spraying environments.

Chapter 5. Evaluation of mist spraying environment considering mist wettedness

Chapter 5. Evaluation of mist spraying environment considering mist wettedness

5.1. Background and objectives

Global temperatures have been warming over the last century [89]. In addition, many studies have shown that hot outdoor environments affect human health and mortality [2–5]. Therefore, the impact of urban heat island and climate change on the human body has become a critical issue. Outdoor environments are also important in sustainable cities because they include daily pedestrian traffic and outdoor activities that contribute to the urban environment and vitality [90]. However, due to the dynamic fluctuation of outdoor environmental conditions, it is difficult to clearly determine the effect of the thermal environment on the human body. Therefore, various kinds of studies have been conducted to understand thermal sensations in outdoor environments. In earlier studies, human thermal sensations in outdoor environments were investigated by using subjective assessment and measuring environmental factors [91,92]. Stathopoulos et al. examined the surveys and field measurements to investigate the correlation between environmental factors and thermal comfort [93]. Lai et al. predict skin temperature using a physiological thermoregulation model to understand human thermal conditions in outdoor environments [72]. They found a good correlation between average skin temperature and thermal sensation in various outdoor conditions, and their studies showed the possibility of predicting the thermal sensation and thermal state of the body in outdoor environments. Xie et al. were investigated a comparison of the thermal sensation in the outdoor environment with the prediction results by the UCB model (UC-Berkeley thermal comfort model) [94]. In outdoor environments, UCB models do not reflect actual thermal sensations that are sensitive to wind speed and solar radiation. In addition, Xie et al. tracked the trend of outdoor hot spots in Hong Kong for two years, and they found a human's heat adaptation in outdoor environments for seasons using a probit analysis [95].

Recently, in hot outdoor environments, mist spraying systems have been widely used as a means to reduce high temperatures [11,12,17]. In general, mist spray systems are useful for relieving thermal stress and improving thermal comfort in hot outdoor environments [15]. However, due to the high humidity in which many mist particles are suspended in the atmosphere, the mist spray environment is a more complex thermal environment than the outdoor environment. Sulfur etc. The mist spray system has confirmed that it can lower the air temperature to 5–7 °C in a hot environment [11] In the climate chamber experiments, the mist spraying system was able to lower the air temperature to 10 °C [12].

However, while the study focused only on changes in temperature and humidity, changes in other

environmental factors have not been fully investigated. Consideration should also be given to solar irradiation, which greatly affects thermal comfort in outdoor environments [46]. Although there are considerable studies evaluating the thermal state of humans in hot weather conditions in outdoor and mist spraying environments, there is a lack of research on the thermal effects of mist spraying environments on the human body, especially taking into account the environmental factors that can affect them. Therefore, it is necessary to compare the internal and external environmental factors of the mist spraying environment, including air temperature, humidity, radiation, and airspeed to verify the effect of the mist spraying system on the thermal sensation and the outdoor environment conditions. Oh et al. studied to understand the impact of the mist spraying system on hot outdoor environments by comparing the difference between the internal and external environmental factors of the mist spray environment [27]. However, in this study, since the mist spray environment has a sunshade, the effect of radiation was significantly less than in outdoor environments. Thus, the independent cooling effect of the mist spraying system on the thermal sensations and thermal comfort under the same radiation conditions as the outdoor environment is not yet known.

Shivering, blood flow rate change and sweating are part of the body's thermoregulating physiological response. These physiological responses are closely related to the thermal sensation as a thermal interaction between the environment and the human body. Farnham et al. confirmed the forearm temperature changed after entering the mist spraying environment, and the skin temperature dropped to 1–3 °C [15]. However, it is still difficult to understand the effect of the mist spraying environment on human physiological responses by investigating temperature changes only in parts of the body. To fully investigate the effect on the human body, it is important to understand the thermal state of the whole-body scale. Ulpiani et al. measured the thermal sensation, thermal comfort, and environmental factors, evaluated the mist spraying environment to understand the thermal effects using the universal thermal climate index (UTCI) index [16]. However, conventional indices have a limitation in assessing thermal sensations and thermal comfort because these indices do not consider the evaporative heat loss on the body surface due to the mist particles [27].

In conventional mist spraying methods, the mist is generally diffused without an air blowing mode. However, this type of mist spraying system has a limitation that the cooled air cannot be properly delivered to the vicinity of the human body. When strong winds blow from the outside, it is very difficult to deliver cooled air and mist to the desired location. For this reason, a mist spray system equipped with an air blowing fan has been inspected [15]; This method has been found to be more effective in relieving heat stress and improving thermal comfort in a person compared to systems without a blower fan. Nevertheless, the main environmental factors that influence the maximization of the mist's evaporative cooling effect when the mist is diffused by forced air are not clearly explored. In addition, in addition to the blowing, operating parameters of the mist system such as the spray amount of the mist particles were not investigated. To increase the effectiveness of the evaporative

cooling of the mist system, it is necessary to check the various modes of operation.

In order to solve the above-mentioned issues, thermal sensations, and thermal comfort, overall environmental factors (air temperature, radiation, humidity, and airspeed), and overall skin temperature changes in outdoor and mist spraying environments were examined. In addition, the effects of an operation mode of mist spraying systems on these assessments were additionally investigated. In order to estimate the independent impact of the mist spraying system on the thermal environment, the radiation conditions inside and outside the mist spraying environment were measured. Through the survey research, subjective assessments were performed using the modified thermal sensation vote (mTSV), thermal sensation vote (TSV), and comfort sensation vote (CSV) scales. In addition, the overall skin temperature was monitored to understand the thermal state of the body and physiological responses during the experiment. The measured skin temperature and subjective evaluation results were analyzed to verify the cooling effect of the mist spraying system. The results of this study are expected to be used to correctly understand the effects of the mist spraying environment on the human body. In addition, experimental data from the operation of the mist spraying system in different modes of operation can provide a basic understanding of the control variables affecting this system. In addition, the analysis of this study can be useful for identifying physical phenomena in the human body and for predicting thermal conditions and physiological reactions under the influence of outdoor and mist spraying environments.

5.2. Experimental setup

5.2.1. Operation conditions of mist spraying system

As shown in Table 5-1, four different modes were conducted considering different amounts of mist spraying and presence of air blowing mode. The mist droplet size was set as 9–11 μm so that the mist particles can be fully evaporated when they are suspended in the air. The height of the mist spraying nozzle was 3.0 m above the ground. In Table 5-1, CASE-1 was set as the baseline operating mode that has a droplet size of 11 μm with a mist spraying amount of 300 cm^3/min in the air blowing mode. CASE-2 sprays the same amount of water as CASE-1 but has no air blowing mode. The effects of air blowing mode on the assessment of the mist spraying system can be confirmed. CASE-3 sprays less water than CASE-1 and controlled as 240 cm^3/min. The effects of the amount of spraying water on the assessment of the mist spraying environment can be understood by comparing the results of CASE-1 and CASE-3. CASE-4 refers to an air blowing mode without spraying of water.

Table 5-1. Operation modes of mist spraying system.

Variables	CASE-1 (baseline)	CASE-2 (without air blowing)	CASE-3 (less mist)	CASE-4 (without mist)
mist droplet size*	11	11	9	-
amount of spraying water (cm^3/min)	300	300	240	-
existence of air blowing	O	X	O	O

Note: Mist droplet size* is the mean particle size of water spraying distribution, which is the value of the Sauter mean diameter measured by laser diffraction instrument [96].

5.2.2. Measurements of environmental factors

The field experiments with considering mist wettedness were performed from July 23 to August 4, 2018. Mist spraying system was installed at the Institute of Industrial Science, University of Tokyo, Japan (Fig. 5-1). Subject experiments were performed only during the day (10 am–4 pm) corresponding to hot weather. The following environmental factors were simultaneously measured both inside and outside the mist spraying environment: temperature, radiation, humidity, and airspeed. Details of the measuring equipment and installation locations are listed in Table 5-2, and the installation of this spray system, measuring equipment and target experiments is shown in Fig. 5-1. All measurements were made at a height of 1.1 m, corresponding to the center of the standing human body [88].

Previous studies have shown that mist droplets make it difficult to accurately measure environmental factors in a mist spraying environment [15,76]. If the sensor gets wet, it cannot be measured by evaporative heat loss. Therefore, a device was developed to measure air temperature and relative humidity with sucking air in the opposite direction of the mist spraying direction by using an air compressor to prevent the measurement equipment from getting wet (Fig. 5-2c).

Environmental factors were measured by placing temperature and humidity sensors inside the developed equipment. The flow rate of the air compressor was set to 5.5 L/min. For cross-validation of measured data, relative humidity was further measured and compared using an infrared H_2O analyzer capable of detecting the mole fraction of water vapor in the air. The relative humidity measured by the humidity sensor and infrared H_2O analyzer was about the same. On the other hand, the hot wire anemometer was used because it is impossible to measure when wet or blocked flow. All measurement data was recorded at 1-second intervals.

In outdoor environments, shading greatly affects the thermal comfort of a person [46]. As the sunshade is greatly reduced when using the sunshade as in Chapter 4, it is important to design the same radiation environment as the outdoor environment in order to confirm the independent cooling effect of the mist spraying system. In this experiment, the measurement locations for outdoor and mist

spraying environments were chosen so that the radiation effects of the surrounding buildings and the sun were the same. As shown in Fig. 5-1b, radiation was obtained using short and longwave radiation meters and direct radiation meters. The direct solar radiation measurement equipment was measured only inside the mist because the outdoor and mist environment was the same.

Table 5-2. Measurements for mist wettedness.

Instrument	Measurement variables	Location†	Height (m)	Range	Accuracy
EK-H4 (SHT71)	air temperature (T_a)	inside* / inside** / outside	1.1	0–60 °C	±0.4 °C
	relative humidity (RH)			0–100%	±0.3%
CGY-81000	airspeed (v)	inside** / outside	1.1	0–60 m/s	±0.3%
LI-7200 RS	relative humidity (RH)	inside* / outside	1.1	0–95%	
MR-60	radiation ($S\uparrow, S\downarrow, L\uparrow, L\uparrow$)	inside** / outside	1.1		
STR-22G	direct solar radiation (I_{dn})	inside**	-		

Note: Location † is position of instruments inside and outside the mist spraying environment. Inside* is the area wet by mist droplets. Inside** is the area that does not get wet with mist droplets. The inside*, inside**, and external locations † are described in (Fig. 5-1b).

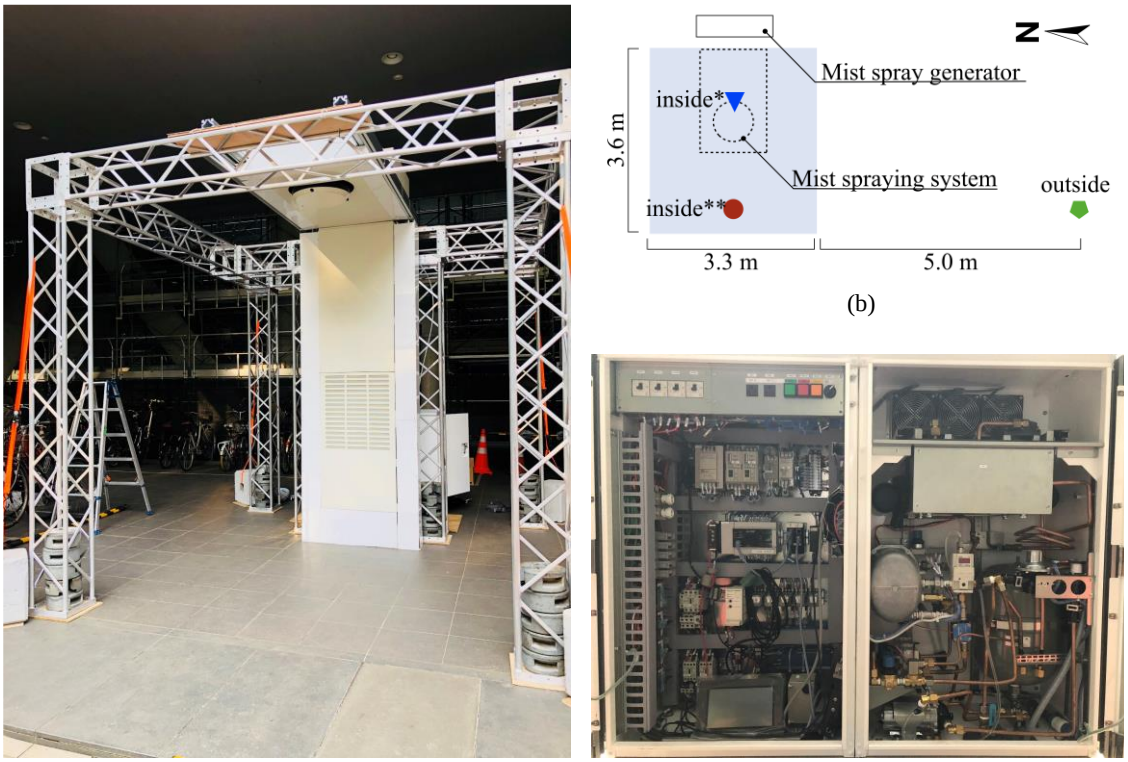

Fig. 5-1. Mist spraying system installed at the Institute of Industrial Science of the University of Tokyo, Japan (July 23–August 4, 2018): (a) overall appearance of the mist spraying system; (b) a top view of the mist spraying system and the location of instruments; (c) Mist spraying generators (i.e. pressure pumps, water tanks and control devices).

(a) (b)

(c)

Fig. 5-2. Equipment for measuring environmental factors in outdoor and mist spraying environments. (a) inside** representing shortwave and longwave radiation, direct solar radiation, and ultrasonic anemometers; inside* representing infrared H_2O analyzers and air temperature and humidity sensor; (b) displays air temperature and humidity sensor, shortwave and longwave radiation meters, ultrasonic anemometers, infrared H_2O analyzers installed outside, and (c) showing air temperature and humidity sensors in inside*.

5.2.3. Measuring mean radiant temperature (MRT)

Humphreys has proposed the use of a 40 mm diameter table-tennis ball to measure average radiant temperature (MRT) in indoor and outdoor environments [97] and widely have been used. In the outdoor environment, however, Wang and Li confirmed that the thermal response of the ping-pong ball is not suitable for estimating the MRT of the outdoor environment [98]. Therefore, in the present study, MRT was calculated based on Equation (5-1) to understand the effect of radiation on the human body. The sun was tracked and measured direct solar radiation, long and short radiation was measured using an upper and lower bidirectional radiation meter. These environmental factors were measured

where the effects of mist particles were minimal (outside and inside** location for measurements in Fig. 5-1).

$$T_{\mathrm{mrt}} = \sqrt[4]{\frac{1}{\sigma}\left(f_{\mathrm{eff}}\left(\frac{\alpha_{\mathrm{k}}}{\varepsilon}\cdot\frac{I_{\mathrm{dH}}+S\uparrow}{2}+\frac{L\downarrow+L\uparrow}{2}\right)+\frac{\alpha\cdot f_{\mathrm{p}}}{\varepsilon}\cdot I_{\mathrm{dN}}\right)}-273.15 \quad (5\text{-}1)$$

where, σ is the Stefan-Boltzmann constant (5.67×10^{-8}, W m^{-2} K^{-4}), f_{eff} is the effective body area factor of the radiation (assumed as 0.87), I_{dH} is the diffuse solar radiation on a horizontal surface calculated using the downward short radiation of $S\downarrow$, the direct solar radiation on normal surface of I_{dN}, and the solar altitude of β (i.e., $I_{\mathrm{dH}} = S\downarrow - I_{\mathrm{dN}}\cdot sin\beta$). $S\uparrow$ is the upward shortwave radiation, $L\downarrow$ is the downward longwave radiation, $L\uparrow$ is the upward longwave radiation, α is the absorptivity of the clothed human body by the shortwave radiation assumed as 0.7. The emissivity rate ε by the longwave on human body was assumed as 0.95. The project area coefficient f_{p} of a standing person by the direct solar radiation can be calculated using Equation (5-2) suggested by Park and Tuller [79].

$$f_{\mathrm{p}} = 3.01\times10^{-7}\beta^3 - 6.46\times10^{-5}\beta^2 + 8.34\times10^{-4}\beta + 0.298 \quad (5\text{-}2)$$

The altitude of the sun β was calculated with the logged time and location of the Institute of Industrial Science, the University of Tokyo (latitude of 35° 66'N, longitude of 139° 68'E location information was obtained from Google map).

5.2.4. Subject experiment setup

65 subjects participated in the field experiment. The average age, weight, height and BMI of all participants were 26.6 ± 8.4 years, 59.6 ± 10.1 kg, 1.67 ± 0.072 m and 21.1 ± 2.4, respectively, as listed in Table 5-3. A schematic of this experimental protocol is shown in Fig. 5-3. The experimental procedure was approved by the University of Tokyo Ethics Committee (No. 18-114), and all participating subjects received written consent (see Appendix 3). At the initial stage of the field experiment, the subjects rested for 20 minutes in an indoor environment, controlling the air temperature to 26 °C with an air conditioner, considering the usual cooling setpoint temperature in the summer season. After a break, they walked outside for 10 minutes and then stayed inside the mist spraying environment for 10 minutes. The subject reported the first survey after 10 minutes of walking.

Second and third surveys were performed at 3 and 10 minutes after the subject entered the mist spraying environment, respectively.

Table 5-3. Characteristics of subjects.

	Age (year)	Weight (kg)	Height (m)	BMI
	Mean ± SD (standard deviation)			
Men (n = 41)	25.1 ± 6.1	63.7 ± 9.6	1.71 ± 0.056	21.6 ± 2.7
Women (n = 24)	29.5 ± 11.2	52.3 ± 5.8	1.61 ± 0.046	20.1 ± 1.6
Total (n = 65)	26.6 ± 8.4	59.6 ± 10.1	1.67 ± 0.072	21.1 ± 2.4

n is number of subjects.

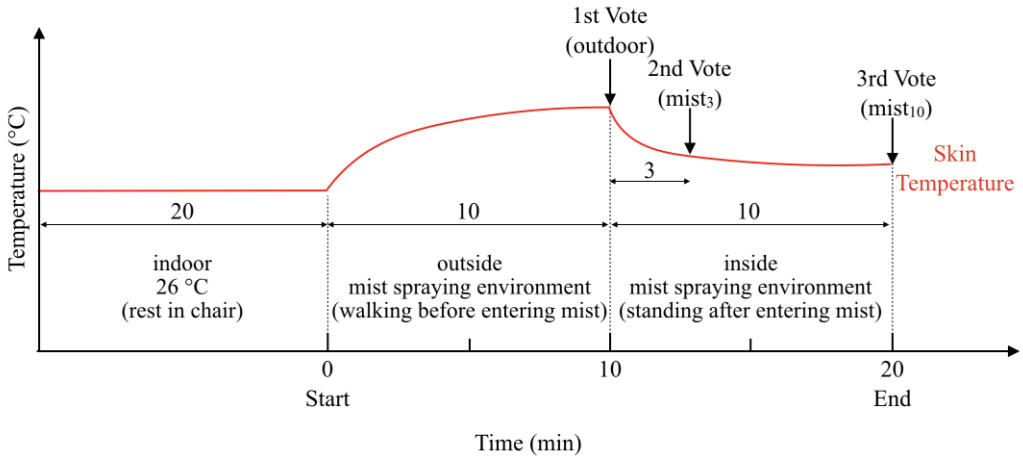

Fig. 5-3. Schematic diagram of subject experimental protocol showing timetable. Experimental conditions for outdoor and mist spraying environments correspond to (outside) and (inside*, inside**) in Table 5-1b, respectively.

In relation to the physiological response, skin temperature was measured to check the thermal state of the body. Skin temperature was measured by a thermocouple (accuracy: ± 0.5 °C) and recorded at 5-second intervals by LR-8430 (HIOKI Corporation, Japan). The thermocouple was attached to the skin surface of the subject with surgical tape. The mean skin temperature T_{overall} was calculated of an area-weighted average of the body segments: head, torso, forearm, hand, thigh, leg and foot (T_i is the surface temperature of body segment i) using the equation (4-6) proposed by Hardy and Dubois [80,87].

5.2.5. Statistical analysis

Statistical analysis was performed using MATLAB version R2018a. First, the impact of

environmental factors and subjective evaluations on the control variables of the mist system was confirmed by analyzing the results of the various modes of operation. For example, the effect of spraying quantity on the cooling effect can be estimated by comparing the results of CASE-1 (reference) with those of other cases. Survey results from two comparable but different modes of operation were analyzed by paired t-tests and are typically used to compare the mean difference between two variables. The null hypothesis assumes that the mean of the variable between the two groups is zero [99].

Second, Pearson's correlation coefficient, a statistical indicator, was used to assess the correlation between total skin temperature and thermal sensation. Pearson's correlation coefficient can be derived from the range -1 to 1. Closer to 1 indicates that the two variables are positively correlated. Close to -1 indicates that these variables are negatively correlated. The null hypothesis of Pearson's analysis is that the two comparison variables are not statistically correlated.

5.3. Concepts of mist wettedness

The mist spraying environment, mist particles are sprayed in an air and cool down the air temperature. By the way, the sprayed mist droplets are not completely dried in an air. Therefore, the water particles are attached to the surface of the body and evaporated. The evaporation of water particles from the surface makes the additional cooling effect. The schematic diagram of heat loss mechanism by skin wettedness and mist wettedness is illustrated in Fig. 5-4. Evaporative heat loss due to skin wettedness occurs on the skin surface. On the other hand, the mist droplets adhere to the body surface and evaporation on there. Thus, if the body part is covered by clothes, heat loss by mist wettedness occurs on the clothing surface. Otherwise, heat loss happens on the skin surface. Therefore, in 3NM calculation, both conditions are necessary to be considered, but the only clothed condition is necessary for 2NM calculation.

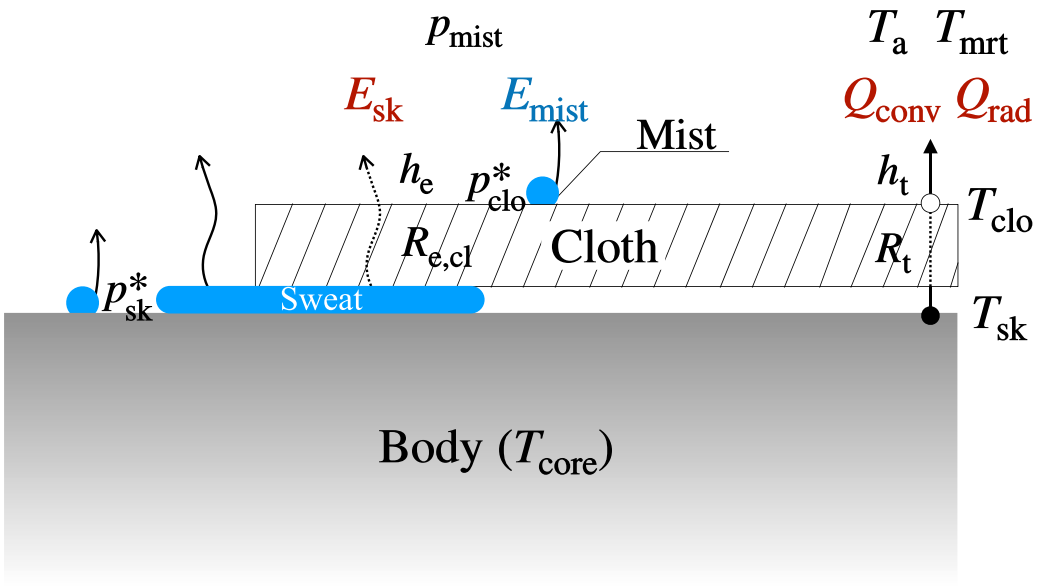

Fig. 5-4. Schematic diagram of heat loss on body surface by skin wettedness and mist wettedness.

5.3.1. Design of mist wettedness meter

Evaporative heat loss at the surface is determined by the surface temperature and the partial pressure of water in the air. However, as the measuring evaporative heat loss on the body surface directly is difficult, as a simplified method, a globe thermometer was utilized as described in Fig. 5-5. The sensors and measuring instruments for measuring mist wettedness are listed in Table 5-4. Two ceramic heaters were attached inside the globe thermometer to control the skin temperature. The power of the heating elements was controlled by SSR, and the surface temperature is measured by two film types PT100 and the average value was calculated. The surface temperature of the heating globe thermometer was controlled at 35 °C by PID controller. Fig. 5-6 shows the actual heating globe thermometer (mist wettedness meter) and its controller.

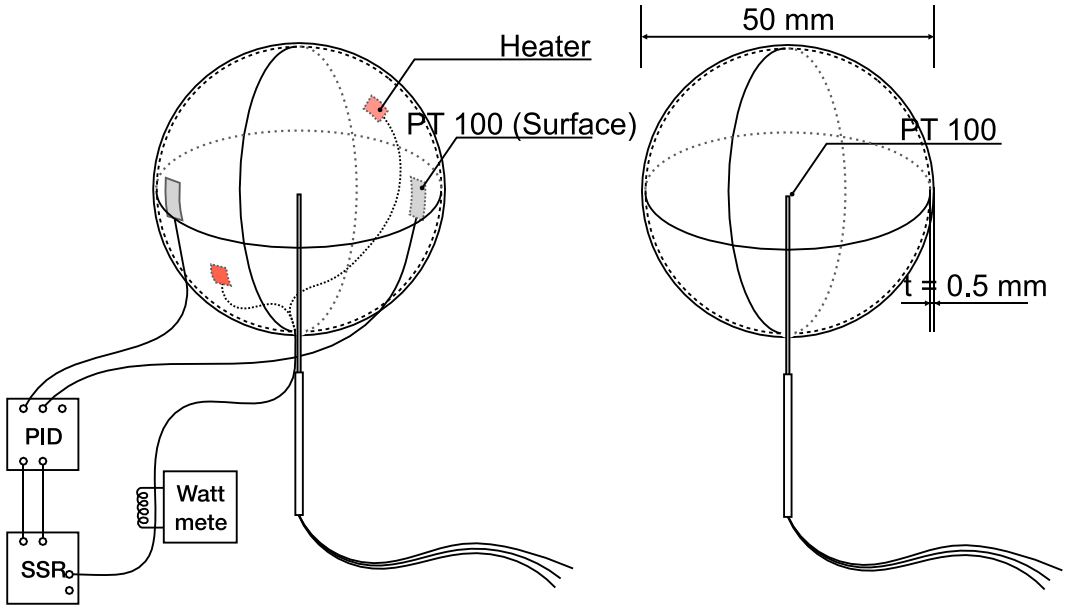

Fig. 5-5. Design of heating globe thermometer for measuring mist wettedness.

Table 5-4. Measurements for mist wettedness.

Instrument	Measurement variables	Height (m)	Range	Accuracy
EK-H4 (SHT71)	air temperature (T_a and T_{mist})	1.1	0–60 °C	±0.4 °C
	relative humidity (RH) for p_{mist}	1.1	0–100%	±3.0%
CGY-81000	airspeed (v) for h_c calculation	1.1	0–60 m/s	±1.0%
PT100	globe temperature (T_g and T_{gh})	1.1	up to 200 °C	±0.1 °C
	surface temperature*			
NFR-CF-PT100	heat input (H)	-	up to 200 °C	±0.1 °C
DW-777		-	0–9999 W	±1.0%

Note: The surface temperature* of heating globe thermometer was measured with two thermometers, and the average value was set to 35 °C.

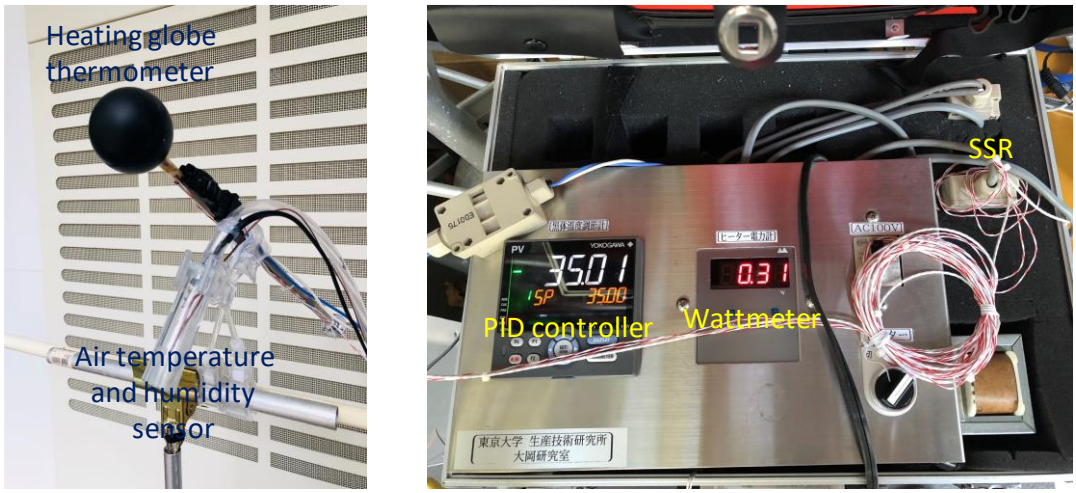

Fig. 5-6. Mist wettedness meter and its controller.

5.3.2. Mist wettedness measurement

The evaporative heat loss on the skin is caused by natural diffusion of water through the skin and the sweating for the thermoregulation control. The skin wettedness (ω_{sk}) is defined as the ratio of the actual evaporative heat loss on a skin surface to maximum possible evaporative heat loss [100]. Similarly, the mist wettedness can be defined as the ratio of the actual evaporative heat loss due to the mist droplets on the surface of the body for the maximum possible evaporative heat loss under the same conditions. The heat loss due to skin wettedness occurs at the skin surface, but heat loss due to mist wettedenss occurs at the surface of the body (skin or cloth) where get wet by the mist droplets.

However, since heat loss from the body surface by mist droplets is difficult to measure directly, a heating globe thermometer was introduced to investigate the heat loss by mist droplets on the body surface as shown in Fig. 5-7. The water evaporation capability on the surface depends on surface temperature and water vapor pressure in the air. The heating globe thermometer was controlled at the skin temperature level to determine the evaporative heat loss on the surface of the body. As a similar manner, Nakayoshi et al. measured wind speed and shortwave and longwave radiation fluxes using three globe thermometers in an outdoor environment [101]. However, the evaporative heat loss on the surface cannot simply be measured because of complex heat exchanges between globe thermometer and outdoor and mist spraying environments. Thus, another normal globe thermometer of the same size as the heating globe thermometer was placed near the mist spraying environment.

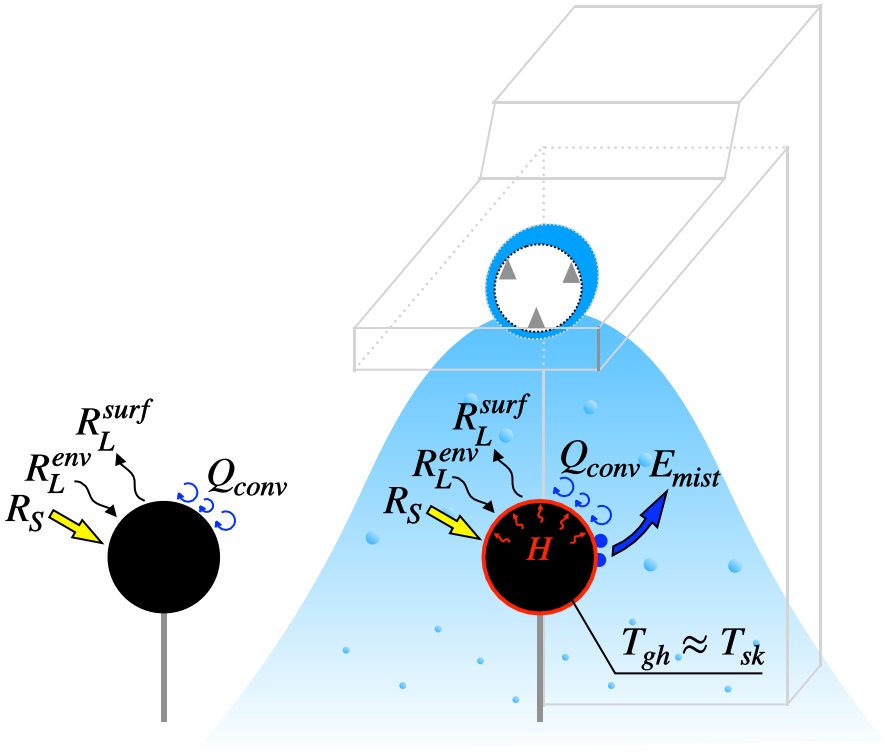

Fig. 5-7. Schematic diagram of measuring mist wettedness using heating globe thermometer. Heating globe thermometer and globe thermometer are placed in wetted and non-wetted areas inside mist spraying environment, respectively.

Heat balance equations on globe thermometer and heating globe thermometer can be expressed Equation (5-3) and Equation (5-4), respectively.

$$\frac{C_g}{A}\left(\frac{dT_g}{dt}\right) = (1-\alpha)\,S + \varepsilon\,L - \varepsilon\,\sigma\,T_g^4 - h_c\left(T_g - T_a\right) \tag{5-3}$$

$$\frac{C_g}{A}\left(\frac{dT_{gh}}{dt}\right) = (1-\alpha)\,S + \varepsilon\,L - \varepsilon\,\sigma\,T_{gh}^4 - h_c\left(T_{gh} - T_{mist}\right) - E + \frac{H}{A} \tag{5-4}$$

C_g is the heat capacity of the globe thermometer (In the present study, the heat capacity of 13.52 J/K globe thermometer with 50 mm diameter and 0.5 mm thickness copper was used. cf. 150 mm globe thermometer has 124.75 J/K heat capacity), A is a surface area of 50 mm globe thermometer (7.9×10^{-3} m^2). α is albedo of globe thermometers, ε is emissivity of globe thermometers, and σ is

the Stefan-Boltzmann constant. S is shortwave radiation flux from environment to the globe thermometer, L is longwave radiation flux from environment to the globe thermometer. h_c is convective heat transfer coefficient of globe thermometer. T_g is inside temperature of globe thermometer, and T_{gh} is inside temperature of the heating globe thermometer. T_a and T_{mist} are the air temperature around the globe thermometer and heating globe thermometer, respectively.

Assuming the effects of the radiation environment on the globe thermometer and the heating globe thermometer are the same, the evaporative heat loss (E) Equation (5-5) can be obtained from heat balance Equations (5-3) and (5-4), and unknown parameters S and L can be neglected.

$$E = \frac{C_g}{A}\left(\frac{dT_g}{dt} - \frac{dT_{gh}}{dt}\right) + \varepsilon\,\sigma\left(T_g^4 - T_{gh}^4\right) + h_c\left(T_g - T_a\right) - h_c\left(T_{gh} - T_{mist}\right) + \frac{H}{A} \tag{5-5}$$

H is heat input into the heating globe thermometer and determined by measuring input power by a wattmeter. h_c is the convective heat transfer coefficient on surface of globe thermometer. The convective heat transfer in sphere can be calculated using Equation (5-6) [102]. v is the airspeed (m s^{-1}), D is the diameter of globe thermometer (0.05 m), and k is the thermal conductivity of air (e.g. 26.3 × 10^{-3} W m^{-1} K^{-1} at 27 °C). Equation (5-7). indicate the Nusselt number Nu which is the ratio of convective heat transfer to fluid conductive heat transfer under the same conditions. Pr is the Prandtl number of air (e.g. approximately 0.707 at 27 °C). The Reynolds number (Re) can be calculated by Equation (5-8). ν is Kinematic viscosity of air at atmospheric pressure (e.g. 15.89 × 10^{-6} m^2 s^{-1} at 27 °C).

$$h_c = \frac{\mathrm{Nu}\,k}{D} \tag{5-6}$$

$$\mathrm{Nu} = 2 + \left(0.4 + \mathrm{Re}^{1/2} + 0.06\,\mathrm{Re}^{2/3}\right)\mathrm{Pr}^{0.4} \tag{5-7}$$

$$\mathrm{Re} = \frac{v\,D}{\nu} \tag{5-8}$$

In stable state condition terms of time derivatives become zero, and evaporative heat loss obtained using Equation (5-9).

$$E = \varepsilon\,\sigma\left(T_g^4 - T_{gh}^4\right) + h_c\left(\left(T_g - T_{gh}\right) - \left(T_a - T_{mist}\right)\right) + \frac{H}{A} \tag{5-9}$$

In addition, heat loss can be written using mist wettedness as Equation (5-10). LR is the coefficient of Lewis relation, p^*_{gh} is the saturated water vapor pressure at surface temperature of heating globe thermometer, and p_{mist} is the partial water vapor pressure in mist spraying environment.

$$E = \mathrm{LR}\,h_{\mathrm{c}}\,\omega_{\mathrm{mist}}\left(p^*_{\mathrm{gh}} - p_{\mathrm{mist}}\right) \tag{5-10}$$

The saturated water vapor pressure p^* for the temperature T of moist air can be calculated using Equation (5-11) [103].

$$p^* = 0.6105\exp\left(\frac{17.269\,T}{237.3 + T}\right), \qquad T \geq 0\,°C \tag{5-11}$$

The mist wettedness can be obtained by combining the Equation (5-5) and (5-10). To determine the mist wettedness using Equation (5-12), Heating globe temperature T_{gh}, globe temperature T_{g}, air temperature around the heating globe temperature T_{mist} and globe temperature T_{a}, airspeed and relative humidity inside the mist spraying environment, and heat input H into the heating globe thermometer are necessary to measure. The measuring instruments are listed in Table 5-4.

$$\omega_{\mathrm{mist}} = \frac{\frac{C_{\mathrm{g}}}{A}\left(\frac{\mathrm{d}T_{\mathrm{g}}}{\mathrm{d}t} - \frac{\mathrm{d}T_{\mathrm{gh}}}{\mathrm{d}t}\right) + \varepsilon\,\sigma\left(T_{\mathrm{g}}^4 - T_{\mathrm{gh}}^4\right) + h_{\mathrm{c}}\left(\left(T_{\mathrm{g}} - T_{\mathrm{a}}\right) - \left(T_{\mathrm{gh}} - T_{\mathrm{mist}}\right)\right) + \frac{H}{A}}{\mathrm{LR}\,h_{\mathrm{c}}\left(p^*_{\mathrm{gh}} - p_{\mathrm{mist}}\right)} \tag{5-12}$$

5.4. Results and discussion

5.4.1. Environmental factors

Environmental factors measured in outdoor and mist spray environments were compared and analyzed. The measurement results are shown in Fig. 5-8 by averaging data measured at 1-second intervals at 10-minute intervals. By comparing the results of the external environmental factors at the same time, the impact of the mist system on the outdoor environment was confirmed. The mist spray system was measured 65 times for four operating modes. There was no significant difference in temperature and relative humidity in the outdoor environment for each operating mode. The measured

MRT values were similar for CASE-1 (baseline) and CASE-2 (without air blowing). However, CASE-3 (less mist) and CASE-4 (without mist) were not similar because of solar radiation. On the other hand, the temperature and relative humidity showed a significant difference in the mist spray environment. However, unlike other environmental factors, the airspeed did not change significantly in other modes of operation ($p > 0.5$).

However, changes in absolute humidity (mean ± SD) of CASE-1 and CASE-2 were 0.7 ± 0.7 and 1.0 ± 0.5 (g / kg DA), respectively, indicating that water droplets make water droplets difficult to evaporate. air. Thus, the sprayed water droplets at a height of 3.0 m above the ground escape faster in the initial stage, cooling the ambient air in the air injection mode than in the air injection mode. Therefore, since cold air has a lower partial vapor pressure than warm air, the total evaporation (absolute humidity gap in Table 5-5) was greater in CASE-2 than in CASE-1 ($p < 0.05$). In addition, if the mist droplets hit the same surface as the ground, the evaporative cooling effect can be reduced. As a result, it is essential to allow mist droplets to evaporate through the air in a short time [7]. Without air blow operation, the evaporation time of mist droplets can be delayed until it reaches the ground. On the other hand, when the mist is sprayed on the blowing fan, the air-cooling effect is increased by forced convection heat transfer, and the evaporation phenomenon is relatively reduced.

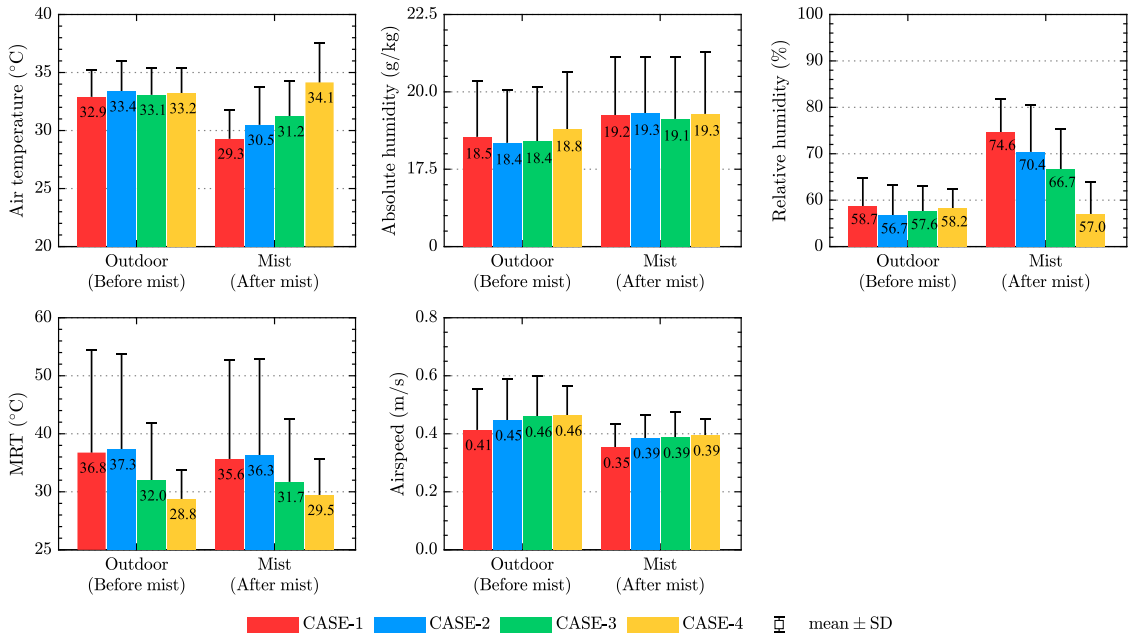

Fig. 5-8. Results of environmental factors (mean ± SD) in outdoor and mist spraying environment for operation modes.

Table 5-5 shows the results of the environmental factors measured in the outdoor and mist spray environments and the difference between the inside and outside of the mist spray environment. For

CASE-1, the air temperature most varied from 32.9 ± 2.6 °C outdoors to 29.3 ± 2.5 °C in a mist spray environment. The decrease in air temperature in CASE-2 and CASE-3 was not greater than CASE-1. In the case of CASE-4, which did not spray mist, the temperature rose. In the mist spray environment of CASE-1, the relative humidity change increased significantly from 58.7 ± 6.1% of outdoor to 74.6 ± 7.1%. Although the change was not greater than that of CASE-1, the relative humidity of CASE-2 was larger than that of CASE-3. Absolute humidity was the largest in CASE-2 and the least in CASE-4. This change in absolute humidity suggests that fog temperatures can evaporate faster at higher ambient temperatures [104]. Therefore, the amount of spray mist is an important control variable to lower the temperature in a hot outdoor environment. The presence of blowing also has a significant effect on the air temperature drop and the increase in relative humidity.

A temperature drop in hot summer can improve thermal comfort, but an increase in humidity can cause thermal discomfort. Therefore, the effect of the air blowing mode on the cooling efficiency of the mist spraying system needs to be investigated by not only measuring environmental factors but also analyzing subjective evaluations based on the results of the survey.

The MRT was about 1 °C lower inside the mist spraying environment than outside due to the low surface temperature of the ground. The airspeed was not significantly affected by other modes of operation. This can be inferred that air blowing does not affect the convective heat transfer on the human body surface. However, in the mist spraying environment, subjects were aware of the different air movements depending on the standing position, and the difference in air movement when the blower fan was turned on and off.

Table 5-5. Environmental factors in outdoor and mist spraying environments.

		CASE-1 (baseline)	CASE-2 (without air blowing)	CASE-3 (less mist)	CASE-4 (without mist)
		n = 65, Mean ± SD (standard deviation)			
Air temperature (°C)	outdoor	32.9 ± 2.3	33.4 ± 2.6	33.1 ± 2.3	33.2 ± 2.2
	mist	29.3 ± 2.5	30.5 ± 3.3	31.2 ± 3.0	34.1 ± 3.4
	gap†	−3.6 ± 1.4	−2.9 ± 1.2	−1.9 ± 0.9	0.9 ± 2.0
Relative humidity (%)	outdoor	58.7 ± 6.1	56.7 ± 6.6	57.6 ± 5.4	58.2 ± 4.3
	mist	74.6 ± 7.1	70.4 ± 10.2	66.6 ± 8.6	57.0 ± 6.8
	gap†	15.9 ± 4.7	13.7 ± 5.0	9.1 ± 4.4	1.2 ± 5.1
Absolute humidity (g/kg DA)	outdoor	18.5 ± 1.8	18.4 ± 1.7	18.4 ± 1.8	18.8 ± 1.9
	mist	19.2 ± 1.9	19.3 ± 1.8	19.1 ± 2.0	19.3 ± 2.0
	gap†	0.7 ± 0.7	0.9 ± 0.5	0.7 ± 0.9	0.5 ± 0.6
MRT (°C)	outdoor	36.8 ± 17.6	37.3 ± 16.5	32.0 ± 9.9	28.8 ± 5.1
	mist	35.6 ± 17.1	36.3 ± 16.5	31.7 ± 10.9	29.5 ± 6.2
	gap†	−1.2 ± 0.6	−1.0 ± 0.4	−0.3 ± 1.1	0.7 ± 1.8
Airspeed (m/s)	outdoor	0.44 ± 0.18	0.45 ± 0.15	0.45 ± 0.15	0.47 ± 0.11
	mist	0.37 ± 0.12	0.38 ± 0.08	0.38 ± 0.09	0.41 ± 0.08
	gap†	−0.07 ± 0.11	−0.07 ± 0.10	−0.07 ± 0.09	−0.06 ± 0.07

Note: gap† is difference between outdoor environment results and mist spraying environment results (mist − outdoor).

5.4.2. Perspective on environmental index

ince the environmental index can express the complex thermal effects of the thermal environment on the human body in a single value, there is an advantage that the thermal environment can be easily identified. The outdoor and mist spray environments were evaluated and compared using SET*, PET and UTCI, which are most widely used in outdoor environments. Fig. 5-9 shows the results of each environmental index obtained using the measured environmental factors. Due to the continuous change in outdoor environmental conditions, it was lower in CASE-3 and CASE-4 than in CASE-1 and CASE-2. This is because MRT was formed low in CASE-3 and CASE-4. Therefore, in order to evaluate the cooling effect of the mist spray environment, it is necessary to confirm the difference from the outdoor environment.

The difference between the outdoor environment and mist spraying environment showed the same pattern in all environmental indices and showed the biggest change in CASE-1. The difference was in the order of CASE-1, CASE-2, CASE-3, and CASE-4. However, since the existing environmental indices do not consider the evaporative heat loss caused by the wetness of mist, the results in the mist environment are considered to be lower.

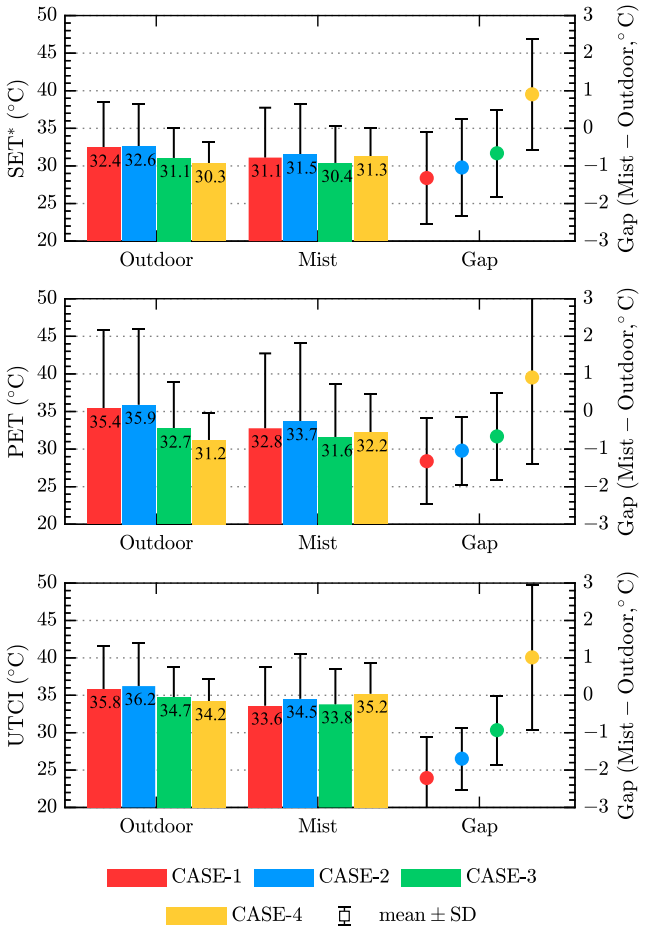

Fig. 5-9. Existing environmental indices in outdoor environment and mist spraying environments (gap is difference of result of outdoor and mist spraying environments).

5.4.3. Mist wettedness

The mist wettedness calculated and averaged every minute for the purpose of the physiological human model calculation. Strong winds make the mist droplets hard to reach the appropriate location because of the open space. Therefore, the mist wettedness showed drastic change by the wind condition. The result of mist wettedness on the surface of the heating globe thermometer was 0.25 ± 0.086 (Mean ± SD, n = 58). The skin temperature was calculated using the proposed physiological prediction human model as mentioned in the previous chapter with the measured environmental factors and mist wettedness and was validated by experimental results.

5.4.4. Review of spraying condition

The effect of spraying the amount of water and height of mist spraying was additionally reviewed.

Scaffoldings were used for subjects' standing to reduce the relative distance between the spraying nozzle and subject because the height of the spraying nozzle was hard to change as shown in Fig. 5-10. The subject experiment (n = 5) was conducted on August 27, 2018. The spraying amount of water was increased from 300 to 400 cm^3/min compared to the baseline case (CASE-1) in the first additional case. In the second additional case, the amount of water was set as 240 cm^3/min as same as CASE-3. The nozzle was changed 3 to 4 in both additional cases to make better uniform mist spraying distribution. In addition, and the height of scaffoldings was 20 cm and it was used in both additional cases (The relative distance between nozzle and feet was changed from 3 m to 2.8 m).

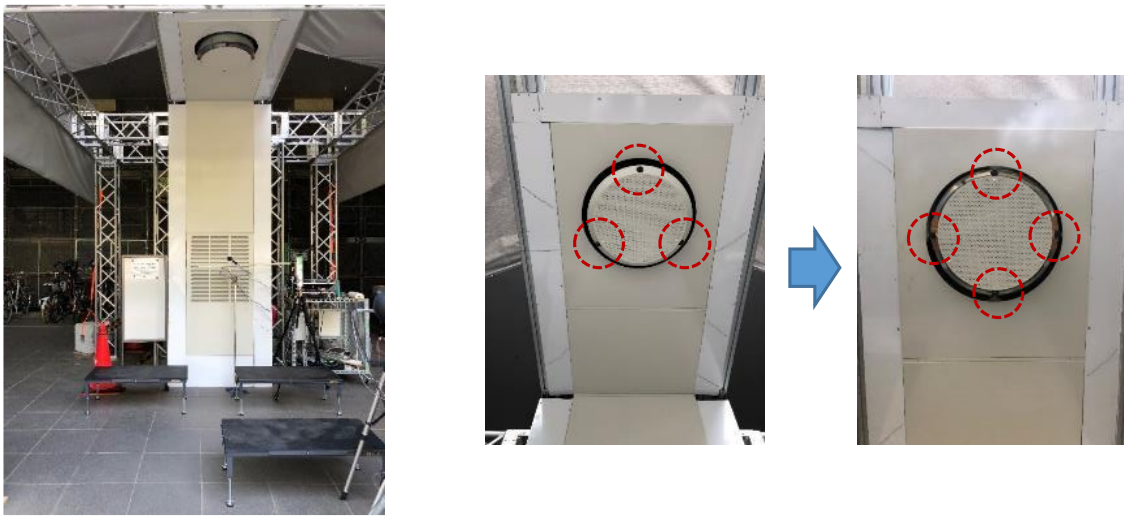

Fig. 5-10. Additional experiment was conducted with 20 cm scaffoldings, and subjects were stood on there during experiment (n = 5).

The results of environmental factors outdoor and mist spraying environment in additional cases was listed in Table 5-6. The results do not show significant differences compared to the baseline, because the measurement point was not changed, and the outdoor environment was hotter compared to the main experiment. Subjects reported that the mTSV, TSV, and CSV were significantly improved in additional experiments than the main experiments as shown in Fig. 5-11.

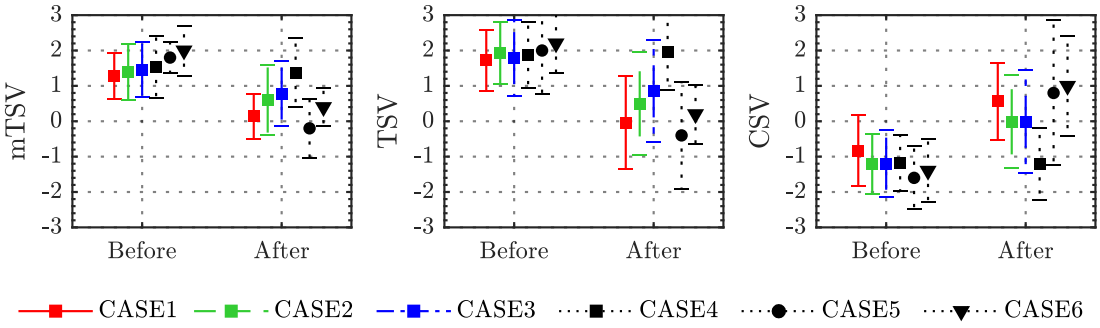

Fig. 5-11. Thermal sensation and thermal comfort results in outdoor and mist spraying environments for different operation mode of mist spraying system.

Table 5-6. The results of environmental factors in additional experiment.

		CASE-1 (baseline, 300 cm³/min)	ADD-1 (more mist, 400 cm³/min)	ADD-2 (240 cm³/min)
		Mean ± SD (standard deviation)		
Air temperature (°C)	outdoor	32.9 ± 2.3	34.5 ± 1.0	34.0 ± 1.4
	mist	29.3 ± 2.5	32.1 ± 1.1	31.3 ± 1.9
	gap†	−3.6 ± 1.4	−2.4 ± 2.1	−2.6 ± 0.5
Relative humidity (%)	outdoor	58.7 ± 6.1	18.5 ± 0.1	18.0 ± 1.9
	mist	74.6 ± 7.1	20.1 ± 0.7	19.5 ± 0.1
	gap†	15.9 ± 4.7	1.6 ± 0.5	1.5 ± 0.3
Absolute humidity (g/kg DA)	outdoor	18.5 ± 1.8	53.6 ± 3.4	53.8 ± 5.3
	mist	19.2 ± 1.9	66.3 ± 2.0	67.6 ± 7.4
	gap†	0.7 ± 0.7	12.8 ± 5.4	13.9 ± 2.2
MRT (°C)	outdoor	36.8 ± 17.6	38.6 ± 8.3	29.0 ± 3.9
	mist	35.6 ± 17.1	37.8 ± 10.1	27.8 ± 4.3
	gap†	−1.2 ± 0.6	−0.8 ± 1.8	−1.2 ± 0.4
Airspeed (m/s)	outdoor	0.44 ± 0.18	0.81 ± 0.15	0.49 ± 0.05
	mist	0.37 ± 0.12	0.56 ± 0.01	0.41 ± 0.04
	gap†	−0.07 ± 0.11	−0.25 ± 0.15	−0.07 ± 0.01

Note: gap† is difference between outdoor environment results and mist spraying environment results (mist − outdoor).

5.4.5. Subjective assessments

Fig. 5-12 shows the results of the survey before and after entering the spray environment. The first column is mTSV, the second column is TSV, and the third column is the result of CSV. Each row in the figure represents the results in the operating mode of Table 5-1 of the mist spraying system. Except for CASE-4, the mTSV and TSV decreased and the CSV increased after entering the mist spraying

environment from the outdoor environment regardless of the operation mode, resulting in improved thermal sensations and thermal comfort.

The standard deviation of mTSV and TSV resulted 0.7 to 1.2 and 0.9 to 1.5, respectively. This means that the results of mTSV are more concentrated than TSV due to the different sensation scale. In the baseline operation mode CASE-1, mTSV, TSV, and CSV varied from slightly hot (1.3 ± 0.7), warm (1.7 ± 0.9), and slightly uncomfortable (−0.8 ± 1.1) to neutral (0.1 ± 1.4), neutral (0.0 ± 1.3) and slightly comfortable (0.6 ± 1.1), respectively. Also, mTSV and TSV after 10 min of entering the mist spraying environment were lower than their corresponding results after 3 min. This implies that the subjects were experienced continuous cooling for 10 min while standing inside the mist environment. On the other hand, when the mist spraying system was controlled in the absence of mist (CASE-4), mTSV ($p = 0.25$), TSV ($p = 0.56$), and CSV ($p = 0.79$), both before and after entering the mist spraying system, were not significantly different. In this case, there is no evaporation, so the temperature does not drop, and you cannot feel cool because the outdoor temperature is as high as the skin temperature.

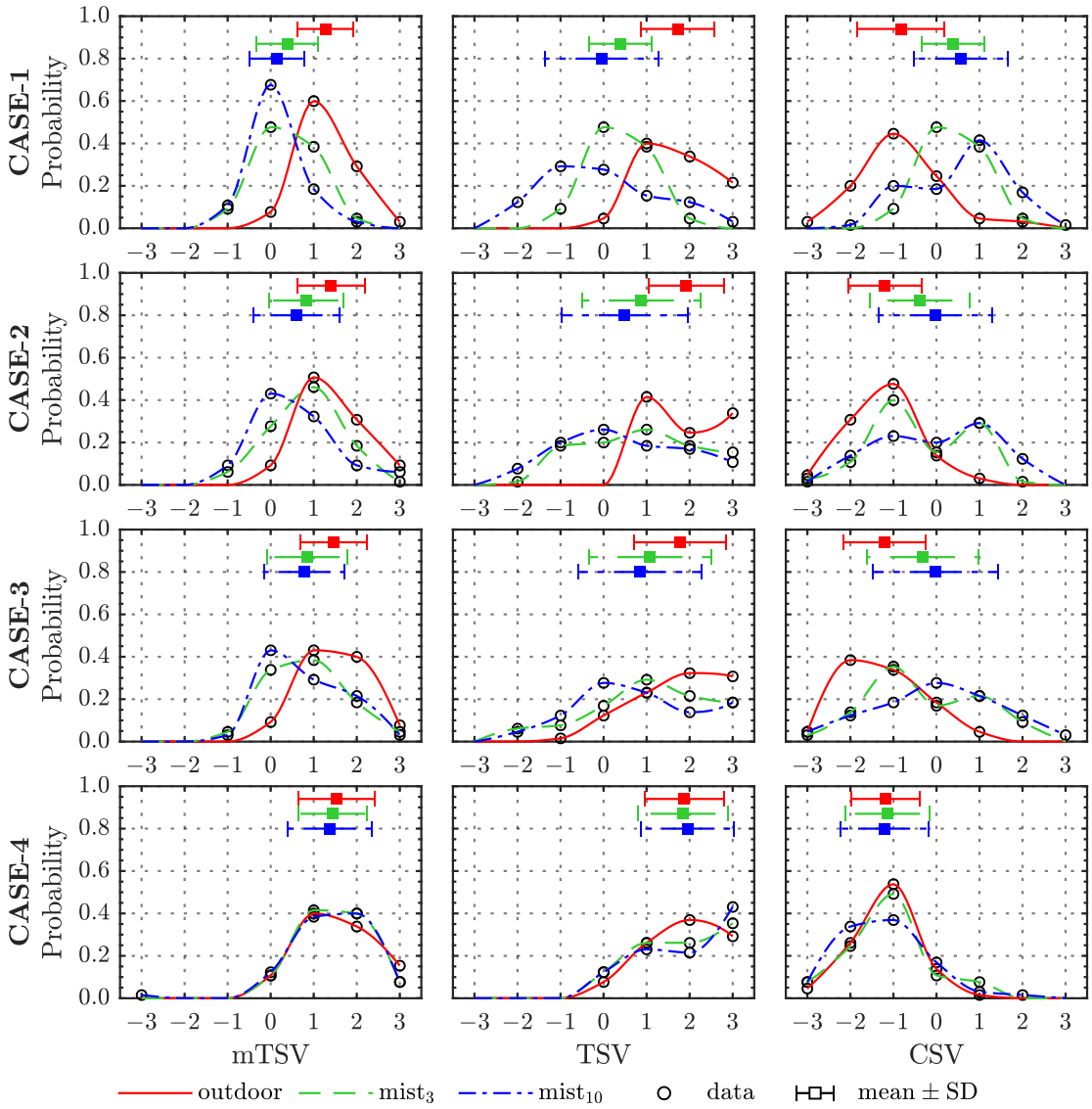

Fig. 5-12. Thermal sensations (mTSV, and TSV) and thermal comfort results in outdoor and mist spraying environments. (outdoor: before entering the mist spraying system, $mist_3$: 3 min. after entering the mist spraying system, $mist_{10}$: 10 min. after entering mist spraying environment)

Because the widths of each sensation scale in mTSV, TSV and CSV are different [105], comparing the indexes with other scales may seem inappropriate, but comparative analysis of these indices is another operation mode of the mist spraying system for human thermal sensation and thermal comfort. This can be useful for estimating the mode.

Therefore, the results of mTSV, TSV and CSV compared the results before and after entering the mist environment in each operating mode. In Fig. 5-13, the results of mTSV, TSV and CSV were compared in the survey after 10 minutes of walking outdoors and after 10 minutes of experiencing the

mist spraying environment. In CASE-1, mTSV, TSV and CSV showed a significant difference before and after entering the mist environment compared to other operation modes. The difference of mTSV, TSV and CSV before and after entering the mist spraying environments were −1.1 ± 0.7, 1.7 ± 1.3 and 1.4 ± 1.2, respectively. In addition, while mTSV and TSV changed more than CASE-2 than CASE-3, there was no significant difference in CASE-4. In each case, the difference between the mean and standard deviation of TSV was greater than that of mTSV. Also, except for CASE-4, CSV did not show significant changes in each case ($p > 0.1$).

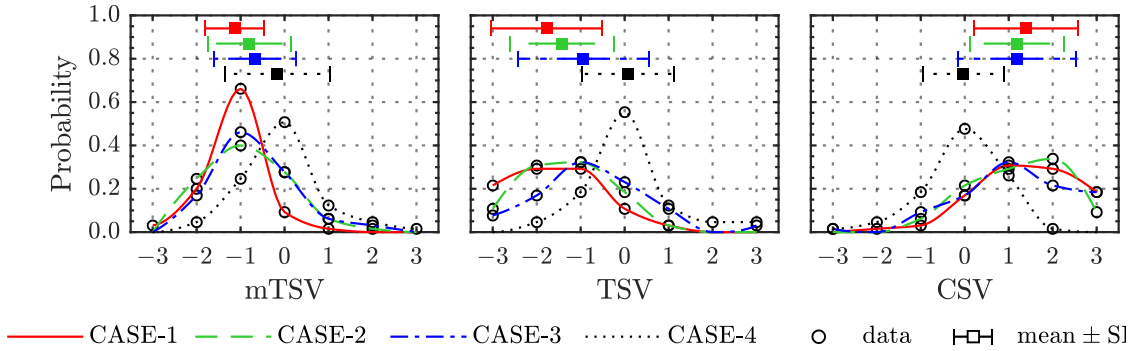

Fig. 5-13. Changes in Individual thermal sensations (mTSV and TSV) and thermal comfort (CSV) in outdoor and mist spray environments.

Table 5-7. Environmental factor results in outdoor and mist spraying environments. (baseline: standard condition, without air blowing: mist only, less mist: less amount of mist spray, without mist: air blowing only).

		mTSV	TSV	CSV
		n = 65, Mean ± SD (standard deviation)		
CASE-1 (baseline)	outdoor	1.3 ± 0.6	1.7 ± 0.9	−0.8 ± 1.0
	$mist_3$	0.4 ± 0.7	0.4 ± 0.7	0.4 ± 0.7
	$mist_{10}$	0.1 ± 0.6	0.0 ± 1.3	0.6 ± 1.1
	gap†	−1.1 ± 0.7	−1.7 ± 1.3	1.4 ± 1.2
CASE-2 (without air blowing)	outdoor	1.4 ± 0.8	1.9 ± 0.9	−1.2 ± 0.9
	$mist_3$	0.8 ± 0.9	0.9 ± 1.4	−0.4 ± 1.2
	$mist_{10}$	0.6 ± 1.0	0.5 ± 1.5	0.0 ± 1.3
	gap†	−0.8 ± 0.9	−1.4 ± 1.2	1.2 ± 1.1
CASE-3 (less mist)	outdoor	1.5 ± 0.8	1.8 ± 1.1	−1.2 ± 1.0
	$mist_3$	0.8 ± 0.9	1.1 ± 1.4	−0.3 ± 1.3
	$mist_{10}$	0.8 ± 0.9	0.8 ± 1.4	0.0 ± 1.5
	gap†	−0.7 ± 0.9	−0.9 ± 1.5	1.2 ± 1.3
CASE-4 (without mist)	outdoor	1.5 ± 0.9	1.9 ± 0.9	−1.2 ± 0.8
	$mist_3$	1.4 ± 0.8	1.8 ± 1.0	−1.1 ± 1.0
	$mist_{10}$	1.4 ± 1.0	2.0 ± 1.1	−1.2 ± 1.0
	gap†	−0.2 ± 1.2	0.1 ± 1.1	0.0 ± 0.9

Note: gap† is difference between results before entering mist spraying environment (outdoor) and results after 10 min ($mist_{10}$) entering mist spraying environment ($mist_{10}$ − outdoor).

To investigate the effect of control variables on improvement of the subject's thermal sensation and thermal comfort, a gap† (the difference of mTSV, TSV, and CSV between before entering the mist spraying and after 10 min of entering the mist spraying environment, $mist_{10}$ − outdoor) between before entering the mist spray and after 10 minutes entered the mist spraying environment was confirmed. The probability value (*p*-value) of this result was confirmed using the paired *t*-test analysis (Table 5-8). In comparison results of CASE-1 and CASE-2, significant differences were observed in mTSV ($p \leq 0.05$), but not in TSV and CSV.

It implicates that the operation of air blowing mode can be distinguished by the mTSV scale in the subjective assessment. In Table 5-5, the ambient temperature was lower in CASE-1 than in CASE-2, and the airspeed showed a similar trend. Based on this fact, the control parameters of the air blowing mode did not directly affect the body's convective heat transfer but lowered the air temperature inside the mist spraying environment. Among the subjective assessment, the only mTSV was able to capture these environmental factors change under activation of the air blowing mode. This means that the mTSV scale is more sensitive than TSV scale.

The mTSV and TSV in CASE-1 and CASE-3 were quite different before and after entering the mist spraying environment, but no significant difference was observed for CSV. In other words, the

sensation scale of mTSV and TSV could reflect the different amounts of spraying water, but CSV did not. Comparison of CASE-1 and CASE-4 shows that all sensory scales showed a highly significant difference. This suggests that the mist spraying itself has a big impact on all sensations. In addition, applying air blowing in the mist spraying system improves additional thermal sensations. Thus, the basic operation of the mist spraying system tends to significantly improve subjective evaluation on all sensations.

In Table 5-8, the *p*-value is displayed as "ns" (not significant). This means that no significant difference was found in the mTSV, TSV and CSV results between the two cases under different operating conditions. Even if the comparison in the two cases is "ns", this does not mean that the operation of the mist injection system itself did not affect the findings.

Table 5-8. Statistical analysis of effects of operation modes on thermal sensations and thermal comfort. Statistical significance was confirmed by probability value (*p*-value) in paired t-test. (CASE-1: baseline, CASE-2: without air blowing, CASE-3: less mist, CASE-4: without mist)

Comparison (n = 65)	Difference	Significance (p-value)		
		mTSV	TSV	CSV
CASE-1 vs. CASE-2	Air blowing	*	ns	ns
CASE-1 vs. CASE-3	Amount of spraying water	***	***	ns
CASE-1 vs. CASE-4	Water spray	**	***	***

Significant indicator of probability value represents (ns: p > 0.05, *: p ≤ 0.05, **: p ≤ 0.01, ***: p ≤ 0.001).

5.4.6. Overall skin temperature changes

The mean and 95% confidence intervals (CI) of overall skin temperature of body changes measured in the experiment are shown in Fig. 5-14. In each case, the initial overall skin temperature of all subjects was not the same because the outdoor thermal environment was not constant. The mean initial skin temperature in all cases was 33.8–34.1 °C. Except for CASE-4 (excluding the mist), the skin temperature of the subject gradually increased during walking in the outdoor environment (0–10 minutes), and then gradually decreased during stayed in the mist spraying environment (10–20 minutes). However, the overall skin temperature in CASE-4 increased continuously from the start of the experiment, regardless of the environment. This shows that there is no cooling effect on the human body because only air blowing exists in the mist spraying environment. When the subjects experienced a mist spraying environment, the average overall skin temperature varied greatly in the order of CASE-1, CASE-2, CASE-3, and CASE-4.

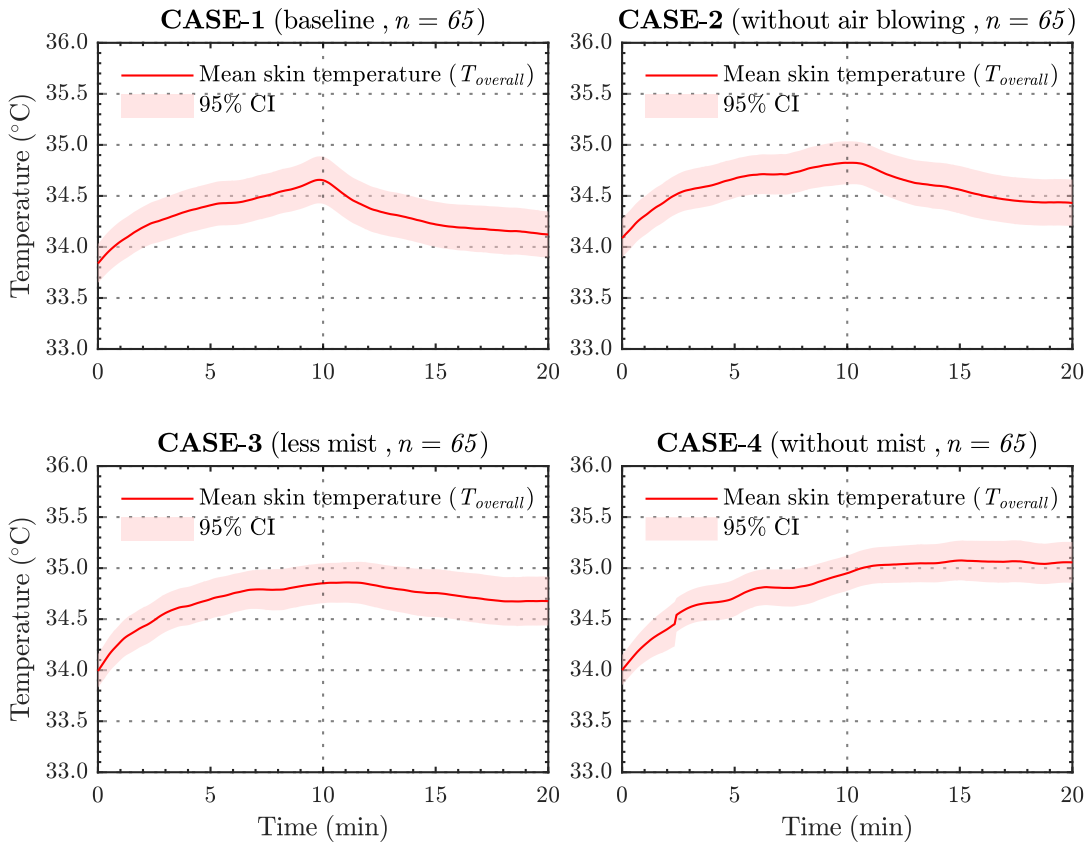

Fig. 5-14. The mean of overall skin temperature and 95% CI variations with different operating conditions for the mist spraying system.

Fig. 5-14 presents the mean and 95% CI (lower 95% limit, the upper 95% limit) of overall skin temperature variations of each body segment during the subjects' stay in the mist spraying environment. The skin temperature dropped maximally in the head in CASE-1 and CASE-3. But it was lowered the most in the arm in CASE-2 (without air-blowing). The temperature variations, which were derived from the mean overall skin temperature and temperatures of each body segment while the subjects were staying inside the mist system, were −0.55 °C (95% CI: −0.63, −0.43), −0.39 °C (95% CI: −0.51, −0.27), −0.17 °C (95% CI: −0.29, −0.05), and 0.11 °C (95% CI: 0.00, 0.22) for CASE-1, 2, 3, and 4, respectively.

5.4.7. Temperature differences in body segments

The skin temperatures on the upper parts of the body were lower in CASE-1 than in CASE-2, indicating that the air blowing operation helped cool these parts. As shown in Fig. 5-15, the skin temperature on the head was lower in CASE-1 than in CASE-2 even though the overall skin

temperature variations had no significant difference between these cases. The skin temperature variations in CASE-1 and CASE-2 were similar: −1.10 °C (95% CI: −1.41, −0.79) in CASE-1, and −0.48 °C (95% CI: −0.63, −0.33) in CASE-2 as listed in Table 5-9. The face is the most sensitive part among the human body segments in thermal sensations. People prefer to cool the head when they are exposed to a hot outdoor environment [106]. According to the survey results in the field experiment, the subjective assessment of CASE-1 was analyzed as better than that of CASE-2. Therefore, a possibility exists that the improvement on the subjective assessment in CASE-1 could result from the further cooling down in the thermally sensitive face area in CASE-1.

Between CASE-2 and CASE-3, no significant difference was found in the temperature change of the head region before and after entering the mist spraying environment. However, in CASE-2, the overall skin temperature was lowered with a wide range of temperature changes, resulting in a cooler sensation was reported in CASE-2 than in CASE-3. In CASE-4, the skin temperature of all body parts increased slightly even after the subject entered the fog system. The highest increase was recorded for hands [0.28 °C (95% CI: 0.11, 0.45)] and lowest for the abdomen [0.06 °C (95% CI: −0.04, 0.16)].

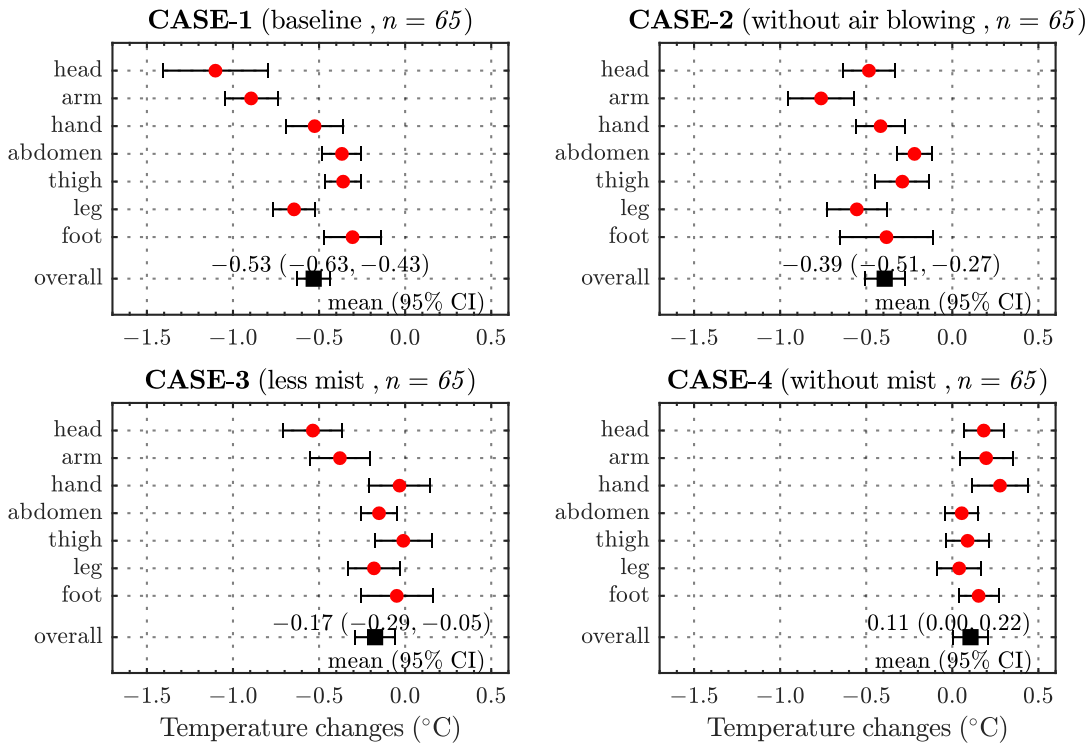

Fig. 5-15. Skin temperature changes in each body segment after entering the mist spraying environment.

Table 5-9. The mean and 95% CI of the changes in skin temperature of each body segment before and after entering the mist spraying environment.

Segment	CASE-1 (baseline)	CASE-2 (without air blowing)	CASE-3 (less mist)	CASE-4 (without mist)
	Mean ± SD (standard deviation) Temperature changes (°C, mean (lower 95% limit, the upper 95% limit))			
Head	−1.10 (−1.41, −0.79)	−0.48 (−0.63, −0.33)	−0.53 (−0.71, −0.35)	0.19 (0.07, 0.31)
Arm	−0.89 (−1.05, −0.73)	−0.76 (−0.96, −0.56)	−0.37 (−0.55, −0.19)	0.20 (0.04, 0.36)
Hand	−0.53 (−0.69, −0.35)	−0.41 (−0.56, −0.26)	−0.03 (−0.21, 0.15)	0.28 (0.11, 0.45)
Abdomen	−0.36 (−0.48, −0.24)	−0.21 (−0.31, −0.11)	−0.15 (−0.26, −0.04)	0.06 (−0.04, 0.16)
Thigh	−0.36 (−0.47, −0.25)	−0.29 (−0.45, −0.13)	−0.01 (−0.18, −0.16)	0.09 (−0.04, 0.22)
Leg	−0.64 (−0.77, −0.51)	−0.56 (−0.73, −0.37)	−0.18 (−0.34. −0.02)	0.04 (−0.09, 0.17)
Foot	−0.31 (−0.47, −0.13)	−0.38 (−0.66, −0.10)	−0.04 (−0.25, 0.17)	0.16 (0.04, 0.28)
Overall	−0.53 (−0.63, −0.43)	−0.39 (−0.51, −0.27)	−0.17 (−0.29, −0.05)	0.11 (0.00, 0.22)

5.4.8. Skin temperature changes in maximum evaporative cooling condition

In this chapter, the mist spraying system utilized mist spraying to cool the air and take advantage of the evaporative heat loss by the mist on the human body surface. However, as the body is wet by the mist too much, which may cause discomfort. Therefore, as another approach, mist spraying systems that cool the body by making the ambient air as low as possible by mist spraying without wetting the human body can be imagined. As listed in Table 1-1 of the introduction section, the evaporative cooling effect of the mist spraying system can be obtained additionally until the relative humidity of the surrounding air reaches 100%. However, the increase in relative humidity may cause a decrease in latent heat loss on the body surface, which may cause thermal discomfort. Therefore, it is necessary to investigate the thermal effect on the human body in conditions of the maximum cooling effect. 2NM was used as a predictive model, and the calculation conditions are listed in Table 5-10. The skin temperature changes for 10 min in mist spraying environments showed 0.38 degrees (Fig. 5-17). This result shows that the cooling effect is inferior to the reference condition (CASE-1), and the control of the mist spraying system focusing only on the cooling effect of the air temperature is not good.

Table 5-10. Calculation conditions of 2NM in maximum possible temperature drop condition by mist spraying system.

Factor	Variables	Value	
Human	Metabolic rate (met)	1.2	
	Clothing insulation (clo)	0.5	
	Initial mean skin temperature (°C)	33.7	
	Initial core temperature (°C)	36.8	
	Initial core temperature (°C)	$T_{\mathrm{body}} = 0.1\,T_{\mathrm{sk}} + 0.9\,T_{\mathrm{core}}$	
	Neutral mean skin temperature (°C)	$T_{\mathrm{sk}}^{n} = 33.7$	
	Neutral core temperature (°C)	$T_{\mathrm{core}}^{n} = 36.8$	
	Neutral body temperature (°C)	$T_{\mathrm{body}}^{n} = 36.49, (0.1\,T_{\mathrm{sk}} + 0.9\,T_{\mathrm{core}})$	
		Outdoor environment*	Mist spraying environment
Environment	Air temperature (°C)	32.9	26.7
	Relative humidity (%)	58.7	100
	MRT (°C)	36.8	36.8
	Airspeed (m/s)	0.41	0.41

*Note: mean outdoor environment condition obtained from field experiment.
The calculation was considered that the subjects rested for 20 min in an indoor environment (26 °C, 60% RH)

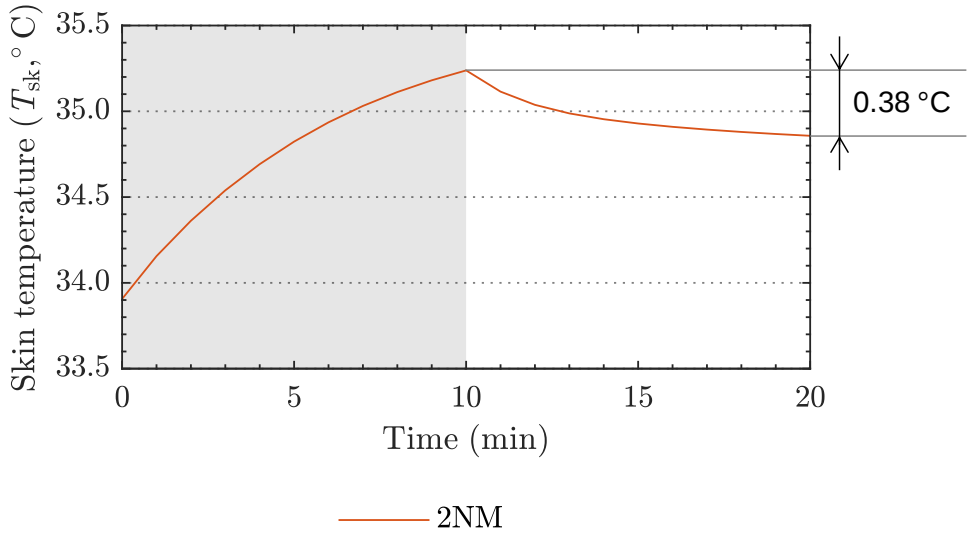

Fig. 5-16. Correlation between air temperature and TSV in outdoor and mist spraying environments.

5.4.9. Overall skin temperature and thermal sensations

Since the thermal sensation (mTSV and TSV) reflects the thermal state of the human body, we analyzed the correlation between skin temperature and thermal sensation. The Pearson correlation coefficients and probability values have calculated and compared the results of the outdoor environment (n = 260) and the mist spraying environment (n = 195) regardless of the operating conditions of the mist spray system. The result of the correlation between systemic skin temperature and thermal sensation is shown in Fig. 5-17.

Skin temperature and reported thermal sensations in the first (after 10 min walking in outdoor) and third (after 10 min staying inside the mist, Fig. 5-3)vote were compared. The Pearson's correlation coefficients (r) between overall skin temperature and mTSV were 0.38 (n = 260, $p \leq 0.001$) and 0.61 (n = 195, $p \leq 0.001$) in outdoor and mist spraying environment, respectively. The r values between overall skin temperature and TSV were 0.27 (n = 260, $p \leq 0.001$) in outdoor and 0.55 (n = 195, $p \leq 0.001$) in mist spraying environment. In conclusion, the overall skin temperature was more highly correlated with mTSV than TSV in both outdoor and mist spraying environments.

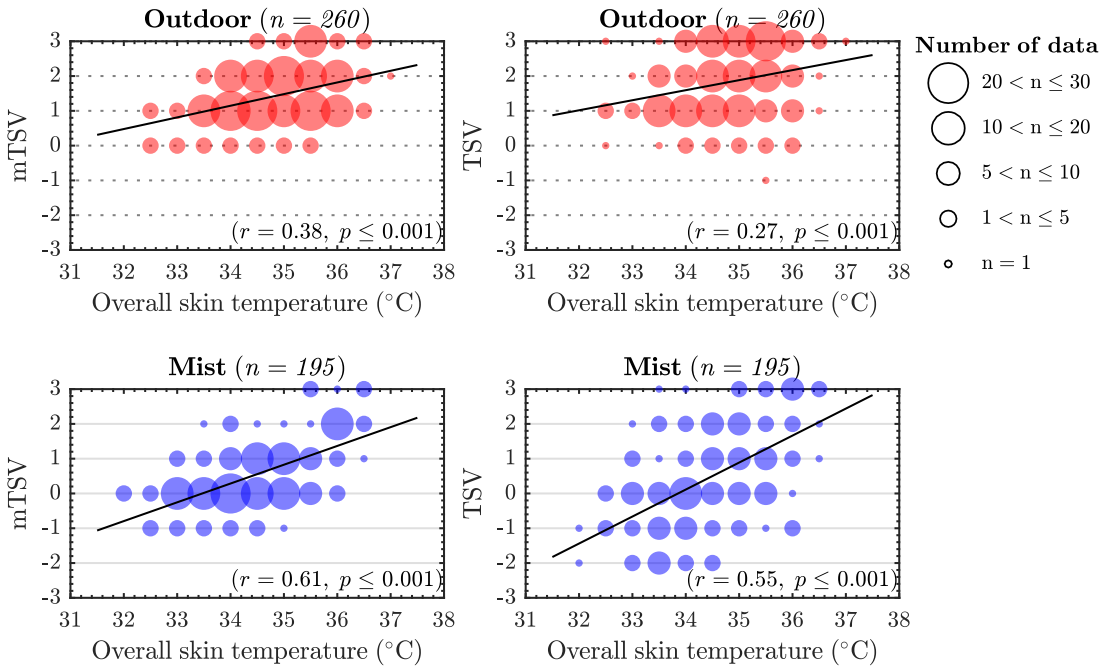

Fig. 5-17. Correlation between overall skin temperature and thermal sensations (mTSV and TSV). Pearson's correlation coefficient (r) and probability value (p) are represented.

The results of correlation analysis between skin temperature and thermal sensation of each body part are listed in Table 5-11. As an empirical and psychological effect on the mist spray environment

[107], it may be thought that subjects felt a cool sensation. However, a significant correlation between skin temperature and the thermal sensation was confirmed which is the objective evidence that the mist spray environment has a thermal effect on the human body. On the other hand, skin temperature tended to have a higher correlation coefficient with mTSV than TSV in most body parts. It is also suggested that the higher the value of the correlation coefficient (r) for the mist environment, the more the skin temperature of all body parts is affected than the outdoor environment. In particular, the r values of arms, hands, legs, and feet were relatively higher than the r values of other parts, while the values of the abdomen were the lowest. It can be considered that parts of the body that has no thermal resistance by clothing can be directly affected by the external environment.

Table 5-11. Mean and 95% CI of the changes in skin temperature of each body segment before and after entering mist spraying environment.

Segment	Outdoor (n = 260)				Mist (n = 195)			
	mTSV		TSV		mTSV		TSV	
	r	p	r	p	r	p	r	p
Head	0.32	***	0.30	***	0.38	***	0.35	***
Arm	0.41	***	0.31	***	0.61	***	0.56	***
Hand	0.40	***	0.37	***	0.59	***	0.54	***
Abdomen	0.19	**	0.11	ns	0.38	***	0.34	***
Thigh	0.35	***	0.21	***	0.55	***	0.44	***
Leg	0.38	***	0.25	***	0.60	***	0.57	***
Foot	0.35	***	0.32	***	0.61	***	0.56	***
Overall	0.38	***	0.27	***	0.61	***	0.55	***

Significant indicator of probability value represents (ns: $p > 0.05$, *: $p \leq 0.05$, **: $p \leq 0.01$, ***: $p \leq 0.001$).

5.4.10. Correlation between thermal sensations and thermal comfort

In relationship between thermal sensation and thermal comfort in non-uniform environment research, it was confirmed that the thermal sensation change with time affects thermal comfort significantly [108,109]. Fig. 5-18 and Fig. 5-19 are the correlation between the results of thermal sensations (TSV and mTSV) and thermal comfort (CSV). Correlation analysis results in outdoor and mist environments are shown, respectively. Moreover, the correlation analysis of TSV, mTSV, and CSV was conducted before and after entering the mist spraying environment. The difference in the correlation coefficient between CSV and TSV and CSV and mTSV was not significant. The linear regression equations are listed in Equation (5-13)–(5-16). Meanwhile, the slope result of linear regression with CSV was greater in mTSV than in TSV. In the same CSV change, it means that the change of TSV is larger than mTSV.

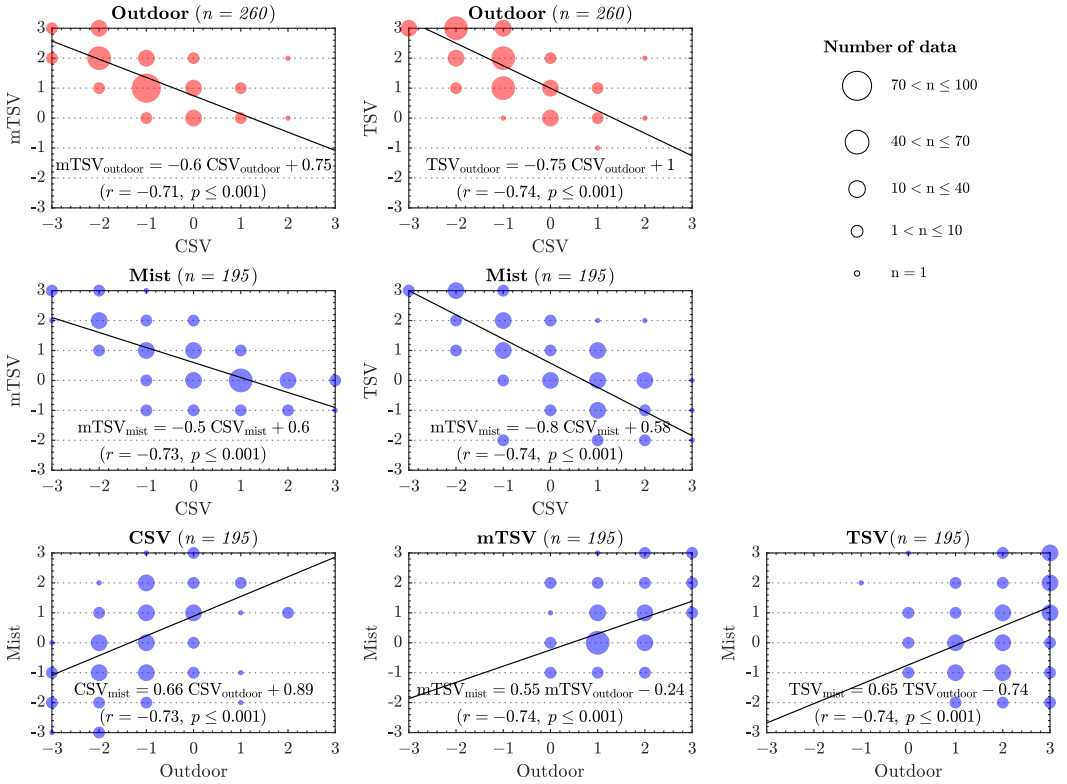

Fig. 5-18. Correlation analysis of survey results. Pearson's correlation coefficient (*r*) and probability value (*p*) are represented.

$$\mathrm{mTSV_{outdoor}} = -0.60\ \mathrm{CSV_{outdoor}} + 0.75 \tag{5-13}$$

$$\mathrm{mTSV_{mist}} = -0.50\ \mathrm{CSV_{mist}} + 0.60 \tag{5-14}$$

$$\mathrm{TSV_{outdoor}} = -0.75\ \mathrm{CSV_{outdoor}} + 1.00 \tag{5-15}$$

$$\mathrm{TSV_{mist}} = -0.80\ \mathrm{CSV_{mist}} + 0.58 \tag{5-16}$$

The linear regression equations for CSV, TSV, and mTSV before and after entering the mist spraying environment are shown in Equation (5-17)–(5-19).

$$\mathrm{CSV_{mist}} = 0.66\ \mathrm{CSV_{outdoor}} + 0.89 \tag{5-17}$$

$$\mathrm{mTSV_{mist}} = 0.55\ \mathrm{mTSV_{outdoor}} - 0.24 \tag{5-18}$$

$$\mathrm{TSV_{mist}} = 0.65\ \mathrm{TSV_{outdoor}} - 0.74 \tag{5-19}$$

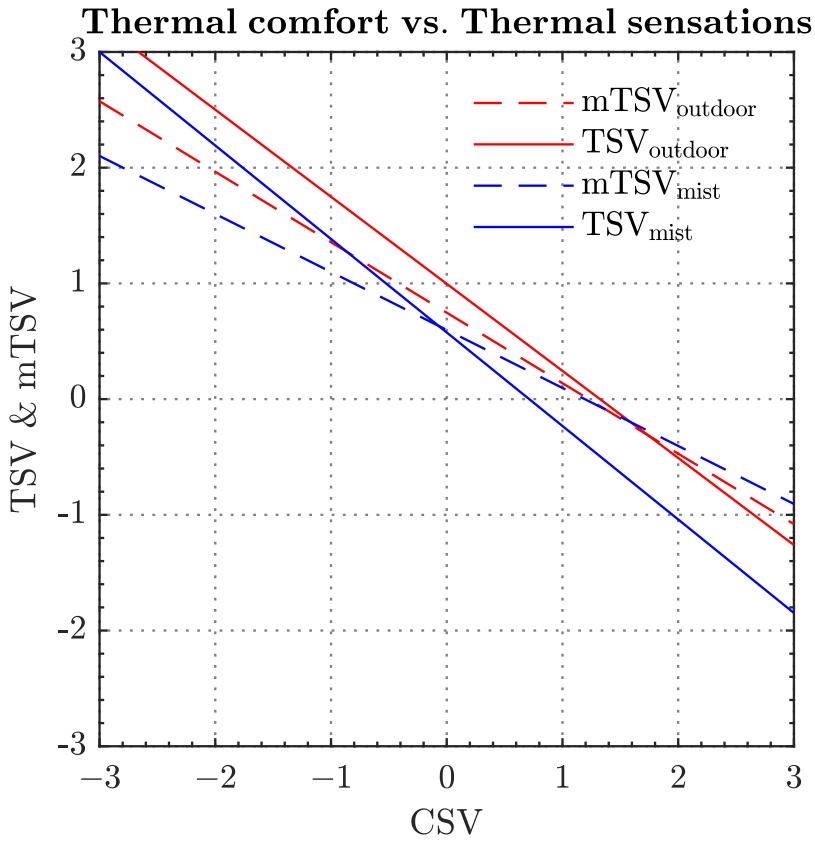

Fig. 5-19. Correlation between thermal sensations (mTSV and TSV). Pearson's correlation coefficient (*r*) and probability value (*p*) are represented.

5.4.11. Comparison with other outdoor researches

A study on the correlation analysis of the human body's thermal sensation and the UTCI index in the outdoor environment was conducted by Pantavou et al. [110]. The result of the linear correlation analysis is shown in Fig. 5-20. The results of UTCI and mean TSV in outdoor and mist spraying

environments for each operation mode obtained in this chapter were compared. The results of the outdoor environment tended to be very similar to the result of Pantavou et al. However, the TSV results in the mist spraying environment showed lower than expected. This result is considered to be the effect of evaporative heat loss by mist on the human body surface.

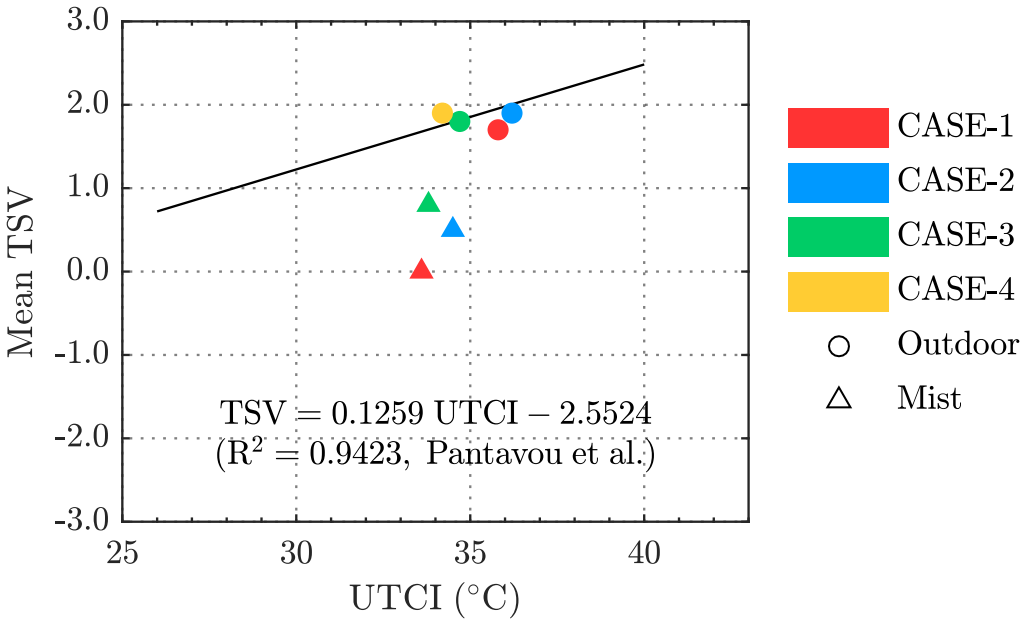

Fig. 5-20. Results of UTCI and mean TSV in outdoor and mist spraying environments.

5.4.12. Perspective on adaptive thermal comfort

Comfort temperature in outdoor and mist spraying environments can be calculated using correlation between air temperature and TSV as shown in Fig. 5-21. The regression equations can be expressed in Equation (5-20) and Equation (5-21). The comfort temperatures were 18.8 °C for outdoor environment and 27.9 °C for mist spraying environment. The mean air temperatures of outdoor and mist spraying environment were 33.1 °C and 30.3 °C, respectively. This result represents peoples were tolerated in the mist spraying environment than the outdoor environment.

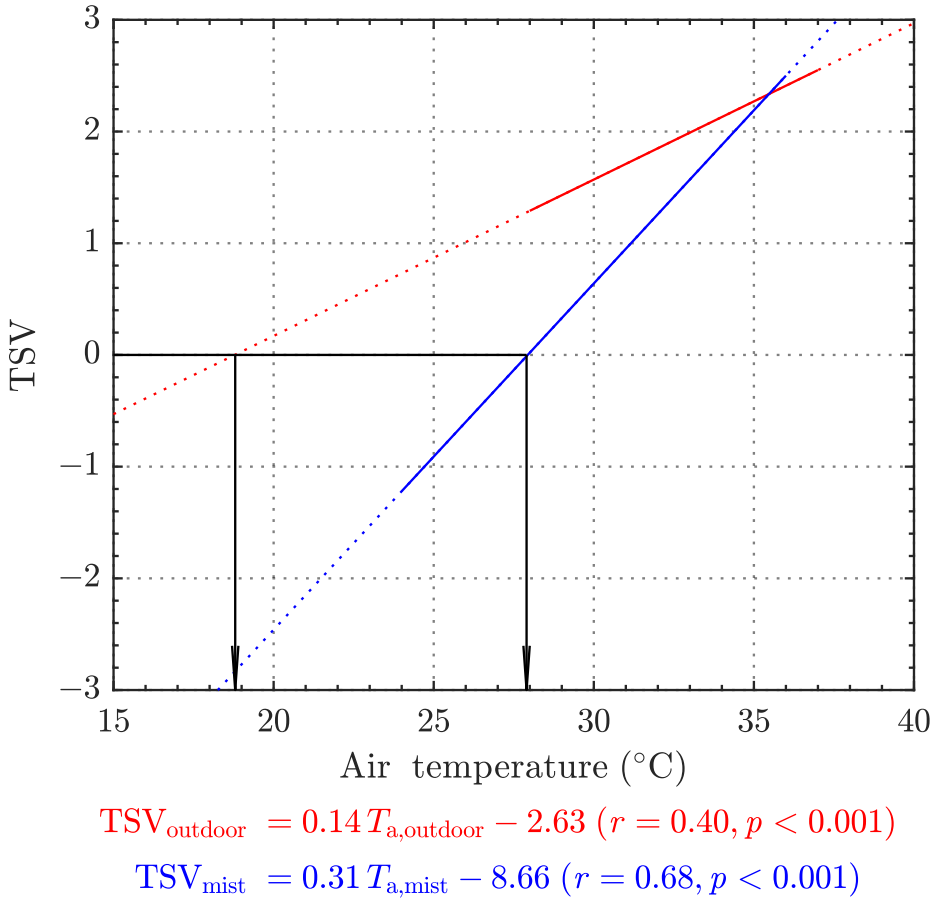

Fig. 5-21. Correlation between air temperature and TSV in outdoor and mist spraying environments.

$$\mathrm{TSV}_{\mathrm{outdoor}} = 0.14\,T_{\mathrm{a,outdoor}} - 2.63, (n = 222, r = 0.40, p < 0.001) \quad (5\text{-}20)$$

$$\mathrm{TSV}_{\mathrm{mist}} = 0.31\,T_{\mathrm{a,mist}} - 8.66, (n = 171, r = 0.68, p < 0.001) \quad (5\text{-}21)$$

However, in outdoor environments, the results of TSV are concentrated in hot feeling conditions, resulting in abnormally low comfort temperatures. Therefore, the comfort temperature in outdoor environments was derived using the Griffiths constant. Griffith constant of 0.5 /°C value is widely used in thermal comfort researches. However, it is not clear whether it can be applied as it is to the outdoor environment. Thus, the value of 0.31 /°C obtained from the mist spraying environment was utilized. The comfort temperature using the Griffiths constant was calculated using Equation (5-22).

The comfort temperature and mean air temperature in outdoor and mist spraying environment are summarized in Table 5-12.

$$T_c = T_a - \frac{\mathrm{TSV}}{G} \tag{5-22}$$

Table 5-12. Comfort temperature and mean air temperature in outdoor and mist spraying environments

	Mean TSV	Comfort temperature (°C)	Mean air temperature (°C)
Outdoor environment	1.80	27.3	33.1
Mist spraying environment	0.47	27.9	30.3

A review of the correlation between comfort temperature and air temperature in outdoor and semi-outdoor was conducted by Rijal [111]. Forty-nine studies were used to compare the comfort temperature and monthly mean outdoor temperature as shown in Fig. 5-22. The higher the temperature, the higher the comfort. Compared to the previous studies, the comfort temperatures in the outdoor and mist spraying environments showed similar results, but the value of comfort temperature showed relatively higher gaps in the outdoor environment than the mist spraying environment, which means that the outdoor environment was more thermal discomfort than the mist spraying environment. Additionally, because all conditions of the present study were controlled, it is difficult to compare directly with adaptive thermal comfort researches.

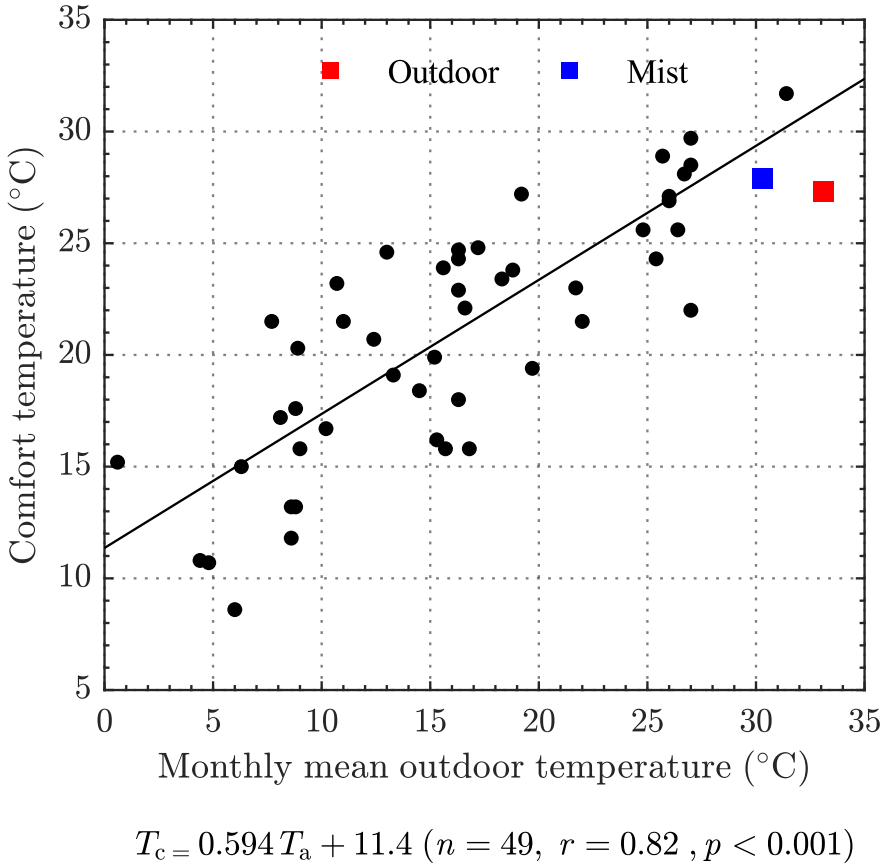

Fig. 5-22. Comparison with other outdoor thermal comfort studies.

5.5. Conclusion

The effects of control variables of the mist spraying system in the hot summer season on thermal sensations, thermal environment, and skin temperature were investigated. In the field experiment, the mist spraying system attaching an air blowing fan was devised. It was different from the conventional mist system that does not consider the air blowing operation concurrently. The devised mist spraying system was examined under four different operating conditions with different spraying water amounts and the inactivation/activation of the air blowing mode: CASE-1 (baseline), CASE-2 (without air blowing), CASE-3 (less mist), and CASE-4 (without mist). The influence of the control variables on the cooling effect of the system was compared with the comparative case study. Moreover, thermal sensations (mTSV, and TSV) were investigated by comparing subjects' subjective assessments (n = 65) before and after entering the mist spraying system in each case. The measured environmental

factors, including air temperature, humidity, MRT, and airspeed were analyzed and compared between before and after the subjects entered the mist spraying environment. By evaluating variations in environmental factors measurements, the cooling effect of the mist system of each operation mode was confirmed. To estimate subjects' physiological responses, skin temperatures on the surface of the seven body parts were collected and correlations between the reported subjective assessments were assessed. The major results obtained from this study can be summarized as follows:

- With the baseline operation of the mist spraying system, the air temperature dropped from 32.9 ± 2.3 °C to 29.3 ± 2.5 °C, relative humidity increased from 58.7 ± 6.1% to 74.6 ± 7.1%. MRT in the mist spraying environment was approximately 1 °C lower than that in the outdoor environment.
- In survey results (n = 65), mTSV, TSV, and CSV changed from slightly hot (1.3 ± 0.6), hot (1.7 ± 0.9), and slightly uncomfortable (−0.8 ± 1.0) to neutral (0.1 ± 0.6), neutral (0.0 ± 1.3) and slightly comfortable (0.6 ± 1.1), respectively due to the cooling effect of the mist spraying system.
- The overall skin temperature dropped by 0.53 °C [n = 65, (95% CI: 0.43, 0.63)] after 10 min of stay inside the mist spraying environment. Moreover, the skin temperature decreased most significantly for the head: the average skin temperature decrease of this part was 1.10 °C [n = 65, (95% CI: 0.79, 1.41)].
- When the mist spraying system was controlled with an increased amount of spraying water, both skin temperature and air temperature were lowered more; the thermal sensation was also better improved. Moreover, this cooling effect was further maximized when the air blowing mode was additionally activated.
- CSV was improved when subjects finished experiencing the mist spraying environment regardless of the operating conditions. However, unlike mTSV and TSV, the sensation scale of CSV did not show any significant correlation with the thermal sensation, which the subjects reported differently when the amount of spraying water increased or the air blowing mode was added ($p > 0.1$).
- The overall skin temperature showed positive correlation with thermal sensations. The correlation coefficients between overall skin temperature and TSV were 0.38 (n = 260, $p < 0.001$) in outdoor and 0.27 (n = 195, $p < 0.001$) in the mist spraying environment. In the case of mTSV, the coefficients were 0.61 (n = 260, $p < 0.001$) in outdoor and 0.55 (n = 195, $p < 0.001$) in the mist spraying environment.

In conclusion, the mist spraying system has been found effective in lowering skin temperature and has been proven to improve thermal sensations (mTSV and TSV) and thermal comfort in hot outdoor

environments. Physiological responses also showed a positive correlation with thermal sensation. Based on these results, human thermal sensitivity can be estimated when skin temperature changes can be predicted in a given outdoor and mist spray environment. If it is possible to properly predict the skin temperature of the human body, correlation analysis can be used to estimate the thermal sensations and thermal state of the human body in outdoor and mist spraying environments.

Chapter 6. Physiological human model considering mist wettedness

Chapter 6. Physiological human model considering mist wettedness

6.1. Background and objectives

6.1.1. Background and literature review

Mist spraying systems have been widely used to mitigate the heat stress in an outdoor hot environment. Although there have been many kinds of mist spraying systems, several studies have shown that mist spraying environments improve thermal sensations and thermal comfort in hot weather [15–17,112]. Some studies attempted to evaluate the mist spraying environment using environmental indices by measuring environmental factors (air temperature, MRT [mean radiant temperature], relative humidity, and wind speed) because survey research takes a long time and is an expensive task that may be difficult to objectify [11,16,17,112]. The mist spraying environments have water droplets in the air which might cause a cooling effect on the human body. However, evaporative heat loss by mist droplets on the body surface—an additional environmental factor in mist spraying environments—has not been reported despite its existence and has also been underestimated because of the difficulties in the measurement. For this reason, thermal sensations and thermal comfort proved to be cooler and more comfortable in mist spraying environment than the outdoor environment, although the environmental index value was the same [27]. Therefore, it is necessary to measure and quantify the evaporation heat loss from the surface of the human body surface due to the mist droplets. By applying this heat loss to the physiological human model, existing environmental indices can be extended to the mist spraying environment.

In regard to the physiological human model, Gagge and Nishi proposed the two-node model (2NM) [75], which has two thermal nodes (the core compartment and skin compartment) from Stolwijk's 25-node model [113]. In addition, Gagge et al. suggested the new effective temperature (ET*) [36] and standard effective temperature (SET*) [39] indices for evaluating thermal environment. The 2NM has an advantage of predicting the thermal physiological state of the whole body considering physiological responses such as shivering, sweating, and blood flow rate without any complicated multi-node model. Zolfaghari and Maerefat proposed the three-node model (3NM) which has three thermal nodes [62] to examine the temperature difference between bare and clothed body parts. The 2NM assumes that all of skin is covered by a uniform clothing level. On the other hand, the skin node is separated into two nodes in 3NM: bare parts and clothed parts. Therefore, the 3NM can confirm the skin temperature of both the bare part and clothed part.

Thermal state of the human body is highly linked to the thermal sensations and thermal comfort. Hence, most research conducted in the survey investigates the effects of mist spraying systems on

humans, and several researchers have examined the skin temperature changes of body parts (the arm and hand) [15,112]; but, thermal conditions of the whole body have not been sufficiently investigated. Recently, Oh et al. reported the results of the whole-body skin temperature changes and corresponding outdoor and mist spraying environmental conditions [114]. In addition, the prediction of skin temperature changes in an outdoor environment was validated by Lai et al. [72] and Melnikov et al. [115], but the feasibility of the physiological thermal state of the human body in the mist spray environment has not been examined using prediction models. Moreover, existing models do not consider heat loss by external causes such as rain or mist droplets. Therefore, it is inevitable to modify the existing models to grasp the thermal sensations and thermal comfort in a specific environmental condition such as the mist spraying environment.

6.1.2. Objectives of developing human model considering mist wettedness

A key aim of the present study is to develop a prediction model considering physiological responses of the human body in the mist spraying environment. In addition, the physical phenomena between the mist spray environment and the human body can be clarified with the prediction models. To achieve this goal, evaporative heat loss from the body surface by mist droplets in a mist spraying environment—which had been underestimated—was measured and applied to the prediction model of physiological responses. Moreover, whether the existing models can be utilized in the mist spraying environment for predicting the physiological thermal state of the human body was confirmed, and the accuracy of the modified prediction model was verified by comparing it with the experimental result. The thermal state of the human body, thermal sensations, and thermal comfort in the mist spraying environment are expected to predict the outdoor environments and the mist spraying environments by using the prediction model.

6.1. Methodology

6.1.1. Environmental factors

The effects of mist spraying systems on the outdoor hot environment conditions were conducted at the Institute of Industrial Science, University of Tokyo from July 23–August 4, 2018 [114]. The results of environmental conditions for outdoor and mist spraying experiments are displayed in Fig. 6-1. The main experiment consists of two parts of environmental conditions: (b) the outdoor environment and (c) mist spraying environment. Before starting the experiment, the subjects rested for 20 min in an indoor environment and experienced hot outdoor and mist spraying environments for 10 min each. The 65 datasets of environmental factors were able to be referenced, but the number of available complete datasets were 58.

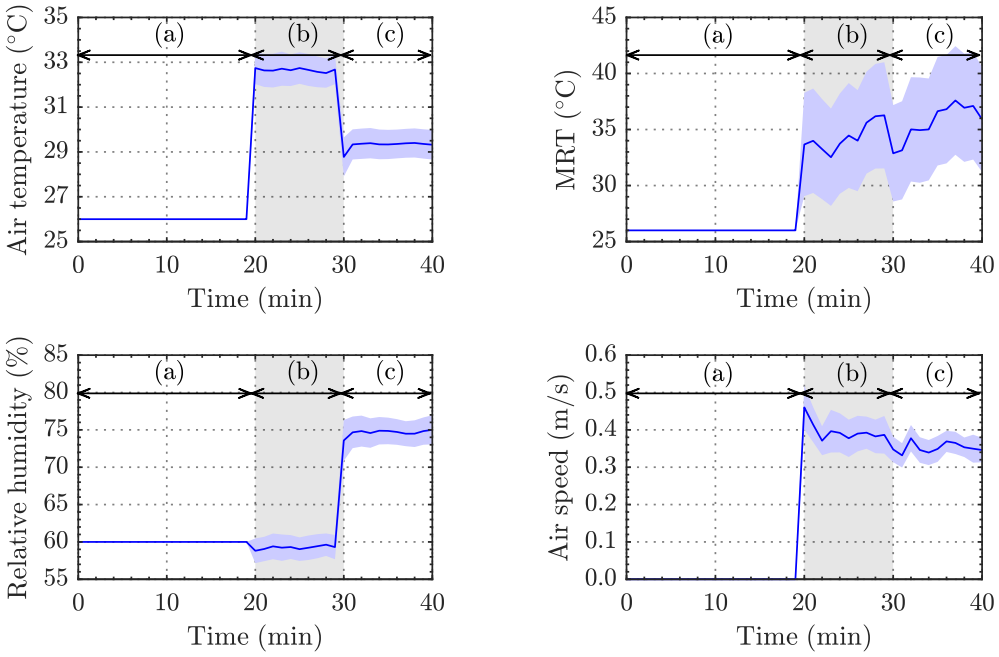

Fig. 6-1. Result of environmental conditions in the experiment (mean and 95% CI [confidence interval], n = 58). (a) air conditioning room, (b) outdoor environment, and (c) mist spraying environment.

The schematic diagram and thermal resistance network diagram of the 2NM and 3NM considering mist wettedness are described in Fig. 6-2. The following descriptions focused on the 3NM because the 2NM can be easily understood considering only the clothed parts of the 3NM. The energy balance equations in each node can be expressed as Equations (6-1) to (6-3).

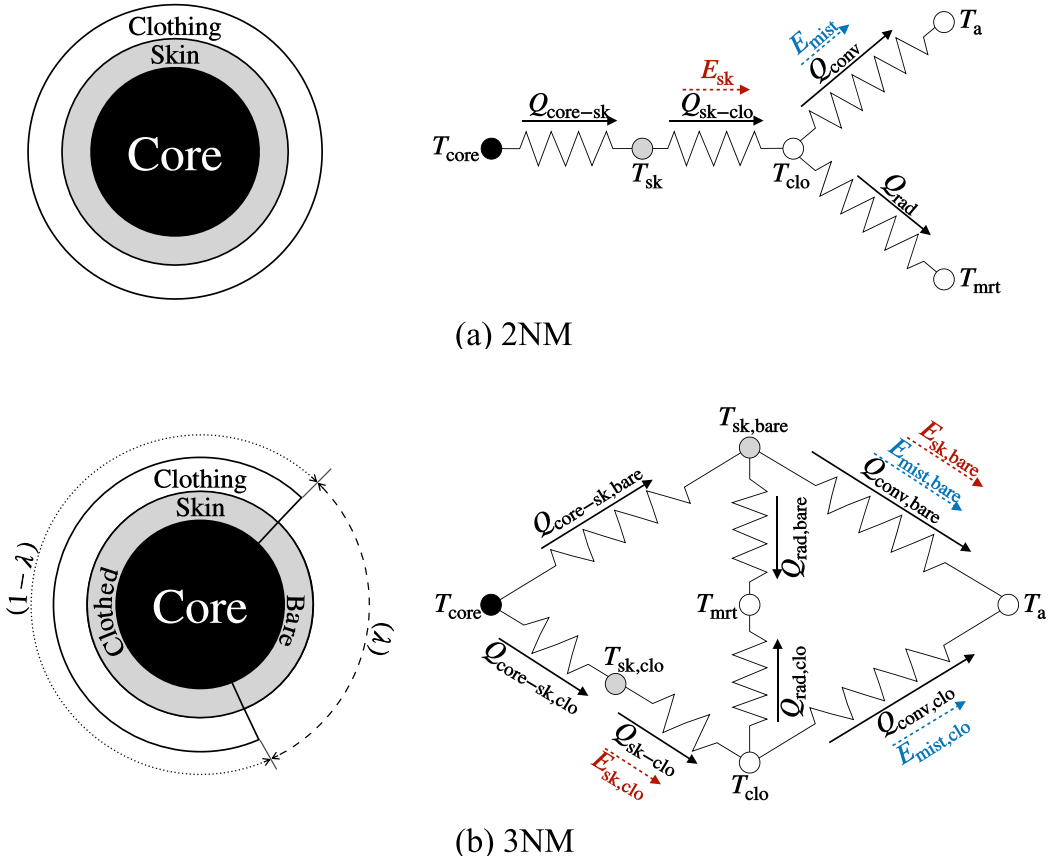

Fig. 6-2. Schematic diagram and thermal resistance network diagram of physiological thermal model considering mist wettedness. (a) 2NM with mist wettedness (b) 3NM with mist wettedness. (Thermal resistance, which affects heat transfer and evaporative heat loss is not the same, but it was simplified as a total resistance for easy understanding.)

$$S_{\mathrm{core}} = M - W - Q_{\mathrm{res}} - \lambda\, Q_{\mathrm{core\text{-}sk,bare}} - (1-\lambda)\, Q_{\mathrm{core\text{-}sk,clo}} \tag{6-1}$$

$$S_{\mathrm{sk,bare}} = Q_{\mathrm{core\text{-}sk,bare}} - \left(Q_{\mathrm{conv,bare}} + Q_{\mathrm{rad,bare}} + E_{\mathrm{sk,bare}} + E_{\mathrm{mist,bare}}\right) \tag{6-2}$$

$$S_{\mathrm{sk,clo}} = Q_{\mathrm{core\text{-}sk,clo}} - \left(Q_{\mathrm{conv,clo}} + Q_{\mathrm{rad,clo}} + E_{\mathrm{sk,clo}} + E_{\mathrm{mist,clo}}\right) \tag{6-3}$$

where S_{core}, $S_{\mathrm{sk,bare}}$, and $S_{\mathrm{sk,clo}}$ are heat storage rate in the core, bare skin, and clothed skin in W/m^2. In the core compartment, the heat is produced by metabolism M, and some portions of it could be used as external work W. In addition, the heat loss by respiration Q_{res} and heat transfer from the

core to skin ($Q_{\mathrm{core-sk,bare}}$ and $Q_{\mathrm{core-sk,clo}}$) occur. The heat transfer from the core to the skin is calculated considering area ratio λ of the bare segments of the human body by Equation (6-4) (q.v. Appendix 4 and Appendix 5). Q_{conv} and Q_{rad} are convective and radiative heat loss from skin, respectively. E_{sk} and E_{mist} are latent heat loss by regulatory sweating and natural diffusion of vapor from skin and evaporative heat loss by mist droplets. The subscripts bare and clo correspond to the segments where evaporation occurs.

$$\lambda = \frac{A_{\mathrm{bare}}}{A_{\mathrm{total}}} \tag{6-4}$$

Considering the heat capacity, the temperature change in each node according to the heat storage can be derived using Equations (6-5) to (6-7).

$$S_{\mathrm{core}} = M - W - Q_{\mathrm{res}} - \lambda\, Q_{\mathrm{core-sk,bare}} - (1-\lambda)\, Q_{\mathrm{core-sk,clo}} \tag{6-5}$$

$$S_{\mathrm{sk,bare}} = Q_{\mathrm{core-sk,bare}} - \left(Q_{\mathrm{conv,bare}} + Q_{\mathrm{rad,bare}} + E_{\mathrm{sk,bare}} + E_{\mathrm{mist,bare}}\right) \tag{6-6}$$

$$S_{\mathrm{sk,clo}} = Q_{\mathrm{core-sk,clo}} - \left(Q_{\mathrm{conv,clo}} + Q_{\mathrm{rad,clo}} + E_{\mathrm{sk,clo}} + E_{\mathrm{mist,clo}}\right) \tag{6-7}$$

where α_{sk} is a mass fraction of skin compartment of the body and is determined by the blood flow rate according to the thermal state of the body (Equation (6-8)) and is assumed 0.1 for physiological thermal neutrality. Accordingly, $(1-\alpha_{\mathrm{sk}})$ is a mass fraction of the core compartment of the body. m is total mass of the body in kg, $C_{\mathrm{p,body}}$ is the specific heat of body (3500 J kg^{-1} K^{-1}), and A_D is surface area of the body in m^2. The temperatures of core, bare skin, and clothed skin nodes are expressed T_{core}, $T_{\mathrm{sk,bare}}$, and $T_{\mathrm{sk,clo}}$ in that order. μ is the mass ratio of the bare segments for the total mass of the body and can be expressed in Equation (6-9) (q.v. Appendix 4).

$$\alpha_{\mathrm{sk}} = 0.0418 + \frac{0.745}{3600\,\dot{m}_{\mathrm{bl}} + 0.585} \tag{6-8}$$

$$\mu = \frac{m_{\mathrm{bare}}}{m} \tag{6-9}$$

The peripheral blood flow rate $\dot{m}_{bl}$ (L s^{-1} m^{-2}) depends on skin and core temperature deviations from their physiological thermal neutral temperature (Equation (6-10)); neutral conditions were considered as 36.8 °C for the core $T_{core,n}$ and 33.7 °C for the skin $T_{sk,n}$ [88].

$$\dot{m}_{bl} = \frac{BFN + c_{dil}\left(T_{core} - T_{core,n}\right)}{3600\left(1 + S_{tr}\left(T_{sk,n} - T_{sk,ov}\right)\right)} \quad (6\text{-}10)$$

$$T_{sk,ov} = \lambda\, T_{sk,bare} + (1-\lambda)\, T_{sk,clo} \quad (6\text{-}11)$$

where overall skin temperature $T_{sk,ov}$ was calculated by area weighted average temperature of bare skin and clothed skin (Equation (6-11)). The limitation of blood flow rate ranged from 0.5 to 90 (L m^{-2} hr^{-1}) due to vasoconstriction and vasodilation. For average persons, the coefficients BFN, c_{dil}, and S_{tr} are 6.3, 50, and 0.5 [44,88].

The heat transfer from the core to skin compartment on each segment can be calculated using Equations (6-12) and (6-13).

$$Q_{core-sk,bare} = \left(K + \rho_{bl}\, C_{p,bl}\, \dot{m}_{bl}\right)\left(T_{core} - T_{sk,bare}\right) \quad (6\text{-}12)$$

$$Q_{core-sk,clo} = \left(K + \rho_{bl}\, C_{p,bl}\, \dot{m}_{bl}\right)\left(T_{core} - T_{sk,clo}\right) \quad (6\text{-}13)$$

where the effective conductance K between core and skin and was considered as 5.28 W m^{-2} K^{-1}, and ρ_{bl} is density of blood (1.06 kg L^{-1}). The specific heat of blood $C_{p,bl}$ was set as 4190 J kg^{-1} K^{-1}.

Heat exchange by respiration Q_{res} which caused by dry heat loss and latent heat loss can be calculated using Equation (6-14).

$$Q_{res} = 0.0014\, M\,(34 - T_a) + 0.0173\, M\,(5.87 - P_a) \quad (6\text{-}14)$$

where p_a is partial water vapor pressure in the air (kPa).

The total sensible heat transfer from bare skin to the environment is calculated using Equation (6-15).

$$Q_{\text{core-sk,bare}} = \left(K + \rho_{\text{bl}}\, C_{\text{p,bl}}\, \dot{m}_{\text{bl}}\right)\left(T_{\text{core}} - T_{\text{sk,bare}}\right) \tag{6-15}$$

where h_{c} and h_{r} are the convective and radiative heat transfer coefficient of the human body. The heat transfer coefficients in each segment of the body for airspeed can be referenced to previous studies [50,116,117]. T_{a}, T_{mrt}, and T_{sk} are the air temperature, mean radiant temperature around the human body, and skin surface temperature. f_{r} is the effective radiation area factors for the whole body: 0.70 for a sitting person and 0.73 for a standing person [35].

The total sensible heat transfer from clothed skin is calculated with Equation (6-16). In addition, the total sensible heat transfer should be matched to the sum of convective and radiative heat loss from clothing surface to the environment as Equation (6-17). Therefore, Equations (6-16) and (6-17) are equal, and T_{clo} is determined by solving two equations using Newton's method.

$$Q_{\text{sk-clo}} = \frac{T_{\text{sk,clo}} - T_{\text{clo}}}{R_{\text{clo}}} \tag{6-16}$$

$$Q_{\text{sk-clo}} = Q_{\text{conv,clo}} + Q_{\text{rad,clo}} = f_{\text{clo}}\left[h_{\text{c}}\left(T_{\text{clo}} - T_{\text{a}}\right) + f_{\text{r}}\, h_{\text{r}}\left(T_{\text{clo}} - T_{\text{mrt}}\right)\right] \tag{6-17}$$

where f_{clo} is the ratio of the clothing area to the whole-body surface area. T_{clo} and R_{clo} are clothing surface temperature and clothing insulation.

The evaporative heat loss from the skin surface is a combination of the heat loss by the natural diffusion of water through the skin E_{diff} and the regulatory sweating E_{rsw} as expressed in Equation (6-20). The maximum evaporative heat loss E_{max} occurs when the skin surface is completely wet ($\omega_{\text{sk}} = 1$) and is proportional to the difference between saturated water vapor pressure at skin temperature and partial water vapor pressure in the air. The natural diffusion of water through the skin does not occur as much as the surface area is wetted by sweating in Equation (6-21).

$$\omega_{\mathrm{diff}} = \frac{E_{\mathrm{diff}}}{E_{\mathrm{max}}} = 0.06 \tag{6-18}$$

$$\omega_{\mathrm{rsw}} = \frac{E_{\mathrm{rsw}}}{E_{\mathrm{max}}} \tag{6-19}$$

$$\omega_{\mathrm{sk}} = \omega_{\mathrm{rsw}} + \omega_{\mathrm{diff}} \tag{6-20}$$

$$\omega_{\mathrm{diff}} = 0.06\,(1 - \omega_{\mathrm{rsw}}) \tag{6-21}$$

Evaporation heat loss using mist wettedness under skin wettedness conditions can be considered as shown in Fig. 6-3. The skin surface is wet as the value of skin wettedness as expressed in Equation (6-22). The mist wettedness by the experimental method was obtained under a dry body surface condition. The mist wettedness was obtained by the heating globe thermometer, and skin wettedness was not considered in the experimental method. Therefore, evaporative heat loss by the mist wettedness under given skin wettedness should be calculated. Even if the mist droplets are attached to the wetted surface, it does not affect the total evaporation heat loss, and the area ratio affecting evaporation heat loss by the mist wettedness can be expressed, as shown in Equation (6-23).

$$\frac{A_{\mathrm{sk}}}{A_{\mathrm{D}}} = \omega_{\mathrm{sk}} \tag{6-22}$$

$$\frac{A_{\mathrm{mist}}}{A_{\mathrm{D}}} = (1 - \omega_{\mathrm{sk}})\,\omega_{\mathrm{mist}} \tag{6-23}$$

The evaporative heat loss by skin wettedness can be determined by using Equation (6-24) for the bare node and Equation (6-25) for the clothed node.

$$E_{\mathrm{sk,bare}} = \omega_{\mathrm{sk}}\,\left(p^{*}_{\mathrm{sk,bare}} - p_{\mathrm{a}}\right)/\left(\frac{1}{h_{\mathrm{e}}}\right) \tag{6-24}$$

$$E_{\mathrm{sk,clo}} = \omega_{\mathrm{sk}}\,\left(p^{*}_{\mathrm{sk,clo}} - p_{\mathrm{a}}\right)/\left(R_{\mathrm{e,clo}} + \frac{1}{f_{\mathrm{clo}}\,h_{\mathrm{e}}}\right) \tag{6-25}$$

where h_{e} is the evaporative heat transfer coefficient for the outer air layer of a bare or clothed body

in W m^{-2} kPa^{-1}, $R_{e,clo}$ is the evaporative heat transfer resistance of clothing in kPa m^2 W^{-1}, and p^*_{sk} is saturated water vapor pressure at skin temperature.

The evaporative heat loss by mist wettedness can be determined by using Equation (6-26) for the bare node and Equation (6-27) for the clothed node. Unlike skin wettedness, heat loss by mist droplets does not consider clothing insulation.

$$E_{mist,bare} = (1 - \omega_{sk})\, \omega_{mist}\, (p^*_{sk,bare} - p_a) / \left(\frac{1}{h_e}\right) \tag{6-26}$$

$$E_{mist,clo} = (1 - \omega_{sk})\, \omega_{mist}\, (p^*_{clo,clo} - p_a) / \left(\frac{1}{f_{clo}\, h_e}\right) \tag{6-27}$$

where p^*_{clo} is saturated water vapor pressure at clothing temperature.

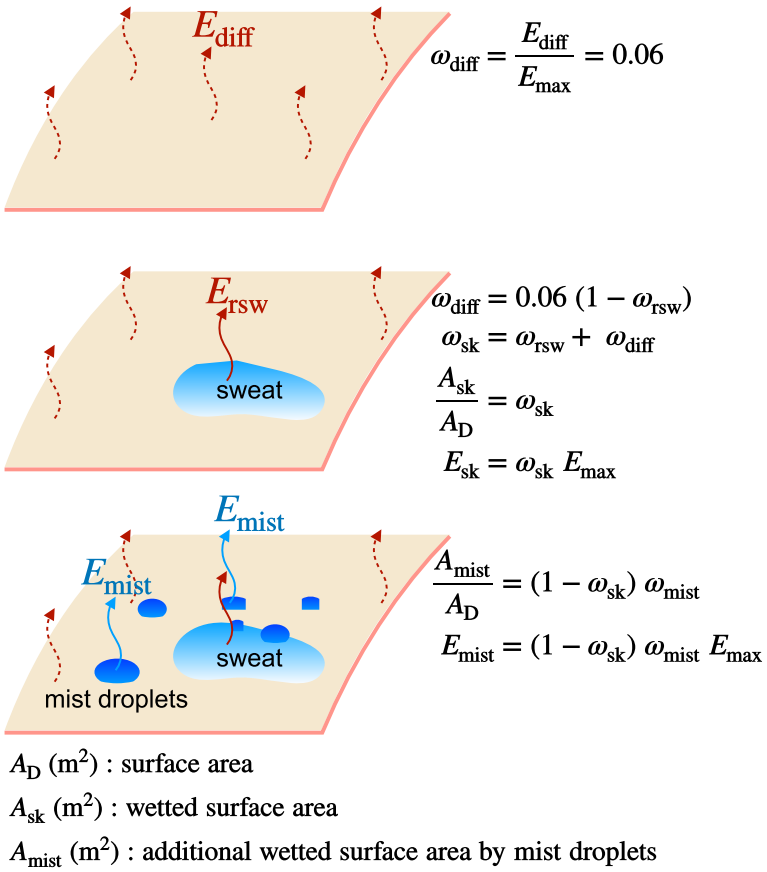

Fig. 6-3. Evaporative heat loss concepts by skin wettedness and mist wettedness.

6.2. Results and discussion

6.2.1. Skin temperature variations

The overall skin temperature was calculated by proposed 2NM and 3NM using measured environmental factors. In addition, the results of the predicted skin temperature were compared with the measured overall skin temperature as shown in Fig. 6-4. The measured overall skin temperature was calculated as the area-weighted average of seven parts of body segments, which was suggested by Hardy et al. [80]. The 65 overall skin temperatures were measured and calculated properly. The experiment result showed that skin temperature gradually rose in the outdoor environment (b) and decreased in the mist spraying environment (c). In the result of existing 2NM and 3NM which did not involve mist wettedness, skin temperature rose in the outdoor environment. On the other hand, the skin temperature did not steadily decrease in the mist spraying environment. Applying the mist wettedness to 2NM and 3NM, the skin temperature showed continuously decreased in the mist spraying environment. However, the skin temperature gap between measurement and prediction showed 0.52 °C for 2NM and 0.56 °C for 3NM at the end of the experiment. When the human enters the mist spraying environment, the body is not uniformly wet by the mist droplets (e.g. if the human body is exposed to a mist spraying system which is sprayed the water from the side, the body's back is not directly wet). Therefore, the effectiveness factor of the evaporative heat loss by mist wettedness on the body can be considered.

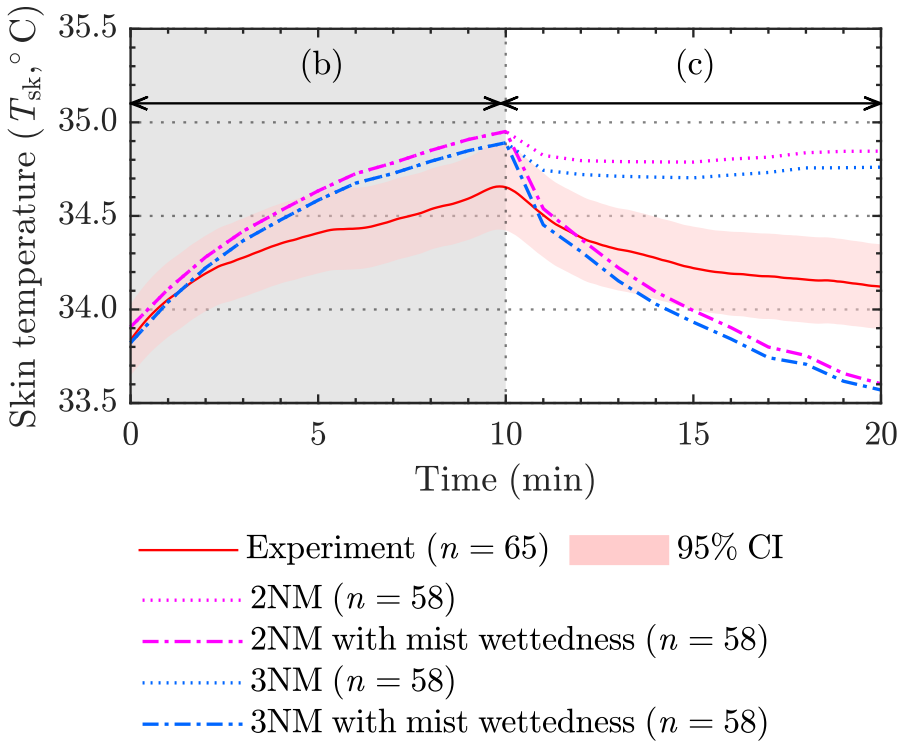

Fig. 6-4. Comparison of results of overall body skin temperature by experiment (*n* = 65) and prediction (*n* = 58), (b) is for outdoor environment, and (c) is for mist spraying environment.

6.2.2. Heat loss causes in outdoor and mist spraying environment

Heat loss causes were investigated to understand the thermal effects of outdoor and mist spraying environments on the human body. Environmental conditions were selected as the mean value of measured experiment data of outdoor and mist spraying environments (see Table 6-1). The heat losses were calculated considering that the physiological thermal neutral condition of the body was exposed to each environment for 10 min which was the same time as the experiment. The results showed that the sweating was the most important factor to diffuse the heat from the body in outdoor environment, and the mist wettedness was the most important role for heat loss on human body in mist spraying environment as shown in Fig. 6-5.

Table 6-1. Environmental factors for calculation of heat loss causes in outdoor and mist spraying environments using 2NM and 3NM.

Environmental factor	Outdoor environment	Mist spraying environment
Air temperature T_a (°C)	32.9	29.3
Relative humidity RH (%)	58.7	74.6
Mean radiant temperature T_{mrt} (°C)	36.8	35.6
Airspeed v (m/s)	0.41	0.35
Mist wettedness ω_{mist}	-	0.25

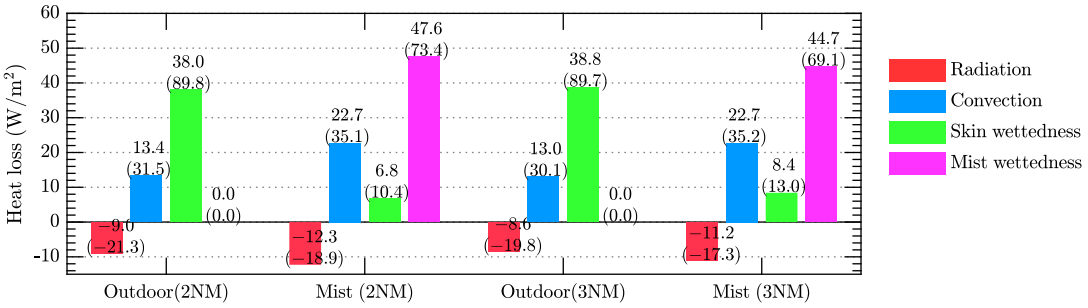

Fig. 6-5. Comparison of the results of heat loss by radiation, convection, evaporation on the human body in outdoor and mist spraying environments considering mist wettedness.

6.2.3. Effectiveness area factor of evaporative heat loss by mist droplets

The effectiveness factor of evaporative heat loss by mist wettedness η_{mist} was applied to 2NM and 3NM and can be summarized in Table 6-2. Therefore, all kinds of evaporative heat losses at the bare node and clothed node can be described as Equations (6-28) and (6-29). The summation of skin wettedness and mist wettedness cannot exceed one.

$$E_{bare} = h_e \left(\omega_{sk} + \eta_{mist} \left(1 - \omega_{sk}\right) \omega_{mist}\right) \left(p^*_{sk,bare} - p_a\right) \tag{6-28}$$

$$E_{clo} = f_{clo}\, h_e \left[\frac{\omega_{sk} \left(p^*_{sk,clo} - p_a\right)}{f_{clo}\, h_e\, R_{e,clo} + 1} + \eta_{mist} \left(1 - \omega_{sk}\right) \omega_{mist} \left(p^*_{clo,clo} - p_a\right)\right] \tag{6-29}$$

The effectiveness area factor assumed constant value while the human body is in the mist spraying environment. Skin temperature variations for the effectiveness factor value in the mist spraying environment are calculated as shown in Fig. 6-6. The least skin temperature difference between the

experiment and the prediction resulted when the effectiveness factor was 0.72 for 2NM and 0.64 for 3NM. Meanwhile, the initial skin temperature of the predicted result was different from the measured value in the mist spraying environment. Therefore, when the initial skin temperature was adjusted to the experimental value, the least skin temperature difference between the experiment and the prediction occurred when the effect factor was 0.34 for 2NM and 0.32 for 3NM.

However, further research is necessary because the initial physiological thermal state of the body should be matched in prediction and the experiment to gain an accurate value of mist wettedness.

Table 6-2. The evaporative heat losses in 2NM and 3NM.

	E_{sk}	E_{mist}
2NM	$\omega_{\mathrm{sk}}\left(p^{*}_{\mathrm{sk,clo}}-p_{\mathrm{a}}\right)/\left(R_{\mathrm{e,clo}}+\frac{1}{f_{\mathrm{clo}}\,h_{\mathrm{e}}}\right)$	$\eta_{\mathrm{mist}}(1-\omega_{\mathrm{sk}})\,\omega_{\mathrm{mist}}\,\left(p^{*}_{\mathrm{clo,clo}}-p_{\mathrm{a}}\right)/\left(\frac{1}{f_{\mathrm{clo}}\,h_{\mathrm{e}}}\right)$
3NM (bare)	$\omega_{\mathrm{sk}}\,\left(p^{*}_{\mathrm{sk,bare}}-p_{\mathrm{a}}\right)/\left(\frac{1}{h_{\mathrm{e}}}\right)$	$\eta_{\mathrm{mist}}\,(1-\omega_{\mathrm{sk}})\,\omega_{\mathrm{mist}}\,\left(p^{*}_{\mathrm{sk,bare}}-p_{\mathrm{a}}\right)/\left(\frac{1}{h_{\mathrm{e}}}\right)$
3NM (clothed)	$\omega_{\mathrm{sk}}\left(p^{*}_{\mathrm{sk,clo}}-p_{\mathrm{a}}\right)/\left(R_{\mathrm{e,clo}}+\frac{1}{f_{\mathrm{clo}}\,h_{\mathrm{e}}}\right)$	$\eta_{\mathrm{mist}}\,(1-\omega_{\mathrm{sk}})\,\omega_{\mathrm{mist}}\,\left(p^{*}_{\mathrm{clo,clo}}-p_{\mathrm{a}}\right)/\left(\frac{1}{f_{\mathrm{clo}}\,h_{\mathrm{e}}}\right)$

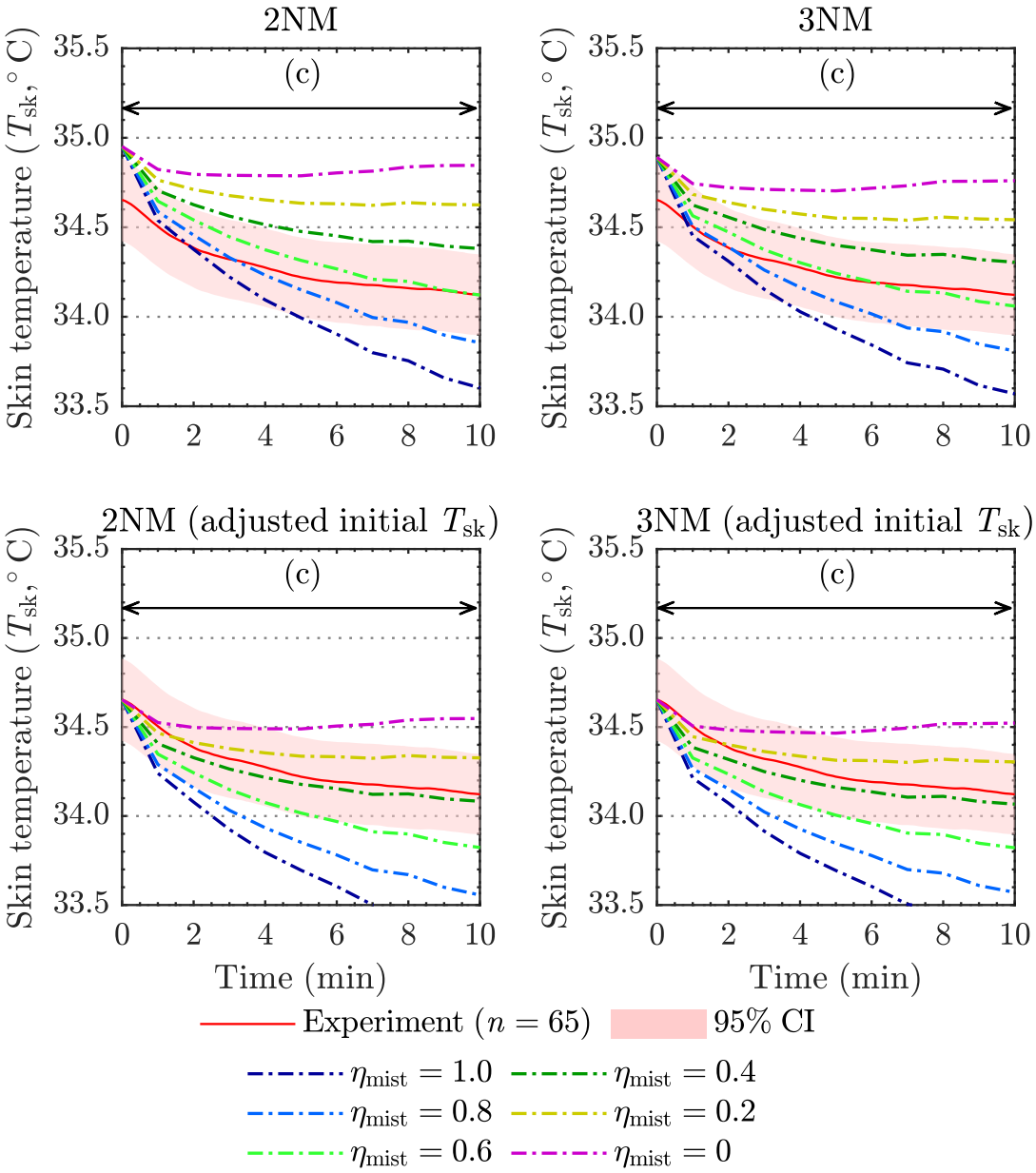

Fig. 6-6. Skin temperature variations for the effectiveness area factor of evaporative heat loss by mist wettedness.

6.2.4. Heat loss causes considering effectiveness area factor

The heat loss from the body surface can be confirmed using the proposed prediction model. The conditions of the outdoor and mist spraying environments used the mean of measured environmental factors (Table 6-3), and heat losses were calculated considering that the physiological thermal neutral condition of the body was exposed to each environment for 10 min. (a) and (b) display the ratio of heat loss causes to total heat loss for effectiveness area factor in 2NM and 3NM, respectively. (c) and

(d) show the results of the heat loss causes in outdoor and mist spray environments in 2NM and 3NM when the effect factor is 0.5, respectively. The effectiveness area factor η_{mist} was set as 0 to 1. The results of heat losses on surface of the body are shown in Fig. 6-7. In the outdoor environment, evaporative heat loss due to skin wettedness was the dominant cause of heat loss from the surface of the human body. In contrast, in the mist spraying environment, the convective heat loss on the surface of the human body was largest. In addition, evaporative heat loss due to mist wettedness showed a significant effect on the total heat loss, corresponding to 37.4% for 2NM and 35.1% for 3NM.

Table 6-3. Environmental factors for calculation of heat losses causes in outdoor and mist spraying environments using 2NM and 3NM.

Environmental factor	Outdoor environment	Mist spraying environment
Air temperature T_{a} (°C)	32.9	29.3
Relative humidity RH (%)	58.7	74.6
Mean radiant temperature T_{mrt} (°C)	36.8	35.6
Airspeed v (m/s)	0.41	0.35
Mist wettedness ω_{mist}	-	0.25
Effectiveness area factor η_{mist}	-	0 to 1

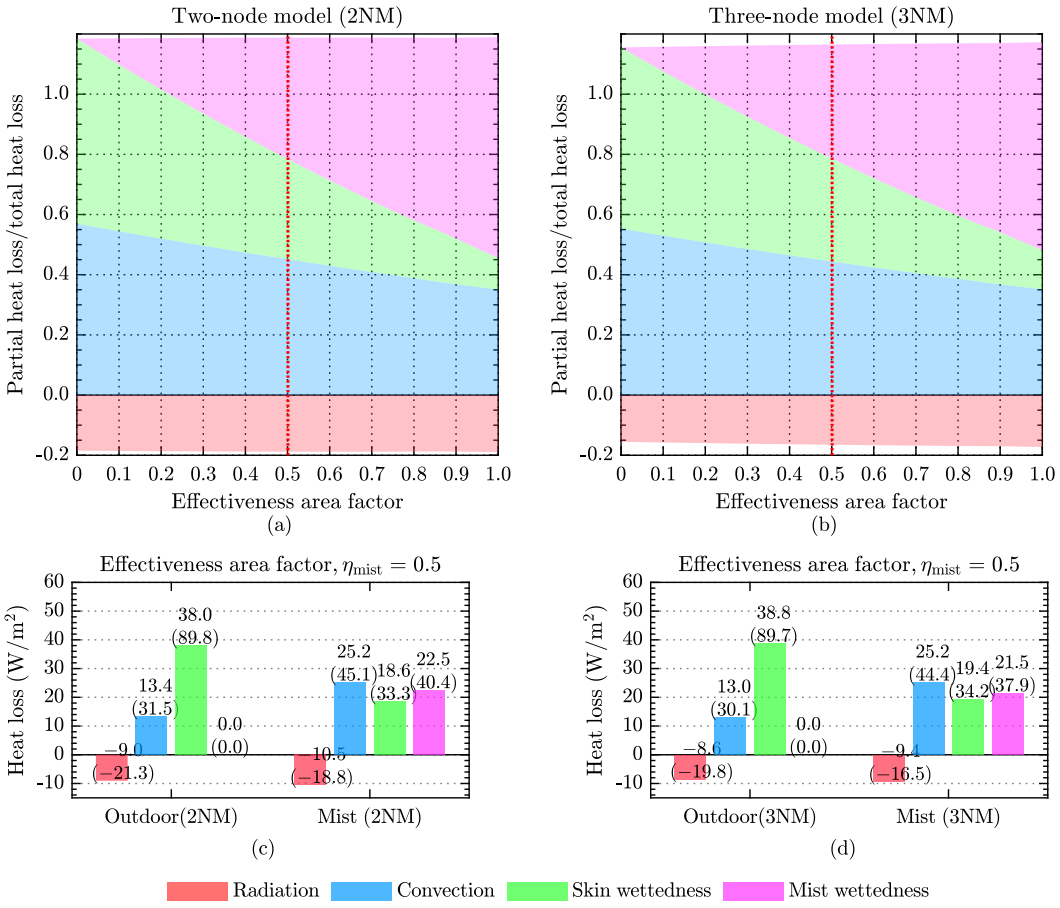

Fig. 6-7. Comparison of the results of heat loss by radiation, convection, evaporation on the human body in outdoor and mist spraying environments considering mist wettedness and effectiveness area factor (the parentheses value is each heat loss percentage (%) for the total heat loss). (a): Ratio of heat loss causes to total heat loss for effectiveness area factor (2NM), (b): Ratio of heat loss causes to total heat loss for effectiveness area factor (3NM), (c): Results of heat loss causes in outdoor and mist spraying environments (2NM), and (d): Results of heat loss causes in outdoor and mist spraying environments (3NM).

6.3. Conclusion

The verification of 2NM and 3NM in outdoor and mist spraying environments was confirmed by the comparison with the experimental result of skin temperature. The mist wettedness was proposed as a new environmental factor in the mist spraying environment. In addition, the mist wettedness was measured using a heating globe thermometer and modified the existing prediction models for mist spraying environment considering the mist wettedness. The results obtained from the present study are listed below.

- The mist wettedness on the surface of the heating globe thermometer in the mist spraying environment was measured as 0.25 ± 0.086 (Mean ± SD, n = 58).
- In the outdoor environment, the existing models predicted skin temperature with an error of 0.24 °C (2NM) and 0.3 °C (3NM) for 10 min, and the modified model showed the same results.
- In the mist spraying environment, predicted skin temperature by existing models had stabilized and did not reflect the continuously decreasing experimental results, but the modified models reflected the continuously decreasing tendency with an error of 0.52 °C (modified 2NM) and 0.56 °C (modified 3NM).
- The effectiveness of evaporative heat loss by mist droplets η_{mist} was proposed and expected a range of 0.34–0.72 for modified 2NM and 0.32–0.64 for modified 3NM.
- The mist wettedness contributed to total heat loss from the body surface with 40.4% for the modified 2NM and 37.9% for the modified 3NM and was found to be a very important environmental factor (when η_{mist} was 0.5).

The physiological human model can be extended to the mist spraying environment by modified models considering mist wettedness. In addition, the physical phenomena between environments and the human body can be more clarified with prediction models. Moreover, the thermal state of the human body, thermal sensations, and thermal comfort in the mist spraying environment are expected to predict results in the outdoor and mist spraying environments by using the prediction model in future research.

Chapter 7. Proposal of new assessments for outdoor and mist spraying environments

Chapter 7. Proposal of new assessments for outdoor and mist spraying environments

7.1. Proposal of O-PMV index

A schematic diagram of deriving outdoor predicted mean vote (O-PMV) index is shown in Fig. 7-1. In experiment, environmental factors such as air temperature, mean radiant temperature, relative humidity, and airspeed were measured in outdoor and mist spraying environments. In addition, subjective assessments were collected through survey research. The skin temperature of subjects was measured to investigate the thermal state of the body. The skin temperature can be predicted using the measured environmental factors. The physiological thermoregulation human model verified by comparing the skin temperature between experiment and predicted results.

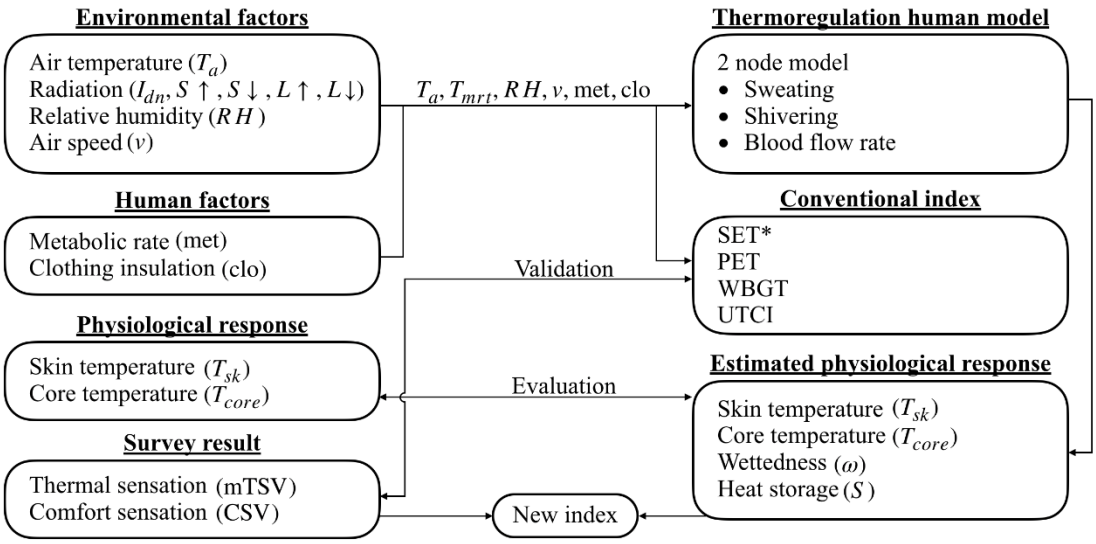

Fig. 7-1. Overall research flow for proposing new environmental index.

Fanger proposed PMV index by using the correlation between thermal sensation vote (TSV) and heat storage (S) on human body as expressed in Equation (7-1). PMV can be able to use to evaluate the thermal sensation of a thermal environment by simply measuring four basic environmental factors.

$$\mathrm{PMV} = \frac{\delta \mathrm{TSV}}{\delta S} \times S$$
$$\mathrm{PMV} = f(x) \times S \qquad (7\text{-}1)$$

where, the TSV is the result of the thermal sensation vote results, and S is the heat storage rate.

However, since the PMV index does consider physiological responses, such as sweating, shivering, and blow flow rate changes [118], it is not suitable to estimate the thermal sensation in extremely hot environments, such as hot outdoor environments and mist spraying environments. It is also known that the PMV index is suitable for almost comfortable indoor environments.

For this reason, instead of introducing the concept of PMV, the present study attempted to apply it to special environments such as outdoor and mist spraying environments by further considering the physiological response using a two-node model. The predictability of the two-node model was verified by field experiments and the results are described in Chapter 5. To suggest a new environmental index, 2NM was used to calculate the heat storage rate in the human body in environmental conditions. In addition, since the thermal sensation in the outdoor and mist spray environment is different from the indoor environment, the thermal sensation (mTSV) obtained through the experiment was used (Equation (7-2)).

$$\mathrm{OPMV} = \frac{\delta \mathrm{mTSV}}{\delta S(\mathrm{2NM})} \times S(\mathrm{2NM})$$
$$\mathrm{O\text{-}PMV} = f(x) \times S \tag{7-2}$$

The SET* index proposed through 2NM calculation assuming a person exposed to the environment for 60 minutes. However, since the heat storage rate converges to zero due to the thermoregulation of the human body, the heat storage rate in the thermal equilibrium condition cannot be utilized. Therefore, the heat storage rate was calculated when the human body was exposed to an outdoor and mist spraying environment for 10 minutes at the same time as surveying time. Fig. 7-2 shows the heat losses that occur inside and outside the mist spraying environments for a specific time (10 minutes).

On the outside and inside the mist system, the sensible heat losses (Mean ± SD) were 22.6 ± 13.1 W/m^2 and 52.0 ± 6.1 W/m^2, the latent heat losses (Mean ± SD) were 28.0 ± 6.9 W/m^2 and 12.3 ± 2.3 W/m^2, and the total heat losses (Mean ± SD) were 50.6 ± 6.2 W/m^2 and 64.3 ± 4.3 W/m^2, respectively. In the paired t-test analysis of the sensible ($p < 0.001$), latent ($p < 0.001$), and total heat loss ($p < 0.001$) from the body between outside and inside the mist spraying environment, a probability value (p-value) was shown as less than 0.05. Therefore, it can be inferred that heat losses from the body are significantly different between staying in outdoor and mist spraying environment.

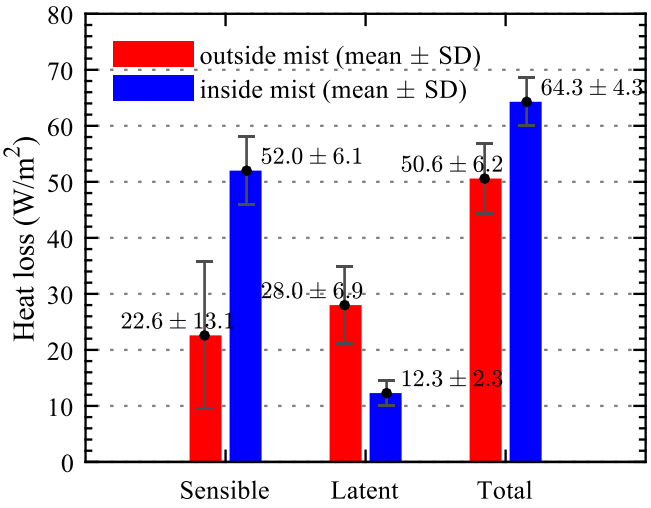

Fig. 7-2. Heat loss in outdoor and mist spray environments (10 minutes). The statistically significant differences between outside and inside the mist spraying environment was analyzed by paired *t*-test.

To determine the relationship between the heat storage rate and mTSV, Pearson's correlation coefficient was calculated. (cf. The null hypothesis of Pearson's correlation analysis is that there is no statistically significant relationship between the comparison variables). Fig. 7-3 shows the result of the correlation between heat storage rate and mTSV in outdoor and mist spraying environments. The linear regression equations are represented by equation (7-3), which can be used as a new environmental index (O-PMV) to evaluate outdoor and mist spraying environments.

Pearson's correlation coefficient (r) was 0.31 in outdoor and 0.28 in the mist spraying environment, respectively. In order to generalize the O-PMV index, it is necessary to update the correlation by measuring the thermal sensation and environmental factors in a wider range of environmental conditions. However, this study is limited in sample size and requires additional experiments to obtain more robust regression equations for O-PMV. According to the O-PMV results, it has been observed that even at the same heat storage rate, humans can feel colder in mist spraying environments than in normal outdoor environments.

$$\begin{aligned} \text{O-PMV}_{\text{outdoor}} &= 0.05\,S + 0.51,\ (n = 72,\ r = 0.31,\ p < 0.01) \\ \text{O-PMV}_{\text{mist}} &= 0.06\,S - 0.13,\ (n = 60,\ r = 0.28,\ p < 0.05) \end{aligned} \tag{7-3}$$

Subjects reported that even at the same heat storage rate, they were cooler in the mist spraying environment than in the outdoor environment, which may be due to evaporation from the human

surface by the mist. Therefore, further studies must be conducted to clearly understand the thermal interactions between the human body and the thermal environment in a mist spraying environment.

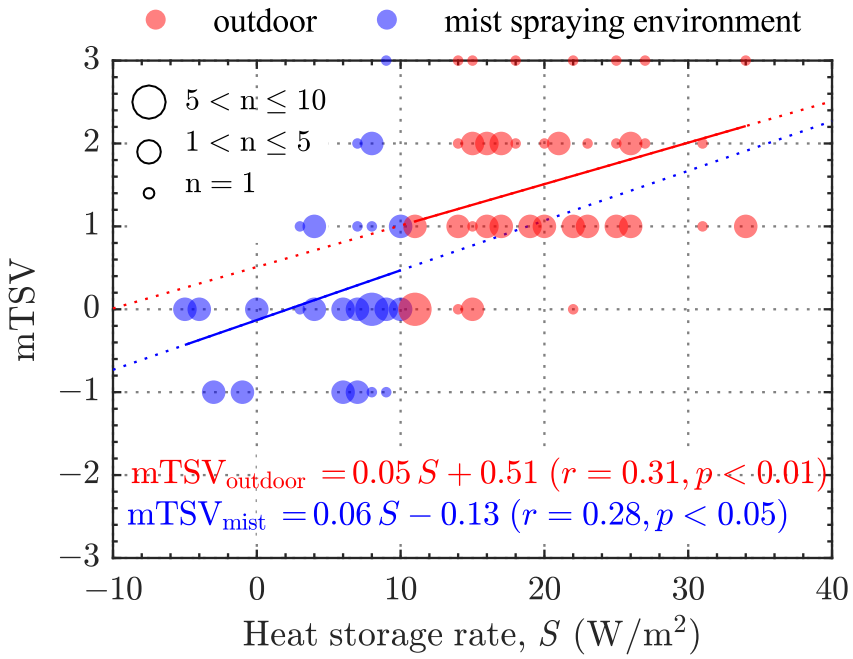

Fig. 7-3. Correlation between heat storage rate and mTSV (*n* is 72 for outdoor environment and 60 for mist spraying environment, *r* is the Pearson's correlation coefficient, and *p* is probability value).

The O-PMV index was proposed using experimental data in 2017 [27]. However, due to the shortage number of subject's data, the proposed O-PMV index was necessary to be updated by applying additional experimental results. A further experiment was conducted in 2018 as explained in Chapter 5. The summation of data that was used in the updated O-PMV was 294 in the outdoor environment and 231 in the mist spraying environment, as listed in Table 7-1.

Table 7-1. Utilized number of data for O-PMV index.

Environment condition	2017 experiment (sunshade)	2018 experiment (without sunshade)	Total
Outdoor environment	72	222	294
Mist spraying environment	60	171	231

The updated O-PMV result is showed in Fig. 7-4. As a result, the range of heat storage rates was wider and Pearson's correlation coefficient was larger than before. In addition, the probability value

became smaller which was indicating a higher significant correlation between the heat storage rate and mTSV. Equation (7-4) shows the result of the updated O-PMV.

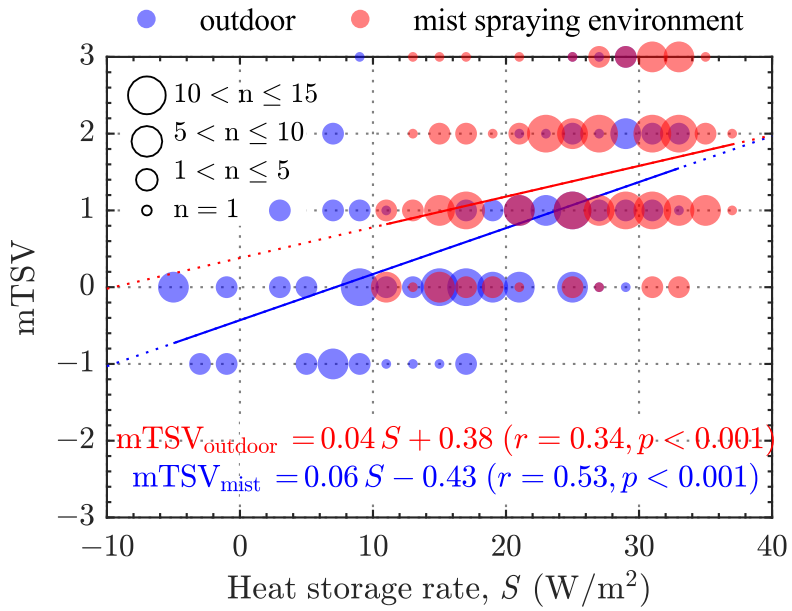

Fig. 7-4. Correlation between heat storage rate and mTSV (*n* is 294 for outdoor environment and 231 for mist spraying environment, *r* is the Pearson's correlation coefficient, and *p* is probability value).

$$\begin{aligned} \text{O-PMV}_{\text{outdoor}} &= 0.04\,S + 0.38,\ (n = 294,\ r = 0.34,\ p < 0.001) \\ \text{O-PMV}_{\text{mist}} &= 0.06\,S - 0.43,\ (n = 231,\ r = 0.53,\ p < 0.001) \end{aligned} \tag{7-4}$$

*7.2. Proposal of SET** index*

The SET* index assumes the human body with the physiologically thermoneutral condition is exposed to a given environmental condition for one hour. The air temperature of the standard environment conditions which makes the same skin temperature and wettedness of the results of 2NM is the SET* value. The SET* considers the basic 4 environmental conditions (air temperature, radiation, humidity, and airspeed). Thus, SET* in a mist spraying environment is difficult to utilize due to additional thermal influence exists. To overcome these problems, measuring the additional thermal effects in a mist spraying environment, mist wettedness meter was developed and measured as explained in Chapter 5. In addition, physiological human models were revised considering mist wettedness as described in Chapter 6.

From these results, it is possible to propose environmental factors that consider the five

environmental factors in the mist spraying environment which are the all environmental effects of the thermal environment on a human body. As shown in Fig. 7-5, we suggest the SET** index that considers mist wettedness.

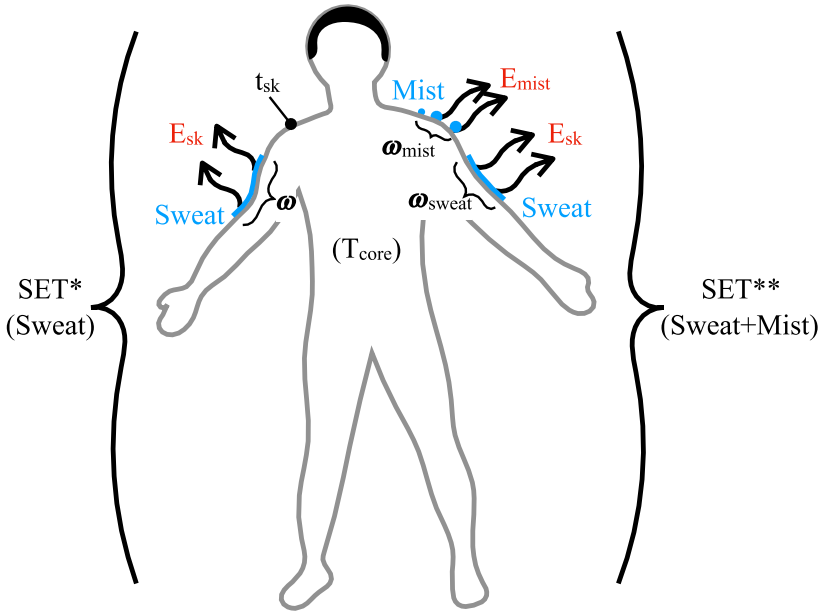

Fig. 7-5. Concept of SET** index considering skin wettedness and mist wettedness.

The SET** is an environmental index considering mist wettedness such as inside the mist spraying environment, which value is perfectly consistent with SET* for without mist wettedness conditions. The correlation results of SET* and SET** between in outdoor and mist spraying environments are expressed in Fig. 7-6 and its regression results are Equation (7-5). The SET* and SET** changes of an outdoor environment by mist spraying system can be estimated using the results of regression analysis. For example, in an outdoor environment where SET* is 30 °C, SET* and SET** becomes 28.7 °C and 26.9 °C in a mist spraying environment. This result implicates that the cooling effect by mist wettedness which is not considered in SET* is about 1.8 °C.

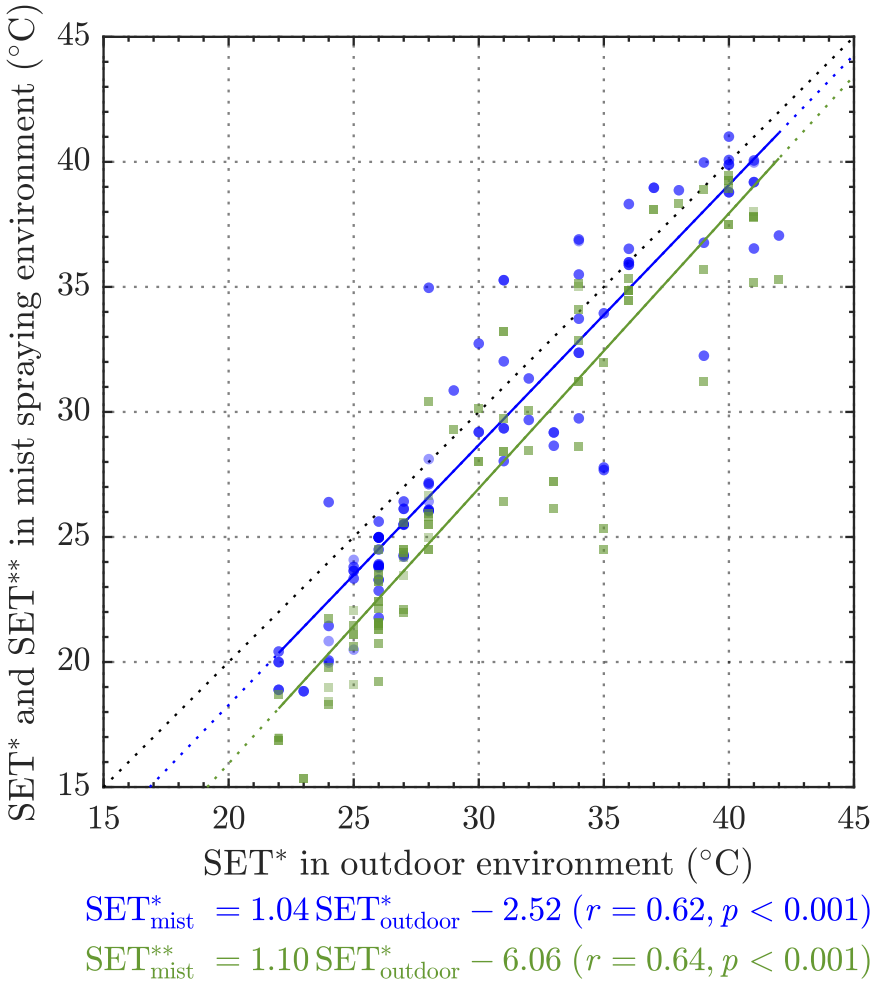

Fig. 7-6. Correlation between results of SET* and SET** in outdoor and mist spraying environment.

$$\begin{aligned} \mathrm{SET}^{*}_{\mathrm{mist}} &= 1.04\,\mathrm{SET}^{*}_{\mathrm{outdoor}} - 2.52 \quad (r = 0.62,\ p < 0.001) \\ \mathrm{SET}^{**}_{\mathrm{mist}} &= 1.10\,\mathrm{SET}^{*}_{\mathrm{outdoor}} - 6.06 \quad (r = 0.64,\ p < 0.001) \end{aligned} \tag{7-5}$$

Fig. 7-7 shows the correlation results of mTSV to SET* and SET** and linear regression results are shown in Equation (7-6). The thermal sensation (mTSV) corresponding to the measured environment can be predicted and evaluated using the results of regression equation, when SET* or SET** is calculated by measuring environment factors in outdoor and mist spraying environments.

The results of SET* and SET** in the mist spraying environment differed depending on the consideration of the mist wettedness, and the difference was 2.2 °C under the same thermal sensation (mTSV).

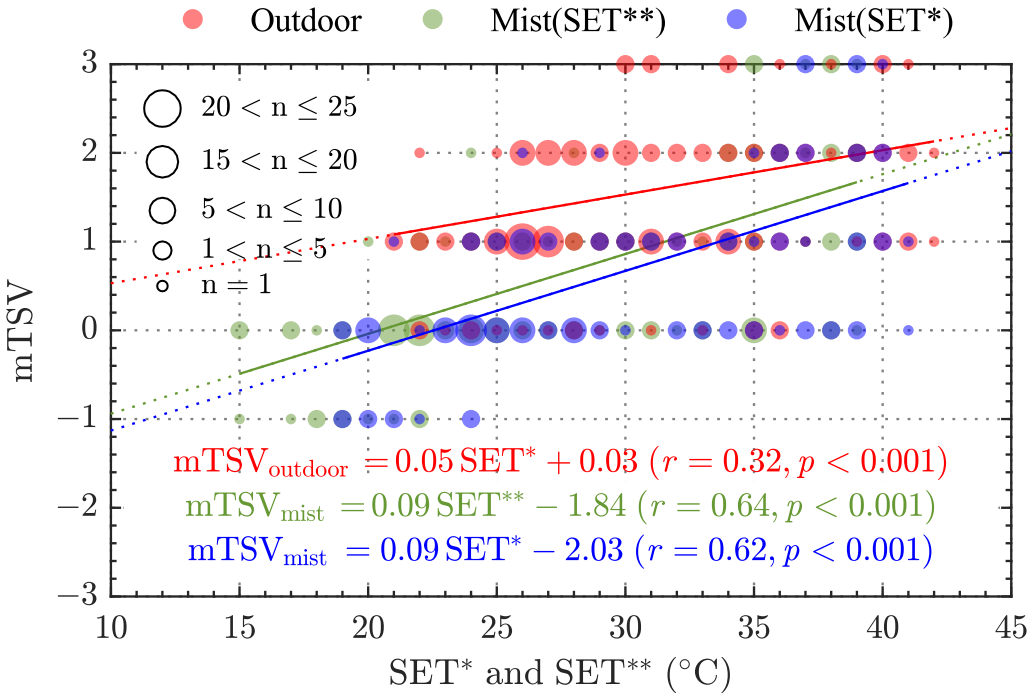

Fig. 7-7. Correlation results of mTSV to SET* and SET**.

$$\begin{aligned} \mathrm{mTSV_{outdoor}} &= 0.05\ \mathrm{SET^{*}} + 0.03 \quad (r = 0.32,\ p < 0.001) \\ \mathrm{mTSV_{mist}} &= 0.09\ \mathrm{SET^{**}} - 1.84 \quad (r = 0.64,\ p < 0.001) \\ \mathrm{mTSV_{mist}} &= 0.09\ \mathrm{SET^{*}} - 2.03 \quad (r = 0.62,\ p < 0.001) \end{aligned} \tag{7-6}$$

Fig. 7-8 shows the correlation results of TSV to SET* and SET** and linear regression results are shown in Equation (7-7). The thermal sensation (mTSV) corresponding to the measured environment can be predicted and evaluated using the results of regression equation, when SET* or SET** is calculated by measuring environment factors in outdoor and mist spraying environments.

The results of SET* and SET** in the mist spraying environment differed depending on the consideration of the mist wettedness, and the difference was 2.0 °C under the same thermal sensation (TSV).

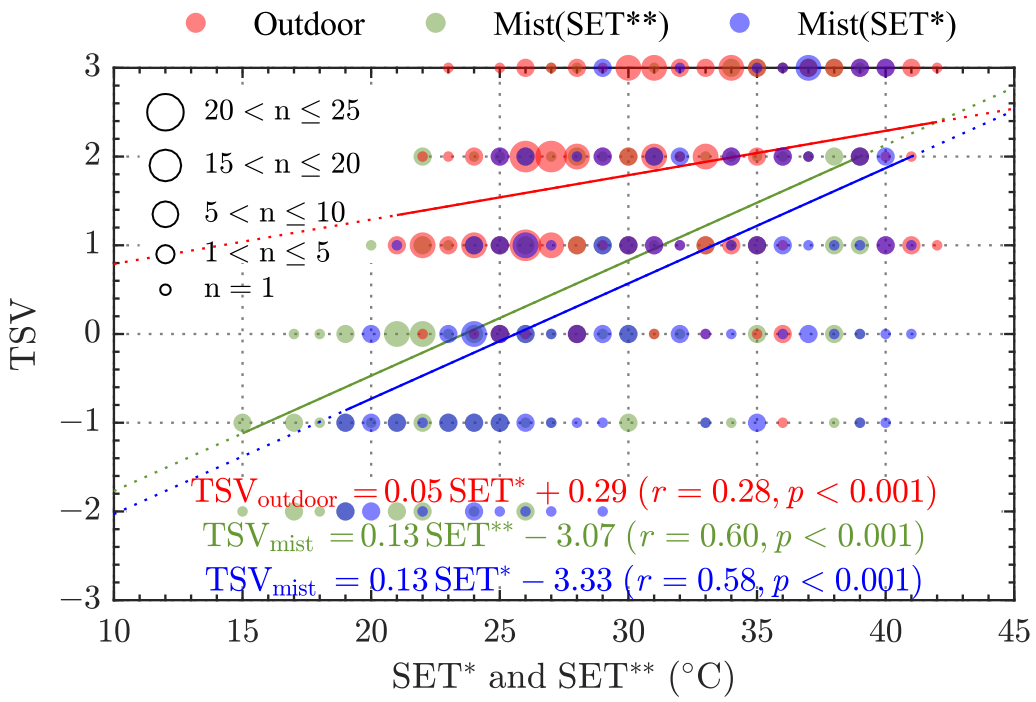

Fig. 7-8. Correlation results of TSV to SET* and SET**.

$$\begin{aligned} \mathrm{TSV_{outdoor}} &= 0.05\ \mathrm{SET^{*}} + 0.29 \quad (r = 0.28,\ p < 0.001) \\ \mathrm{TSV_{mist}} &= 0.13\ \mathrm{SET^{**}} - 3.07 \quad (r = 0.60,\ p < 0.001) \\ \mathrm{TSV_{mist}} &= 0.13\ \mathrm{SET^{*}} - 3.33 \quad (r = 0.58,\ p < 0.001) \end{aligned} \tag{7-7}$$

7.3. Proposal of mPMV index

The main reason why the PMV index cannot be applied directly to the mist spraying environment is that the thermal sensation is different from the results of PMV due to unusual environmental conditions. Therefore, a new environmental index (modified predicted mean vote (mPMV)) can be proposed by following the same calculation manner of PMV with replacing the corresponding thermal sensation (mTSV) for the heat storage rate results of the environmental conditions. PMV has been proposed from the correlation between thermal sensation and heat storage rate. Heat storage rate can be calculated using the Fanger's heat balance Equation (7-8). The heat storage rate S on the human body in the mist spraying environment calculated using measured environmental factors. The heat storage is the difference between the left and right side of Equation (7-9).

$$S_{\text{body}} = (M - W) - E_{\text{sk}} - Q_{\text{res}} - Q_{\text{rad}} - Q_{\text{conv}} \tag{7-8}$$

$$\begin{aligned} M - W = {} & 3.96 \cdot 10^{-8} f_{\text{clo}} \left[(T_{\text{clo}} + 273)^4 + (T_{\text{mrt}} + 273)^4 \right] + f_{\text{clo}} h_{\text{c}} (T_{\text{clo}} - T_a) \\ & + 3.05 \left[5.73 - 0.007 \, (\text{M} - \text{W}) - p_{\text{air}} \right] + 0.42 \left[(M - W) - 58.15 \right] \\ & + 0.0173 \, M \, (5.87 - p_{\text{air}}) + 0.0014 \, M \, (34 - T_{\text{air}}) \end{aligned} \tag{7-9}$$

The activity and clothing insulation levels were set at 1.2 met and 0.5 clo. The environmental factors and thermal sensations inside (n = 222) and outside (n = 222) the mist spraying environment which were obtained from the field experiments in 2018 were used for correlation analysis. Fig. 7-9 shows the correlation between heat storage calculated using PMV method and mTSV in outdoor environment and mist spraying environments, and the results of linear regression equations are listed in (7-10).

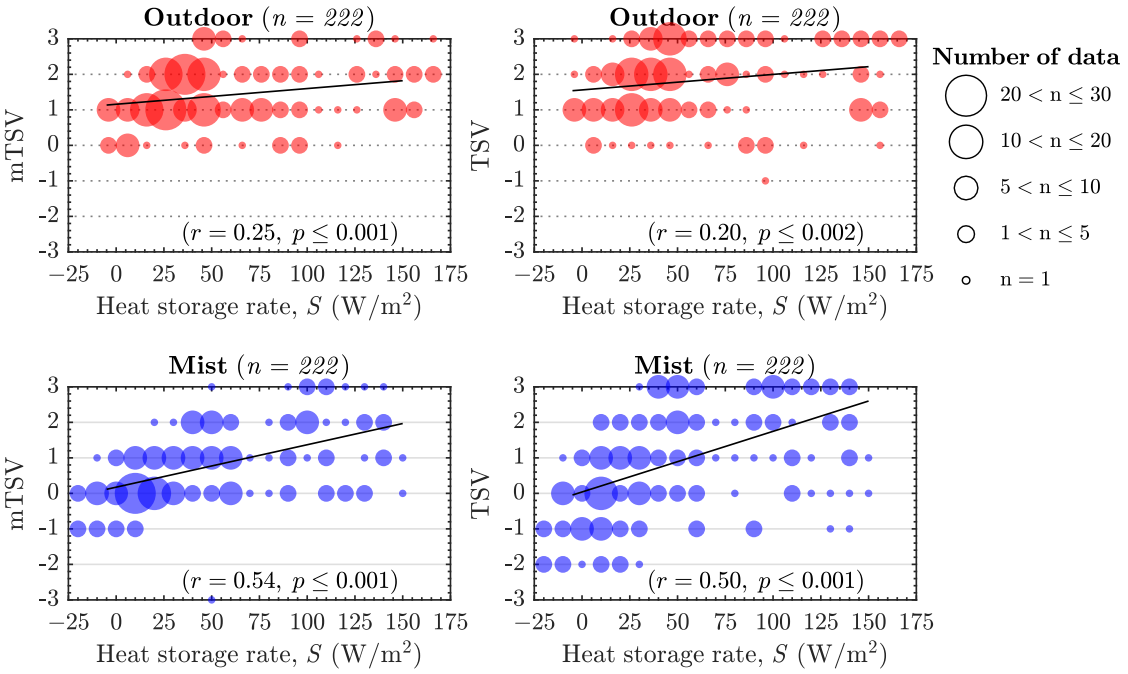

Fig. 7-9. Correlation between heat storage (PMV method) and thermal sensations (mTSV and TSV) in outdoor environment and mist spraying environments.

$$\begin{aligned} \mathrm{mTSV}_{\mathrm{outdoor}} &= 0.004\,S_{\mathrm{PMV}} + 1.157 \quad (r = 0.25,\ p < 0.001) \\ \mathrm{mTSV}_{\mathrm{mist}} &= 0.012\,S_{\mathrm{PMV}} + 0.174 \quad (r = 0.54,\ p < 0.001) \\ \mathrm{TSV}_{\mathrm{outdoor}} &= 0.004\,S_{\mathrm{PMV}} + 1.561 \quad (r = 0.20,\ p < 0.001) \\ \mathrm{TSV}_{\mathrm{mist}} &= 0.017\,S_{\mathrm{PMV}} + 0.039 \quad (r = 0.50,\ p < 0.001) \end{aligned} \tag{7-10}$$

The thermal sensation evaluation using the PMV calculation method showed a similar level of correlation results with O-PMV index, and it is easier to use because the calculation method is simpler than O-PMV index. However, there is a disadvantage that the thermal state of the human body, physiological responses, and environmental factors causing the thermal sensations are unknown.

7.4. Comparison of proposed different environmental indices

As a practical example, three proposed environmental indices were calculated and compared (Table 7-2). The environmental conditions of outdoor and mist spraying environments were utilized the average values obtained from the field experiments as shown in Table 6-3. The SET* index showed 32.05 °C in the outdoor environment and 30.48 °C in the mist spraying environment. Considering the mist wettedness in the mist spraying environment, the SET** value showed 27.23 °C. As a result of mTSV predicted by different environmental indices, the results of O-PMV and SET** were almost the same in the outdoor environment, and mPMV and SET** were similar in the mist spraying environment. However, O-PMV in the mist spraying environment showed about 0.5 higher thermal sensation than that of SET** and mPMV in the mist spraying environment.

Table 7-2. Comparison of three different environmental indices.

	mTSV		TSV		Temperature (°C)	
Index	Outdoor	Mist	Outdoor	Mist	Outdoor	Mist
O-PMV	1.64	1.16	-	-	-	-
SET*(*)	1.63	0.71 (0.61†)	1.89	0.63 (0.46†)	32.05	30.48 (27.23†)
mPMV	1.39	0.67	1.79	0.75	-	-

†Note: values were calculated considering mist wettedness (mist wettedness and effectiveness area factor of mist wettedness were considered 0.25 and 0.5, respectively).

7.5. Conclusion

This chapter contains proposed three environmental indices to evaluate the thermal sensations in outdoor and mist spraying environments. O-PMV index is a method to evaluate the thermal sensation

only by measuring four basic environmental factors. The result shows that human feels cooler in a mist spraying environment than an outdoor hot environment at the same conditions of heat load. Table 7-3 shows the summary of proposed new indices for outdoor and mist spraying environments.

SET** index is calculated using a modified 2NM which considers the mist wettedness. In general environments, SET** shows the same value at the SET* index and has been proposed to extend the applicability to the mist spray environment. As the SET** index expressed in a temperature value, it's easy to use and understand. SET** shows the cooling effect of mist wettedness is 2.1 °C. Meanwhile, to obtain SET** in mist spraying environment, it is necessary to measure the mist wettedness value.

Finally, as a thermal sensation evaluation method using the most widely used PMV, we proposed an index (mPMV) that is the simplest to calculate and can be evaluated by measuring only four basic environmental factors of outdoor and mist spraying environments.

Table 7-3. Summary of proposed new indices for outdoor and mist spraying environments

Index	Necessary environmental factors	Physiological responses estimation	Expression	Note
O-PMV	Air temperature MRT Relative humidity Airspeed	Applicable	mTSV	Mist wettedness cannot be measured
SET**	Air temperature MRT Relative humidity Airspeed Mist wettedness	Applicable	Temperature / mTSV / TSV	Most recommended
mPMV	Air temperature MRT Relative humidity Airspeed	Not applicable	mTSV / TSV	Mist wettedness cannot be measured, and the prediction of physiological responses is not necessary

Chapter 8. Conclusion and further research

Chapter 8. Conclusion and further research

In the present study, new three environmental indices were proposed to evaluate the thermal sensations in outdoor and mist spraying environments as summarized in Fig. 8-1. Through the present study, the improvement of thermal sensations and thermal comfort was confirmed in hot outdoor environments by the utilization of mist spraying systems in summer. In addition, the cooling effects of the mist spraying system were investigated by measuring environmental factors and skin temperatures inside and outside of the mist spraying environment. Moreover, the effects of operating conditions of the mist spraying system on thermal sensation and cooling performance also investigated.

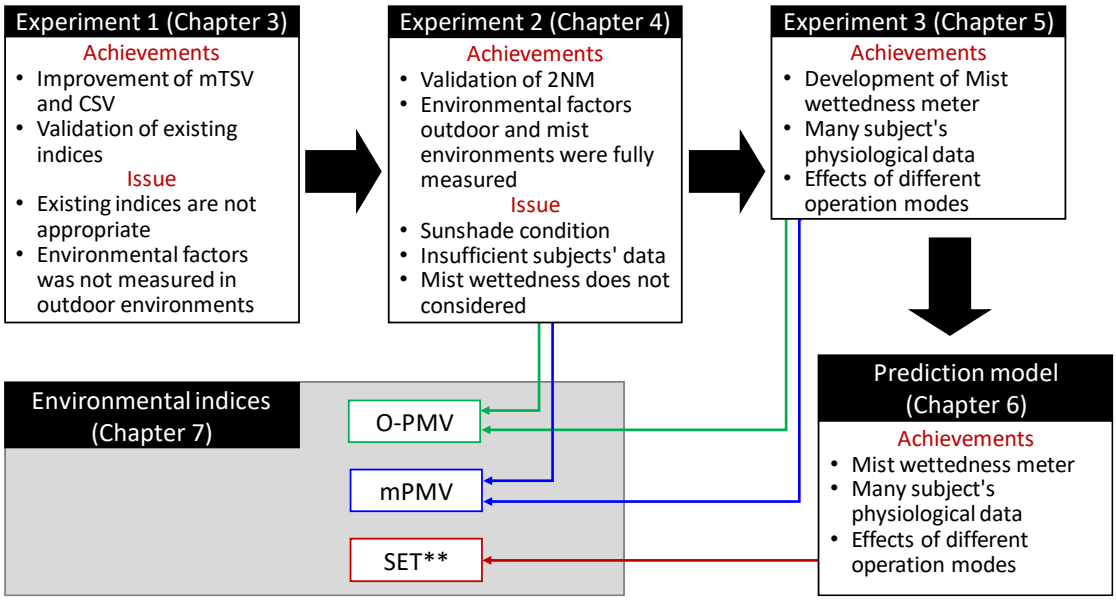

Fig. 8-1. Summary of research flow.

Since the outdoor environment is an open space, the heat exchange phenomenon with the surrounding environment occurs continuously. Therefore, a high-efficiency cooling system such as a mist spraying system is useful. The humidity increases rapidly, and the air is supersaturated when the mist spraying system applied to an indoor environment, thereby the cooling performance decreased, and condensation risks increased. The control variable of the mist spraying system that has the greatest influence on the cooling effect and the thermal sensation was an amount of spraying water. The cooling effect was drastically decreased when the amount of spraying water was reduced. Therefore, it is necessary to spray a sufficient amount of water in a hot environment. However, if the spray amount is too large, it is likely to cause discomfort, so it is necessary to control it appropriately. In the present

study, the size of mist spray particles was adjusted to about 10 m. The larger mist particle size, the evaporation rate becomes slow, and the body is easy to wet. In addition, when the air blowing operation additionally applied, the mist particles evaporate fast, and the cooling effect also increased.

As a result of evaluating thermal sensations in a mist spraying environment using existing environmental indices (SET*, WBGT, PET, and UTCI), these environmental indices did not properly reflect the thermal sensations. Because there is an additional thermal effect on a human body in the mist spraying environment except for the four basic environmental factors, people feel cooler than the general outdoor environment. Therefore, it was not appropriate to evaluate the thermal sensations in a mist spraying environment using conventional environmental indices. Based on the results of environmental factors and surveys, the new environmental indices which can be applied to outdoor and mist spraying environment were suggested as below.

The O-PMV index was derived from the correlation between predicted physiological responses in 2NM and survey results of thermal sensations. The validation of the prediction model was confirmed by comparing it with skin temperatures of 12 subjects. Predicted skin temperature which was calculated from the 2NM using only measured four basic environmental factors (air temperature, radiation, humidity, and airspeed) showed high accuracy in outdoor and mist spraying environments. In addition, the predicted physiological response well reflected the thermal sensations in outdoor and mist spraying environments. The results of O-PMV showed that the mist spraying environment made a person cooler than the outdoor hot environment at the same heat load condition.

Skin temperature steadily decreased in a mist spraying environment with sunshade, and the results of the prediction model showed the tendency of decreasing skin temperature too. However, in a mist spraying environment without sunshade, the skin temperature dropped, but the prediction model could not predict the decreasing skin temperature, because the prediction model does not consider the evaporative heat loss (mist wettedness) on the body surface by mist droplets.

Since there has not been studied mist wettedness measuring method in mist spraying environment, mist wettedness meter was newly developed and physiological human models were also revised to consider the cooling effect of mist wettedness. In addition, to verify the revised physiological prediction model, 65 subjects participated in the experiment and skin temperatures were measured. As input variables of the prediction model, environmental factors in outdoor and mist spraying environments were recorded simultaneously. The improved predictive model, which considers the mist wettedness, the skin temperatures were predicted well with an error of 0.5 degrees even in mist spraying environment without a sunshade.

By the way, since the mist is not uniformly distributed inside the mist spraying environment, the degrees of wet skin by mist droplets are different for the position. In our approach, it is difficult to determine the effect on the whole body because seven environmental factors must be measured to

determine the mist wettedness of a single point. Therefore, the mist wettedness effects on the overall body are necessary to be studied in further research.

In the present study, SET** was proposed in consideration of heat loss when the surface of the human body was wet by external causes so that SET* could be extended to the mist spraying environment. In addition, SET** can be easily used as an environmental index to understand the thermal environment because it is expressed in temperature. The difference of SET* and SET** results in mist spraying environments was 2.1 degrees, which corresponds to the cooling effects of mist wettedness. Moreover, the thermal sensation can be evaluated in both outdoor and mist spraying environments under any conditions by correlation analysis between the SET** and the survey results. The thermal state of the human body and physiological responses can be estimated using the revised prediction model. Although it had not possible to quantify the effects of environmental factors on the human body in the mist spraying environment, the revised predictive model was able to determine the influence of each environmental factor. Temperature drops and mist wettedness in mist spraying environment have proven to be important environmental factors.

However, due to the difficulty of measuring mist wetting and the complexity of the 2NM calculation, it is not easy to obtain SET** results in the experiment. Therefore, we proposed another approach to assess thermal sensation in outdoor and mist spraying environments using only four basic environmental factors by the correlation analysis between the heat load of the human body by PMV calculation and the thermal sensation by questionnaire. The correlation coefficient results showed similar to that of O-PMV. However, there is a disadvantage that cannot confirm the thermal state and physiological response of the human body.

For further studies, it is necessary to investigate the extent of mist wettedness on the whole body in the mist spraying environment which was insufficient in the present study. In addition, due to the difficulty of measuring mist wettedness, it is important to study the prediction of mist wettedness according to outdoor environmental conditions. It is expected that the proposed thermal sensation evaluation indices can be used for the optimal control of the mist spraying system for the weather conditions.

Appendix

Appendix 1. Survey questionnaires for preliminary experiment.

グリーンエアコン　－お客様アンケート－
Survey questionnaire

ミストを浴びる前、ミストを浴びた後の感想をお答えいただきます.
Please answer the questionnaires before and after entering the mist spraying environment.
「服」や「肌」にミストが当たり、濡れることがあります.
The 'clothes' and 'skins' could be wetted after entered the mist spraying environment.
お客さまはいつでもやめることはできます.
You can stop the survey whenever you want.

説明内容を理解し、アンケートにご協力いただけますか？
Do you agree to participate in the questionnaire?
■はい (Yes)

Q1. あなたの年齢は？
What is your age?
□10 才代 (10's)
□20 才代 (20's)
□30 才代 (30's)
□40 才代 (40's)
□50 才代 (50's)
□60 才代 (60's)
□70 才代 (70's)

Q2. あなたの性別は？
What is your gender?
□男 (Male)
□女 (Female)
□回答しない (Do not answer)

Q3. あなたの身長は？
What is your height?
□140cm 未満 (Under 140 cm)
□150cm 台 (about 140 cm)
□160cm 台 (about 150 cm)
□170cm 台 (about 160 cm)
□180cm 台 (about 170 cm)
□180cm 以上 (over 180 cm)
□140cm 台 (about 140 cm)

Q4. 現在のあなたの着衣は？（いくつでも）
What are you wearing now (multiple response is possible)?
トップス（上衣）Tops
□ノースリーブ Sleeveless
□半そで Short sleeve
□長そで Long sleeve
ボトムス（下衣）Bottoms
□短パン Short pants
□膝丈ズボン Knee length pants
□長ズボン Long pants
□膝上丈スカート Skirt above the knee
□膝丈スカート Knee length skirt
□ロングスカート Long skirt
その他 etc
□帽子 Hat
□めがね Glasses
□スカーフ Scarf

今の状態は？（次の質問にお進みください.）
Your present status?
■まだ、敷地内におり、ミストを浴びていない (I haven't entered the mist spray system yet)

Q5. 今のあなた自身の暑さ、寒さはどの程度ですか？
How do you feel at this moment?
□非常に暑い (Very Hot)
□暑い (Hot)
□やや暑い (Slightly Hot)
□どちらでもない (Neutral)
□やや寒い (Slightly Cold)
□寒い (Cold)
□非常に寒い (Very Cold)

Q6. 今の暑さ、寒さがどうあれば、あなたにとってよいですか？
How would you like the environment to be?
□今より暖かいほうがよい (Warmer)
□このままでよい (As it is)
□今よい涼しいほうがよい (Cooler)

Q7. 今の暑さ、寒さをあなたは受けいれることができますか？
Is the present thermal environment acceptable?
□受け入れられる (Acceptable)
□どちらかというと受け入れられる (Barely Acceptable)
□どちらかというと受け入れられない (Barely Unacceptable)
□受け入れられない (Unacceptable)

Q8. 汗による今の肌や衣類のぬれは、あなた自身にとってどうですか？
How is the wettedness of your cloth and skin due to sweat?
□非常にぬれている (Very Wet)
□ぬれている (Wet)
□ややぬれている (Slightly Wet)
□ぬれていない (Not wet)

Q9. 今の肌や衣類のぬれ具合をあなたは受け入れられますか？受け入れられませんか？
Is the wettedness of your cloth and skin acceptable?
□受け入れられる (Acceptable)
□どちらかというと受け入れられる (Barely Acceptable)
□どちらかというと受け入れられない (Barely Unacceptable)
□受け入れられない (Unacceptable)

Q10. 今の状態は総合的に考えて、あなたにとって快適ですか？不快ですか？
In total, do you feel your present condition to be comfortable?
□非常に快適 (Very Comfortable)
□快適 (Comfortable)
□やや快適 (Slightly Comfortable)
□どちらでもない (Neutral)
□やや不快 (Slightly Uncomfortable)
□不快 (Uncomfortable)
□非常に不快 (Very Uncomfortable)

今の状態をお聞きします.（次の質問にお進みください.）
Your present status?
■ミストを浴び終わった (I already stayed in mist spray system)

Q11. 今のあなた自身の暑さ、寒さはどの程度ですか？
How do you feel at the moment?
□非常に暑い (Very Hot)
□暑い (Hot)
□やや暑い (Slightly Hot)
□どちらでもない (Neutral)
□やや寒い (Slightly Cold)
□寒い (Cold)
□非常に寒い (Very Cold)

Q12. 今の暑さ、寒さがどうあれば、あなたにとってよいですか？
How would you like the environment to be?
□今より暖かいほうがよい (Warmer)
□このままでよい (As it is)
□今よい涼しいほうがよい (Cooler)

Q13. 今の暑さ、寒さをあなたは受けいれることができますか？
Is the present thermal environment acceptable?
□受け入れられる (Acceptable)
□どちらかというと受け入れられる (Barely Acceptable)
□どちらかというと受け入れられない (Barely Unacceptable)
□受け入れられない (Unacceptable)

Q14. 汗による今の肌や衣類のぬれは、あなた自身にとってどうですか？
How is the wettedness of your cloth and skin due to sweat?
□非常にぬれている (Very Wet)
□ぬれている (Wet)
□ややぬれている (Slightly Wet)
□ぬれていない (Not wet)

Q15. ミストによる今の肌や衣類のぬれは、あなた自身にとってどうですか？
How is the wettedness of your cloth and skin due to mist?
□非常にぬれている (Very Wet)
□ぬれている (Wet)
□ややぬれている (Slightly Wet)
□ぬれていない (Not wet)

Q16. 今の肌や衣類のぬれ具合をあなたは受け入れられますか？受け入れられませんか？
Is the wettedness of your cloth and skin acceptable?
□受け入れられる (Acceptable)
□どちらかというと受け入れられる (Barely Acceptable)
□どちらかというと受け入れられない (Barely Unacceptable)
□受け入れられない (Unacceptable)

Q17. ミスト噴霧機器内の状態は総合的に考えて、あなたにとって快適ですか？不快ですか？
In total, do you feel comfortable at the moment?
□非常に快適 (Very Comfortable)
□快適 (Comfortable)
□やや快適 (Slightly Comfortable)
□どちらでもない (Neutral)
□やや不快 (Slightly Uncomfortable)
□不快 (Uncomfortable)
□非常に不快 (Very Uncomfortable)

Q18. ミスト噴霧機器が発生する騒音のレベルはどうですか？
How do you feel the sound generated by the mist spray system?
□とてもうるさい (Very Noisy)
□うるさい (Noisy)
□ややうるさい (Slightly Noisy)
□静か (Quiet)

Q19. ミスト噴霧機器が発生する騒音を、滞在中や会話シーンなどを想定して、 受け入れることができますか？
Is the sound generated by the mist spray system acceptable for conversation?
□受け入れられる (Acceptable)
□どちらかというと受け入れられる (Barely Acceptable)
□どちらかというと受け入れられない (Barely Unacceptable)
□受け入れられない (Unacceptable)

お願い実験参加者調査票
(Survey questionnaire)

・実施日　　年　月　日午前・午後
Participation Date(DD/MM/YYYY)

被験者番号(ID)

・お名前
Name

・性別　□男 (Male) □女 (Female)
Gender

・年齢　　歳(years old)
Age

・体重　　kg　　lb
Weight

・身長　　cm　　ft
Height

・出身地
Hometown

・前日の睡眠時間
How long did you sleep yesterday?
　　時間(hours)

・暑がりですか、寒がりですか？（該当するもの全てを選んでください。）
Are you sensitive to hot and cold conditions? (multiple answers allowed)

□暑さに強い	□暑さに弱い	□寒さに弱い	□寒さに強い	□いずれでもない
Tolerant of heat	Sensitive to heat	Sensitive to cold	Tolerant of cold	None of the above

・今日の体調はいかがですか？
How is your health conditions today?

□とても良い	□良い	□普通	□悪い	□とても悪い
Very well	Well	Fair	Poor	Very poor

ケース１：被験者実験の主観評価シート
CASE1: Questionnaires

・１回目：グーリンエアコンに「入る前」/ ２回目：グリーンエアコンに「入った後」
Questionnaire1: Before entering the mist spraying system / Questionnaire2: After 3 minutes from entering the mist spray system

1）今のあなたの自身の暑さ、寒さはどの程度ですか？
How do you feel at the moment?

−3	−2	−1	0	1	2	3
非常に寒い Very Cold	寒い Cold	やや寒い Slightly Cold	とちらでもない Neutral	やや暑い Slightly Hot	暑い Hot	非常に暑い Very Hot

2）今の暑さ、寒さがどうあれば、あなたにとってよいですか？
How would you like the environment to be?

−1	0	1
今より涼しいほうがよい Cooler	このままでよい As it is	今より暖かいほうがよい Warmer

3）今の暑さ、寒さをあなたは受けいれることができますか？
Is the present thermal environment acceptable?

−2	−1	1	2
受け入れられない Unacceptable	どちらかというと受け入れられない Barely unacceptable	どちらかというと受け入れられる Barely acceptable	受け入れられる Acceptable

4）汗による今の肌や衣類のぬれは、あなた自身にとってどうですか？
How is the wettedness of your cloth and skin due to sweat?

0	1	2	3
ぬれていない Not Wet	ややぬれている Slightly Wet	ぬれている Wet	非常にぬれている Very Wet

5）今の肌や衣類のぬれ具合をあなたは受け入れられますか？受け入れられませんか？
Is the wettedness of your cloth and skin acceptable?

−2	−1	1	2
受け入れられない Unacceptable	どちらかというと受け入れられない Barely unacceptable	どちらかというと受け入れられる Barely acceptable	受け入れられる Acceptable

6）今の状態は総合的に考えて、あなたにとって快適ですか？不快ですか？
In total, do you feel your present condition to be comfortable?

−3	−2	−1	0	1	2	3
非常に不快 Very Uncomfortable	不快 Uncomfortable	やや不快 Slightly Uncomfortable	とちらでもない Neutral	やや快適 Slightly Comfortable	快適 Comfortable	非常に快適 Very Comfortable

7）今のあなたの自身の温冷感はどの程度ですか？
How do you feel at the moment?

−3	−2	−1	0	1	2	3
寒い Cold	涼しい Cool	やや涼しい Slightly Cool	とちらでもない Neutral	やや暖かい Slightly Warm	暖かい Warm	暑い Hot

Appendix 3. The result of the research ethics committee review for the subject experiment.

意　見　書

平成３０年７月１３日

東京大学**生産**技術研究所長　殿

東京大学倫**理**審査専門委員会委員長

審査**番**号：　１８－１１４
研究課題：　「屋外ミスト機器における暑さ評価手法の研究」
申　請　者：　**生産**技術研究所　教授　大岡　龍三

記

上記研究計**画**について、平成 30 年 8 月 7 日開催予定の倫**理**審査専門委員会にて審査の予定であるが、実施予定日が同年 7 月 23 日であるため事前に審査することはできない。

そのため、委員長は平成 30 年 7 月 13 日付けで提出された研究計**画申**請書について、参加者の負担とならない軽微な介入実験であること、適切な説明文書と同意書が準備されていることから、実施に当たって**特**段の問題となる点はないと判断した。

ただし、委員会での審査時に研究計**画**の修正あるいは追加を**求**める意見があった場合は研究計**画**の変更の**申**請と、必要に応じて参加者に対する再同意を**求**めることとする。

以上

Surface area fraction and mass fraction of each segment of the human body are listed in Appendix 4 (These values were referenced by the previous research (Tanabe et al. [63])).

Appendix 4. Surface area fraction and mass fraction of each segment of body.

i	Segment (i)	Area	Mass	Presence of clothing	
				Summer	Winter
1	Head	0.075	0.054	×	×
2	Cheat	0.093	0.168	○	○
3	Back	0.086	0.148	○	○
4	Pelvis	0.118	0.236	○	○
5	Left shoulder	0.051	0.029	○	○
6	Right shoulder	0.051	0.029	○	○
7	Left arm	0.034	0.018	×	○
8	Right arm	0.034	0.018	×	○
9	Left hand	0.027	0.005	×	○
10	Right hand	0.027	0.005	×	×
11	Left thigh	0.112	0.094	○	×
12	Right thigh	0.112	0.094	○	○
13	Left leg	0.060	0.045	×	○
14	Right leg	0.060	0.045	×	○
15	Left foot	0.030	0.006	○	○
16	Right foot	0.030	0.006	○	○
	Total	1.000	1.000	-	-

Note: Standard clothes for the summer season considered short sleeve shirts and short pants.

Convective heat transfer coefficients of each segment of body for the sitting and standing posture in different wind speed (v) are listed in Appendix 5 (These values were referenced by the previous research (de Dear et al. [116])).

Appendix 5. Convective heat transfer coefficients for the sitting and standing posture of thermal manikin.

i	Segment (*i*)	Natural convective heat transfer (v < 0.1 m/s, W m^{-2} K^{-1})		Natural convective heat transfer (W m^{-2} K^{-1})	
		Sitting	Standing	Sitting	Standing
1	Head	3.7	3.6	4.9 $v^{0.73}$	3.2 $v^{0.97}$
2	Cheat	3.0	3.0	9.1 $v^{0.59}$	9.1 $v^{0.59}$
3	Back	2.6	2.9	8.9 $v^{0.63}$	8.9 $v^{0.63}$
4	Pelvis	2.8	3.4	8.2 $v^{0.65}$	8.8 $v^{0.59}$
5	Left shoulder	3.4	2.9	11.2 $v^{0.62}$	11.2 $v^{0.62}$
6	Right shoulder	3.4	2.9	11.6 $v^{0.66}$	11.6 $v^{0.66}$
7	Left arm	3.8	3.7	11.6 $v^{0.62}$	11.6 $v^{0.62}$
8	Right arm	3.8	3.7	11.9 $v^{0.63}$	11.9 $v^{0.63}$
9	Left hand	4.5	4.1	14.3 $v^{0.61}$	14.3 $v^{0.60}$
10	Right hand	4.5	4.1	12.6 $v^{0.60}$	12.6 $v^{0.60}$
11	Left thigh	3.7	4.1	8.9 $v^{0.60}$	10.1 $v^{0.52}$
12	Right thigh	3.7	4.1	8.9 $v^{0.60}$	10.1 $v^{0.52}$
13	Left leg	4.0	4.1	12.9 $v^{0.56}$	12.7 $v^{0.50}$
14	Right leg	4.0	4.1	13.4 $v^{0.58}$	13.1 $v^{0.51}$
15	Left foot	4.2	5.1	12.8 $v^{0.55}$	11.9 $v^{0.50}$
16	Right foot	4.2	5.1	13.0 $v^{0.54}$	12.1 $v^{0.49}$
	Total	3.3	3.4	10.1 $v^{0.61}$	10.4 $v^{0.56}$

Note: Standard clothes for the summer season were considered short sleeve shirts and short pants.

Appendix 6. Matlab code for 2NM calculation considering mist wettedness and effective area factor.

```
function [T, Q, B, E, Wet, SET_Var] = Func_e2NM(TA,TR,VEL,RH,WetMist,InitialSKIN,InitialCORE,Eff)
%--------------------------------------------------------------------------
%                          Two-node model (2NM) Input model
%--------------------------------------------------------------------------
% TA = 35;
% TR = 35;
% VEL = 0.25;
% RH = 50;
% WetMist = 0;
% InitialSKIN = 0;
% InitialCORE = 0;
% Eff = 1;
SUBJECT.MET = 1.2;                                          % Metabolic rate [MET]
SUBJECT.CLO = 0.5;                                          % Clothing level [CLO]
SUBJECT.CLOTHING = 'Summer';                                % type of clothing
Facl = 1 + 0.3 * SUBJECT.CLO;                               % Clothing area factor
Rcl = 0.155 * SUBJECT.CLO;                                  % Resistance of clothing
SUBJECT.WEIGHT = 69.9;                                                  %[kg]
SUBJECT.HEIGHT = 1.7;                                                   %[m]
SUBJECT.AREA = 0.202*SUBJECT.WEIGHT^0.425*SUBJECT.HEIGHT^0.725;         %[m2]
SUBJECT.WORK = 0;                                           % External work [W/m2]
SUBJECT.POSTURE = 'Standing';
METFACTOR = 58.2;                                                       %[W/m2]
Const.P0 = 101.3273;          %Atmospheric pressure [kPa] 1atm = 101.3273kpa
Const.P = 101.3273;           %Atmospheric pressure [kPa] 1atm = 101.3273kpa
Const.SBC = 5.6697 * 10^(-8);                %Stefan-Boltzmann constant[W/m2K4]
Const.LR = 16.5;                                                        %Lewis ratio
Q.M = SUBJECT.MET * METFACTOR;
Q.W = SUBJECT.WORK * METFACTOR;
%--------------------------------------------------------------------------
%                      Physiological thermal neutral condition
%                Experimental results by Stolwijk JA and Hardy JD
%--------------------------------------------------------------------------
Neutral.SKIN = 33.7;                                                    %[C]
Neutral.CORE = 36.8;                                                    %[C]
Neutral.Alpha = 0.1;                          % mass fraction of skin compartment
Neutral.BODY = Neutral.Alpha*Neutral.SKIN    + (1 - Neutral.Alpha) * Neutral.CORE;
%--------------------------------------------------------------------------
%                                  Initial Condition
%--------------------------------------------------------------------------
%------------------------- Storage Statement ----------------------
COEFF = Func_Human(SUBJECT.CLOTHING,SUBJECT.POSTURE,0);
T.SKIN(1) = Neutral.SKIN;                                       %Initial Value
T.CORE(1) = Neutral.CORE;                                       %Initial Value
T.BODY(1) = Neutral.Alpha * T.SKIN(1) + (1 - Neutral.Alpha) * T.CORE(1);
ALPHA = Neutral.Alpha;
if length(TA) == 1
    TIME = 60;
    ENV.TA = TA * ones(TIME,1);
    ENV.TR = TR * ones(TIME,1);
    ENV.VEL = VEL * ones(TIME,1);
    ENV.RH = RH * ones(TIME,1);
    Wet.MIST = WetMist * ones(TIME+1,1);
else
    TIME = length(TA);
    ENV.TA = TA;
    ENV.TR = TR;
    ENV.VEL = VEL;
```

```
        ENV.RH = RH;
end
if InitialSKIN == 0 && InitialCORE == 0
        T.SKIN(1) = Neutral.SKIN;
        T.CORE(1) = Neutral.CORE;
else
        T.SKIN(1) = InitialSKIN;
        T.CORE(1) = InitialCORE;
end
if length(WetMist) == 1
        Wet.MIST = WetMist * ones(TIME,1);
else
        Wet.MIST = WetMist;
end
%---------------------------------------------------------------------------

for i = 1:TIME
        Vapor.Partial = ENV.RH(1)/100*Func_Ps(ENV.TA(i));
        ENV.VEL(i) = max(ENV.VEL(i), 0.1);
        COEFF = Func_Human(SUBJECT.CLOTHING,SUBJECT.POSTURE,ENV.VEL(i));
        COEFF.HR = 4.0 * Const.SBC * (T.SKIN(i)/2.0 + 273.15)^3 * COEFF.Fr;
        COEFF.HT = COEFF.HR + COEFF.HC;
        Ra = 1.0/(Facl * COEFF.HT);
        HE = Const.LR * COEFF.HC;
        if(SUBJECT.CLO <= 0)
                WCRIT = 0.38*(ENV.VEL(i))^(-0.29);        %Maximum Wettedness by wind
                ICL = 1.0;                                %Vapor permeability of clithing
        else
                WCRIT = 0.59*(ENV.VEL(i))^(-0.08);
                ICL = 0.45;
        end
        Rea = 1.0/(Const.LR*Facl*COEFF.HC);     %Evaporative resistance of air layer
        Recl = Rcl/(Const.LR*ICL);              %Evaporative resistance of clothing (icl=.45)
        Ret = Rea + Recl;                       %Total Evaporative resistance of clothed body

        % ----------- Cold and warm temperature receptor -----------
        SIG.WARM_SKIN = max(0,T.SKIN(i) - Neutral.SKIN);
        SIG.WARM_CORE = max(0, T.CORE(i) - Neutral.CORE);
        SIG.WARM_BODY = max(0, T.BODY(i) - Neutral.BODY);
        SIG.COLD_SKIN = max(0, Neutral.SKIN - T.SKIN(i));
        SIG.COLD_CORE = max(0, Neutral.CORE - T.CORE(i));
        T.BODY(i) = ALPHA * T.SKIN(i) + (1 - ALPHA) * T.CORE(i);

        Wet.SK(i) = Func_PWET(SIG.WARM_BODY, SIG.WARM_SKIN, WCRIT, T.SKIN(i), Vapor.Partial, Ret);

        % --------------- Estimating cloth temperature -----------------
        TOP = (COEFF.HR * ENV.TR(i) + COEFF.HC * ENV.TA(i)) / COEFF.HT;
        T.CLO = TOP + (T.SKIN(i) - TOP) / (COEFF.HT * (Ra + Rcl));
        FLUX1 = 100; FLUX2 = 50;
        while abs(FLUX1 - FLUX2) > 0.001
                Q.CONV(i) = Facl * COEFF.HC * (T.CLO - ENV.TA(i));
                Q.RAD(i) = Facl * COEFF.HR * (T.CLO - ENV.TR(i));
                E.SKIN(i) = Wet.SK(i) * (Func_Ps(T.SKIN(i)) - Vapor.Partial) / (Recl +1 / (Facl * HE));
%               E.MIST(i) = Wet.MIST(i) * (Func_Ps(T.CLO) - Vapor.Partial) / (1 / (Facl * HE));
                E.MIST(i) = Eff * (1 - Wet.SK(i)) * Wet.MIST(i) * (Func_Ps(T.CLO) - Vapor.Partial) / (1 / (Facl * HE));
                E.ALL(i) = E.SKIN(i) + E.MIST(i);
                E.MAX = Func_Ps(T.SKIN(i) - Vapor.Partial) / Ret;
                E.ALL(i) = min(E.ALL(i), E.MAX * WCRIT);
                FLUX1 = Q.CONV(i) + Q.RAD(i) + E.ALL(i);
                T.CLO = T.SKIN(i) - Rcl * FLUX1;
                FLUX2 = (T.SKIN(i) - T.CLO) / Rcl;
        end
        Q.RES(i) = 0.0014 * Q.M * (34- ENV.TA(i)) + 0.0173 * Q.M * (5.85 - Vapor.Partial);
```

```
        B(i) = Func_Blood(SIG.WARM_CORE, SIG.COLD_SKIN)*3600;
        F(i) = (5.28 + 1.06 * 4190 * Func_Blood(SIG.WARM_CORE, SIG.COLD_SKIN)) * (T.CORE(i) - T.SKIN(i));

        MSHIV = Func_Shiv(SIG.COLD_SKIN, SIG.COLD_CORE);
        % ---------------------- Heat storage -----------------------
        S.CORE(i) = Q.M - Q.W + MSHIV - Q.RES(i) - F(i);
        S.SKIN(i) = F(i) - (Q.CONV(i) + Q.RAD(i) + E.ALL(i));

        SamplingTime = 60;                                              %1 min.
        ALPHA = 0.0417737+0.7451833/(Func_Blood(SIG.WARM_CORE, SIG.COLD_SKIN) * 3600 + 0.585417);
        dT.CORE = S.CORE(i) * SUBJECT.AREA / (1 - ALPHA) / SUBJECT.WEIGHT / 3500;
        dT.SKIN = S.SKIN(i) * SUBJECT.AREA / ALPHA / SUBJECT.WEIGHT / 3500;
        T.CORE(i+1) = T.CORE(i) + dT.CORE * SamplingTime;
        T.SKIN(i+1) = T.SKIN(i) + dT.SKIN * SamplingTime;
        T.BODY(i+1) = ALPHA * T.SKIN(i+1) + (1-ALPHA) * T.CORE(i+1);

        % ----------- Definition of ASHRAE Standard Environment    -----------
        HSK = Q.CONV(i) + Q.RAD(i) + E.ALL(i); %Total heat loss from skin
        W = Wet.SK(i);
        PSSK = Func_Ps(T.SKIN(i+1));
        COEFFS.HR = COEFF.HR;
        %Definition of ASHRAE standard environment
%       if SUBJECT.MET < 0.85
%           COEFFS.HC = 3.0;
%       else
%           COEFFS.HC = 5.66*(SUBJECT.MET-0.85)^0.39;
%           COEFFS.HC = max(COEFFS.HC,3.0);
%       end
        COEFF = Func_Human(SUBJECT.CLOTHING,SUBJECT.POSTURE,0);
        COEFFS.HC = COEFF.HC;
        COEFFS.HT = COEFFS.HC + COEFFS.HR;
        % ASHRAE Standard 2013
%       RCLOS = 1.52 / (SUBJECT.MET - SUBJECT.WORK / METFACTOR + 0.6944) - 0.1835;
        % Nishi Y. and Gagge, A.P. 1977, Effective temperature scale useful for hypo- and hyperbaric environments.
        RCLOS = 1.33 / (SUBJECT.MET - SUBJECT.WORK / METFACTOR + 0.74) - 0.095;
        RCLS = 0.155 * RCLOS;
        KCLO = 0.25;
        FACLS = 1.0 + KCLO * RCLOS;
        FCLS = 1.0 / (1.0 + 0.155 * FACLS * COEFFS.HT * RCLOS);
        IMS = 0.45;
        ICLS = IMS * COEFFS.HC / COEFFS.HT * (1 - FCLS) / (COEFFS.HC / COEFFS.HT - FCLS * IMS);
        RAS = 1.0/(FACLS * COEFFS.HT);
        REAS = 1.0/(Const.LR * FACLS * COEFFS.HC);
        RECLS = RCLS / (Const.LR * ICLS);
        HD_S = 1.0 / (RAS + RCLS);
%       HE_S = Const.LR * COEFFS.HC;
        HE_S = 1.0 / (REAS + RECLS);    %SET determined using Newton's iterative solution
        DELTA = .0001;
        dx = 100.0;
        SET_OLD = T.SKIN(i+1) - HSK/HD_S;                               %Lower bound for SET
        while abs(dx) > .01
            ERR1 = (HSK - HD_S * (T.SKIN(i+1) - SET_OLD) - W * HE_S * (PSSK - 0.5 * Func_Ps(SET_OLD)));
            ERR2 = (HSK - HD_S * (T.SKIN(i+1) - (SET_OLD + DELTA)) - W * HE_S * (PSSK - 0.5 *
                Func_Ps((SET_OLD + DELTA))));
            SET = SET_OLD - DELTA * ERR1 / (ERR2 - ERR1);
            dx = SET - SET_OLD;
            SET_OLD = SET;
        end
        SET_Var(i+1) = SET;
    end
    T.SET = SET_Var(TIME+1);
    end
```

```
%%                  Saturated Vapor Pressure in Specific Temperature
function [SaturatedVaporPressure] = Func_Ps(T) % (Celsius & kPa)
if T >= 0
      SaturatedVaporPressure = 0.6105 * exp((17.269 * T) / (237.3 + T));
else
      SaturatedVaporPressure = 0.6105 * exp((21.875 * T) / (265.5 + T));
end
% SaturatedVaporPressure = 0.61121*exp((18.678-T/234.5)*(T/(257.14+T)));
end

%%                                  Sweat production
function [PWET] = Func_PWET(WARMB,WARMSK,WCRIT,Temperature,Pa,Ret)
CSW = 170;        %Driving coefficient for regulatory sweating [170g/(m2hr)]
ERSW = CSW*WARMB*exp(WARMSK/10.7);
ERSW = min(ERSW,670);
ERSW = 2430000/1000/3600*ERSW;                          %Phase change 2430000J/kg
EMAX = (Func_Ps(Temperature)-Pa)/(Ret);
PRSW = ERSW/EMAX;                                              %Wettedness by Sweat
PWET = 0.06+0.94*PRSW;
if PWET > WCRIT
      PWET = WCRIT;
      PRSW = WCRIT / (1 - 0.06);
      ERSW = PRSW * EMAX;
      EDIFF = 0.06 * (1 - PRSW) * EMAX;
      PWET = (ERSW + EDIFF) / EMAX;
end
if EMAX < 0
      EDIF = 0;
      ERSW = 0;
      PWET = WCRIT;
end
end

%%                                  Blood flow rate
function [SkinBloodFlow] = Func_Blood(WARM_CORE, COLD_SKIN)
SkinBloodFlowNeutral = 6.3;                                          %[Liter/m2hr]
CDIL = 200;                                 %Driving coefficient for vasoconstriction
CSTR = 0.5;                                                        %vasoconstriction
SkinBloodFlow = (SkinBloodFlowNeutral+CDIL*(WARM_CORE))/(1+CSTR*(COLD_SKIN));
SkinBloodFlow = max(0.5,min(90,SkinBloodFlow));
SkinBloodFlow = SkinBloodFlow/3600;                                  %Liter/s m2
end

%%                          Human's bared fraction of segments
function [Answer] = Func_Human(Season,Posture,VEL)
if strcmp('Summer', Season) == 1
      i = 1;
elseif strcmp('Winter', Season) == 1
      i = 2;
else
end
if strcmp('Sitting', Posture) == 1
      j = 1;
       Answer.Fr = 0.70;                          %Radiation effective area factor
elseif strcmp('Standing', Posture) == 1
      j = 2;
     Answer.Fr = 0.725;                          %Radiation effective area factor
else
end
%-------------------------Tanabe et al.-------------------------------
% 1st column : Area fraction, 2nd column : Mass fraction
Human = [0.075 0.054; 0.093 0.168; 0.086 0.148; 0.118 0.236; 0.051 0.029; 0.051 0.029;...
      0.034 0.018; 0.034 0.018; 0.027 0.005; 0.027 0.005; 0.112 0.094; 0.112 0.094;...
```

```
    0.06 0.045; 0.06 0.045; 0.03 0.006; 0.03 0.006];
% 1st column : Summer, 2nd column : Winter
% 0:Bared, 1:Clothed
Clothed_segment = [0 0;...      %Head
    1 1;...                     %2Chest
    1 1;...                     %3Back
    1 1;...                     %4Pelvis
    1 1;...                     %5Lshoulder
    1 1;...                     %6Rshoulder
    0 1;...                     %7Larm
    0 1;...                     %8Rarm
    0 0;...                     %9Lhand
    0 0;...                     %10Rhand
    1 1;...                     %11Lthigh
    1 1;...                     %12Rthigh
    0 1;...                     %13Lleg
    0 1;...                     %14Rleg
    1 1;...                     %15Lfoot
    1 1];                       %16Rfoot
Bared_Fraction = Human.*(1-Clothed_segment(:,i));
Answer.MassFraction = sum(Bared_Fraction(:,1));                 % Bared area fraction
Answer.AreaFraction = sum(Bared_Fraction(:,2));                  % Bared mass fraction
%-------------------------de Dear et al.-------------------------------
% 1st column : Sitting, 2nd column : Standing
COEFF.HNC = [3.7 3.6; 3.0 3.0; 2.6 2.9; 2.8 3.4; 3.4 2.9; 3.4 2.9; 3.8 3.7; 3.8 3.7; 4.5 4.1; 4.5 4.1;...
    3.7 4.1; 3.7 4.1; 4.0 4.1; 4.0 4.1; 4.2 5.1; 4.2 5.1];
COEFF.HFC_a = [4.9 3.2; 9.1 7.5; 8.9 7.7; 8.2 8.8; 11.2 9.9; 11.6 10.2; 11.6 12.7; 11.9 12.4; 14.3 15.4;...
    12.6 13.4; 8.9 10.1; 8.9 10.1; 12.9 12.7; 13.4 13.1; 12.8 11.9; 13.0 12.1];
COEFF.HFC_b = [0.73 0.97; 0.59 0.66; 0.63 0.63; 0.65 0.59; 0.62 0.61; 0.66 0.64; 0.62 0.53; 0.63 0.55;...
    0.60 0.51; 0.60 0.60; 0.60 0.52; 0.60 0.52; 0.56 0.50; 0.58 0.51; 0.55 0.50; 0.54 0.49];
BARED = Human(:,1).*(1-Clothed_segment(:,i));
CLOTHED = Human(:,1).*(Clothed_segment(:,i));

COEFF.HNC_BARED = sum(COEFF.HNC(:,j).*BARED)/sum(BARED);
COEFF.HNC_CLOTHED = sum(COEFF.HNC(:,j).*CLOTHED)/sum(CLOTHED);
COEFF.HNC_OVERALL = (sum(COEFF.HNC(:,j).*BARED) + sum(COEFF.HNC(:,j).*CLOTHED)) /
            (sum(BARED) + sum(CLOTHED));
COEFF.HFC_BARED = sum(COEFF.HFC_a(:,j).*VEL.^COEFF.HFC_b(:,j).*BARED)/sum(BARED);
COEFF.HFC_CLOTHED = sum(COEFF.HFC_a(:,j).*VEL.^COEFF.HFC_b(:,j).*CLOTHED)/sum(CLOTHED);
COEFF.HFC_OVERALL = (sum(COEFF.HFC_a(:,j).*VEL.^COEFF.HFC_b(:,j).*BARED) +
            sum(COEFF.HFC_a(:,j).*VEL.^COEFF.HFC_b(:,j).*CLOTHED)) / (sum(BARED) +
            sum(CLOTHED));
if VEL > 0.2
    Answer.HC = COEFF.HFC_OVERALL;
else
    Answer.HC = COEFF.HNC_OVERALL;
end
end
%%                              Shivering
function [Shiv] = Func_Shiv(COLDSK, COLDCORE)
Shiv = 19.44*COLDSK*COLDCORE;
end
```

Appendix 7. Matlab code for 3NM calculation considering mist wettedness and effective area factor.

```
function [T, Q, F, E, Wet, SET_Var] = Func_e3NM(TA,TR,VEL,RH,WetMist,InitialSKIN,InitialCORE,Eff)
%-------------------------------------------------------------------------
%                       Three-node model (3NM) Input model
```

```
%--------------------------------------------------------------------
% TA = 35;
% TR = 35;
% VEL = 0.25;
% RH = 50;
% WetMist = 0.2;
% InitialSKIN = 0;
% InitialCORE = 0;
% Eff = 1;
SUBJECT.MET = 1.2;                                          % Metabolic rate [MET]
SUBJECT.CLO = 0.5;                                          % Clothing level [CLO]
SUBJECT.CLOTHING = 'Summer';                                % type of clothing
Facl = 1 + 0.3 * SUBJECT.CLO;                               % Clothing area factor
Rcl = 0.155 * SUBJECT.CLO;                                  % Resistance of clothing
SUBJECT.WEIGHT = 69.9;                                                  %[kg]
SUBJECT.HEIGHT = 1.7;                                                   %[m]
SUBJECT.AREA = 0.202*SUBJECT.WEIGHT^0.425*SUBJECT.HEIGHT^0.725;         %[m2]
SUBJECT.WORK = 0;                                           % External work [W/m2]
SUBJECT.POSTURE = 'Standing';
METFACTOR = 58.2;                                                       %[W/m2]
Const.P0 = 101.3273;          %Atmospheric pressure [kPa] 1atm = 101.3273kpa
Const.P = 101.3273;           %Atmospheric pressure [kPa] 1atm = 101.3273kpa
Const.SBC = 5.6697 * 10^(-8);              %Stefan-Boltzmann constant[W/m2K4]
Const.LR = 16.5;                                                        %Lewis ratio
Q.M = SUBJECT.MET * METFACTOR;
Q.W = SUBJECT.WORK * METFACTOR;
%--------------------------------------------------------------------
%                    Physiological thermal neutral condition
%              Experimental results by Stolwijk JA and Hardy JD
%--------------------------------------------------------------------
Neutral.SKIN = 33.7;                                                    %[C]
Neutral.CORE = 36.8;                                                    %[C]
Neutral.Alpha = 0.1;                          % mass fraction of skin compartment
Neutral.BODY = Neutral.Alpha*Neutral.SKIN    + (1 - Neutral.Alpha) * Neutral.CORE;
%--------------------------------------------------------------------
%                                   Initial Condition
%--------------------------------------------------------------------
%------------------------- Storage Statement ----------------------
COEFF = Func_Human(SUBJECT.CLOTHING,SUBJECT.POSTURE,0);
T.SKIN_CLOTHED(1) = Neutral.SKIN;                                       %Initial Value
T.SKIN_BARED(1) = Neutral.SKIN;
T.SKIN_OV(1) = COEFF.AreaFraction * T.SKIN_BARED(1) + (1 - COEFF.AreaFraction) *
               T.SKIN_CLOTHED(1);
T.CORE(1) = Neutral.CORE;                                               %Initial Value
T.BODY(1) = Neutral.Alpha*T.SKIN_OV(1) + (1 - Neutral.Alpha) * T.CORE(1);
ALPHA = Neutral.Alpha;
if length(TA) == 1
    TIME = 60;
    ENV.TA = TA * ones(TIME,1);
    ENV.TR = TR * ones(TIME,1);
    ENV.VEL = VEL * ones(TIME,1);
    ENV.RH = RH * ones(TIME,1);
    Wet.MIST = WetMist * ones(TIME+1,1);
else
    TIME = length(TA);
    ENV.TA = TA;
    ENV.TR = TR;
    ENV.VEL = VEL;
    ENV.RH = RH;
end
if InitialSKIN == 0 && InitialCORE == 0
    T.SKIN(1) = Neutral.SKIN;
    T.CORE(1) = Neutral.CORE;
```

```
else
    T.SKIN(1) = InitialSKIN;
    T.CORE(1) = InitialCORE;
end
if length(WetMist) == 1
    Wet.MIST = WetMist * ones(TIME,1);
else
    Wet.MIST = WetMist;
end
%---------------------------------------------------------------------

for i = 1:TIME
    Vapor.Partial = ENV.RH(1)/100*Func_Ps(ENV.TA(i));
    ENV.VEL(i) = max(ENV.VEL(i), 0.1);
    COEFF = Func_Human(SUBJECT.CLOTHING,SUBJECT.POSTURE,ENV.VEL(i));
    COEFF.HR_CLOTHED = 4.0 * Const.SBC * (T.SKIN_CLOTHED(i)/2.0 + 273.15)^3 * COEFF.Fr;
    COEFF.HR_BARED = 4.0 * Const.SBC * (T.SKIN_BARED(i)/2.0 + 273.15)^3 * COEFF.Fr;
    COEFF.HR_OVERALL = COEFF.AreaFraction * COEFF.HR_BARED + (1 - COEFF.AreaFraction) *
        COEFF.HR_CLOTHED;
    COEFF.HT_BARED = COEFF.HR_BARED + COEFF.HC_BARED;
    COEFF.HT_CLOTHED = COEFF.HR_CLOTHED + COEFF.HC_CLOTHED;
    COEFF.HT_OVERALL = COEFF.HR_OVERALL + COEFF.HC_OVERALL;
    Ra = 1.0/(Facl * COEFF.HT_OVERALL);
    HE = Const.LR * COEFF.HC_CLOTHED;
    if(SUBJECT.CLO <= 0)
        WCRIT = 0.38*(ENV.VEL(i))^(-0.29);      %Maximum Wettedness by wind
        ICL = 1.0;                              %Vapor permeability of clithing
    else
        WCRIT = 0.59*(ENV.VEL(i))^(-0.08);
        ICL = 0.45;
    end
    Rea = 1.0/(Const.LR*Facl*COEFF.HC_CLOTHED);%Evaporative resistance of air layer
    Recl = Rcl/(Const.LR*ICL);                 %Evaporative resistance of clothing (icl=.45)
    Ret = Rea + Recl;                          %Total Evaporative resistance of clothed body

    % ---------- Cold and warm temperature receptor ----------
    SIG.WARM_SKIN_CLOTHED = max(0,T.SKIN_CLOTHED(i) - Neutral.SKIN);
    SIG.WARM_SKIN_BARED = max(0, T.SKIN_BARED(i) - Neutral.SKIN);
    SIG.WARM_SkIN_OV = max(0, T.SKIN_OV(i) - Neutral.SKIN);
    SIG.WARM_CORE = max(0, T.CORE(i) - Neutral.CORE);
    SIG.WARM_BODY = max(0, T.BODY(i) - Neutral.BODY);
    SIG.COLD_SKIN_CLOTHED = max(0, Neutral.SKIN - T.SKIN_CLOTHED(i));
    SIG.COLD_SKIN_BARED = max(0, Neutral.SKIN - T.SKIN_BARED(i));
    SIG.COLD_SKIN_OV = max(0, Neutral.SKIN - T.SKIN_OV(i));
    SIG.COLD_CORE = max(0, Neutral.CORE - T.CORE(i));
    T.SKIN_OV(i) = COEFF.AreaFraction * T.SKIN_BARED(i) + (1 - COEFF.AreaFraction) *
        T.SKIN_CLOTHED(i);
    T.BODY(i) = ALPHA * T.SKIN_OV(i) + (1 - ALPHA) * T.CORE(i);

    Wet.SK_CLOTHED(i) = Func_PWET(SIG.WARM_BODY, SIG.WARM_SKIN_CLOTHED, WCRIT,
        T.SKIN_CLOTHED(i), Vapor.Partial, Ret);
    Wet.SK_BARED(i) = Func_PWET(SIG.WARM_BODY, SIG.WARM_SKIN_BARED, WCRIT,
        T.SKIN_BARED(i), Vapor.Partial, Rea);
    Wet.SK_OV(i) = COEFF.AreaFraction * Wet.SK_BARED(i) + (1 - COEFF.AreaFraction) *
        Wet.SK_CLOTHED(i);

    % ---------- Estimating cloth temperature ----------
    TOP = (COEFF.HR_CLOTHED * ENV.TR(i) + COEFF.HC_CLOTHED * ENV.TA(i)) /
        COEFF.HT_CLOTHED;
    T.CLO = TOP + (T.SKIN_CLOTHED(i) - TOP) / (COEFF.HT_CLOTHED * (Ra + Rcl));
    FLUX1 = 100; FLUX2 = 50;
    while abs(FLUX1 - FLUX2) > 0.001
        Q.CONV_CLOTHED(i) = Facl * COEFF.HC_CLOTHED * (T.CLO - ENV.TA(i));
```

```
        Q.RAD_CLOTHED(i) = Facl * COEFF.HR_CLOTHED * (T.CLO - ENV.TR(i));
        E.CLOTHED_SKIN(i) = Wet.SK_CLOTHED(i) * (Func_Ps(T.SKIN_CLOTHED(i)) - Vapor.Partial) /
            (Recl +1 / (Facl * HE));
%           E.CLOTHED_MIST(i) = Wet.MIST(i) * (Func_Ps(T.CLO) - Vapor.Partial) / (1 / (Facl * HE));
        E.CLOTHED_MIST(i) = Eff * (1 - Wet.SK_CLOTHED(i)) * Wet.MIST(i) * (Func_Ps(T.CLO) -
            Vapor.Partial) / (1 / (Facl * HE));
        E.CLOTHED(i) = E.CLOTHED_SKIN(i) + E.CLOTHED_MIST(i);
        E.CLOTHED_MAX = Func_Ps(T.SKIN_CLOTHED(i) - Vapor.Partial) / Ret;
        E.CLOTHED(i) = min(E.CLOTHED(i), E.CLOTHED_MAX * WCRIT);
        FLUX1 = Q.CONV_CLOTHED(i) + Q.RAD_CLOTHED(i) + E.CLOTHED(i);
        T.CLO = T.SKIN_CLOTHED(i) - Rcl * FLUX1;
        FLUX2 = (T.SKIN_CLOTHED(i) - T.CLO) / Rcl;
    end
    Q.RES(i) = 0.0014 * Q.M * (34- ENV.TA(i)) + 0.0173 * Q.M * (5.85 - Vapor.Partial);
    Q.CONV_BARED(i) = COEFF.HC_BARED * (T.SKIN_BARED(i) - ENV.TA(i));
    Q.RAD_BARED(i) = COEFF.HR_BARED * (T.SKIN_BARED(i) - ENV.TR(i));
    E.BARED_SKIN(i) = Wet.SK_BARED(i) * (Func_Ps(T.SKIN_BARED(i)) - Vapor.Partial) / (1/HE);
    Q.CONV(i) = COEFF.AreaFraction * Q.CONV_BARED(i) + (1 - COEFF.AreaFraction) *
        Q.CONV_CLOTHED(i);
    Q.RAD(i) = COEFF.AreaFraction * Q.RAD_BARED(i) + (1 - COEFF.AreaFraction) * Q.RAD_CLOTHED(i);
    %       E.BARED_MIST(i) = Wet.MIST(i) * (Func_Ps(T.SKIN_BARED(i)) - Vapor.Partial) / (1/HE);
    E.BARED_MIST(i) = Eff * (1 - Wet.SK_BARED(i)) * Wet.MIST(i) * (Func_Ps(T.SKIN_BARED(i)) -
        Vapor.Partial) / (1/HE);
    E.BARED(i) = E.BARED_SKIN(i) + E.BARED_MIST(i);
    E.BARED_MAX = Func_Ps(T.SKIN_BARED(i) - Vapor.Partial) / Rea;
    E.BARED(i) = min(E.BARED(i), E.BARED_MAX * WCRIT);
    E.MIST(i) = COEFF.AreaFraction * E.BARED_MIST(i) + (1 - COEFF.AreaFraction) *
        E.CLOTHED_MIST(i);
    E.SK(i) = COEFF.AreaFraction * E.BARED_SKIN(i) + (1 - COEFF.AreaFraction) * E.CLOTHED_SKIN(i);

    F.CLOTHED(i) = (5.28 + 1.06 * 4190 * Func_Blood(SIG.WARM_CORE, SIG.COLD_SKIN_OV)) *
        (T.CORE(i) - T.SKIN_CLOTHED(i));
    F.BARED(i) = (5.28 + 1.06 * 4190 * Func_Blood(SIG.WARM_CORE, SIG.COLD_SKIN_OV)) * (T.CORE(i)
        - T.SKIN_BARED(i));

    MSHIV.CLOTHED = Func_Shiv(SIG.COLD_SKIN_CLOTHED, SIG.COLD_CORE);
    MSHIV.BARED = Func_Shiv(SIG.COLD_SKIN_BARED, SIG.COLD_CORE);
    MSHIV.OVERALL = COEFF.AreaFraction * MSHIV.BARED + (1 - COEFF.AreaFraction) *
        MSHIV.CLOTHED;
    % ---------------------- Heat storage -----------------------
    S.CORE(i) = Q.M - Q.W + MSHIV.OVERALL - Q.RES(i) - COEFF.AreaFraction * F.BARED(i) - (1-
        COEFF.AreaFraction) * F.CLOTHED(i);
    S.SKIN_CLOTHED(i) = F.CLOTHED(i) - (Q.CONV_CLOTHED(i) + Q.RAD_CLOTHED(i) +
        E.CLOTHED(i));
    S.SKIN_BARED(i) = F.BARED(i) - (Q.CONV_BARED(i) + Q.RAD_BARED(i) + E.BARED(i));
    S.SKIN_OV(i) =    COEFF.AreaFraction * S.SKIN_BARED(i) + (1 - COEFF.AreaFraction) *
        S.SKIN_CLOTHED(i);

    SamplingTime = 60;                                                  %1 min.
    ALPHA = 0.0417737+0.7451833/(Func_Blood(SIG.WARM_CORE, SIG.COLD_SKIN_OV) * 3600 +
        0.585417);
    dT.CORE = S.CORE(i) * SUBJECT.AREA / (1 - ALPHA) / SUBJECT.WEIGHT / 3500;
    dT.SKIN_CLOTHED = S.SKIN_CLOTHED(i) * (1 - COEFF.AreaFraction) * SUBJECT.AREA / (1 -
        COEFF.MassFraction) / ALPHA / SUBJECT.WEIGHT / 3500;
    dT.SKIN_BARED = S.SKIN_BARED(i) * COEFF.AreaFraction * SUBJECT.AREA / COEFF.MassFraction /
        ALPHA / SUBJECT.WEIGHT / 3500;
    T.CORE(i+1) = T.CORE(i) + dT.CORE * SamplingTime;
    T.SKIN_CLOTHED(i+1) = T.SKIN_CLOTHED(i) + dT.SKIN_CLOTHED * SamplingTime;
    T.SKIN_BARED(i+1) = T.SKIN_BARED(i) + dT.SKIN_BARED * SamplingTime;
    T.SKIN_OV(i+1) = COEFF.AreaFraction * T.SKIN_BARED(i+1) + (1 - COEFF.AreaFraction) *
        T.SKIN_CLOTHED(i+1);
    T.BODY(i+1) = ALPHA * T.SKIN_OV(i+1) + (1-ALPHA) * T.CORE(i+1);
```

```
        % ---------- Definition of ASHRAE Standard Environment    ----------
        HSK = COEFF.AreaFraction * (Q.CONV_BARED(i) + Q.RAD_BARED(i) + E.BARED(i))...
              + (1 - COEFF.AreaFraction) * (Q.CONV_CLOTHED(i) + Q.RAD_CLOTHED(i) +
                  E.CLOTHED(i)); %Total heat loss from skin
        W = Wet.SK_OV(i);
        PSSK = Func_Ps(T.SKIN_OV(i+1));
        COEFFS.HR = COEFF.HR_OVERALL;
        %Definition of ASHRAE standard environment
%       if SUBJECT.MET < 0.85
%           COEFFS.HC = 3.0;
%       else
%           COEFFS.HC = 5.66*(SUBJECT.MET-0.85)^0.39;
%           COEFFS.HC = max(COEFFS.HC,3.0);
%       end
        COEFF = Func_Human(SUBJECT.CLOTHING,SUBJECT.POSTURE,0);
        COEFFS.HC = COEFF.HC_OVERALL;
        COEFFS.HT = COEFFS.HC + COEFFS.HR;
        % ASHRAE Standard 2013
%       RCLOS = 1.52 / (SUBJECT.MET - SUBJECT.WORK / METFACTOR + 0.6944) - 0.1835;
        % Nishi Y. and Gagge, A.P. 1977, Effective temperature scale useful for hypo- and hyperbaric environments.
        RCLOS = 1.33 / (SUBJECT.MET - SUBJECT.WORK / METFACTOR + 0.74) - 0.095;
        RCLS = 0.155 * RCLOS;
        KCLO = 0.25;
        FACLS = 1.0 + KCLO * RCLOS;
        FCLS = 1.0 / (1.0 + 0.155 * FACLS * COEFFS.HT * RCLOS);
        IMS = 0.45;
        ICLS = IMS * COEFFS.HC / COEFFS.HT * (1 - FCLS) / (COEFFS.HC / COEFFS.HT - FCLS * IMS);
        RAS = 1.0/(FACLS * COEFFS.HT);
        REAS = 1.0/(Const.LR * FACLS * COEFFS.HC);
        RECLS = RCLS / (Const.LR * ICLS);
        HD_S = 1.0 / (RAS + RCLS);
        HE_S = 1.0 / (REAS + RECLS);    %SET determined using Newton's iterative solution
        DELTA = .0001;
        dx = 100.0;
        SET_OLD = T.SKIN_OV(i+1) - HSK/HD_S;                                    %Lower bound for SET
        while abs(dx) > .01
            ERR1 = (HSK - HD_S * (T.SKIN_OV(i+1) - SET_OLD) - W * HE_S * (PSSK - 0.5 *
                Func_Ps(SET_OLD)));
            ERR2 = (HSK - HD_S * (T.SKIN_OV(i+1) - (SET_OLD + DELTA)) - W * HE_S * (PSSK - 0.5 *
                Func_Ps((SET_OLD + DELTA))));
            SET = SET_OLD - DELTA * ERR1 / (ERR2 - ERR1);
            dx = SET - SET_OLD;
            SET_OLD = SET;
        end
        SET_Var(i+1) = SET;
    end
    T.SET = SET_Var(TIME+1);
    end


    %%                  Saturated Vapor Pressure in Specific Temperature
    function [SaturatedVaporPressure] = Func_Ps(T) % (Celsius & kPa)
    if T >= 0
        SaturatedVaporPressure = 0.6105 * exp((17.269 * T) / (237.3 + T));
    else
        SaturatedVaporPressure = 0.6105 * exp((21.875 * T) / (265.5 + T));
    end
    % SaturatedVaporPressure = 0.61121*exp((18.678-T/234.5)*(T/(257.14+T)));
    end

    %%                                  Sweat production
    function [PWET] = Func_PWET(WARMB,WARMSK,WCRIT,Temperature,Pa,Ret)
    CSW = 170;          %Driving coefficient for regulatory sweating [170g/(m2hr)]
```

```
ERSW = CSW*WARMB*exp(WARMSK/10.7);
ERSW = min(ERSW,670);
ERSW = 2430000/1000/3600*ERSW;                          %Phase change 2430000J/kg
EMAX = (Func_Ps(Temperature)-Pa)/(Ret);
PRSW = ERSW/EMAX;                                       %Wettedness by Sweat
PWET = 0.06+0.94*PRSW;
if PWET > WCRIT
      PWET = WCRIT;
      PRSW = WCRIT / (1 - 0.06);
      ERSW = PRSW * EMAX;
      EDIFF = 0.06 * (1 - PRSW) * EMAX;
      PWET = (ERSW + EDIFF) / EMAX;
end
if EMAX < 0
      EDIF = 0;
      ERSW = 0;
      PWET = WCRIT;
end
end

%%                                  Blood flow rate
function [SkinBloodFlow] = Func_Blood(WARM_CORE, COLD_SKIN)
SkinBloodFlowNeutral = 6.3;                                 %[Liter/m2hr]
%SkinBloodFlow = SkinBloodFlowNeutral;
CDIL = 200;                             %Driving coefficient for vasoconstriction
CSTR = 0.5;                                                 %vasoconstriction
SkinBloodFlow = (SkinBloodFlowNeutral+CDIL*(WARM_CORE))/(1+CSTR*(COLD_SKIN));
SkinBloodFlow = max(0.5,min(90,SkinBloodFlow));
SkinBloodFlow = SkinBloodFlow/3600;                         %Liter/s m2
end

%%                          Human's bared fraction of segments
function [Answer] = Func_Human(Season,Posture,VEL)
if strcmp('Summer', Season) == 1
      i = 1;
elseif strcmp('Winter', Season) == 1
      i = 2;
else
end
if strcmp('Sitting', Posture) == 1
      j = 1;
      Answer.Fr = 0.70;                         %Radiation effective area factor
elseif strcmp('Standing', Posture) == 1
      j = 2;
     Answer.Fr = 0.725;                         %Radiation effective area factor
else
end
%-------------------------Tanabe et al.--------------------------------
% 1st column : Area fraction, 2nd column : Mass fraction
Human = [0.075 0.054; 0.093 0.168; 0.086 0.148; 0.118 0.236; 0.051 0.029; 0.051 0.029;...
      0.034 0.018; 0.034 0.018; 0.027 0.005; 0.027 0.005; 0.112 0.094; 0.112 0.094;...
      0.06 0.045; 0.06 0.045; 0.03 0.006; 0.03 0.006];
% 1st column : Summer, 2nd column : Winter
% 0:Bared, 1:Clothed
Clothed_segment = [0 0;...      %Head
      1 1;...                   %2Chest
      1 1;...                   %3Back
      1 1;...                   %4Pelvis
      1 1;...                   %5Lshoulder
      1 1;...                   %6Rshoulder
      0 1;...                   %7Larm
      0 1;...                   %8Rarm
      0 0;...                   %9Lhand
```

```
        0 0;...                         %10Rhand
        1 1;...                         %11Lthigh
        1 1;...                         %12Rthigh
        0 1;...                         %13Lleg
        0 1;...                         %14Rleg
        1 1;...                         %15Lfoot
        1 1];                           %16Rfoot
Bared_Fraction = Human.*(1-Clothed_segment(:,i));
Answer.MassFraction = sum(Bared_Fraction(:,1));                 % Bared area fraction
Answer.AreaFraction = sum(Bared_Fraction(:,2));                  % Bared mass fraction
%-------------------------de Dear et al.-------------------------------
% 1st column : Sitting, 2nd column : Standing
% COEFF.HR = [3.9 4.1; 3.4 4.5; 4.6 4.4; 4.8 4.2; 4.8 5.2; 4.8 5.2; 5.2 4.9; 5.2 4.9; 3.9 4.1; 3.9 4.1;...
%         4.6 4.3; 4.6 4.3; 5.4 5.3; 5.4 5.3; 4.2 3.9; 4.2 3.9];
COEFF.HNC = [3.7 3.6; 3.0 3.0; 2.6 2.9; 2.8 3.4; 3.4 2.9; 3.4 2.9; 3.8 3.7; 3.8 3.7; 4.5 4.1; 4.5 4.1;...
        3.7 4.1; 3.7 4.1; 4.0 4.1; 4.0 4.1; 4.2 5.1; 4.2 5.1];
COEFF.HFC_a = [4.9 3.2; 9.1 7.5; 8.9 7.7; 8.2 8.8; 11.2 9.9; 11.6 10.2; 11.6 12.7; 11.9 12.4; 14.3 15.4;...
        12.6 13.4; 8.9 10.1; 8.9 10.1; 12.9 12.7; 13.4 13.1; 12.8 11.9; 13.0 12.1];
COEFF.HFC_b = [0.73 0.97; 0.59 0.66; 0.63 0.63; 0.65 0.59; 0.62 0.61; 0.66 0.64; 0.62 0.53; 0.63 0.55;...
        0.60 0.51; 0.60 0.60; 0.60 0.52; 0.60 0.52; 0.56 0.50; 0.58 0.51; 0.55 0.50; 0.54 0.49];
BARED = Human(:,1).*(1-Clothed_segment(:,i));
CLOTHED = Human(:,1).*(Clothed_segment(:,i));

COEFF.HNC_BARED = sum(COEFF.HNC(:,j).*BARED)/sum(BARED);
COEFF.HNC_CLOTHED = sum(COEFF.HNC(:,j).*CLOTHED)/sum(CLOTHED);
COEFF.HNC_OVERALL = (sum(COEFF.HNC(:,j).*BARED) + sum(COEFF.HNC(:,j).*CLOTHED)) /
                (sum(BARED) + sum(CLOTHED));
COEFF.HFC_BARED = sum(COEFF.HFC_a(:,j).*VEL.^COEFF.HFC_b(:,j).*BARED)/sum(BARED);
COEFF.HFC_CLOTHED = sum(COEFF.HFC_a(:,j).*VEL.^COEFF.HFC_b(:,j).*CLOTHED)/sum(CLOTHED);
COEFF.HFC_OVERALL = (sum(COEFF.HFC_a(:,j).*VEL.^COEFF.HFC_b(:,j).*BARED) +
                sum(COEFF.HFC_a(:,j).*VEL.^COEFF.HFC_b(:,j).*CLOTHED)) / (sum(BARED) +
                sum(CLOTHED));
if VEL > 0.2
        Answer.HC_BARED = COEFF.HFC_BARED;
        Answer.HC_CLOTHED = COEFF.HFC_CLOTHED;
        Answer.HC_OVERALL = COEFF.HFC_OVERALL;
else
        Answer.HC_BARED = COEFF.HNC_BARED;
        Answer.HC_CLOTHED = COEFF.HNC_CLOTHED;
        Answer.HC_OVERALL = COEFF.HNC_OVERALL;
end
end
%%                                      Shivering
function [Shiv] = Func_Shiv(COLDSK, COLDCORE)
Shiv = 19.44*COLDSK*COLDCORE;
end
```

Reference

[1] Y.A. Cengel, M.A. Boles, Thermodynamics an engineering approach, 8th ed., Mcgraw-Hill, New York, NY, 2015.

[2] M. Burke, F. González, P. Baylis, S. Heft-Neal, C. Baysan, S. Basu, S. Hsiang, Higher temperatures increase suicide rates in the United States and Mexico, Nature Climate Change. 8 (2018). doi:10.1038/s41558-018-0222-x.

[3] D.B. Petitti, D.M. Hondula, S. Yang, S.L. Harlan, G. Chowell, Multiple trigger points for quantifying heat-health impacts: New evidence from a hot climate, Environmental Health Perspectives. 124 (2016) 176–183. doi:10.1289/ehp.1409119.

[4] K.B. Metzger, K. Ito, T.D. Matte, Summer heat and mortality in New York City: How hot is too hot?, Environmental Health Perspectives. 118 (2010) 80–86. doi:10.1289/ehp.0900906.

[5] N. Seltenrich, Between extremes: Health effects of heat and cold, Environmental Health Perspectives. 123 (2015) 276–280. doi:10.1289/ehp.123-A275.

[6] R.A. Mugele, H.D. Evans, Droplet Size Distribution in Sprays, Industrial & Engineering Chemistry. 43 (1951) 1317–1324. doi:10.1021/ie50498a023.

[7] H. Barrow, C.W. Pope, Droplet evaporation with reference to the effectiveness of water-mist cooling, Applied Energy. 84 (2007) 404–412. doi:10.1016/j.apenergy.2006.09.007.

[8] S.S. Kachhwaha, P.L. Dhar, S.R. Kale, Experimental studies and numerical simulation of evaporative cooling of air with a water spray—I. Horizontal parallel flow, International Journal of Heat and Mass Transfer. 41 (1998) 447–464. doi:10.1016/S0017-9310(97)00133-6.

[9] A. Alkhedhair, Z. Guan, I. Jahn, H. Gurgenci, S. He, I. Jahn, Z. Guan, S. He, Numerical simulation of water spray for pre-cooling of inlet air in natural draft dry cooling towers, Applied Thermal Engineering. 61 (2013) 416–424. doi:10.1016/j.applthermaleng.2013.08.012.

[10] A. Hayashi, N. Kodama, M. Tsujimoto, Development of heat island control system with water mist sprayer, in: Proceedings of AIJ annual conference at Hokkaido University, 2004: pp. 805–806.

[11] C. Huang, D. Ye, H. Zhao, T. Liang, Z. Lin, H. Yin, Y. Yang, The research and application of spray cooling technology in Shanghai Expo, Applied Thermal Engineering. 31 (2011) 3726–3735. doi:10.1016/j.applthermaleng.2011.03.039.

[12] K. Zheng, M. Ichinose, N. Hien, Parametric study on the cooling effects from dry mists in a controlled environment, Building and Environment. 141 (2018) 61–70. doi:10.1016/j.buildenv.2018.05.053.

[13] C. Huang, J. Cai, Z. Lin, Q. Zhang, Y. Cui, Solving model of temperature and humidity profiles in spray cooling zone, Building and Environment. 123 (2017) 189–199. doi:10.1016/j.buildenv.2017.06.043.

[14] H. Montazeri, Y. Toparlar, B. Blocken, J.L.M. Hensen, Simulating the cooling effects of water spray systems in urban landscapes: A computational fluid dynamics study in Rotterdam, The Netherlands, Landscape and Urban Planning. 159 (2017) 85–100. doi:10.1016/j.landurbplan.2016.10.001.

[15] C. Farnham, K. Emura, T. Mizuno, Evaluation of cooling effects: Outdoor water mist fan, Building Research and Information. 43 (2015) 334–345. doi:10.1080/09613218.2015.1004844.

[16] G. Ulpiani, E. Di Giuseppe, C. Di Perna, M. D'Orazio, M. Zinzi, Thermal comfort improvement in urban spaces with water spray systems: Field measurements and survey, Building and Environment. 156 (2019) 46–61. doi:10.1016/j.buildenv.2019.04.007.

[17] N.H. Wong, A.Z.M. Chong, Performance evaluation of misting fans in hot and humid climate, Building and Environment. 45 (2010) 2666–2678. doi:10.1016/j.buildenv.2010.05.026.

[18] G. Jendritzky, R. de Dear, G. Havenith, UTCI-Why another thermal index?, International Journal of Biometeorology. 56 (2012) 421–428. doi:10.1007/s00484-011-0513-7.

[19] J. Pickup, R. de Dear, An outdoor thermal comfort index-part I - The model and its assumptions, Biometeorology and Urban Climatology at the Turn of the Millennium. WCASP 50: WMO/TD No.1026. (2000) 279–283.

[20] C.P. Yaglou, D. Minard, Control of heat casualties at military training centers, American Medical Association Archives of Industrial Health. (1957). doi:10.1017/CBO9781107415324.004.

[21] F.R. D'Ambrosio Alfano, J. Malchaire, B.I. Palella, G. Riccio, WBGT index revisited after 60 years of use, Annals of Occupational Hygiene. 58 (2014) 955–970. doi:10.1093/annhyg/meu050.

[22] P. Höppe, The physiological equivalent temperature - a universal index for the biometeorological assessment of the thermal environment, International Journal of Biometeorology. 43 (1999) 71–75. doi:10.1007/s004840050118.

[23] E. Walther, Q. Goestchel, The P.E.T. comfort index: Questioning the model, Building and Environment. 137 (2018) 1–10. doi:10.1016/j.buildenv.2018.03.054.

[24] T. Sharmin, K. Steemers, M. Humphreys, Outdoor thermal comfort and summer PET range: A field study in tropical city Dhaka, Energy and Buildings. 198 (2019) 149–159. doi:10.1016/j.enbuild.2019.05.064.

[25] J. Sen, P.K. Nag, Human susceptibility to outdoor hot environment, Science of The Total Environment. 649 (2019) 866–875. doi:10.1016/j.scitotenv.2018.08.325.

[26] J. Li, J. Niu, C.M. Mak, T. Huang, Y. Xie, Exploration of applicability of UTCI and thermally comfortable sun and wind conditions outdoors in a subtropical city of Hong Kong, Sustainable Cities and Society. 52 (2020) 101793. doi:10.1016/j.scs.2019.101793.

[27] W. Oh, R. Ooka, J. Nakano, H. Kikumoto, O. Ogawa, Environmental index for evaluating thermal sensations in a mist spraying environment, Building and Environment. 161 (2019) 106219. doi:10.1016/j.buildenv.2019.106219.

[28] M. Taleghani, M. Tenpierik, S. Kurvers, A. van den Dobbelsteen, A review into thermal comfort in buildings, Renewable and Sustainable Energy Reviews. 26 (2013) 201–215. doi:10.1016/j.rser.2013.05.050.

[29] L. Hill, H. Barnard, J.H. Sequeira, The Effect of Venous Pressure on the Pulse, The Journal of Physiology. 21 (1897) 147–159. doi:10.1113/jphysiol.1897.sp000648.

[30] J.S. Haldane, The influence of high air temperatures no. I, Journal of Hygiene. 5 (1905) 494–513. doi:10.1017/S0022172400006811.

[31] A.F. Dufton, The eupatheostat, Journal of Scientific Instruments. 6 (1929) 249–251. doi:10.1088/0950-7671/6/8/303.

[32] H.M. Vernon, C.G. Warner, The influence of the humidity of the air on capacity for work at high temperatures, Journal of Hygiene. 32 (1932) 431–462. doi:10.1017/S0022172400018167.

[33] C.-E.A. Winslow, L.P. Herrington, A.P. Gagge, Physiological reactions of the human body to varying environmental temperatures, American Journal of Physiology-Legacy Content. 120 (1937) 1–22. doi:10.1152/ajplegacy.1937.120.1.1.

[34] E.C. Thom, The Discomfort Index, Weatherwise. 12 (1959) 57–61. doi:10.1080/00431672.1959.9926960.

[35] P.O. Fanger, Thermal comfort. Analysis and applications in environmental engineering., Danish Technical Press, Copenhagen, 1970. https://scholar.google.com/scholar?hl=ko&as_sdt=0%2C5&q=Thermal+comfort.+Analysis+and+applications+in+environmental+engineering&btnG=.

[36] A.P. Gagge, J.A.J. Stolwijk, Y. Nishi, An effective temperature scale based on a simple model of human physiological regulatory response, ASHRAE Transactions. 77 (1972).

[37] J.H. Botsford, A wet globe thermometer for environmental heat measurement, American Industrial Hygiene Association Journal. 32 (1971) 1–10. doi:10.1080/0002889718506400.

[38] D.M. Kerslake, The stress of hot environments, Cambridge University Press. (1972) 316. doi:10.1126/science.177.4054.1096.

[39] R.R. Gonzalez, Y. Nishi, A.P. Gagge, Experimental evaluation of standard effective temperature a new biometeorological index of man's thermal discomfort, International Journal of Biometeorology. 18 (1974) 1–15. doi:10.1007/BF01450660.

[40] A. Zolfaghari, M. Maerefat, A new predictive index for evaluating both thermal sensation and thermal response of the human body, Building and Environment. 46 (2011) 855–862. doi:10.1016/j.buildenv.2010.10.011.

[41] D.S. Moran, Y. Shapiro, Y. Epstein, W. Matthew, K.B. Pandolf, A modified discomfort index (MDI) as an alternative to the wet bulb globe temperature (WBGT), Medicine & Science in Sports & Exercise. 30 (1998) 284. doi:10.1097/00005768-199805001-01614.

[42] D.S. Moran, K.B. Pandolf, Y. Shapiro, Y. Heled, Y. Shani, W.T. Mathew, R.R. Gonzalez, An environmental stress index (ESI) as a substitute for the wet bulb globe temperature (WBGT), Journal of Thermal Biology. 26 (2001) 427–431. doi:10.1016/S0306-4565(01)00055-9.

[43] G. Jendritzky, A. Maarouf, H. Staiger, Looking for a universal thermal climate index UTCI for outdoor applications, in: Windsor Conference on Thermal Standards, April 5-8, 2001, Windsor, UK, 2001: pp. 353–367.

[44] ASHRAE, Chapter 9, Thermal comfort, ASHRAE Handbook Fundamentals. (2017).

[45] Z. Fang, Z. Lin, C.M. Mak, J. Niu, K.-T.T. Tse, C.M. Mak, Z. Lin, Z. Fang, K.-T.T. Tse, Investigation into sensitivities of factors in outdoor thermal comfort indices, Building and Environment. 128 (2017) 129–142. doi:10.1016/j.buildenv.2017.11.028.

[46] T.-P. Lin, A. Matzarakis, R.-L. Hwang, Shading effect on long-term outdoor thermal comfort, Building and Environment. 45 (2010) 213–221. doi:10.1016/j.buildenv.2009.06.002.

[47] P. Bröde, D. Fiala, K. Blazejczyk, I. Holmér, G. Jendritzky, B. Kampmann, B. Tinz, G. Havenith, Deriving the operational procedure for the Universal Thermal Climate Index (UTCI), International Journal of Biometeorology. 56 (2012) 481–494. doi:10.1007/s00484-011-0454-1.

[48] I. Holmér, H. Nilsson, M. Bohm, O. Norén, Thermal Aspects of Vehicle Comfort, Applied Human Science. 14 (1995) 159–165. doi:10.1248/cpb.37.3229.

[49] H.O. Nilsson, Thermal comfort evaluation with virtual manikin methods, Building and Environment. 42 (2007) 4000–4005. doi:10.1016/j.buildenv.2006.04.027.

[50] W. Oh, S. Kato, The effect of airspeed and wind direction on human's thermal conditions and air distribution around the body, Building and Environment. 141 (2018) 103–116. doi:10.1016/j.buildenv.2018.05.052.

[51] M. He, N. Li, Y. He, D. He, C. Song, The influence of personally controlled desk fan on comfort and energy consumption in hot and humid environments, Building and Environment. 123 (2017) 378–389. doi:10.1016/j.buildenv.2017.07.021.

[52] M. Chludzińska, A. Bogdan, The role of the front pattern shape in modelling personalized airflow and its capacity to affect human thermal comfort, Building and Environment. 126 (2017) 373–381. doi:10.1016/j.buildenv.2017.10.018.

[53] H.O. Nilsson, I. Holmér, Comfort climate evaluation with thermal manikin methods and computer simulation models, Indoor Air. 13 (2003) 28–37. doi:10.1034/j.1600-0668.2003.01113.x.

[54] ISO 14505-2:2006, Ergonomics of the thermal environment - Evaluation of thermal environments in vehicles - Part2: Determination of equivalent temperature, (2006).

[55] Y. Kurazumi, T. Tsuchikawa, J. Ishii, K. Fukagawa, Y. Yamato, N. Matsubara, Radiative and convective heat transfer coefficients of the human body in natural convection, Building and Environment. 43 (2008) 2142–2153. doi:10.1016/j.buildenv.2007.12.012.

[56] S. Tanabe, E.A. Arens, F. Bauman, H. Zhang, T.L. Madsen, Evaluating thermal environments by using a thermal manikin with controlled skin surface temperature, ASHRAE Transactions. 100 Part 1 (1994) 39–48. https://escholarship.org/uc/item/22k424vp.

[57] M. Asayama, Guideline for the Prevention of Heat Disorder in Japan, Global Environmental Research. 13 (2009) 19–25.

[58] D. Fiala, G. Havenith, P. Bröde, B. Kampmann, G. Jendritzky, UTCI-Fiala multi-node model of human heat transfer and temperature regulation, International Journal of Biometeorology. 56 (2012) 429–441. doi:10.1007/s00484-011-0424-7.

[59] G. Havenith, D. Fiala, K. Błazejczyk, M. Richards, P. Bröde, I. Holmér, H. Rintamaki, Y. Benshabat, G. Jendritzky, The UTCI-clothing model, International Journal of Biometeorology. 56 (2012) 461–470. doi:10.1007/s00484-011-0451-4.

[60] Y. Nishi, A.P. Gagge, Humid operative temperature: A biophysical index of thermal sensation and discomfort, in: Symposium Intetnational de Thermorgulation Comportementale, Lyon, September 7-11 1970, Lyon, 1970: pp. 33–36. http://hdl.handle.net/2115/37923.

[61] R. Ooka, Y. Minami, T. Sakoi, K. Tsuzuki, H.B. Rijal, Improvement of sweating model in 2-Node Model and its application to thermal safety for hot environments, Building and Environment. 45 (2010) 1565–1573. doi:10.1016/j.buildenv.2009.12.012.

[62] A. Zolfaghari, M. Maerefat, A new simplified model for evaluating non-uniform thermal sensation caused by wearing clothing, Building and Environment. 45 (2010) 776–783. doi:10.1016/j.buildenv.2009.08.015.

[63] S. Tanabe, K. Kobayashi, J. Nakano, Y. Ozeki, M. Konishi, Evaluation of thermal comfort using combined multi-node thermoregulation (65MN) and radiation models and computational fluid dynamics (CFD), Energy and Buildings. 34 (2002) 637–646. doi:10.1016/S0378-7788(02)00014-2.

[64] J.A.J. Stolwijk, Mathematical models of thermal regulation, Annals of the New York Academy of Sciences. 335 (1980) 98–106. doi:10.1111/j.1749-6632.1980.tb50739.x.

[65] W. Oh, R. Ooka, J. Nakano, H. Kikumoto, O. Ogawa, Study on thermal indices under mist spray condition through thermal sensation and comfort, in: WINDSOR CONFERENCE: Rethinking comfort, 2018: p. Vol 10, pp110-127.

[66] T. Horikoshi, N. Isoda, Y. Kobayashi, Experimental study on the effect on the human body of the thermal conditions in the wind tunnel in Japanese, in: The Society of Heating, Air-Conditioning Sanitary Engineers of Japan, 1974: pp. 22–30.

[67] M. Takasu, R. Ooka, H.B. Rijal, M. Indraganti, M.K. Singh, Study on adaptive thermal comfort in Japanese offices under various operation modes, Building and Environment. 118 (2017) 273–288. doi:10.1016/j.buildenv.2017.02.023.

[68] H.B. Rijal, M.A. Humphreys, J.F. Nicol, Towards an adaptive model for thermal comfort in Japanese offices, Building Research and Information. 45 (2017) 717–729. doi:10.1080/09613218.2017.1288450.

[69] N.A.S. Taylor, N.K. Allsopp, D.G. Parkes, Preferred Room Temperature of Young vs Aged Males: The Influence of Thermal Sensation, Thermal Comfort, and Affect, The Journals of Gerontology Series A: Biological Sciences and Medical Sciences. 50A (1995) M216–M221. doi:10.1093/gerona/50A.4.M216.

[70] G. Havenith, D. Fiala, Thermal indices and thermophysiological modeling for heat stress, Comprehensive Physiology. 6 (2016) 255–302. doi:10.1002/cphy.c140051.

[71] K. Nagano, T. Horikoshi, New index indicating the universal and separate effects on human comfort under outdoor and non-uniform thermal conditions, Energy and Buildings. 43 (2011) 1694–1701. doi:10.1016/j.enbuild.2011.03.012.

[72] D. Lai, X. Zhou, Q. Chen, Measurements and predictions of the skin temperature of human subjects on outdoor environment, Energy and Buildings. 151 (2017) 476–486. doi:10.1016/j.enbuild.2017.07.009.

[73] M. Nikolopoulou, N. Baker, K. Steemers, Improvements to the Globe Thermometer for Outdoor Use, Architectural Science Review. 42 (1999) 27–34. doi:10.1080/00038628.1999.9696845.

[74] S. Thorsson, F. Lindberg, I. Eliasson, B. Holmer, Different methods for estimating the mean radiant temperature in an outdoor urban setting, International Journal of Climatology. 27 (2007) 1983–1993. doi:10.1002/joc.1537.

[75] A.P. Gagge, Y. Nishi, Heat exchange between human skin surface and thermal environment, Comprehensive Physiology. (2011). doi:10.1002/cphy.cp090105.

[76] C. Farnham, M. Nakao, M. Nishioka, M. Nabeshima, T. Mizuno, Study of mist-cooling for semi-enclosed spaces in Osaka, Japan, Procedia Environmental Sciences. 4 (2011) 228–238. doi:10.1016/j.proenv.2011.03.027.

[77] R. Hreiz, R. Lainé, J. Wu, C. Lemaitre, C. Gentric, D. Fünfschilling, On the effect of the nozzle design on the performances of gas-liquid cylindrical cyclone separators, International Journal of Multiphase Flow. 58 (2014) 15–26. doi:10.1016/j.ijmultiphaseflow.2013.08.006.

[78] N. Walikewitz, B. Jänicke, M. Langner, F. Meier, W. Endlicher, The difference between the mean radiant temperature and the air temperature within indoor environments: A case study during summer conditions, Building and Environment. 84 (2015) 151–161. doi:10.1016/j.buildenv.2014.11.004.

[79] S. Park, S.E. Tuller, Human body area factors for radiation exchange analysis: Standing and walking postures, International Journal of Biometeorology. 55 (2011) 695–709. doi:10.1007/s00484-010-0385-2.

[80] J.D. Hardy, E.F. Du Bois, G.F. Soderstrom, The technic of measuring radiation and convection, The Journal of Nutrition. 15 (1938) 461–475. doi:10.1093/jn/15.5.461.

[81] N.L. Ramanathan, A new weighting system for mean surface temperature of the human body, Journal of Applied Physiology. 19 (1964) 531–533. doi:10.1152/jappl.1964.19.3.531.

[82] D. Mitchell, C.H. Wyndham, Comparison of weighting formulas for calculating mean skin temperature, Journal of Applied Physiology. 26 (1969) 616–622. doi:10.1152/jappl.1969.26.5.616.

[83] E.R. Nadel, J.W. Mitchell, J.A.J. Stolwijk, Differential thermal sensitivity in the human skin, Pflügers Archiv: European Journal of Physiology. 340 (1973) 71–76. doi:10.1007/BF00592198.

[84] L.I. Crawshaw, E.R. Nadel, J.A.J. Stolwijk, B.A. Stamford, Effect of local cooling on sweating rate and cold sensation, Pflügers Archiv European Journal of Physiology. 354 (1975) 19–27. doi:10.1007/BF00584500.

[85] J.A.J. Stolwijk, J.D. Hardy, Partitional calorimetric studies of man during exposures to thermal transients., Journal of Applied Physiology. 21 (1966) 1799–1806. doi:10.1152/jappl.1966.21.6.1799.

[86] A.C. Burton, Human calorimetry: II. The average temperature of the tissues of the body, The Journal of Nutrition. 9 (1935) 261–280. doi:10.1093/jn/9.3.261.

[87] J.K. Choi, K. Miki, S. Sagawa, K. Shiraki, Evaluation of mean skin temperature formulas by infrared thermography, International Journal of Biometeorology. 41 (1997) 68–75. doi:10.1007/s004840050056.

[88] ANSI/ASHRAE, Standard 55-2013: Thermal environmental conditions for human occupancy, (2013).

[89] IPCC, Climate Change 2013 - The Physical Science Basis, Cambridge University Press, New York, 2013. doi:10.1017/CBO9781107415324.

[90] L. Chen, E. Ng, Outdoor thermal comfort and outdoor activities: A review of research in the past decade, Cities. 29 (2012) 118–125. doi:10.1016/j.cities.2011.08.006.

[91] M. Nikolopoulou, S. Lykoudis, Thermal comfort in outdoor urban spaces: Analysis across different European countries, Building and Environment. 41 (2006) 1455–1470. doi:10.1016/j.buildenv.2005.05.031.

[92] J. Spagnolo, R. de Dear, A field study of thermal comfort in outdoor and semi-outdoor environments in subtropical Sydney Australia, Building and Environment. 38 (2003) 721–738. doi:10.1016/S0360-1323(02)00209-3.

[93] T. Stathopoulos, H. Wu, J. Zacharias, Outdoor human comfort in an urban climate, Building and Environment. 39 (2004) 297–305. doi:10.1016/j.buildenv.2003.09.001.

[94] Y. Xie, T. Huang, J. Li, J. Liu, J. Niu, C.M. Mak, Z. Lin, Evaluation of a multi-nodal thermal regulation model for assessment of outdoor thermal comfort: Sensitivity to wind speed and solar radiation, Building and Environment. 132 (2018) 45–56. doi:10.1016/j.buildenv.2018.01.025.

[95] Y. Xie, J. Liu, T. Huang, J. Li, J. Niu, C. Ming, T. Lee, B. Services, T. Hong, K. Polytechnic, H. Kong, C.M. Mak, T. Lee, Outdoor thermal sensation and logistic regression analysis of comfort range of meteorological parameters in Hong Kong, Building and Environment. 155 (2019) 175–186. doi:10.1016/j.buildenv.2019.03.035.

[96] D.L. Black, M.Q. McQuay, M.P. Bonin, Laser-based techniques for particle-size measurement: A review of sizing methods and their industrial applications, Progress in Energy and Combustion Science. 22 (1996) 267–306. doi:10.1016/S0360-1285(96)00008-1.

[97] M.A. Humphreys, The optimum diameter for a globe thermometer for use indoors, Annals of Occupational Hygiene. (1977). doi:10.1093/annhyg/20.2.135.

[98] S. Wang, Y. Li, Suitability of acrylic and copper globe thermometers for diurnal outdoor settings, Building and Environment. 89 (2015) 279–294. doi:10.1016/j.buildenv.2015.03.002.

[99] H. Hsu, P.A. Lachenbruch, Paired t Test, in: Wiley Encyclopedia of Clinical Trials, John Wiley & Sons, Inc., Hoboken, NJ, USA, 2008: pp. 1–3. doi:10.1002/9780471462422.eoct969.

[100] ASHRAE, Chapter 9, Thermal comfort, ASHRAE Handbook Fundamentals. (2013).

[101] M. Nakayoshi, M. Kanda, R. Shi, R. de Dear, Outdoor thermal physiology along human pathways: a study using a wearable measurement system, International Journal of Biometeorology. 59 (2014) 503–515. doi:10.1007/s00484-014-0864-y.

[102] T.L. Bergman, A.S. Lavine, F.P. Incropera, D.P. Dewitt, A.S. Lavigne, F.P. Incropera, D.P. Dewitt, Fundamentals of heat and mass transfer, Eighth Ed., John Wiley & Sons, Danvers, 2017. doi:10.1016/j.applthermaleng.2011.03.022.

[103] M. Pinterić, Building Physics, Springer International Publishing, Cham, 2017. doi:10.1007/978-3-319-57484-4.

[104] C. R. Camp, E. J. Sadler, W. J. Busscher, A Water Droplet Evaporation and Temperature Model, Transactions of the ASAE. 32 (1989) 0457–0462. doi:10.13031/2013.31026.

[105] F. Nicol, M. Humphreys, S. Roaf, Adaptive thermal comfort: Foundations and analysis, London, 2016.

[106] M. Nakamura, T. Yoda, L.I. Crawshaw, S. Yasuhara, Y. Saito, M. Kasuga, K. Nagashima, K. Kanosue, Regional differences in temperature sensation and thermal comfort in humans, Journal of Applied Physiology. (2008) 1897–1906. doi:10.1152/japplphysiol.90466.2008.

[107] C. Farnham, Y. Okazaki, K. Emura, M. Kubota, J. Yuan, A. Md Alan, The effect of the visual cue of mist cooling on perceived thermal comfort, in: WINDSOR CONFERENCE: Rethinking comfort, 2018: p. Vol 10, pp99-109.

[108] Y. Zhang, R. Zhao, Relationship between thermal sensation and comfort in non-uniform and dynamic environments, Building and Environment. 44 (2009) 1386–1391. doi:10.1016/j.buildenv.2008.04.006.

[109] D. Lai, C. Chen, Comparison of the linear regression, multinomial logit, and ordered probability models for predicting the distribution of thermal sensation, Energy and Buildings. 188–189 (2019) 269–277. doi:10.1016/j.enbuild.2019.02.027.

[110] K. Pantavou, G. Theoharatos, M. Santamouris, D. Asimakopoulos, Outdoor thermal sensation of pedestrians in a Mediterranean climate and a comparison with UTCI, Building and Environment. 66 (2013) 82–95. doi:10.1016/j.buildenv.2013.02.014.

[111] S. Kato, K. Hiyama, Ventilating Cities, Springer Netherlands, Dordrecht, 2012. doi:10.1007/978-94-007-2771-7.

[112] K. Zheng, C. Yuan, N.H. Wong, C. Cen, Dry mist systems and its impact on thermal comfort for the tropics, Sustainable Cities and Society. 51 (2019) 101727. doi:10.1016/j.scs.2019.101727.

[113] J.A.J. Stolwijk, J.D. Hardy, Temperature regulation in man - A theoretical study, Pflügers Archiv Für Die Gesamte Physiologie Des Menschen Und Der Tiere. 291 (1966) 129–162. doi:10.1007/BF00412787.

[114] W. Oh, R. Ooka, J. Nakano, H. Kikumoto, O. Ogawa, Evaluation of mist-spraying environment on thermal sensations, thermal environment, and skin temperature under different operation modes, Building and Environment. 168 (2020) 106484. doi:10.1016/j.buildenv.2019.106484.

[115] V. Melnikov, V. V. Krzhizhanovskaya, M.H. Lees, P.M.A. Sloot, System dynamics of human body thermal regulation in outdoor environments, Building and Environment. 143 (2018) 760–769. doi:10.1016/j.buildenv.2018.07.024.

[116] R. de Dear, E.A. Arens, Z. Hui, M. Oguro, Convective and radiative heat transfer coefficients for individual human body segments, International Journal of Biometeorology. 40 (1997) 141–156. doi:10.1007/s004840050035.

[117] S. Gao, R. Ooka, W. Oh, Formulation of human body heat transfer coefficient under various ambient temperature, air speed and direction based on experiments and CFD, Building and Environment. 160 (2019) 106168. doi:10.1016/j.buildenv.2019.106168.

[118] S. Becker, O. Potchter, Y. Yaakov, Calculated and observed human thermal sensation in an extremely hot and dry climate, Energy and Buildings. 35 (2003) 747–756. doi:10.1016/S0378-7788(02)00228-1.

Publications

Peer-reviewed journals

[1] W. Oh, R. Ooka, J. Nakano, H. Kikumoto, O. Ogawa, Environmental index for evaluating thermal sensations in a mist spraying environment, Building and Environment. 161 (2019) 106219. doi:10.1016/j.buildenv.2019.106219.

[2] S. Gao, R. Ooka, W. Oh, Formulation of human body heat transfer coefficient under various ambient temperature, air speed and direction based on experiments and CFD, Building and Environment. 160 (2019) 106168. doi:10.1016/j.buildenv.2019.106168.

[3] W. Oh, R. Ooka, J. Nakano, H. Kikumoto, O. Ogawa, Evaluation of mist-spraying environment on thermal sensations, thermal environment, and skin temperature under different operation modes, Building and Environment, 168 (2020) 106484. 10.1016/j.buildenv.2019.106484.

[4] W. Oh, R. Ooka, J. Nakano, H. Kikumoto, O. Ogawa, W. Choi, Development of physiological human model considering mist wettedness for mist-spraying environments (under-review)

Conference proceeding papers (International)

[1] W. Oh, R. Ooka, J. Nakano, H. Kikumoto, O. Ogawa, Study on thermal indices under mist spray condition through thermal sensation and comfort, in: WINDSOR CONFERENCE: Rethinking comfort, 2018: p. Vol 10, pp110-127.

[2] R. Ooka, W. Oh, J.Nakano, H. Kikumoto, O. Ogawa, Field experiment of mist spray system with supporting air blow for the mitigation of hot outdoor environment, International Conference on Urban Climate, 6-10 August 2019, New York, NY.

[3] S. Gao, R. Ooka, W. Oh, Effects of ambient temperature, airspeed, and wind direction on heat transfer coefficient for the human body by means of manikin experiments and CFD analysis, E3S Web of Conferences. 111 (2019) 02041. doi:10.1051/e3sconf/201911102041

[4] Q. Guo, R. Ooka, W. Oh, W. Choi, D. Lee, Effect of insulation on indoor thermal comfort in a detached house with a floor heating system, E3S Web of Conferences. 111 (2019) 02049. doi:10.1051/e3sconf/201911102049

[5] W. Oh, R. Ooka, J. Nakano, H. Kikumoto, O. Ogawa, Validation of thermoregulation human model considering mist wettedness on mist spraying environment, in: IAQVEC Conference, 5-7 September 2019, Bari, Italy.

Conference proceeding papers (Domestic)

[1] W. Oh, R. Ooka, J. Nakano, H. Kikumoto, O. Ogawa, Study on the thermal environmental indices and human thermal sensation under mist spray condition (in Japanese), in: Technical

papers of annual meeting, the Society of Heating, Air-Conditioning and Sanitary Engineers of Japan at Kochi University of Technology, 2017: pp. 109–112.

[2] W. Oh, R. Ooka, J. Nakano, H. Kikumoto, O. Ogawa, Development of a new environmental index for outdoor and mist spray environments (Part 1) Study on evaluation and verification of 2 node model (in Japanese), in: in: Proceedings of AIJ annual conference at Tohoku University, 2018: pp. 393–394.

[3] S. Gao, R. Ooka, W. Oh, Q. Guo, Study of non-uniform wall temperature effects on micro-climate around human body with coupled analysis of convection and radiation (Part 1) Cases description and study of skin surface temperature (in Japanese), in: Proceedings of AIJ annual conference at Tohoku University, 2018: pp. 433–434.

[4] Q. Guo, R. Ooka, W. Oh, S. Gao, Study of non-uniform wall temperature effects on micro-climate around human body with coupled analysis of convection and radiation (Part 2) Study of heat transfer coefficient and heat loss (in Japanese), in: Proceedings of AIJ annual conference at Tohoku University, 2018: pp. 435–436.

[5] W. Oh, R. Ooka, J. Nakano, H. Kikumoto, O. Ogawa, Development of a new environmental index for outdoor and mist spray environments (Part 2) Proposal of a new index using thermal sensation votes, in: Technical papers of annual meeting, the Society of Heating, Air-Conditioning and Sanitary Engineers of Japan at Daido University, 2018: pp. 1–4.

[6] S. Gao, R. Ooka, W. Oh, H. Nagano, Study on the convective heat transfer coefficients under calm environment with different ambient temperature by using thermal manikin (in Japanese), in: Technical papers of annual meeting, the Society of Heating, Air-Conditioning and Sanitary Engineers of Japan at Daido University, 2018: pp. 361–364.

[7] Q. Guo, R. Ooka, W. Oh, W. Choi, Evaluation of thermal sensation and comfort of radiant heating system in an environmental test room (in Japanese), in: Technical papers of annual meeting, the Society of Heating, Air-Conditioning and Sanitary Engineers of Japan at Daido University, 2018: pp. 365–368.

[8] W. Oh, R. Ooka, J. Nakano, H. Kikumoto, O. Ogawa, Development of a new environmental index for outdoor and mist spray environments (Part 3) Effect of operation mode on environmental factors and subjective assessments (in Japanese), in: Proceedings of AIJ annual conference at Kanazawa Institute of Technology, 2019: pp. 563–564.

[9] S. Gao, R. Ooka, W. Oh, Study on the evaluation of thermal environment around the human body using thermal manikin: Effects of airspeed and wind direction on convective heat transfer coefficient for human body (in Japanese) , in: Proceedings of AIJ annual conference at Kanazawa Institute of Technology, 2019: pp. 527–528.

[10] Q. Guo, R. Ooka, W. Oh, W. Choi, D. Lee, Effects of insulation on indoor thermal comfort in a detached house with a floor heating system (in Japanese), in: Proceedings of AIJ annual conference at Kanazawa Institute of Technology, 2019: pp. 305–306.

[11] W. Oh, R. Ooka, J. Nakano, H. Kikumoto, O. Ogawa, Development of a new environmental index for outdoor and mist spray environments (Part 4) Study on skin temperature changes and thermal sensations in outdoor and mist spraying environment (in Japanese), in: Technical papers of annual meeting, the Society of Heating, Air-Conditioning and Sanitary Engineers of Japan at Hokkaido University of Science, 2019: pp. 177–180.

[12] S. Gao, R. Ooka, W. Oh, Evaluation of the thermal environment around the human body using a thermal manikin The effect of air speed and direction on convective heat transfer coefficient for the clothing human body (in Japanese), in: Technical papers of annual meeting, the Society of Heating, Air-Conditioning and Sanitary Engineers of Japan at Hokkaido University of Science, 2019: pp. 49–52

[13] Q. Guo, R. Ooka, W. Oh, W. Choi, D. Lee, Simulation of indoor thermal environment of a radiant floor heating system in an environmental test room (in Japanese), in: Technical papers of annual meeting, the Society of Heating, Air-Conditioning and Sanitary Engineers of Japan at Hokkaido University of Science, 2019: pp. 353–356.

Acknowledgments

I would like to express my gratitude to all who helped me to write this doctoral thesis.

The completion of this doctoral dissertation involved the labor and support of many people. I would like to express my gratitude to all who helped and supported me to finish this dissertation.

First and foremost, I would like to express the deepest appreciation to my supervisor, Prof. Ryozo Ooka for his support and guidance to complete my doctoral course. His perceptive advice, kind encouragement, and willing assistance helped bring this dissertation to a successful conclusion.

I would like to thank Prof. Shinsuke Kato. The fundamental studies and the way of solving problems I learned from him during my master course became a solid foundation for my research in the doctoral course.

And a very special thanks to Assoc. Prof. Junta Nakano whose experienced and skilled advice leaded to advance this research with further developments. Also, I would like to thank to his students who assisted filed experiments despite the hot weather.

My sincere gratitude also goes to Prof. Kikumoto Hideki for his sincere advice on research. His insightful advice and guidance helped me all the time to improve my doctoral dissertation.

I wish to express my gratitude to Prof. Yasunori Akashi. As a co-advisor, he had given me help and encouragement every semester during the doctoral course. Constructive criticism what he had offered helped me to refine this dissertation.

Also, I would like to record my appreciation to Prof. Hom Bahadur Rijal who was generously reviewed this dissertation, offering detailed and invaluable comments. Especially, I was pleased to learn a technical know-how about surveying analysis and adaptive thermal comfort.

I am also very grateful to Research Assoc. Wonjun Choi for offering valuable suggestions on designing and making a heating globe thermometer, one of the key instruments of the field experiments conducted in this dissertation.

I am also indebted to Ms. Doyun Lee and Ms. Shan Gao, for their assistance in the field experiment

and subject experiments. This dissertation would be never been complete without their support and encouragement.

This doctoral dissertation was made possible by support from Mr. Osamu Ogawa who supported this research through industry-academic cooperation. To him, I owe special thanks for the help and technical assistance I have received to progress the research perfectly as planned.

Also, I am grateful to my seniors, colleagues and members of Ooka and Kikumoto Laboratory who lead me in a good direction during my life of studying abroad. They are Dr. Mengtao Han, Mr. Mingzhe Liu, Mr. Qi Zhou, Mr. Bingchao Zhang, Mr. Hongyuan Jia, Mr. Ke Wen, Mr. Chao Lin, Mr. Christopher O'Malley, Ms. Qianwen Guo, Mr. Daisuke Inagaki, Mr. Naoto Uchida, Ms. Hong Hu, Ms. Yunchen Bu, Mr. Chaoyi Hu, and Ms. Shuyuan Hu.

Finally, my most sincere thanks go to my family who always providing all sorts of tangible and intangible support.